


CA3 ONHW Q90

82 U6507

v.4

Hydrogeological
investigations of the
Upper Ottawa Street
Landfill site - appendix
Reference 23



Digitized by the Internet Archive
in 2024 with funding from
Hamilton Public Library

<https://archive.org/details/hydrogeologicali04unse>

HAMILTON PUBLIC LIBRARY

APR 3 - 1987

COPY

URBAN MUNICIPAL

MAY 4 1987

GOVERNMENT DOCUMENTS

Reference 23

Appendix A

PROTOCOLS EMPLOYED FOR CHEMICAL SAMPLING

Figure A-1 describes the sequence in which groundwater samples for the various chemical parameters were obtained at the Upper Ottawa Street site. Other routine procedures associated with the taking of water samples are also included, such as the measurement of water depth, removal of standing water and determination of field temperature, pH and electrical conductance. When a sample for an individual chemical parameter was not to be taken at a particular point, it was simply omitted from the sequence and the remaining samples obtained in the order indicated.

Special measures were employed at piezometers where recharge rates were too slow to obtain all of the desired samples within approximately three hours. When a slow recharge rate was suspected, a 1-l aliquot of the standing water initially removed from the well was saved in an amber glass bottle prepared for extractable organics analysis. If the well failed to recharge after 24 hours, the saved water was used either as an extractable organics or a major ions/nitrogen species/bulk parameters sample. If recharge within 24 hours was sufficient, the earlier sample was discarded and the newly-recharged water removed and saved for the desired chemical analyses.

Clean water-level tape with deionized H_2O

↓
Measure depth to water

↓
Select pumping apparatus (b)

↓
Clean tubing for pumping apparatus (b)

↓
Lower tip of tube to bottom of piezometer,
then lift up approximately 10 cm

↓
Remove standing water (b)

↓
Collect initial TOC/Cl sample (c)

↓
Purgeable organics (d)

↓
Extractable organics (d)

↓
Field temperature, pH and electrical conductance (e)

↓
Major ions/nitrogen species/bulk parameters (f)

↓
Heavy metals (f)

↓
Dissolved oxygen (g)

↓
Dissolved methane (h)

↓
Aqueous isotopes (i)

↓
Final TOC/Cl (c)

Clean sampling tubing as described in section (b)
then wipe outside with cloth soaked in methanol
(reagent grade) to remove residual organic material

a. Methods for sample container preparation

1. EXTRACTABLE ORGANICS

A. bottles (1-litre, amber glass, narrow-necked)

1. Rinse thoroughly with hot tap water. Remove label(s).
2. Add a few ml Extran (neat).
3. Fill to rim with hot tapwater
4. Allow to soak overnight
5. Empty and rinse with deionized water until soap appears to be gone (no bubbles).
6. Rinse with 10% HNO_3 (concentrated nitric acid diluted with organic-free deionized water).
7. Rinse 3 times with small aliquots (10 ml) of organic-free deionized water.
8. Rinse 2 times with either spectroscopic-grade acetone or methanol (acetone preferred), using a 30 ml aliquot and thoroughly covering all inner surfaces. Drip dry in hood.
9. Rinse 2 times with either spec-grade hexane or spec-grade methylene chloride (hexane preferred), again using a 30 ml aliquot and thoroughly covering all inner surfaces. Drip dry in hood.
10. Bake at 100°C overnight.
11. Cap with Teflon face of liner against bottle lip.

B. Caps (unlined) + Liners (Teflon-faced silicone rubber septa)

1. Remove liners from used caps. Discard liners which are discoloured.
2. Rinse cap-liners well with tapwater.
3. Place caps and liners in separate beakers filled with dilute Extran.
4. Soak for at least 2 hours.
5. Rinse caps and liners thoroughly with deionized water until soap appears to be gone.
6. Soak caps and liners in 10% HNO₃.
7. Rinse both 3 times with organic-free water.
8. Dry both at 80°C for at least 3 hrs.

II. PURGEABLE ORGANICS

A. Bottles (250-ml, amber glass)

1. Follow procedure for extractable organics bottles, steps 1 through 7.
2. Dry in oven at 100°C
3. Cap while still warm.
4. Purge with nitrogen flowing at approximately 100 ml/min for 5 minutes.
5. Re-cap immediately

B. Caps (1-urilled) + Liners (Teilon-faced silicone rubber septa)

1. Prepare caps for extractable organics bottle caps.
2. Dispose of old liners - wash new ones with organic-free water 3 times.

III. SYRINGES

A. Plastic (for dissolved oxygen)

1. Rinse well with tapwater, remove label(s) and needles.
2. Shake off excess water.
3. Air dry in laboratory.

B. Glass (for methane)

1. Rinse well with tapwater, remove labels and needles.
2. Rinse with dilute (2-5%) HNO_3
3. Rinse well with tapwater
4. Gently shake off excess water.
5. Air dry in laboratory.

IV. 60-ml Plastic bottles (used for aqueous isotopes samples)

1. Rinse well with tapwater, remove labels, shake out excess water and air dry in lab.

V. 1-l Plastic bottles (used to hold MOE samples from JT points prior to filtration, and for enriched tritium samples)

1. Extran soak for one hour. Remove all labels and visible dirt.
2. Rinse out soap with deionized H_2O
3. Acid wash with 10% HCl
4. Rinse with deionized H_2O
5. Air dry in lab.

b. Design, operation and cleaning of pumping equipment

Three different types of pumping apparatus were used to obtain groundwater samples for chemical analysis: A peristaltic pump, a triple tube sampler and a gas-squeeze pump. When the water surface in the piezometer was within vacuum lift height (i.e., 8 m), the peristaltic pump was used. The triple-tube was used for nearly all piezometers where the water surface was beyond vacuum lift height (> 8 m), the only exceptions being the larger-diameter (1.5-in) standpipes, UW2b and UW2c, where the gas-squeeze pump was employed.

1. Peristaltic Pump

(a) Apparatus

A variable-speed peristaltic pump (PP) was used in conjunction with PTFE (polytetrafluoro-ethylene, or Teflon R) tubing to obtain samples from points where the depth to water was within vacuum lift height (approximately 8 m). The tubing is mounted on a wooden spool lined with PTFE sheeting to facilitate cleaning and minimize cross-contamination among consecutive samples. For sampling, the free end of the tubing is fed down the piezometer tube to the desired depth. The opposite end of the tube remains fixed to the spool and is connected internally to a stainless steel port on one side of the spool. After the sampling tube is lowered into the piezometer, the connection to the PP is completed using a short length of PTFE tubing.

with one end affixed to the spool access port by a Swagelok (R) fitting and the other connected either to the flow-through system for organics sampling (see section d below) or directly to the PP for all other samples.

Standing water was removed from all piezometers sampled with the PP by pumping out at least 2 l (wherever recharge rates permitted) before obtaining any samples for chemical analysis.

(b) Cleaning

1. Wipe outside of tubing with a clean cloth soaked in reagent-grade methanol as the tubing is withdrawn from the piezometer.
2. Pump one or two 50-ml aliquots of 10% nitric acid through PTFE tubing and PP.
3. Pump two or three 50-ml aliquots of reagent-grade methanol through entire apparatus.
4. Pump 1 l of deionized water through apparatus.
5. Wipe outside of tubing while it is being lowered into piezometer, using a cloth soaked with deionized water.

(2) Triple-Tube Pump

(a) Apparatus

The triple-tube (JT) is a gas-driven, positive displacement pump used to obtain samples from narrow-diameter piezometers (Robin et al., 1982). As with the PP tubing, the JT tubing is made of PTFE and mounted on a

wooden spool lined with PTFE sheeting. During sampling with this apparatus, groundwater contacts only PTFE, stainless steel (or brass), a short length of latex tubing and organic-free nitrogen gas.

The design and operation of the JT pump are described by Robin et al. (1982). Standing water was removed from all piezometers sampled with the JT by removing two JT tube volumes (where recharge rates permitted) prior to obtaining any samples for chemical analysis.

(b) Cleaning

The methods used for cleaning the JT pump during sampling operations are identical to those used for the PP tubing (described above).

(c) Gas-squeeze (IEA) pump

(a) Apparatus

The IEA pump (Industrial and Environmental Analysts, Inc., Essex Junction, VT) is a gas-squeeze pump which was used to sample the larger-diameter standpipes (UW26-2 and UW28-2). The principle of operation of this device is described by Gillham et al. (1983).

(b) Cleaning

Prior to sampling, the IEA pump was rinsed with dilute nitric acid, reagent-grade methanol and deionized water.

(4) Tube bailing

At those piezometers where none of the three methods described above proved to be effective in obtaining water, a simple bailing technique was employed. After appropriate

cleaning, the PP tube was led down to the bottom of the sampling point with its upper end open to the atmosphere. The upper end was then blocked and the tubing, containing sample held by suction, raised out of the piezometer. Sample was then delivered by opening the sealed end. This procedure was repeated until a sufficient volume of sample was obtained.

c. Methods for Collecting Groundwater Samples for Specific Chemical Parameters

1. Total Organic Carbon/Chloride

Samples were collected in new, 20-ml glass scintillation vials from the effluent end of either the PP or the 3T apparatus. The vials were sealed with foil-lined screw caps and packed in ice for transport to the laboratory, where they were stored at approximately 4°C until analysed.

2. Purgeable and Extractable Organic Compounds

Samples for purgeable and extractable organic compounds were obtained in amber glass bottles (purgeables: 250 ml; extractables: 1 l) using the apparatuses depicted in figure A-2 and figure A-3. Sample bottles were connected in line with the PTFE sampling lines by threaded stainless-steel caps. Gas-tight seals at the bottle necks were ensured by using Vitron (R) O-rings imbedded within the caps.

(1) Peristaltic Pump Procedure

Bottles for purgeable and extractable organics samples were installed in series upstream from the peristaltic pump as shown in Figure A-2.

At least 750 ml of groundwater were pumped through the system before any purgeable organics samples were taken. If the piezometer recharge rate was sufficiently high, at least two litres of groundwater were pumped before any organics samples were taken. The vacuum seal was broken by loosening the stainless steel fitting at the effluent port on the tubing spool. The purgeable organics bottle was then unscrewed from its stainless steel cap, spiked with 1 ml of organic-free HCl (1 + 1) as a preservative (Longbottom and Lichtenberg, 1982), and sealed without a headspace using a PTFE-lined-septum-fitted cap. Extractable organics samples were obtained by unscrewing the 1-l bottle from its stainless-steel cap and sealing it with a minimum headspace using a PTFE lined-septum-fitted cap. Both purgeable and extractable organics samples were packed in ice as soon as possible for transport back to the laboratory. Replicate samples were obtained by placing clean bottles into the stainless steel caps, re-connecting the sample line to the tube spool and repeating the above procedure. Samples were obtained from slowly-recharging points by pumping a smaller volume of water through the system before samples were taken, or by returning within 24 hours to complete the operation.

(2) Triple-Tube Procedure

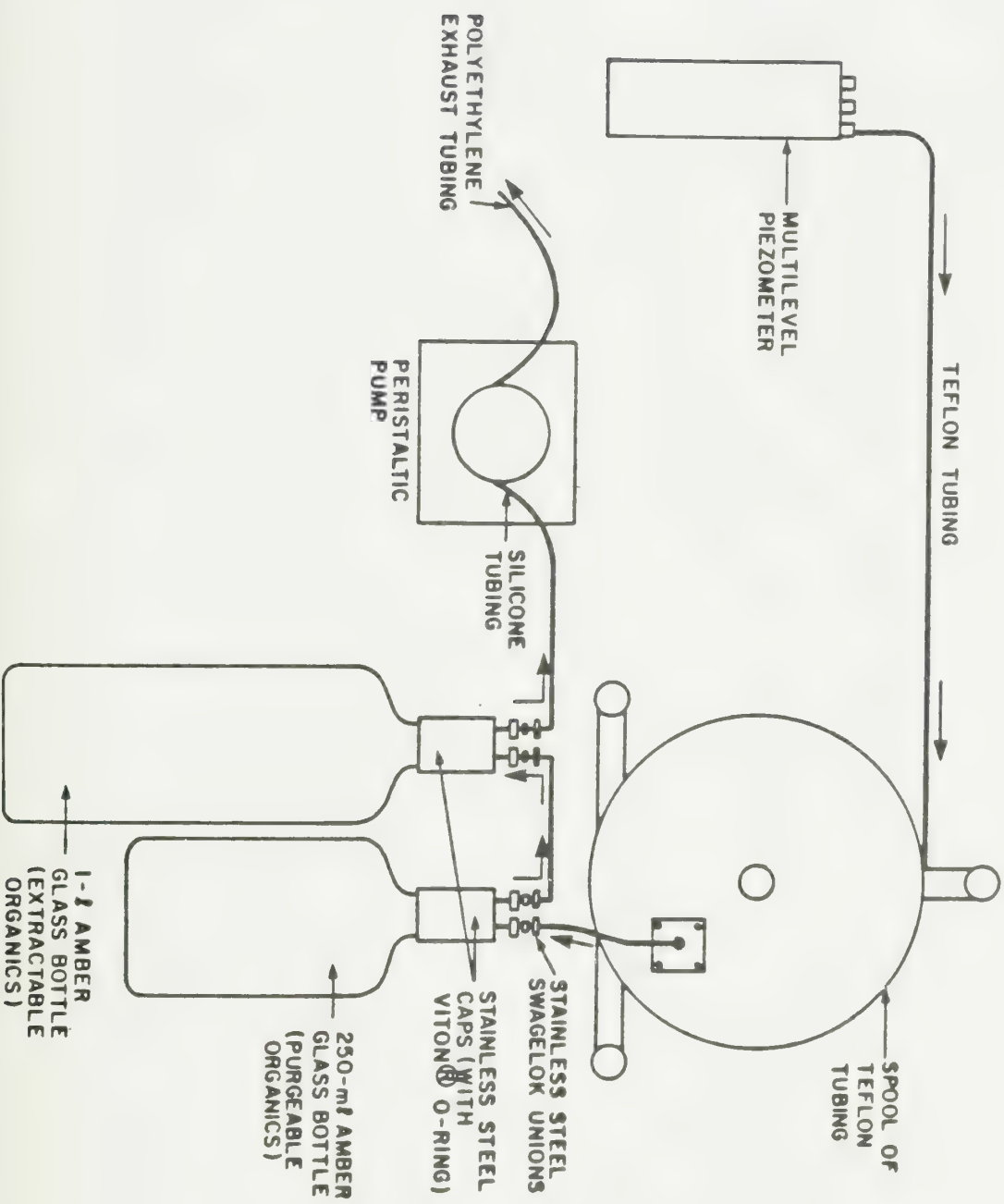


Figure A-2 Groundwater sampling using a multistage pump

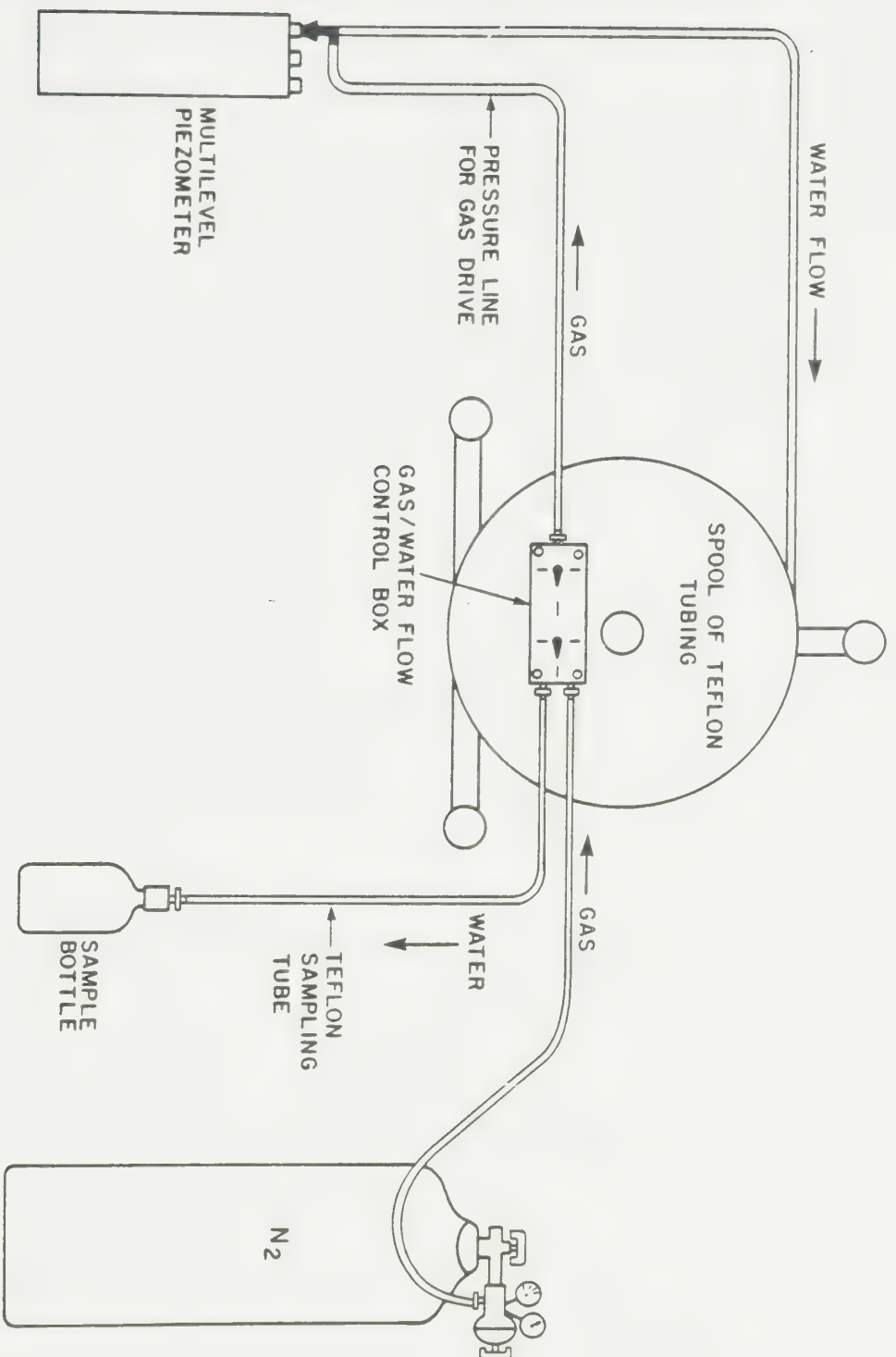


Figure A-3. Groundwater sampling using a triple-tube sampler (Robin et al., 1982).

Samples were taken individually at the sample outlet of the pump, using the appropriate stainless-steel cap for each of the two types of samples. When the recharge rate was sufficiently high at an individual piezometer, the first two triple-tube volumes were discarded, and sampling commenced on the third, after taking the initial TOC/Cl sample. If the recharge rate was too slow to refill the piezometer, within approximately thirty minutes, the initial effluent was saved as an extractable organics (or, if preferred, a major ions/nitrogen species) sample. In these instances, purgeable organics samples were taken from the initial effluent on the following day. A sample for purgeable or extractable organics was taken by unscrewing the filled bottle from its stainless steel cap preserving, sealing and transporting it in the same manner as that used for the Peristaltic Pump Procedure for organics (described above).

a. Field Measurement of Selected Chemical Parameters

If samples for major ions/nitrogen species/bulk parameters or heavy metals were to be taken, the groundwater temperature, pH and electrical conductance were measured in the field prior to obtaining these samples.

(1) Peristaltic Pump Procedure

At piezometers where the recharge rate was rapid enough to provide a steady stream of water, a field thermometer, pH probe, (Can Lab, H5503-30) and three pH buffer solutions (pH

- 4.00, 7.00 and 10.00) were brought to thermal equilibrium with the groundwater in a plexiglass flow-through cell. The effluent stream from the cell discharged into a plastic beaker containing an electrical conductance probe (Y.S.I.-) which was also allowed to equilibrate thermally with the water. When the thermometer reading stabilized, the pH meter was calibrated with the buffer solutions. Measurements of temperature, pH and electrical conductance were then recorded once a stable value for each was obtained.

At sampling points where recharge was too slow to provide a steady stream of water, a 20-ml glass vial and a small plastic beaker were filled with the discharged groundwater and the water temperature measured immediately. The groundwater, thermometer, pH probe, buffer solutions and electrical conductance probe were then allowed to reach air temperature. After calibration of the pH meter, electrical conductance and pH were measured and recorded.

During the field season, the electrical conductance meter and probe were calibrated periodically with a standard NaCl solution, using the technique outlined by Wood, (1981). In all cases, the cell constant was found to be 1.1 ± 0.1 . Consequently, electrical conductance values measured in the field were not corrected for variations in meter response.

(2) Triple-Tube Procedure

Because the triple-tube pump usually provides a groundwater effluent stream for a relatively short period of time, field measurements of water temperature, pH and electrical conductance could not be made under conditions of continuous flow. As a result, temperature was measured immediately, on the second triple-tube volume, while pH and electrical conductance measurements were made using the air-equilibration technique described in the previous section.

f. Major Ions, Nitrogen Species, Bulk Parameters and Heavy Metals

Water samples for the analysis of major ions, nitrogen species, bulk parameters and heavy metals were filtered in the field in order to eliminate chemical interferences introduced by the presence of suspended solids. The field filtration apparatus consisted of a glass fibre pre-filter and a membrane filter (0.45 μ m), both held in a plexiglass tripod filter holder (Geotech Environmental Equipment, Inc.; Denver, CO). Originally, a membrane filter made of PTFE was used. During the sampling program, however, an experiment was carried out in which one set of samples of distilled water were drawn through the filtration apparatus using PTFE membrane filters, while another set were filtered using cellulose acetate membranes. Chemical analysis of these samples (see Table 3) demonstrated that the filtration material (PTFE, cellulose acetate, glass fibre or plexiglass) did not contribute significant quantities of

major ions, nitrogen species or heavy metals, relative to a distilled water blank. Consequently, cellulose acetate filters were substituted for the more expensive PTFE membranes for the remainder of the investigation.

Samples for major ions, bulk parameters and nitrogen species were taken in a 1-litre glass bottle prepared for this purpose and supplied by the Ontario Ministry of the Environment (MOE). The bottles were filled with filtered sample, sealed with a minimum head space and packed in ice for transport to the MOE laboratory in Rexdale, Ontario. Filtered water samples for heavy metals analysis were taken initially in 500-ml polyethylene bottles (also supplied by the MOE), acidified with 1 ml of 10% nitric acid sealed with a minimum head space and transported, unrefrigerated, to the MOE laboratory. For purposes of convenience, polystyrene bottles were substituted for the polyethylene ones by the MOE during the course of the sampling program. Initially as well, a separate, unacidified sample was taken in another 500-ml plastic bottle for boron and arsenic analysis, according to MOE guidelines (Ontario MOE, 1979). Following revised MOE procedures, (M. Rawlings, personal communication), this was found to be unnecessary, so that only a single acidified sample was submitted to the MOE for all metals analyses during the latter half of the program.

Between samples, the filters were discarded and the filtration apparatus was disassembled and rinsed with

deionized water. Dilute (10%) nitric acid was used to rinse the apparatus after particularly turbid samples, followed by a thorough rinse with deionized water. In these instances, the metals sample was taken before the major ions/nitrogen species/bulk parameters sample at the next piezometer, in order to minimize contamination of the latter sample by residual nitric acid from the washing procedure. Fresh filters and pre-filters were used for all samples.

(1) Peristaltic Pump Procedures

The use of a variable-speed peristaltic pump at its minimum pumping rate made it possible to filter the groundwater as it was removed from the piezometer and to fill the sample bottles directly. The major ions/nitrogen species/bulk parameters sample was taken first, the metals sample second.

(2) Triple-Tube Procedure

The high rate of sample discharge from the triple-tube apparatus could not be accommodated by the filtration apparatus. As a result, the discharge from the triple-tube was directed into an acid-washed, 1-l plastic bottle which was kept sealed when not receiving sample. When a sufficient volume was obtained, this water was pumped through the filtration apparatus into the appropriate containers using the peristaltic pump. The samples were then preserved, sealed and transported to the MOE laboratory as described above.

2. Dissolved Oxygen

Water samples for dissolved oxygen analysis were taken in triplicate in plastic, 50-ml, wax-coated syringes. At the commencement of the program, the analytical results from quadruplicate samples using plastic syringes were compared with those from gas-tight glass syringes at two sampling points (UW6-2 and UW9-2). No significant differences were observed. Because they are less fragile and costly than the glass syringes, the plastic syringes were therefore used for dissolved oxygen samples throughout the study.

Prior to sampling, each syringe was connected by silicone tubing to a tank of organic-free nitrogen, flushed two to three times to displace any residual oxygen, and sealed with a needle imbedded in a rubber stopper. When the peristaltic pump was being used, the pumping rate was reduced to a minimum before taking the sample. Where the triple-tube pump was used, the nitrogen pressure was reduced immediately before the discharge step, then increased slowly to provide a minimum rate of sample delivery. For both methods, the remainder of the procedure was identical, viz:

1. Remove stoppered needle from syringe.
2. Flush syringe twice with approximately 40 ml of groundwater
3. Fill syringe a third time with approximately 50 ml of water

4. Holding syringe with the needle end up, tap sides and depress plunger to obtain 40 ml of bubble-free sample. Maintain positive pressure on plunger to avoid entry of atmospheric oxygen.
5. Add 0.4 ml of manganous sulfate reagent by syringe into the convex meniscus exposed at tip of sample syringe.

NOTE: The remainder of this procedure was carried out away from direct sunlight and wearing rubber gloves.

6. Add 0.4 ml of alkaline iodide/arsite reagent, also by syringe.
7. Replace stoppered needle onto sample syringe.
8. Invert fifteen times to mix contents.
9. Allow iloc to settle until it fills less than two thirds of the sample volume.
10. Repeat steps eight and nine.
11. Remove stoppered needle and add 0.4 ml of sulfuric acid.

NOTE: In the middle of the sampling program, phosphoric acid was substituted for the sulfuric acid, both because it is less corrosive, and for better pH control (Richards, 1969).

12. Replace needle and mix contents by inverting syringe fifteen times.

13. Store sample on ice for transport to the University of Waterloo laboratory.

The chemical analysis consisted of a Winkler titration (Standard Methods, 1981), incorporating modifications introduced by Carpenter (1965) and Richards (1960).

h. Dissolved Methane

Samples were obtained in duplicate or (where recharge rates permitted) triplicate using gas-tight glass syringes. The syringes were prepared by flushing with nitrogen gas. Water was pumped into the syringes in a manner identical to that used for the dissolved oxygen procedure. The syringe was filled with samples and emptied twice. After the syringe was filled a third time, water and bubbles were expelled until 25 ml of bubble-free water remained. The syringe was then capped with a stoppered needle and stored on ice for transport back to the laboratory.

i. Aqueous Isotopes

Groundwater samples for the analysis of ^{18}O , deuterium (^2H) and tritium (^3H) were taken in 40-ml polyethylene bottles directly from the peristaltic pump or triple-tube outlet. Samples taken for enriched tritium analysis were obtained in 1-litre plastic bottles. All samples were sealed tightly with minimal head space and stored at room temperature until analysed.

APPENDIX B. Methods for the chemical analysis of groundwater samples.

| Chemical Parameter | Analytical Laboratory | Summary of Analytical Procedure |
|-------------------------------|--|---|
| Total Organic Carbon | UW (i.e. University of Waterloo) | Aqueous carbon analyzer employing UV and chemical oxidation (Dohrmann Carbon Analyzer, DC -80) |
| Chloride | UW | Anion chromatography using a Dionex resin column |
| Purgeable Organic Compounds | UW | <ol style="list-style-type: none"> 1. Transfer sample using PTFE (i.e. Teflon R tubing and nitrogen gas pressure into sparging chamber of a UNACON Model 401 sample concentrator (Envirochem, Inc.; Kemblesville, PA) 2. Analyze via the "purge-and-trap" technique using the UNACON concentrator interfaced with an HP 5840A gas chromatograph and a 30-m DP-5 fused silica column 3. Identify peaks using external standards; quantitate internal standard (para-fluoro-toluene) (Reference: United States Environmental Protection Agency Method 602 for Purgeable Aromatic Compounds [Longbottom and Lichtenberg, 1982].) |
| Purgeable Organic Compounds | MTL (i.e., Mann Testing Laboratories) | Analyze in a manner identical to method employed by UW (see above), employing an Envirocon Model 780B concentrator equipped with either a Superox (similar to Carbowax) or a DB-5 fused silica column and interfaced with a Finnigan 3200 Mass Spectrometer. Internal standard: deuterated chlorobenzene. |
| Extractable Organic Compounds | UW | <ol style="list-style-type: none"> 1. Spike sample with internal standard (containing the following deuterated compounds: anthracene, naphthalene, 2-nitrophenol, phenol) 2. Extract with methylene chloride at pH 11 (Base/Neutral fraction) and pH 2 (Acid fraction). 3. Dry extracts by passing them through a bed of anhydrous sodium sulfate. 4. Concentrate extracts to 1 ml on a Kuderna-Danish concentrator 5. Analyse by gas chromatography using external standards and a 30-m Carbowax fused silica column. (Reference: United States Environmental Protection Agency Method 625 for Base/Neutral and Acid Compounds [Longbottom and Lichtenberg, 1982]). |

| | | |
|---|--|---|
| Extractable Organic Compounds (Base/Neutral and Acid Fractions) | MTL (using extracts obtained from UW) | Base/Neutral Fraction: Analyze by chromatography/mass spectrometry. Acid Fraction: Analyze by gas chromatography/mass spectrometry following derivatization (methylation) with diazomethane |
| Polychlorinated Biphenyls (PCBs) and Organochlorine Pesticides | MOE (i.e., Ontario Ministry of the Environment) | <ol style="list-style-type: none"> 1. Extract sample with organic solvent 2. Dry extract and concentrate to 1 ml 3. Clean up and separate PCB and pesticide fractions by passage through a Florisil column 4. Analyse by electron capture gas chromatography (References: Ministry of the Environment [1981]; Longbottom and Lichtenberg [1982, Method 608]). |
| Field pH, Temperature and Electrical Conductance | - | See section 3, Appendix |
| pH (laboratory) | MOE | Measured with a pH electrode on a stirred aliquot of sample at room temperature. (Reference for all analyses performed by the MOE, unless otherwise indicated: Ministry of the Environment [1981]). |
| Electrical Conductance (laboratory) | MOE | Measured with a conductivity meter at 25°C |
| Hardness | MOE | Calculated as sum of calcium and magnesium concentrations (C. Lee, MOE, personal communication). |
| Calcium | MOE | Atomic absorption spectroscopy |
| Magnesium | MOE | Atomic absorption spectroscopy |
| Sodium | MOE | Atomic absorption spectroscopy |
| Potassium | MOE | Atomic absorption spectroscopy |
| Chloride | MOE | Titration with silver nitrate |
| Alkalinity | MOE | Titration with sulfuric acid |
| Sulfate | MOE | Colorimetric analysis using barium chloride and methyl thymol blue with an Auto Analyser system. |
| Fluoride | MOE | <ol style="list-style-type: none"> 1. Distill sample from sulphuric acid. 2. Analyse colorimetrically with Auto Analyser after reaction with lanthanum nitrate and Alizarin Blue. |
| Nitrate | MOE | <ol style="list-style-type: none"> 1. Filter sample 2. Reduce nitrate to nitrite using hydrazine sulphate 3. Diazotise nitrite with sulphanilamide and N (1-naphthyl) ethylenediamine hydrochloride 4. Analyse using an Auto Analyser system. 5. Subtract concentration of nitrite measured by above procedure, without the hydrazine sulphate reduction (step 2). |

| | | |
|--|-----|---|
| Nitrite | MOE | Procedure identical to that for nitrate, without the hydrazine sulfate reduction (step 2) |
| Kjeldahl Nitrogen | MOE | <ol style="list-style-type: none"> 1. Digest sample with sulphuric acid, mercuric oxide and potassium sulphate. 2. Analyze colorimetrically by the alkaline phenol-hypochlorite method adapted to an Auto Analyser system. |
| Ammonia | MOE | Filter sample and analyze colorimetrically by the alkaline phenol-hypochlorite method adapted to an Auto Analyser system. |
| Dissolved Organic Carbon | MOE | <ol style="list-style-type: none"> 1. Remove inorganic carbon and oxidize analyte in an ultraviolet digester using an acid-persulphate medium. 2. Pass evolved carbon dioxide through a gas permeable membrane into a weakly buffered, alkaline phenolphthalein solution. 3. Measure decrease in absorbance of phenolphthalein solution resulting from the presence of carbon dioxide. |
| Iron (total) | MOE | Acid digestion followed by atomic absorption spectroscopy. |
| Manganese | MOE | Acid digestion followed by atomic absorption spectroscopy. |
| Boron Cadmium Chromium Copper Nickel Lead Zinc | MOE | <ol style="list-style-type: none"> 1. Twenty-fold preconcentration by boiling in presence of concentrated nitric acid. 2. Analyze by Inductively coupled plasma atomic emission spectroscopy (B. Loescher, MOE, personal communication). |
| Arsenic | MOE | <ol style="list-style-type: none"> 1. Digestion in nitric acid/sulfuric acid solution overnight at 130°C. 2. Analyze by automated hydride generation atomic absorption spectroscopy. (B. Loescher, MOE, personal comm.). |
| Selenium | MOE | <ol style="list-style-type: none"> 1. Digestion in nitric acid/sulfuric acid solution overnight at 130°C. 2. Analyze by automated hydride generation atomic absorption spectroscopy. (B. Loescher, MOE, personal comm.). |
| Dissolved Oxygen | UW | Winkler titration, modified for use with a 50-ml syringe (see section g of Appendix for details of method). |
| Dissolved Methane | UW | Partition methane into an inert gas (helium) and analyze with a gas partitioner (Reference: Barker, 1979). |
| Aqueous Isotopes Oxygen-18 Deuterium Tritium (direct) Tritium (enriched) | UW | Mass Spectrometry (Reference: Hoefs, 1973). |

APPENDIX C.

Results of Routine Chemical Analyses - Inorganic and Volatile Organic Parameters, Environmental Isotopes and Dissolved Gases

Symbols Used

- ° - Approximate Value;
Analytical Interference
- ? - Unreliable or Questionable Analysis
- NA - Not Analysed
- < - Less Than Detection Limit
- - Not Detected; Less Than 0.05 mg/l usually

SAMPLING POINT:

INORGANIC ELANKS

| | | |
|----------------|------------------|-------------------|
| Sampling date: | 04/10/83 | 31/10/83 |
| FIELD DATA | (After UW9-2) | (After UW22-1) |
| temp (C) | NA | NA |
| En (mv) | NA | NA |
| pH | NA | NA |
| cond. (uS) | NA | NA |
| LAB DATA | | |

| | | |
|------------------|--------|--------|
| pH | 6.75 | 6.93 |
| cond. (uS) | 6.60 | 4.30 |
| hardness (CaCO3) | <0.5 | 2.1 |
| Ca (mg/l) | <0.5 | 0.5 |
| Mg | <0.10 | 0.20 |
| Na | <0.1 | <0.1 |
| K | <0.05 | <0.05 |
| Cl | <0.6 | <0.2 |
| Alk., as CaCO3 | 2.8 | 4.4 |
| SO4 | <0.5 | <0.5 |
| F | <0.01 | 0.01 |
| NO3, as N | <0.1 | <0.1 |
| NO2, as N | <0.01 | <0.01 |
| Kjeld. N, as N | 0.2 | 0.6 |
| NH3, as N | <0.1 | 0.2 |
| TCC | NA | NA |
| BCC | NA | 0.3 |
| E | 0.18 | 0.26 |
| Fe (tot) | 0.027 | 0.007 |
| Mn | <0.005 | <0.002 |
| As | <0.001 | <0.001 |
| Cd | <0.005 | <0.005 |
| Cr | <0.025 | <0.005 |
| Cu | 0.008 | <0.005 |
| Ni | 0.006 | <0.006 |
| Pb | <0.030 | <0.030 |
| Se | <0.001 | <0.001 |
| Zn | 0.033 | 0.011 |

SAMPLING POINT:

D# 1-2

Sampling date: 30/09/82 17/11/82 13/05/83 12/09/83
 FIELD DATA

| | 30/09/82 | 17/11/82 | 13/05/83 | 12/09/83 |
|------------|----------|----------|----------|----------|
| temp (C) | 9.22 | NA | 11.8 | 229.0 |
| Eh (mV) | -79 | NA | NA | NA |
| pH | 6.62 | NA | 6.25 | 6.65 |
| cond. (uS) | NA | NA | 6300 | 5500 |

LAB DATA

| | 30/09/82 | 17/11/82 | 13/05/83 | 12/09/83 |
|------------------|----------|----------|----------|----------|
| pH | 7.37 | 7.30 | 6.90 | 6.70 |
| cond. (uS) | 8980 | 9320 | 9050 | 9650 |
| hardness (CaCO3) | 1389 | 2696 | 2782 | 3390 |
| Ca (mg/l) | 412.0 | 810.0 | 830.0 | 1000 |
| Mg | 87.0 | 164.0 | 173.0 | 217.5 |
| Na | 1000 | 990.0 | 980.0 | 1050 |
| K | 152.0 | 162.0 | 128.0 | 156.5 |
| Cl | 1658 | 1533 | 1572 | 1900 |
| Alk., as CaCO3 | 1348 | 1373 | 734.2 | 1405 |
| SO4 | NA | 1775 | 1900 | 1875 |
| F | 0.63 | 0.70 | 0.59 | 0.62 |
| NO3, as N | 0.2 | <0.1 | <0.1 | 0.2 |
| NO2, as N | 0.02 | <0.01 | <0.01 | 0.04 |
| Kjeld. N, as N | 142.0 | 289.5 | 141.0 | 695.0 |
| NH3, as N | 133.0 | 146.0 | 129.0 | 142.0 |
| TOC | 92 | 100 | 90.7 | 104 |
| DOC | NA | NA | 2110.0 | 200.0 |
| B | 0.60 | 0.93 | 5.60 | 6.20 |
| Fe (tot) | 0.260 | 0.07 | 0.036 | 0.35 |
| Mn | 0.049 | 0.014 | 0.034 | 0.075 |
| As | <0.030 | <0.030 | 0.001 | 0.002 |
| Cd | 0.0008 | <0.002 | 0.015 | 0.0009 |
| Cr | 0.019 | 0.020 | <0.050 | 0.009 |
| Cu | 0.045 | 0.070 | 0.074 | 0.017 |
| Ni | 0.023 | 0.028 | 0.040 | 0.018 |
| Pb | 0.053 | 0.050 | 0.096 | 0.005 |
| Se | <0.030 | <0.030 | <0.001 | 0.001 |
| Zn | 0.013 | 0.010 | <0.010 | 0.016 |

DISSOLVED GASES

Sampling Date: 30/09/82 17/11/82 05/07/83 12/09/83

| | 30/09/82 | 17/11/82 | 05/07/83 | 12/09/83 |
|-----|----------|----------|----------|----------|
| CH4 | 400 | 1200 | 370 | 460 |
| O2 | NA | NA | ND | ND |

PURGEABLE ORGANICS

Sampling Date: 12/09/83 12/09/83

| | (A) | (E) |
|---------------|-------|-------|
| benzene | 1.393 | 2.157 |
| toluene | 0.325 | 0.337 |
| chlorobenzene | 0.017 | 0.011 |
| ethylbenzene | 0.008 | 0.916 |
| p-xylene | 0.920 | 1.205 |
| o-xylene | 0.460 | 0.592 |
| cumene | 0.085 | 0.100 |
| 1,2,4-TMB | 0.021 | 0.427 |
| naphthalene | 0.022 | 0.070 |

AQUEOUS ISOTOPES

Sampling Date: 30/09/82 17/11/82 13/05/83

| | 30/09/82 | 17/11/82 | 13/05/83 |
|----------------|----------|----------|----------|
| Delta C-18 | -10.0 | -10.1 | -9.9 |
| Delta H-2 | NA | NA | -6.1 |
| Tritium (T.U.) | 120 | 109 | 88 |

SAMPLING POINT:

UW 1-3

Sampling date: 13/09/83 14/09/83
FIELD DATA

temp (C) NA 16.0
Eh (mV) NA NA
pH NA 6.45
cond. (uS) NA 1900

LAB DATA

pH 6.48
cond. (uS) 72000
hardness (CaCO3) 25100
Ca (mg/l) 6440
Mg 2200
Na 9400
K 164.0
Cl 31000
Alk., as CaCO3 225.0
SO4 1213
F NA
NO3, as N 0.5
NO2, as N 0.03
Kjeld. N, as N 32.0
NH3, as N 27.0
TOC 49.5
DOC 210.0
B 4.40
Fe (tot) 9.80
Mn 1.080
As 0.003
Cd 0.073
Cr 0.064
Cu 0.350
Ni 0.019
Pb 0.040
Se <0.001
Zn 0.190

DISSOLVED GASES

Sampling Date: 14/09/83

CH4 190
CO2 ND

PURGEABLE ORGANICS

Sampling Date: 12/09/83

benzene 1.469
toluene 2.513
chlorobenzene --
ethylbenzene 0.277
p-xylene 0.409
o-xylene 0.434
cumene --
1,2,4-TMB 0.695
naphthalene 0.659

SAMPLING POINT:

U#1-4

Sampling date:
FIELD DATA

30/09/82 02/11/82 13/05/83 22/09/83

| | | | | |
|------------|------|----|-------|-------|
| temp (C) | NA | NA | 11.0 | 14.5 |
| En (mV) | -145 | NA | NA | 7.25 |
| pH | 6.64 | NA | 6.45 | NA |
| cond. (uS) | NA | NA | 32000 | 15300 |

LAB DATA

| | | | | |
|------------------|--------|--------|-------|--------|
| pH | 7.16 | 7.71 | 7.50 | 7.62 |
| cond. (uS) | 21300 | 21940 | 3970 | 30600 |
| hardness (CaCO3) | 6598 | 5138 | 12552 | NA |
| Ca (mg/l) | 1845 | 1390 | 3300 | NA |
| Mg | 485.0 | 406.0 | 1050 | NA |
| Na | 2700 | 2660 | 5500 | 3700 |
| K | 56.0 | 60.0 | 87.50 | 71.0 |
| Cl | 7910 | 6204 | 14530 | 11000 |
| Alk., as CaCO3 | 299.4 | 114.8 | 123.6 | 284.0 |
| SO4 | NA | 1500 | 900.0 | 1500 |
| F | 0.73 | 0.55 | 0.70 | 0.55 |
| NO3, as N | 0.2 | <0.1 | <0.1 | 0.2 |
| NO2, as N | <0.01 | 0.03 | 0.02 | 0.03 |
| Kjeld. N, as N | 04.5 | NA | NA | 10.2 |
| NH3, as N | 06.8 | 7.0 | 11.4 | 9.3 |
| TOC | 22 | 2.7 | 20.9 | 9.4 |
| DOC | NA | NA | NA | 2060 |
| B | 3.50 | 3.60 | 4.40 | 1.80 |
| Fe (tot) | 0.068 | 0.12 | 0.082 | 0.089 |
| Mn | 0.150 | 0.172 | 1.80 | 0.310 |
| As | 0.050 | 0.040 | 0.062 | 0.077 |
| Cd | 0.006 | <0.002 | 0.016 | <0.005 |
| Cr | 0.022 | 0.020 | 0.072 | 0.038 |
| Cu | 0.076 | 0.110 | 0.280 | 0.20 |
| Ni | 0.005 | 0.006 | 0.032 | 0.011 |
| Pb | 0.110 | 0.050 | 0.090 | <0.030 |
| Se | <0.030 | <0.030 | 0.001 | 0.001 |
| Zn | 0.034 | 0.017 | 0.026 | 0.120 |

DISSOLVED GASES

Sampling Date:

30/09/82 05/11/82 07/07/83 22/09/83

| | | | | |
|-----|-----|-----|----|-----|
| CH4 | 370 | 310 | ND | 160 |
| O2 | NA | NA | ND | ND |

PURGEABLE ORGANICS

Sampling Date:

19/07/83 22/09/83

| | | |
|---------------|-------|-------|
| benzene | 0.063 | 0.381 |
| toluene | 1.831 | 3.395 |
| chlorobenzene | -- | -- |
| ethylbenzene | 1.332 | 0.303 |
| p-xylene | 0.916 | 0.508 |
| o-xylene | 0.322 | 0.225 |
| cumene | -- | -- |
| 1,2,4-TMB | 0.111 | 0.262 |
| naphthalene | 0.127 | 0.830 |

AQUEOUS ISOTOPES

Sampling Date:

30/09/82 02/11/82 13/05/83 12/10/83

| | | | | |
|----------------|------|------|------|-------|
| Delta O-18 | -9.9 | -9.8 | -9.4 | |
| Delta H-2 | NA | NA | -71 | |
| Tritium (T.U.) | ND | 21 | ND | 3 (1) |

SAMPLING POINT:

UW 1-5

Sampling date:

FIELD DATA

temp (C)
Eh (mV)
pH
Cond. (uS)

LAB DATA

pH
Cond. (uS)
hardness (CaCO3)
Ca (mg/l)
Mg
Na
K
Cl
Alk., as CaCO3
SO4
F
NO3, as N
NO2, as N
Kjeld. N, as N
NH3, as N
TOC
DOC
E
Fe (tot)
Mn
As
Cd
Cr
Cu
Ni
Pb
Se
Zn

DISSOLVED GASES

Sampling Date:

CH4
O2

PURGEABLE ORGANICS

Sampling Date:

benzene
toluene
chlorobenzene
ethylbenzene
p-xylene
o-xylene
cumene
1,2,4-TMB
naphthalene

AQUEOUS ISOTOPES

Sampling Date: 17/08/83

Delta C-18 -7.9
Delta H-2 -66
Tritium (T.U.) 40

SAMPLING POINT:

UN 1-6

Sampling date:

FIELD DATA

temp (C)
Eh (mV)
pH
cond. (uS)

LAB DATA

pH
cond. (uS)
hardness (CaCO₃)
Ca (mg/l)
Mg
Na
K
Cl
Alk., as CaCO₃
SO₄
F
NO₃, as N
NO₂, as N
Kjeld. N, as N
NH₃, as N
TOC
DOC
E
Fe (tot)
Mn
As
Cd
Cr
Cu
Ni
Pb
Se
Zn

DISSOLVED GASES

Sampling Date:

CH₄
O₂

PURGEABLE ORGANICS

Sampling Date:

benzene
toluene
chlorobenzene
ethylbenzene
p-xylene
o-xylene
cumene
1,2,4-TMB
naphthalene

AQUEOUS ISOTOPES

Sampling Date: 17/08/83

Delta O-18 -8.5
Delta H-2 -71
Tritium (T.U.) ND

SAMPLING POINT:

UW 2-1

Sampling date: 05/10/82 17/11/82
 FIELD DATA

temp (C) 18.0
 Eh (mV) +33
 pH 6.73
 Cond. (uS) NA

LAB DATA

| | | |
|------------------|--------|--------|
| pH | 7.32 | 7.19 |
| cond. (uS) | 4327 | 4168 |
| hardness (CaCO3) | 1334 | 1185 |
| Ca (mg/l) | 363.0 | 330.0 |
| Mg | 104.0 | 88.0 |
| Na | 340.0 | 255.0 |
| K | 24.0 | 17.0 |
| Cl | 471.6 | 576.4 |
| Alk., as CaCO3 | 543.4 | 523.6 |
| SO4 | NA | 1030 |
| F | 0.44 | 0.45 |
| NO3, as N | <0.1 | <0.1 |
| NO2, as N | <0.01 | <0.03 |
| Kjeld. N, as N | 19.0 | 212.4 |
| NH3, as N | 18.0 | 18.1 |
| TOC | 38 | 9.2 |
| DOC | NA | NA |
| E | 1.80 | 2.80 |
| Fe (tot) | 0.910 | 0.05 |
| Mn | 1.20 | 1.830 |
| As | <0.030 | <0.030 |
| Cd | 0.001 | <0.002 |
| Cr | 0.017 | 0.016 |
| Cu | 0.042 | 0.049 |
| Ni | 0.010 | 0.011 |
| Pb | 0.027 | 0.036 |
| Se | <0.030 | <0.030 |
| Zn | 0.120 | 0.008 |

DISSOLVED GASES

Sampling Date: 05/10/82 17/11/82

| | | |
|-----|-----|-----|
| CH4 | 240 | 440 |
| O2 | NA | NA |

PURGEABLE ORGANICS

Sampling Date:

benzene
 toluene
 chlorobenzene
 ethylbenzene
 p-xylene
 o-xylene
 cumene
 1,2,4-TMB
 naphthalene

AQUEOUS ISOTOPES

Sampling Date: 05/10/82 17/11/82

| | | |
|----------------|------|------|
| Delta O-18 | -9.8 | -9.6 |
| Delta H-2 | NA | NA |
| Tritium (T.U.) | 90 | |

SAMPLING POINT:

Uw2-2

| Sampling date: | 13/05/83 | 14/09/83 | 15/09/83 | 15/09/83 |
|----------------|----------|----------|----------|----------|
| FIELD DATA | | | Cell.Ac. | Teflon |
| | | | Filter | Filter |
| temp (C) | 10.5 | 17.0 | NA | NA |
| Eh (mV) | NA | NA | NA | NA |
| pH | 6.65 | 6.70 | NA | NA |
| cond. (uS) | 3950 | NA | NA | NA |

LAE DATA

| | | | | |
|-------------------------------|--------|--------|---------|-------|
| pH | 7.24 | 6.85 | 6.75 | 6.85 |
| cond. (uS) | 5650 | 5800 | 5800 | 5800 |
| hardness (CaCO ₃) | 2227 | 2221 | 2241 | 2296 |
| Ca (mg/l) | 600.0 | 600.0 | 590.0 | 620.0 |
| Mg | 177.5 | 176.0 | 187.0 | 182.0 |
| Na | 522.2 | 615.0 | 525.0 | 515.0 |
| K | 21.25 | 18.0 | 17.25 | 18.0 |
| Cl | 1080 | 949.0 | 862.0 | 888.0 |
| Alk., as CaCO ₃ | NA | 445.0 | 427.8 | 444.6 |
| SO ₄ | 1888 | 1788 | 1800 | 1813 |
| F | 0.75 | 0.70 | 0.73 | 0.72 |
| NO ₃ , as N | 0.2 | <0.1 | <0.1 | <0.1 |
| NO ₂ , as N | 0.02 | <0.01 | <0.01 | <0.01 |
| Kjeld. N, as N | 7.1 | 4.8 | 5.0 | 5.3 |
| NH ₃ , as N | 7.6 | 3.2 | 2.7 | 3.5 |
| TOC | 42.4 | 31.9 | NA | NA |
| DOC | 12.4 | 15.9 | 14.6 | 14.9 |
| E | 2.80 | 2.80 | 2.80 | NA |
| Fe (tot) | 0.068 | 0.07 | <0.03 | 0.08 |
| Mn | 0.110 | 0.110 | 0.110 | 0.105 |
| As | <0.001 | <0.001 | <0.001 | |
| Cd | <0.010 | 0.0005 | <0.0002 | |
| Cr | <0.050 | 0.005 | 0.004 | |
| Cu | 0.060 | 0.012 | 0.015 | |
| Ni | 0.028 | 0.006 | 0.003 | |
| Pb | <0.060 | 0.004 | <0.003 | |
| Se | 0.002 | <0.001 | <0.001 | |
| Zn | <0.010 | 0.009 | 0.008 | |

DISSOLVED GASES

| Sampling Date: | 05/07/83 | 15/09/83 |
|-----------------|----------|----------|
| CH ₄ | 130 | 180 |
| O ₂ | ND | ND |

PURGEABLE ORGANICS

| Sampling Date: | 14/09/83 | 14/09/83 |
|----------------|----------|----------|
| benzene | 0.055 | 0.122 |
| toluene | 0.022 | 0.026 |
| chlorobenzene | -- | -- |
| ethylbenzene | 0.002 | 0.010 |
| p-xylene | 0.030 | 0.032 |
| o-xylene | 0.015 | 0.009 |
| cumene | -- | -- |
| 1,2,4-TMB | 0.036 | 0.017 |
| Napthalene | 0.071 | -- |

AQUEOUS ISOTOPES

| Sampling Date: | 13/05/83 |
|----------------|----------|
| Delta O-18 | -9.4 |
| Delta H-2 | -60 |
| Tritium (T.U.) | 102 |

SAMPLING POINT:

U-2-3

Sampling date: 14/09/83

FIELD DATA

| | |
|------------|------|
| temp (C) | 27.0 |
| En (mV) | NA |
| pH | 6.45 |
| cond. (uS) | NA |

LAB DATA

| | |
|------------------|--------|
| pH | 6.74 |
| cond. (uS) | 7000 |
| hardness (CaCO3) | 2640 |
| Ca (mg/l) | 750.0 |
| Mg | 187.5 |
| Na | 740.0 |
| K | 51.50 |
| Cl | 1299 |
| Alk., as CaCO3 | 538.6 |
| SO4 | 1725 |
| F | 0.91 |
| NO3, as N | <0.1 |
| NO2, as N | <0.01 |
| Kjeld. N, as N | 19.3 |
| NH3, as N | 17.0 |
| TOC | 35.3 |
| DOC | 32.0 |
| B | 3.30 |
| Fe (tot) | 0.15 |
| Mn | 0.110 |
| As | 0.001 |
| Cd | 0.0004 |
| Cr | 0.008 |
| Cu | 0.018 |
| Ni | 0.005 |
| Pb | <0.003 |
| Se | <0.001 |
| Zn | 0.003 |

DISSOLVED GASES

Sampling Date: 15/09/83

| | |
|-----|-----|
| CH4 | 150 |
| C2 | ND |

PURGEABLE ORGANICS

| Sampling Date: | 14/09/83 | 14/09/83 |
|----------------|----------|----------|
| | (A) | (E) |
| benzene | 0.739 | 0.362 |
| toluene | 0.574 | 0.373 |
| chlorobenzene | -- | -- |
| ethylbenzene | 0.033 | 0.016 |
| p-xylene | 0.094 | 0.074 |
| o-xylene | 0.045 | 0.095 |
| cumene | -- | -- |
| 1,2,4-IMB | 0.052 | 0.042 |
| naphthalene | 0.005 | 0.099 |

AQUEOUS ISOTOPES

Sampling Date: 14/09/83

| | |
|----------------|------|
| Delta O-18 | -9.5 |
| Delta H-2 | -67 |
| Tritium (T.U.) | 60 |

SAMPLING POINT:

UW2-4

Sampling date: 18/08/83 24/08/83 20/09/83
 FIELD DATA

| | 18/08/83 | 24/08/83 | 20/09/83 |
|------------|----------|----------|----------|
| temp (C) | NA | NA | 228.0 |
| Eh (mV) | NA | NA | NA |
| pH | NA | NA | 6.45 |
| cond. (uS) | NA | NA | NA |

LAB DATA

| | 18/08/83 | 24/08/83 | 20/09/83 |
|------------------|----------|----------|----------|
| pH | 6.70 | NA | 6.66 |
| cond. (uS) | 124000 | NA | 131000 |
| hardness (CaCO3) | 51474 | NA | 58700 |
| Ca (mg/l) | 12800 | NA | 15200 |
| Mg | 4750 | NA | 5050 |
| Na | 19600 | NA | 20800 |
| K | 297.0 | NA | 324.0 |
| Cl | 65360 | NA | 70000 |
| Alk., as HCO3 | 127.8 | NA | 119.4 |
| SO4 | 880.0 | NA | 895.0 |
| F | NA | NA | NA |
| NO3 | <0.1 | NA | <0.1 |
| NO2, as N | 0.02 | NA | 0.03 |
| Kjeld. N, as N | NA | NA | NA |
| NH3, as N | 42.0 | NA | 41.4 |
| TOC | 98.6 | 95.3 | 84.2 |
| DOC | 2200.0 | NA | 930.0 |
| B | 4.70 | NA | |
| Fe (tot) | 0.20 | 0.320 | |
| Mn | 1.150 | 0.920 | |
| As | <0.001 | <0.001 | |
| Cd | NA | <0.002 | |
| Cr | NA | 0.069 | |
| Cu | NA | 0.670 | |
| Ni | NA | 0.007 | |
| Pb | NA | 0.041 | |
| Se | NA | <0.001 | |
| Zn | NA | 0.150 | |

DISSOLVED GASES

Sampling Date: 08/10/82 24/08/83 20/09/83

| | 08/10/82 | 24/08/83 | 20/09/83 |
|-----|----------|----------|----------|
| CH4 | 0.50 | NA | 40 |
| O2 | NA | ND | ND |

PURGEABLE ORGANICS

Sampling Date: 13/09/83 15/09/83

| | 13/09/83 | 15/09/83 |
|---------------|----------|----------|
| benzene | 2.019 | 1.222 |
| toluene | 3.255 | 2.389 |
| chlorobenzene | 0.039 | 0.031 |
| ethylbenzene | 6.263 | 0.204 |
| p-xylene | 0.776 | 0.591 |
| o-xylene | 1.083 | 0.237 |
| cumene | 0.011 | 0.009 |
| 1,2,4-TMB | 0.311 | 0.268 |
| naphthalene | -- | 0.306 |

AQUEOUS ISOTOPES

Sampling Date: 17/08/83

| | 17/08/83 |
|----------------|----------|
| Delta C-18 | -8.2 |
| Delta H-2 | -70 |
| Tritium (T.U.) | 27 |

SAMPLING POINT:

UW2-5

Sampling date:

FIELD DATA

temp (C)
Eh (mV)
pH
cond. (uS)

LAE DATA

pH
cond. (uS)
hardness (CaCO3)
Ca (mg/l)
Mg
Na
K
Cl
Alk., as CaCO3
SO4
F
NO3, as N
NO2, as N
Kjeld. N, as N
NH3, as N
TOC
DOC
E
Fe (tot)
Mn
As
Cd
Cr
Cu
Ni
Pb
Se
Zn

DISSOLVED GASES

Sampling Date:

CH4
O2

PURGEABLE ORGANICS

Sampling Date:

benzene
toluene
chlorobenzene
ethylbenzene
p-xylene
o-xylene
cumene
1,2,4-IMB
naphthalene

AQUEOUS ISOTOPES

Sampling Date: 18/03/83

Delta O-18 -6.7
Delta H-2 -55
Tritium (T.U.) 58

SAMPLING POINT:

UW 3-2

Sampling date: 18/08/83 12/09/83
FIELD DATA

| | | |
|------------|-------|----|
| temp (C) | 232.0 | NA |
| Eh (mV) | NA | NA |
| pH | 7.35 | NA |
| cond. (uS) | 10200 | NA |

LAB DATA

| | | |
|-------------------------------|---------|--------|
| pH | NA | 6.70 |
| cond. (uS) | NA | 64000 |
| hardness (CaCO ₃) | 11510 | 19728 |
| Ca (mg/l) | 3080 | 5500 |
| Mg | 930.0 | 1460 |
| Na | 5050 | 8700 |
| K | 123.0 | 156.0 |
| Cl | 15040 | 27300 |
| Alk., as CaCO ₃ | 398.0 | 298.0 |
| SO ₄ | 1450 | 1325 |
| F | NA | NA |
| NO ₃ , as N | <0.1 | 0.4 |
| NO ₂ , as N | 0.02 | 0.02 |
| Kjeld. N, as N | NA | NA |
| NH ₃ , as N | 53.0 | 28.8 |
| TOC | 23.0 | 100 |
| DOC | ? 160.0 | NA |
| B | NA | 10.0 |
| Fe (tot) | 0.25 | 0.24 |
| Mn | 0.350 | 0.350 |
| As | 0.001 | 0.001 |
| Cd | <0.0002 | 0.005 |
| Cr | 0.007 | 0.040 |
| Cu | 0.064 | 0.30 |
| Ni | <0.001 | 0.013 |
| Pb | <0.003 | <0.030 |
| Se | <0.001 | <0.001 |
| Zn | 0.016 | 0.060 |

DISSOLVED GASES

Sampling Date: 13/09/83

| | |
|-----------------|-----|
| CH ₄ | 480 |
| O ₂ | ND |

PURGEABLE ORGANICS

| Sampling Date: | 13/09/83 | 13/09/83 |
|----------------|----------|----------|
| | (A) | (B) |
| benzene | 0.898 | 1.028 |
| toluene | 0.952 | 1.041 |
| chlorobenzene | -- | -- |
| ethylbenzene | 0.222 | 0.197 |
| p-xylene | 0.573 | 0.547 |
| o-xylene | 0.418 | 0.357 |
| cumene | 0.022 | 0.021 |
| 1,2,4-TMB | 0.306 | 0.267 |
| naphthalene | 0.388 | 1.951 |

AQUEOUS ISOTOPES

Sampling Date: 18/08/83

| | |
|----------------|------|
| Delta O-18 | -9.3 |
| Delta H-2 | -64 |
| Tritium (T.U.) | ND |

SAMPLING POINT:

UW3-3

Sampling date: 06/10/82 13/05/83 14/09/83
 FIELD DATA

| | 06/10/82 | 13/05/83 | 14/09/83 |
|------------|----------|----------|----------|
| temp (C) | 19.0 | 17.0 | |
| Eh (mV) | +16 | NA | |
| pH | 6.26 | 7.35 | |
| cond. (uS) | NA | 6100 | |

LAB DATA

| | 06/10/82 | 13/05/83 | 14/09/83 |
|-------------------------------|----------|----------|----------|
| pH | 7.07 | 7.33 | 6.85 |
| cond. (uS) | 41100 | 10800 | 60000 |
| hardness (CaCO ₃) | 11862 | 2516 | 17903 |
| Ca (mg/l) | 3650 | 695.0 | 4950 |
| Mg | 670.0 | 190.0 | 1350 |
| Na | 6125 | 1450 | 8100 |
| K | 136.0 | 75.50 | 156.0 |
| Cl | 17590 | 2314 | 25000 |
| Alk., as CaCO ₃ | 655.4 | NA | 276.6 |
| SO ₄ | NA | 1600 | 1350 |
| F | NA | 0.64 | NA |
| NO ₃ , as N | 0.1 | 0.7 | 0.3 |
| NO ₂ , as N | 0.02 | 0.02 | 0.03 |
| Kjeld. N, as N | 0.34.0 | 49.0 | NA |
| NH ₃ , as N | 0.35.0 | 45.0 | 32.4 |
| TOC | 65 | 100 | 80.2 |
| DOC | NA | 29.5 | |
| B | 0.52 | 4.0 | |
| Fe (tot) | 0.280 | 0.075 | |
| Mn | 0.20 | 0.580 | |
| As | <0.030 | <0.001 | |
| Cd | 0.0016 | 0.013 | |
| Cr | 0.099 | 0.026 | |
| Cu | 0.180 | 0.082 | |
| Ni | 0.023 | 0.036 | |
| Pb | 0.057 | 0.062 | |
| Se | <0.030 | 0.001 | |
| Zn | 0.640 | <0.010 | |

DISSOLVED GASES

Sampling Date: 06/10/82 05/07/83 21/09/83

| | 06/10/82 | 05/07/83 | 21/09/83 |
|-----------------|----------|----------|----------|
| CH ₄ | 90 | 180 | 180 |
| O ₂ | NA | ND | ND |

PURGEABLE ORGANICS

Sampling Date: 19/07/83 15/09/83 15/09/83 15/09/83
 (A) (b: 20/9) (b: 29/9)

| | 19/07/83 | 15/09/83 (A) | 15/09/83 (b: 20/9) | 15/09/83 (b: 29/9) |
|---------------|----------|--------------|--------------------|--------------------|
| benzene | 0.847 | 0.417 | 0.910 | 0.620 |
| toluene | 2.948 | 2.215 | 2.769 | 0.812 |
| chlorobenzene | -- | -- | -- | -- |
| ethylbenzene | 5.662 | 0.128 | 0.140 | 0.143 |
| p-xylene | 2.318 | 0.339 | 0.377 | 0.424 |
| o-xylene | 1.295 | 0.231 | 0.182 | 0.242 |
| cumene | -- | 0.009 | 0.006 | 0.013 |
| 1,2,4-TMB | 0.136 | 0.173 | 0.160 | 0.186 |
| naphthalene | 0.104 | 0.120 | 0.546 | -- |

AQUEOUS ISOTOPES

Sampling Date: 06/10/82 13/05/83

| | 06/10/82 | 13/05/83 |
|----------------|----------|----------|
| Delta O-18 | -9.8 | -9.1 |
| Delta H-2 | NA | -61 |
| Tritium (T.U.) | 30 | 114 |

SAMPLING POINT:

UW3-4

Sampling date: 06/10/82 17/11/82 13/05/83 13/09/83

FIELD DATA

| | 06/10/82 | 17/11/82 | 13/05/83 | 13/09/83 |
|------------|----------|----------|----------|----------|
| temp (C) | 19.0 | NA | 15.0 | 224.0 |
| En (mV) | +16 | NA | NA | NA |
| pH | 6.48 | NA | 6.15 | 6.50 |
| cond. (uS) | NA | NA | 46000 | NA |

LAB DATA

| | 06/10/82 | 17/11/82 | 13/05/83 | 13/09/83 |
|------------------|----------|----------|----------|----------|
| pH | 6.94 | 7.08 | 2.10 | 6.68 |
| cond. (uS) | 51600 | 42300 | 56200 | 66000 |
| hardness (CaCO3) | 12109 | 12641 | 19415 | 20638 |
| Ca (mg/l) | 3625 | 3550 | 5350 | 5700 |
| Mg | 745.0 | 920.0 | 1475 | 1560 |
| Na | 7400 | 9400 | 7750 | 9100 |
| K | 154.04 | 150.0 | 162.5 | 159.0 |
| Cl | 19000 | 16550 | 21800 | 27600 |
| Alk., as CaCO3 | 573.6 | 531.4 | 321.4 | 265.4 |
| SO4 | NA | 1337 | 1400 | 2700 |
| F | NA | NA | 0.60 | NA |
| NO3, as N | <0.1 | <0.1 | <0.1 | 0.3 |
| NO2, as N | 0.02 | <0.01 | 0.02 | 0.02 |
| Kjeld. N, as N | 0.33 | 224.5 | NA | NA |
| NH3, as N | 0.34.5 | 44.0 | 34.5 | 26.8 |
| TOC | 34 | 23 | 33.2 | 95.4 |
| DOC | NA | NA | NA | NA |
| B | 1.0 | 5.20 | 9.60 | 10.0 |
| Fe (tot) | 1.40 | 0.17 | 0.480 | 0.21 |
| Mn | 0.270 | 0.194 | 0.680 | 0.335 |
| As | <0.030 | <0.030 | 0.001 | <0.001 |
| Cd | 0.001 | 0.002 | 0.014 | 0.003 |
| Cr | 0.085 | 0.033 | 0.072 | 0.036 |
| Cu | 0.10 | 0.170 | 0.380 | 0.360 |
| Ni | 0.010 | 0.010 | 0.024 | 0.009 |
| Pb | 0.054 | 0.085 | <0.060 | <0.030 |
| Se | <0.030 | <0.030 | 0.001 | <0.001 |
| Zn | 0.022 | 0.010 | 0.042 | 0.042 |

DISSOLVED GASES

Sampling Date: 06/10/82 17/11/82 30/11/82 07/07/83 13/09/83

| | 06/10/82 | 17/11/82 | 30/11/82 | 07/07/83 | 13/09/83 |
|-----|----------|----------|----------|----------|----------|
| CH4 | 740 | 1000 | 320 | 260 | 770 |
| O2 | NA | NA | NA | ND | ND |

PURGEABLE ORGANICS

Sampling Date: 19/07/83 19/07/83 13/09/83 13/09/83

| | (A) | (E) | (A) | (B) |
|---------------|-------|-------|-------|-------|
| benzene | 0.772 | 0.970 | 1.210 | 1.654 |
| toluene | 1.294 | 0.571 | 0.260 | 0.424 |
| chlorobenzene | -- | -- | -- | -- |
| ethylbenzene | 2.281 | 0.736 | 0.050 | 0.080 |
| p-xylene | 1.227 | 0.636 | 0.191 | 0.333 |
| o-xylene | 0.498 | 0.233 | 0.074 | 0.112 |
| cumene | -- | -- | 0.033 | 0.040 |
| 1,2,4-TMB | 0.160 | 0.117 | 0.083 | 0.129 |
| naphthalene | 0.014 | 0.089 | -- | -- |

AQUEOUS ISOTOPES

Sampling Date: 06/10/82 17/11/82 30/11/82 13/05/82

| | 06/10/82 | 17/11/82 | 30/11/82 | 13/05/82 |
|----------------|----------|----------|----------|----------|
| Delta O-18 | -9.6 | -9.6 | -10.2 | -9.4 |
| Delta H-2 | NA | NA | NA | -69 |
| Tritium (T.U.) | NA | 80 | 62 | 53 |

SAMPLING POINT:

ALEXION MILL POND (U#30-1)

Sampling date: 16/05/83 11/10/83
 FIELD DATA

| | | |
|------------|------|----|
| temp (C) | 14.0 | NA |
| Em (mV) | NA | NA |
| pH | 8.0 | NA |
| cond. (uS) | 1050 | NA |

LAE DATA

| | | |
|-------------------------------|--------|--------|
| pH | 7.92 | 7.70 |
| cond. (uS) | 1238 | 1600 |
| hardness (CaCO ₃) | 458.3 | 668.0 |
| Ca (mg/l) | 123.5 | 182.0 |
| Mg | 36.50 | 52.0 |
| Na | 85.0 | 100.0 |
| K | 5.50 | 10.0 |
| Cl | 134.8 | 146.6 |
| Alk., as CaCO ₃ | NA | 224.6 |
| SO ₄ | 255.0 | 420.0 |
| F | 0.50 | 0.75 |
| NO ₃ , as N | 1.5 | 1.6 |
| NO ₂ , as N | 0.04 | 0.23 |
| Kjeld. N, as N | 2.2 | 1.8 |
| NH ₃ , as N | 0.9 | 0.7 |
| TOC | 6.7 | NA |
| DOC | 12.3 | 5.5 |
| E | 0.26 | 2.0 |
| Fe (tot) | <0.050 | 0.05 |
| Mn | 0.110 | 0.140 |
| As | <0.001 | <0.001 |
| Cd | <0.010 | 0.0007 |
| Cr | <0.050 | 0.002 |
| Cu | <0.010 | 0.003 |
| Ni | 0.018 | 0.003 |
| Pb | <0.060 | 0.015 |
| Se | <0.001 | <0.001 |
| Zn | <0.010 | 0.001 |

DISSOLVED GASES

Sampling Date: 29/06/83

| | |
|-----------------|-----|
| CH ₄ | ND |
| O ₂ | 2.0 |

PURGEABLE ORGANICS

Sampling Date: 11/10/83

| | |
|---------------|-------|
| benzene | 0.053 |
| toluene | 0.079 |
| chlorobenzene | -- |
| ethylbenzene | 0.021 |
| p-xylene | 0.020 |
| o-xylene | -- |
| cumene | -- |
| 1,2,4-IMB | 0.013 |
| naphthalene | 0.005 |

ΔQUEOUS ISOTOPES

Sampling Date: 16/05/83

| | |
|----------------|------|
| Delta C-18 | -9.1 |
| Delta H-2 | -59 |
| Tritium (T.U.) | 86 |

SAMPLING POINT:

ALEION FALLS SEEPS (UW31-1)

Sampling date: 16/05/83

FIELD DATA

| | |
|------------|----|
| temp (C) | NA |
| Eh (mV) | NA |
| pH | NA |
| Cond. (uS) | NA |

LAB DATA

| | |
|------------------|--------|
| pH | 7.63 |
| Cond. (uS) | 2920 |
| hardness (CaCO3) | 691.9 |
| Ca (mg/l) | 196.5 |
| Mg | 49.0 |
| Na | 370.0 |
| K | 5.75 |
| Cl | 689.0 |
| Alk., as CaCO3 | NA |
| SO4 | 217.5 |
| F | 0.43 |
| NO3, as N | 0.9 |
| NO2, as N | 0.03 |
| Kjeld. N, as N | 1.2 |
| NH3, as N | 0.4 |
| TOC | 22.4 |
| DOC | 3.0 |
| E | 0.26 |
| Fe (tot) | <0.050 |
| Mn | 0.440 |
| As | <0.001 |
| Cd | <0.010 |
| Cr | <0.050 |
| Cu | <0.010 |
| Ni | <0.010 |
| Pb | <0.000 |
| Se | <0.001 |
| Zn | 0.022 |

PURGEABLE ORGANICS

Sampling Date: 11/10/83

| | |
|---------------|-------|
| benzene | 0.089 |
| toluene | 0.119 |
| chlorobenzene | -- |
| ethylbenzene | 0.030 |
| p-xylene | 0.048 |
| o-xylene | -- |
| cumene | -- |
| 1,2,4-TMB | -- |
| naphthalene | -- |

AQUEOUS ISOTOPES

Sampling Date: 16/05/83

| | |
|----------------|------|
| Delta O-18 | -8.8 |
| Delta H-2 | -62 |
| Tritium (T.U.) | 100 |

SAMPLING POINT:

UW4-1

Sampling date:

FIELD DATA

temp (C)
Eh (mV)
pH
Cond. (uS)

LAB DATA

pH
Cond. (uS)
hardness (CaCO₃)
Ca (mg/l)
Mg
Na
K
Cl
Alk., as CaCO₃
SO₄
F
NO₃, as N
NO₂, as N
Kjeld. N, as N
NH₃, as N
TOC
DOC
Fe
Fe (tot)
Mn
As
Cd
Cr
Cu
Ni
Pb
Se
Zn

PURGEABLE ORGANICS

Sampling Date: 09/11/83

| | |
|---------------|-------|
| benzene | 0.504 |
| toluene | 2.114 |
| chlorobenzene | 0.164 |
| ethylbenzene | 0.436 |
| p-xylene | 1.052 |
| o-xylene | 0.623 |
| cumene | -- |
| 1,2,4-TMB | 0.401 |
| naphthalene | 0.305 |

SAMPLING POINT:

U#4-2

Sampling date:

FIELD DATA

temp (C)

Eh (mV)

pH

cond. (uS)

LAB DATA

pH

cond. (uS)

hardness (CaCO3)

Ca (mg/l)

Mg

Na

K

Cl

Alk., as CaCO3

SO4

F

NO3, as N

NO2, as N

Kjeld. N, as N

NH3, as N

TOC

DOC

B

Fe (tot)

Mn

As

Cd

Cr

Cu

Ni

Pb

Se

Zn

PURGEABLE ORGANICS

Sampling Date: 09/11/83 09/11/83

(A)

(E)

benzene

0.792

2.412

toluene

1.607

3.906

chlorobenzene

--

--

ethylbenzene

0.139

0.315

p-xylene

0.388

0.900

o-xylene

0.061

0.267

cumene

--

--

1,2,4-TMB

0.025

0.340

naphthalene

0.151

0.231

SAMPLING POINT:

UW4-3

Sampling date:

FIELD DATA

temp (C)
Eh (mV)
pH
Cond. (uS)

LAB DATA

pH
Cond. (uS)
hardness (CaCO3)
Ca (mg/l)
Mg
Na
K
Cl
Alk., as CaCO3
SO4
F
NO3, as N
NO2, as N
Kjeld. N, as N
NH3, as N
TOC
DOC
E
Fe (tot)
Mn
As
Cd
Cr
Cu
Ni
Pb
Se
Zn

PURGEABLE ORGANICS

Sampling Date: 09/11/83

| | |
|---------------|-------|
| benzene | 2.398 |
| toluene | 3.194 |
| chlorobenzene | 0.148 |
| ethylenzene | 0.202 |
| p-xylene | 0.663 |
| o-xylene | 0.086 |
| cumene | -- |
| 1,2,4-TMB | 0.282 |
| naphthalene | 0.148 |

SAMPLING POINT:

UW4-4

Sampling date:

FIELD DATA

temp (C)

Em (mV)

pH

cond. (uS)

LAB DATA

pd

cond. (uS)

hardness (CaCO3)

Ca (mg/l)

Mg

Na

K

Cl

Alk., as CaCO3

SO4

F

NO3, as N

NO2, as N

Kjeld. N, as N

NH3, as N

TOC

DOC

B

Fe (tot)

Mn

As

Cd

Cr

Cu

Ni

Pb

Se

Zn

PURGEABLE ORGANICS

Sampling Date: 09/11/83

| | |
|---------------|-------|
| benzene | 3.089 |
| toluene | 3.068 |
| chlorobenzene | -- |
| ethylbenzene | 0.045 |
| p-xylene | 0.171 |
| o-xylene | -- |
| cumene | -- |
| 1,2,4-TMB | 0.095 |
| naphthalene | 0.286 |

SAMPLING POINT:

D#5-1

Sampling date: 19/12/83

FIELD DATA

| | |
|------------|----|
| temp (C) | NA |
| En (mV) | NA |
| pH | NA |
| cond. (uS) | NA |

LAB DATA

| | |
|------------------|---------|
| pH | 7.31 |
| cond. (uS) | 1520 |
| hardness (CaCO3) | 555.2 |
| Ca (mg/l) | 140.0 |
| Mg | 50.0 |
| Na | 108.0 |
| K | 4.75 |
| Cl | 182.0 |
| Alk., as CaCO3 | 246.8 |
| SO4 | 273.0 |
| F | 1.15 |
| NO3, as N | 0.2 |
| NO2, as N | <0.01 |
| Kjeld. N, as N | <0.3 |
| NH3, as N | <0.1 |
| TOC | NA |
| DOC | 2.8 |
| B | 0.21 |
| Fe (tot) | 0.68 |
| Mn | 0.140 |
| As | 0.001 |
| Cd | <0.0002 |
| Cr | 0.003 |
| Cu | 0.011 |
| Ni | 0.004 |
| Pb | 0.015 |
| Se | <0.001 |
| Zn | 0.110 |

PURGEABLE ORGANICS

Sampling Date: 09/12/83

| | |
|---------------|-------|
| benzene | 0.050 |
| toluene | 0.894 |
| chlorobenzene | -- |
| ethylbenzene | 0.381 |
| p-xylene | 1.828 |
| o-xylene | 0.531 |
| cumene | -- |
| 1,2,4-TMB | 0.571 |
| naphthalene | 0.367 |

SAMPLING POINT:

UW5-2

Sampling date: 19/12/83

FIELD DATA

| | |
|------------|----|
| temp (C) | NA |
| Eh (mV) | NA |
| pH | NA |
| cond. (uS) | NA |

LAB DATA

| | |
|------------------|---------|
| pH | 7.37 |
| cond. (uS) | 1970 |
| hardness (CaCO3) | 1007 |
| Ca (mg/l) | 260.0 |
| Mg | 87.0 |
| Na | 58.0 |
| K | 5.40 |
| Cl | 144.6 |
| Alk., as CaCO3 | 7361.8 |
| SO4 | 600.0 |
| F | 0.77 |
| NO3, as N | 0.2 |
| NO2, as N | <0.01 |
| Kjeld. N, as N | 0.6 |
| NH3, as N | <0.1 |
| TOC | NA |
| DOC | 10.6 |
| E | 0.31 |
| Fe (tot) | 0.05 |
| Mn | 0.015 |
| As | 0.009 |
| Cd | <0.0002 |
| Cr | 0.012 |
| Cu | 0.015 |
| Ni | 0.002 |
| Pb | 0.013 |
| Se | <0.001 |
| Zn | 0.009 |

PURGEABLE ORGANICS

Sampling Date: 09/12/83

| | |
|---------------|-------|
| benzene | 0.155 |
| toluene | 0.725 |
| chlorobenzene | -- |
| ethylbenzene | 0.463 |
| p-xylene | 1.478 |
| o-xylene | 0.409 |
| cumene | 0.088 |
| 1,2,4-TMB | 1.417 |
| naphthalene | 0.040 |

SAMPLING POINT:

UW5-3

Sampling date:

FIELD DATA

temp (C)
Eh (mV)
pH
cond. (uS)
LAB DATA

pH
cond. (uS)
hardness (CaCO3)
Ca (mg/l)
Mg
Na
K
Cl
Alk., as CaCO3
SO4
F
NO3, as N
NO2, as N
Kjeld. N, as N
NH3, as N
TOC
DOC
E
Fe (tot)
Mn
As
Cd
Cr
Cu
Ni
Pb
Se
Zn

PURGEABLE ORGANICS

Sampling Date: 09/12/83

| | |
|---------------|-------|
| benzene | -- |
| toluene | 1.617 |
| chlorobenzene | -- |
| ethylbenzene | 0.928 |
| p-xylene | 0.810 |
| o-xylene | 0.348 |
| cumene | -- |
| 1,2,4-TMB | 0.832 |
| naphthalene | -- |

SAMPLING POINT:

U#6-2

Sampling date:

FIELD DATA

13/10/82 12/05/83 26/09/83

| | | | |
|------------|------|-------|-------|
| temp (C) | 16.0 | 16.0 | 13.5 |
| Eh (mV) | -167 | NA | NA |
| pH | 6.94 | 6.55 | 6.55 |
| Cond. (uS) | NA | 43000 | 30000 |

LAB DATA

| | | | |
|------------------|--------|--------|--------|
| pH | 7.20 | 7.63 | 6.70 |
| cond. (uS) | 22100 | 30600 | 59000 |
| hardness (CaCO3) | 6084 | 8846 | 21000 |
| Ca (mg/l) | 1680 | 2375 | 5800 |
| Mg | 460 | 710.0 | 1590 |
| Na | 2550 | 3600 | 7350 |
| K | 66.0 | 82.50 | 132.0 |
| Cl | 6785 | 10060 | 24140 |
| Alk., as CaCO3 | 513.2 | 210.0 | 279.4 |
| SO4 | 1340 | 1525 | 1450 |
| F | NA | 1.0 | 01.0 |
| NO3, as N | <0.1 | <0.1 | 0.2 |
| NO2, as N | <0.01 | <0.01 | 0.03 |
| Kjeld. N, as N | 8.0 | 9.8 | 30.0 |
| NH3, as N | 7.2 | 9.2 | 20.0 |
| TOC | 19 | 52.0 | 44.6 |
| DOC | NA | NA | 250.0 |
| B | 4.20 | 6.0 | 3.90 |
| Fe (tot) | NA | 0.046 | 0.240 |
| Mn | NA | 0.230 | 0.570 |
| As | <0.030 | 0.006 | <0.001 |
| Cd | <0.002 | 0.013 | <0.005 |
| Cr | NA | 0.041 | 0.030 |
| Cu | NA | 0.220 | 0.130 |
| Ni | NA | 0.022 | 0.005 |
| Pb | <0.012 | 0.093 | <0.030 |
| Se | <0.030 | <0.001 | <0.001 |
| Zn | NA | 0.034 | 0.006 |

DISSOLVED GASES

Sampling Date: 13/10/82 14/06/83 26/09/83

| | | | |
|-----|-----|----|----|
| CH4 | 140 | 75 | 30 |
| O2 | NA | ND | ND |

PURGEABLE ORGANICS

Sampling Date: 26/09/83 26/09/83

| | (A) | (E) |
|---------------|-------|-------|
| benzene | 1.072 | 0.947 |
| toluene | 0.534 | 0.424 |
| chlorobenzene | -- | -- |
| ethylbenzene | 0.064 | 0.037 |
| p-xylene | 0.146 | 0.190 |
| o-xylene | -- | -- |
| cumene | -- | -- |
| 1,2,4-TMB | 0.078 | 0.072 |
| naphthalene | 0.012 | -- |

AQUEOUS ISOTOPES

Sampling Date: 13/10/82 12/05/83 08/11/83

| | | |
|----------------|------|------|
| Delta C-18 | -9.8 | -9.3 |
| Delta H-2 | NA | -65 |
| Tritium (T.U.) | 20 | ND |

5 (2)

SAMPLING POINT:

UW6-3

Sampling date:

FIELD DATA

temp (C)
Eh (mV)
pH
cond. (uS)

LAE DATA

pH
cond. (uS)
hardness (CaCO3)
Ca (mg/l)
Mg
Na
K
Cl
Alk., as CaCO3
SO4
F
NO3, as N
NO2, as N
Kjeld. N, as N
NH3, as N
TOC
DOC
E
Fe (tot)
Mn
As
Cd
Cr
Cu
Ni
Pb
Se
Zn

PURGEABLE ORGANICS

Sampling Date: 26/09/83

| | |
|---------------|-------|
| benzene | -- |
| toluene | 0.926 |
| chlorobenzene | -- |
| ethybenzene | 0.300 |
| p-xylene | 0.250 |
| o-xylene | 0.034 |
| cumene | -- |
| 1,2,4-TMB | -- |
| naphthalene | -- |

SAMPLING POINT:

Uw6-4

Sampling date: 13/10/82 08/11/83 27/09/83
 FIELD DATA

| | | | |
|------------|------|----|--------|
| temp (C) | 14.0 | NA | 17.0 |
| Eh (mV) | +53 | NA | NA |
| pH | 6.99 | NA | 6.50 |
| cond. (uS) | NA | NA | >50000 |

LAB DATA

| | | |
|------------------|--------|--------|
| pH | 6.74 | |
| cond. (uS) | 79500 | |
| hardness (CaCO3) | 54512 | |
| Ca (mg/l) | 14100 | |
| Mg | 4700 | |
| Na | 24200 | |
| K | 370.0 | |
| Cl | 71520 | |
| Alk., as CaCO3 | 67.4 | |
| SO4 | 835.0 | |
| F | NA | |
| NO3, as N | 0.2 | |
| NO2, as N | 0.02 | |
| Kjeld. N, as N | 35.0 | |
| NH3, as N | 28.6 | |
| TOC | 5.00 | |
| DOC | NA | |
| B | 4.60 | 5.80 |
| Fe (tot) | NA | 0.320 |
| Mn | NA | 0.720 |
| As | <0.030 | 0.002 |
| Cd | <0.002 | <0.005 |
| Cr | NA | 0.035 |
| Cu | NA | 0.430 |
| Ni | NA | <0.006 |
| Pb | <0.012 | 0.074 |
| Se | <0.030 | <0.001 |
| Zn | NA | 0.220 |

DISSOLVED GASES

Sampling Date: 13/10/82

| | |
|-----|----|
| CH4 | ND |
| C2 | NA |

PURGEABLE ORGANICS

Sampling Date: 26/09/83

| | |
|---------------|-------|
| benzene | 4.272 |
| toluene | 0.758 |
| chlorobenzene | -- |
| ethylbenzene | 0.143 |
| p-xylene | 0.137 |
| o-xylene | 0.274 |
| cumene | 0.017 |
| 1,2,4-TMB | 0.091 |
| naphthalene | 0.374 |

SAMPLING POINT:

UW6-5

Sampling date: 08/09/83 27/09/83 08/11/83
 FIELD DATA

| | | | |
|------------|--------|----|--------|
| TEMP (C) | 731.0 | NA | 020.0 |
| EH (mV) | NA | NA | NA |
| PH | 6.10 | NA | 6.25 |
| COND. (uS) | >50000 | NA | >50000 |

LAB DATA

| | | | |
|------------------|--------|--------|--------|
| PH | NA | 5.97 | |
| COND. (uS) | NA | 142000 | |
| hardness (CaCO3) | NA | 60100 | |
| Ca (mg/l) | NA | 17000 | |
| Mg | NA | 4300 | |
| Na | NA | 25000 | |
| K | NA | 390.0 | |
| Cl | NA | 82240 | |
| Alk., as CaCO3 | NA | 157.0 | |
| SO4 | NA | 675.0 | |
| F | NA | NA | |
| NO3, as N | NA | <0.1 | |
| NO2, as N | NA | 0.03 | |
| Kjeld. N, as N | NA | 60.0 | |
| NH3, as N | NA | 45.0 | |
| TOC | 212 | 97.6 | |
| DOC | NA | 780.0 | |
| B | 6.20 | NA | 4.40 |
| Fe (tot) | 24.0 | 43.30 | 26.0 |
| Mn | 2.90 | 4.950 | 8.0 |
| As | 0.001 | NA | <0.001 |
| Cd | <0.010 | NA | <0.010 |
| Cr | 0.120 | NA | 0.110 |
| Cu | 0.720 | NA | 0.570 |
| Ni | 0.014 | NA | 0.029 |
| Pb | 0.150 | NA | 0.110 |
| Se | 0.004 | NA | <0.001 |
| Zn | 0.075 | NA | 0.370 |

DISSOLVED GASES

Sampling Date: 08/09/83 28/09/83

| | | |
|-----|----|-----|
| CH4 | NA | 200 |
| CO2 | ND | |

PURGEABLE ORGANICS

Sampling Date: 27/09/83

| | |
|---------------|-------|
| benzene | 4.692 |
| toluene | 7.720 |
| chlorobenzene | -- |
| ethylbenzene | 0.125 |
| p-xylene | 0.232 |
| o-xylene | 0.009 |
| cumene | 0.099 |
| 1,2,4-IMB | 0.049 |
| naphthalene | -- |

SAMPLING POINT:

UW7-1

Sampling date:

20/10/82 12/05/83 31/05/83 26/10/83

FIELD DATA

| | | | | |
|------------|------|------|------|------|
| temp (C) | 16.0 | 12.5 | 12.0 | 11.5 |
| En (mV) | -37 | NA | NA | NA |
| pH | 6.65 | 6.25 | 6.45 | 6.55 |
| cond. (uS) | NA | 7200 | 7000 | NA |

LAE DATA

| | | | | |
|------------------|--------|--------|--------|--------|
| pH | 7.35 | 7.00 | 6.83 | 6.71 |
| cond. (uS) | 9640 | 9440 | 9380 | 13000 |
| hardness (CaCO3) | 1389 | 1244 | 2283 | 2710 |
| Ca (mg/l) | 260.0 | 177.0 | 610.0 | 740.0 |
| Mg | 180.0 | 195.0 | 185.0 | 210.0 |
| Na | 1260 | 1215 | 1160 | 1450 |
| K | 228.0 | 260.0 | 189.0 | 236.0 |
| Cl | 1686 | 1482 | 1586 | 2320 |
| Alk., as CaCO3 | 1232 | 856.6 | NA | 1799 |
| SO4 | 1500 | 1700 | 1737 | 1680 |
| F | 0.67 | 0.61 | 0.70 | 0.80 |
| NO3, as N | 0.1 | <0.1 | <0.1 | 0.2 |
| NO2, as N | 0.02 | <0.01 | <0.01 | 0.02 |
| Kjeld. N, as N | 190.0 | 136.0 | 136.0 | 150.0 |
| NH3, as N | 118.0 | 134.0 | 121.0 | 135.0 |
| TOC | 140 | 311 | NA | NA |
| DOC | NA | 170.0 | 136.0 | 190.0 |
| B | 1.10 | 6.80 | NA | 7.70 |
| Fe (tot) | <0.01 | 0.086 | 0.120 | 0.110 |
| Mn | 0.024 | 0.030 | 0.032 | 0.032 |
| As | <0.030 | 0.001 | <0.001 | <0.001 |
| Cd | <0.002 | 0.015 | <0.002 | <0.005 |
| Cr | 0.023 | <0.050 | 0.018 | <0.025 |
| Cu | 0.050 | 0.063 | 0.120 | 0.076 |
| Ni | 0.049 | 0.064 | 0.050 | 0.080 |
| Pb | <0.012 | 0.065 | <0.030 | 0.044 |
| Se | <0.030 | 0.005 | <0.001 | <0.001 |
| Zn | 0.120 | <0.010 | 0.012 | 0.033 |

DISSOLVED GASES

Sampling Date: 20/10/82 23/06/83 26/10/83

| | | | |
|-----|------|-----|-----|
| CH4 | 1240 | 230 | 540 |
| O2 | NA | ND | |

PURGEABLE ORGANICS

Sampling Date: 26/10/83 26/10/83

| | (A) | (B) |
|---------------|-------|-------|
| benzene | 4.550 | 4.115 |
| toluene | 2.706 | 2.259 |
| chlorobenzene | 0.080 | 0.099 |
| ethylbenzene | 3.237 | 3.130 |
| p-xylene | 6.981 | 6.668 |
| o-xylene | 3.142 | 2.927 |
| cumene | 0.092 | 0.099 |
| 1,2,4-TMB | 3.765 | 3.735 |
| naphthalene | 0.103 | 0.540 |

AQUEOUS ISOTOPES

Sampling Date: 20/10/82 12/05/83

| | | |
|----------------|-------|-------|
| Delta O-18 | -10.2 | -10.1 |
| Delta H-2 | NA | -54 |
| tritium (T.U.) | 110 | 123 |

SAMPLING POINT:

UW 7-2

Sampling date:
FIELD DATA

20/10/82 12/05/83 31/05/83 26/10/83

| | | | | |
|------------|------|-------|----|------|
| temp (C) | 16.0 | 12.0 | NA | 09.0 |
| Eh (mV) | NA | NA | NA | NA |
| pH | 6.89 | 6.25 | NA | 6.35 |
| cond. (uS) | NA | 19200 | NA | NA |

LAB DATA

| | | | | |
|------------------|--------|--------|--------|--------|
| pH | 7.11 | 6.80 | 6.50 | 6.49 |
| cond. (uS) | 22100 | 25000 | 24000 | 22400 |
| hardness (CaCO3) | 5534 | 7252 | 6776 | 6382 |
| Ca (mg/l) | 1460 | 2000 | 1875 | 1775 |
| Mg | 460.0 | 550.0 | 510.0 | 475.0 |
| Na | 3150 | 3330 | 3180 | 2900 |
| K | 112.0 | 88.50 | 86.0 | 95.0 |
| Cl | 7510 | 8448 | 8148 | 7412 |
| Alk., as CaCO3 | 540.0 | 352.6 | NA | 730.0 |
| SO4 | 1738 | 1625 | 1675 | 1560 |
| F | 0.61 | 1.10 | 0.90 | 0.10 |
| NO3, as N | 0.3 | <0.1 | <0.1 | 0.2 |
| NO2, as N | 0.02 | <0.01 | 0.03 | <0.01 |
| Kjeld. N, as N | 36.5 | 17.4 | NA | 40.0 |
| NH3, as N | 27.6 | 16.3 | 18.0 | 20.7 |
| TOC | NA | 115 | 59.1 | NA |
| DOC | NA | 280.0 | 55.0 | 48.0 |
| B | 6.0 | 8.80 | NA | 7.10 |
| Fe (tot) | 0.07 | 0.078 | 0.064 | 0.110 |
| Mn | 0.040 | 0.140 | 0.110 | 0.110 |
| As | <0.030 | 0.001 | <0.001 | <0.001 |
| Cd | <0.002 | 0.017 | 0.004 | <0.005 |
| Cr | 0.027 | 0.040 | 0.028 | 0.034 |
| Cu | 0.056 | 0.190 | 0.30 | 0.170 |
| Ni | 0.018 | 0.038 | 0.022 | 0.037 |
| Pb | 0.012 | 0.120 | <0.030 | 0.049 |
| Se | <0.030 | <0.001 | <0.001 | <0.001 |
| Zn | 0.033 | <0.010 | 0.032 | 0.021 |

DISSOLVED GASES

Sampling Date: 20/10/82 23/06/83 26/10/83

| | | | |
|-----|-----|-----|-----|
| CH4 | 120 | 100 | 190 |
| O2 | NA | ND | |

PURGEABLE ORGANICS

Sampling Date: 26/10/83 26/10/83

| | (A) | (B) |
|---------------|-------|-------|
| benzene | 0.271 | 0.245 |
| toluene | 0.159 | 0.231 |
| chlorobenzene | -- | -- |
| ethylbenzene | 0.037 | 0.034 |
| p-xylene | 0.146 | 0.153 |
| o-xylene | -- | -- |
| cumene | -- | -- |
| 1,2,4-TMB | 0.080 | 0.091 |
| naphthalene | 0.052 | 0.024 |

AQUEOUS ISOTOPES

Sampling Date: 20/10/82 12/05/83

| | | |
|----------------|-------|------|
| Delta O-18 | -10.1 | -9.7 |
| Delta H-2 | NA | -62 |
| Tritium (T.U.) | 50 | 62 |

SAMPLING POINT:

U#7-3

Sampling date: 25/08/83 07/09/83

FIELD DATA

| | | |
|------------|-------|----|
| temp (C) | 236.0 | NA |
| En (mV) | NA | NA |
| pH | 5.95 | NA |
| Cond. (uS) | 6500 | NA |

LAB DATA

| | | |
|------------------|--------|--------|
| pH | 6.20 | |
| Cond. (uS) | 124000 | |
| hardness (CaCO3) | 8037.9 | |
| Ca (mg/l) | 21500 | |
| Mg | 6500 | |
| Na | 24250 | |
| K | 352.0 | |
| Cl | 65760 | |
| Alk., as CaCO3 | 113.8 | |
| SO4 | 875.0 | |
| F | NA | |
| NO3, as N | 0.17 | |
| NO2, as N | 0.03 | |
| Kjeld. N, as N | 18.0 | |
| NH3, as N | 42.2 | |
| TOC | 277 | 323 |
| DOC | 2300.0 | NA |
| E | NA | 8.20 |
| Fe (tot) | 8.25 | 0.530 |
| Mn | 3.550 | 1.40 |
| As | NA | 0.002 |
| Cd | NA | <0.010 |
| Cr | NA | 0.079 |
| Cu | NA | 0.670 |
| Ni | NA | <0.010 |
| Pb | NA | 0.110 |
| Se | NA | 0.003 |
| Zn | NA | 0.025 |

PURGEABLE ORGANICS

Sampling Date: 27/10/83 27/10/83

| | (A) | (E) |
|---------------|--------|-------|
| benzene | 0.459 | 2.196 |
| toluene | 15.613 | 3.153 |
| chlorobenzene | -- | -- |
| ethybenzene | 0.409 | 0.161 |
| p-xylene | 1.456 | 0.454 |
| o-xylene | 0.881 | 0.289 |
| cumene | -- | -- |
| 1,2,4-IMB | 0.932 | 0.402 |
| naphthalene | 0.473 | 0.354 |

AQUEOUS ISOTOPES

Sampling Date: 25/08/83

| | |
|----------------|------|
| Delta O-18 | -8.5 |
| Delta H-2 | -69 |
| Tritium (T.U.) | ND |

SAMPLING POINT:

UW7-5

Sampling date: 25/08/83

FIELD DATA

| | |
|------------|-------|
| temp (C) | 236.0 |
| Eh (mV) | NA |
| pH | 5.45 |
| cond. (uS) | 6700 |

LAB DATA

| | |
|------------------|--------|
| pH | 6.06 |
| cond. (uS) | 150000 |
| hardness (CaCO3) | 64650 |
| Ca (mg/l) | 18000 |
| Mg | 4600 |
| Na | 72000 |
| K | 420.0 |
| Cl | 88000 |
| Alk., as CaCO3 | 144.2 |
| SO4 | 675.0 |
| F | NA |
| NO3, as N | 0.2 |
| NO2, as N | 0.02 |
| Kjeld. N, as N | 27.0 |
| NH3, as N | 58.0 |
| IOC | 347 |
| DOC | 2260.0 |
| B | 7.20 |
| Fe (tot) | 2.55 |
| Mn | 0.70 |
| As | <0.001 |
| Cd | <0.002 |
| Cr | 0.043 |
| Cu | 0.660 |
| Ni | 0.011 |
| Pb | <0.030 |
| Se | <0.001 |
| Zn | 0.140 |

DISSOLVED GASES

Sampling Date: 25/08/83

| | |
|-----|----|
| CH4 | ND |
| O2 | ND |

PURGEABLE ORGANICS

Sampling Date: 27/10/83

| | |
|---------------|-------|
| benzene | NA |
| toluene | 0.293 |
| chlorobenzene | -- |
| ethylbenzene | 0.049 |
| p-xylene | 0.188 |
| o-xylene | 0.117 |
| cumene | -- |
| 1,2,4-TMB | 0.216 |
| naphthalene | 0.264 |

AQUEOUS ISOTOPEs

Sampling Date: 25/08/83

| | |
|----------------|------|
| Delta C-18 | -5.9 |
| Delta H-2 | -54 |
| Tritium (T.U.) | 116 |

SAMPLING POINT:

UwE-2

Sampling date: 12/10/82 27/10/83
 FIELD DATA

| | | |
|------------|------|------|
| temp (C) | 12.0 | 11.0 |
| En (mV) | -95 | NA |
| pH | 6.55 | 6.35 |
| cond. (uS) | NA | NA |

LAE DATA

| | | |
|------------------|--------|--------|
| pH | 7.15 | 6.59 |
| cond. (uS) | 6800 | 6200 |
| hardness (CaCO3) | 2532 | 2551 |
| Ca (mg/l) | 695.0 | 705.0 |
| Mg | 194.0 | 192.5 |
| Na | 710.0 | 670.0 |
| K | 46.0 | 45.20 |
| Cl | 1229 | 936.0 |
| Alk., as CaCO3 | 747.0 | 766.0 |
| SO4 | 1875 | 1780 |
| F | 0.52 | 0.60 |
| NO3, as N | 0.2 | <0.1 |
| NO2, as N | <0.01 | <0.01 |
| Kjeld. N, as N | 30.2 | 25.5 |
| NH3, as N | 29.5 | 26.2 |
| TOC | 22 | NA |
| DOC | NA | 17.0 |
| B | 3.40 | 3.80 |
| Fe (tot) | NA | 0.039 |
| Mn | NA | 0.10 |
| As | <0.030 | <0.001 |
| Cd | NA | <0.005 |
| Cr | NA | <0.025 |
| Cu | NA | 0.065 |
| Ni | NA | 0.016 |
| Pb | NA | 0.038 |
| Se | <0.030 | <0.001 |
| Zn | NA | 0.009 |

DISSOLVED GASES

Sampling Date: 12/10/82 27/10/83

| | | |
|-----|------|-----|
| CH4 | 1060 | 560 |
| O2 | NA | NA |

PURGEABLE ORGANICS

| Sampling Date: | 27/10/83 | 27/10/83 | 27/10/83 |
|----------------|----------|----------|----------|
| | (A) | (C) | (D) |
| benzene | 0.321 | 0.327 | 0.345 |
| toluene | 0.040 | 0.077 | 0.064 |
| chlorobenzene | -- | -- | -- |
| ethylbenzene | 0.120 | 0.126 | 0.124 |
| p-xylene | 0.169 | 0.208 | 0.198 |
| o-xylene | -- | -- | -- |
| cumene | -- | -- | -- |
| 1,2,4-TMS | 0.000 | 0.001 | 0.063 |
| naphthalene | 0.050 | 0.018 | 0.083 |

AQUEOUS ISOTOPES

Sampling Date: 12/10/82

| | |
|----------------|------|
| Delta O-18 | -9.8 |
| Delta H-2 | NA |
| Tritium (T.U.) | 50 |

SAMPLING POINT:

UW8-3

Sampling date: 12/10/82

FIELD DATA

| | |
|------------|------|
| temp (C) | 14.0 |
| En (mV) | -54 |
| pH | 5.64 |
| cond. (uS) | NA |

LAB DATA

| | |
|------------------|--------|
| pH | 6.55 |
| cond. (uS) | 73200 |
| hardness (CaCO3) | 28099 |
| Ca (mg/l) | 7800 |
| Mg | 2100 |
| Na | 10200 |
| K | 149.0 |
| Cl | 37325 |
| Alk., as HCO3 | 163.0 |
| SO4 | 1270 |
| F | NA |
| NO3 | 0.2 |
| NO2, as N | 0.03 |
| Kjeld. N, as N | 34.5 |
| NH3, as N | 033.8 |
| TOC | 44 |
| DCC | NA |
| B | 3.0 |
| Fe (tot) | NA |
| Mn | NA |
| As | <0.030 |
| Cd | <0.002 |
| Cr | NA |
| Cu | NA |
| Ni | NA |
| Pb | NA |
| Se | <0.030 |
| Zn | NA |

DISSOLVED GASES

Sampling Date: 12/10/82

| | |
|-----|-----|
| CH4 | 270 |
| O2 | NA |

PURGEABLE ORGANICS

Sampling Date:

| |
|---------------|
| benzene |
| toluene |
| chlorobenzene |
| ethylbenzene |
| p-xylene |
| o-xylene |
| cumene |
| 1,2,4-TMB |
| naphthalene |

AQUEOUS ISOTOPES

Sampling Date: 12/10/82

| | |
|----------------|-------|
| Delta O-18 | -10.5 |
| Delta H-2 | NA |
| Tritium (T.U.) | 20 |

SAMPLING POINT:

UW8-4

Sampling date:

FIELD DATA

temp (C)
Eh (mV)
pH
cond. (uS)

LAB DATA

pH
cond. (uS)
hardness (CaCO₃)
Ca (mg/l)
Mg
Na
K
Cl
Alk., as CaCO₃
SO₄
F
NO₃, as N
NO₂, as N
Kjeld. N, as N
NH₃, as N
TOC
DOC
B
Fe (tot)
Mn
As
Cd
Cr
Cu
Ni
Pb
Se
Zn

PURGEABLE ORGANICS

Sampling Date: 17/11/83

| | |
|---------------|-------|
| benzene | 0.264 |
| toluene | 1.431 |
| chlorobenzene | 0.016 |
| ethylbenzene | 0.919 |
| p-xylene | 1.598 |
| o-xylene | 0.328 |
| cumene | -- |
| 1,2,4-IMB | 0.070 |
| naphthalene | 0.481 |

SAMPLING POINT:

UW8-5

Sampling date: 17/11/83

FIELD DATA

| | |
|------------|----|
| temp (C) | NA |
| Eh (mV) | NA |
| pH | NA |
| Cond. (uS) | NA |

LAB DATA

| | |
|------------------|--------|
| pH | 5.86 |
| cond. (uS) | 72000 |
| hardness (CaCO3) | 26005 |
| Ca (mg/l) | 7200 |
| Mg | 1950 |
| Na | 9600 |
| K | 187.0 |
| Cl | 30900 |
| Alk., as CaCO3 | 340.4 |
| SO4 | 1140 |
| F | 01.50 |
| NO3, as N | 0.3 |
| NO2, as N | 0.05 |
| Kjeld. N, as N | NA |
| NH3, as N | 50.0 |
| TOC | NA |
| DOC | 240.0 |
| E | 6.80 |
| Fe (tot) | 0.50 |
| Mn | 1.10 |
| As | <0.001 |
| Cd | <0.010 |
| Cr | 0.210 |
| Cu | 0.360 |
| Ni | 0.015 |
| Pb | <0.000 |
| Se | <0.001 |
| Zn | 0.034 |

PURGEABLE ORGANICS

Sampling Date: 17/11/83

| | |
|---------------|-------|
| benzene | 5.266 |
| toluene | 4.336 |
| chlorobenzene | -- |
| ethylbenzene | 1.919 |
| p-xylene | 1.301 |
| o-xylene | 0.160 |
| cumene | -- |
| 1,2,4-TMB | 0.593 |
| naphthalene | 0.046 |

SAMPLING POINT:

UW 9-1

Sampling date:
FIELD DATA

| 18/11/82 (A) | 18/11/82 (B) | 18/11/82 (C) | 11/05/83 | 31/05/83 | 04/10/83 |
|-----------------|-----------------|-----------------|----------|----------|----------|
|-----------------|-----------------|-----------------|----------|----------|----------|

| | | | | | | |
|------------|----|----|----|------|------|-------|
| temp (C) | NA | NA | NA | 13.0 | 13.5 | 221.0 |
| Eh (mV) | NA | NA | NA | NA | NA | NA |
| pH | NA | NA | NA | 6.75 | 6.50 | 6.65 |
| cond. (uS) | NA | NA | NA | 6000 | 6000 | NA |

LAB DATA

| | | | | | | |
|------------------|--------|--------|--------|--------|--------|--------|
| pH | 7.62 | 7.76 | 7.29 | 7.10 | 6.83 | 6.76 |
| cond. (uS) | 7670 | 7655 | 7660 | 7940 | 7800 | 7800 |
| hardness (CaCC3) | 2516 | 2525 | 2342 | 2309 | 2342 | 2276 |
| Ca (mg/l) | 725.0 | 740.0 | 675.0 | 650.0 | 675.0 | 670.0 |
| Mg | 172.5 | 165.0 | 165.0 | 167.0 | 160.0 | 147.0 |
| Na | 840.0 | 820.0 | 850.0 | 1015 | 980.0 | 905.0 |
| K | 25.50 | 25.0 | 25.50 | 27.0 | 26.0 | 39.0 |
| Cl | 1882 | 1841 | 1848 | 1978 | 1914 | 1965 |
| Alk., as CaCC3 | 444.8 | 441.2 | 441.4 | 428.0 | NA | 456.6 |
| SO4 | 1060 | 1040 | 1050 | 1025 | 1050 | 1120 |
| F | 0.29 | 0.28 | 0.30 | 0.27 | 0.32 | 0.40 |
| NO3, as N | <0.1 | <0.1 | <0.1 | 0.2 | 0.5 | <0.1 |
| NO2, as N | <0.01 | <0.01 | <0.01 | <0.01 | 0.02 | <0.01 |
| Kjeld., N, as N | 4.0 | 3.9 | 3.3 | 3.6 | 3.5 | 7.5 |
| NH3, as N | 2.8 | 2.7 | 2.6 | 2.5 | 2.8 | 2.7 |
| TOC | NA | NA | NA | 38.7 | 19.3 | 21.4 |
| DOC | NA | NA | NA | NA | 217.0 | 216.0 |
| E | 2.80 | 2.80 | 2.90 | 1.40 | NA | 1.60 |
| Fe (tot) | <0.03 | <0.02 | <0.03 | 0.052 | 0.040 | 0.033 |
| Mn | 0.023 | 0.021 | 0.080 | 0.087 | 0.084 | 0.076 |
| As | <0.030 | <0.030 | <0.030 | <0.001 | <0.001 | <0.001 |
| Cd | <0.002 | <0.002 | <0.002 | 0.015 | <0.002 | <0.005 |
| Cr | 0.014 | 0.014 | 0.014 | <0.050 | 0.015 | <0.025 |
| Cu | 0.060 | 0.060 | 0.060 | 0.060 | 0.110 | 0.044 |
| Ni | 0.008 | 0.011 | 0.008 | 0.024 | 0.013 | 0.016 |
| Pb | 0.052 | 0.041 | 0.044 | 0.074 | <0.030 | <0.030 |
| Se | <0.030 | <0.030 | <0.030 | <0.001 | <0.001 | <0.001 |
| Zn | 0.009 | 0.004 | 0.004 | <0.010 | 0.011 | 0.008 |

DISSOLVED GASES

Sampling Date: 23/06/83 04/10/83

| | | |
|-----|----|----|
| CH4 | ND | 40 |
| O2 | ND | ND |

PURGEABLE ORGANICS

Sampling Date: 04/10/83

| | |
|---------------|-------|
| benzene | 0.074 |
| toluene | 0.086 |
| chlorobenzene | -- |
| ethylbenzene | 0.009 |
| p-xylene | 0.015 |
| o-xylene | -- |
| cumene | -- |
| 1,2,4-TMB | 0.010 |
| napthalene | 0.047 |

AQUEOUS ISOTOPES

Sampling Date: 11/05/83

| | |
|----------------|------|
| Delta O-18 | -9.7 |
| Delta H-2 | -62 |
| Tritium (T.U.) | 32 |

SAMPLING POINT:

DW9-2

Sampling date:

12/10/82 11/05/83 31/05/83 04/10/83 04/10/83

FIELD DATA

| | | | | | |
|------------|------|------|------|------|------|
| temp (C) | 12.0 | 14.0 | 14.0 | 14.5 | 14.5 |
| Em (mV) | +55 | NA | NA | NA | NA |
| pH | 6.82 | 6.45 | 6.55 | 6.95 | 6.95 |
| cond. (uS) | NA | 7900 | 7600 | NA | NA |

LAB DATA

| | | | | | |
|------------------|--------|--------|--------|--------|--------|
| pH | 7.40 | 7.07 | 6.88 | 6.86 | 6.86 |
| cond. (uS) | 8810 | 9880 | 9820 | 9800 | 9800 |
| hardness (CaCO3) | 2329 | 2910 | 2952 | 3042 | 2960 |
| Ca (mg/l) | 650.0 | 820.0 | 845.0 | 840.0 | 840.0 |
| Mg | 172.0 | 210.0 | 205.0 | 230.0 | 210.0 |
| Na | 1290 | 1195 | 1150 | 1100 | 1130 |
| K | 38.0 | 40.0 | 41.80 | 47.50 | 48.0 |
| Cl | 2382 | 2854 | 2450 | 2512 | 2513 |
| Alk., as CaCO3 | 578.4 | 448.0 | NA | 468.0 | 466.8 |
| SO4 | 1150 | 1412 | 1400 | 1480 | 1480 |
| F | 0.51 | 0.47 | 0.52 | 0.60 | 0.60 |
| NO3, as N | 0.3 | <0.1 | <0.1 | <0.1 | <0.1 |
| NO2, as N | <0.01 | <0.01 | <0.01 | <0.01 | <0.01 |
| Kjeld. N, as N | 9.4 | 8.8 | 8.9 | 10.0 | 10.0 |
| NH3, as N | 9.4 | 8.6 | 8.7 | 8.5 | 8.5 |
| TOC | 14 | 17.6 | 13.9 | 10.1 | 10.1 |
| DGC | NA | NA | 231.0 | 260.0 | 230.0 |
| B | 2.70 | 2.80 | NA | 2.50 | 2.60 |
| Fe (tot) | NA | 0.320 | 0.081 | 0.063 | 0.072 |
| Mn | NA | 0.250 | 0.190 | 0.160 | 0.160 |
| As | <0.030 | <0.001 | <0.001 | <0.001 | <0.001 |
| Cd | <0.002 | 0.061 | <0.002 | <0.005 | <0.005 |
| Cr | NA | 0.10 | 0.013 | <0.025 | <0.025 |
| Cu | NA | 0.260 | 0.120 | 0.063 | 0.096 |
| Ni | NA | 0.20 | 0.012 | 0.015 | 0.017 |
| Pb | <0.012 | 1.0 | <0.030 | <0.030 | <0.030 |
| Se | <0.030 | <0.001 | <0.001 | <0.001 | <0.001 |
| Zn | NA | 0.042 | 0.014 | 0.010 | 0.030 |

DISSOLVED GASES

Sampling Date:

12/10/82 14/06/83 23/06/83 04/10/83

| | | | | |
|-----|-----|----|-----|-----|
| CH4 | 300 | NA | 150 | 260 |
| O2 | NA | ND | ND | ND |

PURGABLE ORGANICS

Sampling Date:

04/10/83

| | |
|---------------|-------|
| benzene | 0.095 |
| toluene | 0.085 |
| chlorobenzene | -- |
| ethylbenzene | 0.025 |
| p-xylene | 0.029 |
| o-xylene | -- |
| cumene | -- |
| 1,2,4-TMB | 0.020 |
| naphthalene | -- |

AQUEOUS ISOTOPES

Sampling Date:

12/10/82 11/05/83

| | | |
|----------------|-------|------|
| Delta O-18 | -10.0 | -9.8 |
| Delta H-2 | NA | -62 |
| Tritium (T.U.) | 50 | 123 |

SAMPLING POINT:

UW9-3

Sampling date:

12/10/82 03/11/82 06/10/83

FIELD DATA

| | | | |
|------------|------|----|----|
| temp (C) | NA | NA | NA |
| Eh (mV) | +49 | NA | NA |
| pH | 6.45 | NA | NA |
| cond. (uS) | NA | NA | NA |

LAB DATA

| | | | |
|------------------|--------|--------|--------|
| pH | 7.16 | 6.19 | |
| cond. (uS) | 12560 | 10850 | |
| hardness (CaCO3) | 2403 | 813.4 | |
| Ca (mg/l) | 625.0 | 204.0 | |
| Mg | 205.0 | 74.0 | |
| Na | 1820 | 1660 | |
| K | 48.0 | 30.0 | |
| Cl | 3140 | 3248 | |
| Alk., as CaCO3 | 644.4 | 256.8 | |
| SO4 | 515.0 | 194.0 | |
| F | 0.53 | 0.42 | |
| NO3, as N | 9.8 | 1.7 | |
| NO2, as N | 0.03 | <0.01 | |
| Kjeld. N, as N | 14.0 | 11.4 | |
| NH3, as N | 0.13.6 | 5.4 | |
| TDC | 2000 | 2900 | 510 |
| DOC | NA | NA | NA |
| B | 1.60 | 2.0 | 4.40 |
| Fe (tot) | NA | 3.85 | 3.40 |
| Mn | NA | 0.370 | 2.10 |
| As | <0.030 | <0.030 | 0.026 |
| Cd | NA | <0.002 | 0.016 |
| Cr | NA | 2.0 | 0.160 |
| Cu | NA | 0.050 | 0.390 |
| Ni | NA | 0.020 | 0.160 |
| Pb | NA | <0.012 | 0.60 |
| Se | <0.030 | <0.030 | <0.001 |
| Zn | NA | 0.180 | 0.270 |

DISSOLVED GASES

Sampling Date: 12/10/82 05/11/82 02/12/82

| | | | |
|-----|----|-----|-----|
| CH4 | 80 | 260 | 140 |
| C2 | NA | NA | NA |

PURGEABLE ORGANICS

Sampling Date: 21/11/83

| | |
|---------------|-------|
| benzene | -- |
| toluene | 2.256 |
| chlorobenzene | -- |
| ethylbenzene | 0.227 |
| p-xylene | 0.538 |
| o-xylene | 0.099 |
| cumene | -- |
| 1,2,4-TMB | 0.148 |
| napthalene | 0.189 |

AQUEOUS ISOTOPES

Sampling Date: 12/10/82 03/11/82 12/05/83

| | | | |
|----------------|-------|------|-------|
| Delta O-18 | -10.0 | -9.8 | -10.1 |
| Delta H-2 | NA | NA | -72 |
| Tritium (T.U.) | 70 | 81 | 70 |

SAMPLING POINT:

UWS-4

Sampling date: 03/08/83 06/10/83
 FIELD DATA

| | | |
|------------|------|-------|
| temp (C) | 24.0 | 218.0 |
| Eh (mV) | NA | NA |
| pH | 6.05 | 5.75 |
| cond. (uS) | NA | NA |

LAB DATA

| | | |
|------------------|--------|--------|
| pH | 6.33 | 5.75 |
| cond. (uS) | 139000 | 136000 |
| hardness (CaCC3) | 50944 | 50385 |
| Ca (mg/l) | 13000 | 13600 |
| Mg | 4500 | 4000 |
| Na | 27000 | 25000 |
| K | 380.0 | 450.0 |
| Cl | 77880 | 72720 |
| Alk., as HCO3 | 177.6 | 164.6 |
| SO4 | 1088 | 1030 |
| F | NA | NA |
| NO3 | 01.0 | 0.5 |
| NO2, as N | 0.06 | 0.02 |
| Kjeld. N, as N | NA | 51.0 |
| NH3, as N | 53.0 | 51.0 |
| IOC | 30.0 | 15.2 |
| DOC | NA | NA |
| B | 8.40 | 5.0 |
| Fe (tot) | 6.20 | 2.70 |
| Mn | 0.175 | 1.10 |
| As | 0.001 | 0.001 |
| Cd | <0.002 | <0.005 |
| Cr | 0.030 | 0.037 |
| Cu | 0.510 | 0.410 |
| Ni | <0.010 | <0.005 |
| Pb | <0.030 | <0.030 |
| Se | 0.001 | <0.001 |
| Zn | 0.120 | 0.010 |

DISSOLVED GASES

Sampling Date: 06/10/83

| | |
|-----|-----|
| CH4 | 170 |
| O2 | ND |

PURGEABLE ORGANICS

Sampling Date: 06/10/83

| | |
|---------------|-------|
| benzene | 0.923 |
| toluene | 0.608 |
| chlorobenzene | -- |
| ethylbenzene | 0.206 |
| p-xylene | 0.171 |
| o-xylene | -- |
| cumene | -- |
| 1,2,4-TMB | 0.106 |
| naphthalene | 0.082 |

AQUEOUS ISOTOPES

Sampling Date: 03/08/83 19/12/83

| | | |
|----------------|------|--------|
| Delta O-18 | -7.2 | |
| Delta H-2 | -60 | |
| Tritium (T.U.) | ND | 10 (3) |

SAMPLING POINT:

UW10-1

Sampling date:

12/10/82 11/05/83 04/10/83

FIELD DATA

| | | | |
|------------|------|------|----|
| temp (C) | 14.0 | 15.0 | NA |
| Eu (mV) | -09 | NA | NA |
| pH | 6.87 | 6.65 | NA |
| cond. (uS) | NA | 2350 | NA |

LAB DATA

| | | | |
|------------------|--------|--------|--------|
| pH | 7.59 | 7.50 | 6.98 |
| cond. (uS) | 3230 | 2840 | 3000 |
| hardness (CaCO3) | 1652 | 1330 | 1594 |
| Ca (mg/l) | 565.0 | 440 | 545.0 |
| Mg | 59.0 | 56.50 | 57.0 |
| Na | 199.0 | 106.0 | 161.0 |
| K | 13.80 | 11.25 | 16.30 |
| Cl | 270.8 | 176.0 | 202.4 |
| Alk., as CaCO3 | 274.6 | 109.4 | 251.4 |
| SO4 | 1340 | 1275 | 1360 |
| F | 0.69 | 0.70 | 0.80 |
| NO3, as N | <0.1 | 0.3 | <0.1 |
| NO2, as N | <0.01 | <0.01 | 0.02 |
| Kjeld. N, as N | 10.3 | <0.2 | 5.0 |
| NH3, as N | 0.3 | <0.1 | 0.3 |
| TOC | 8.7 | 8.2 | 32.9 |
| DOC | NA | 2.3 | NA |
| B | 0.55 | 0.43 | 0.80 |
| Fe (tot) | NA | 0.048 | 0.610 |
| Mn | NA | 0.052 | 0.047 |
| As | <0.030 | <0.001 | <0.001 |
| Cd | NA | 0.014 | <0.005 |
| Cr | NA | <0.050 | <0.025 |
| Cu | NA | 0.050 | 0.046 |
| Ni | NA | 0.026 | 0.011 |
| Pb | NA | 0.062 | <0.030 |
| Se | <0.030 | 0.006 | <0.001 |
| Zn | NA | <0.010 | 0.009 |

DISSOLVED GASES

Sampling Date:

12/10/82 05/11/82 23/06/83

| | | | |
|-----|----|----|-----|
| CH4 | ND | ND | ND |
| C2 | NA | NA | 2.8 |

PURGEABLE ORGANICS

Sampling Date:

04/10/83

| | |
|---------------|-------|
| benzene | 0.011 |
| toluene | 0.268 |
| chlorobenzene | -- |
| ethylbenzene | -- |
| p-xylene | 0.033 |
| o-xylene | -- |
| cumene | -- |
| 1,2,4-TMB | 0.033 |
| naphthalene | 0.042 |

AQUEOUS ISOTOPES

Sampling Date:

12/10/82 03/11/82 11/05/83

| | | | |
|----------------|------|------|------|
| Delta O-18 | -9.5 | -8.8 | -9.8 |
| Delta H-2 | NA | NA | -66 |
| Tritium (T.U.) | 60 | 72 | 62 |

SAMPLING POINT:

UW10-2

Sampling date:

FIELD DATA

temp (C)
Eh (mV)
pH
cond. (uS)

LAB DATA

pH
cond. (uS)
hardness (CaCO3)
Ca (mg/l)
Mg
Na
K
Cl
Alk., as CaCO3
SO4
F
NO3, as N
NO2, as N
Kjeld. N, as N
NH3, as N
TOC
DOC
B
Fe (tot)
Mn
As
Cd
Cr
Cu
Ni
Pb
Se
Zn

DISSOLVED GASES

Sampling Date:

CH4
C2

PURGEABLE ORGANICS

Sampling Date:

benzene
toluene
chlorobenzene
ethylbenzene
p-xylene
o-xylene
cumene
1,2,4-TMB
naphthalene

AQUEOUS ISOTOPES

Sampling Date: 03/08/83

Delta O-18 -9.6
Delta H-2 -72
Tritium (1.0.) ND

SAMPLING POINT:

UW10-3

Sampling date:

FIELD DATA

temp (C)
Eh (mV)
pH
cond. (uS)

LAB DATA

pH
cond. (uS)
hardness (CaCO3)
Ca (mg/l)
Mg
Na
K
Cl
Alk., as CaCO3
SO4
F
NO3, as N
NO2, as N
Kjeld. N, as N
NH3, as N
TOC
DOC
B
Fe (tot)
Mn
As
Cd
Cr
Cu
Ni
Pb
Se
Zn

PURGEABLE ORGANICS

Sampling Date: 12/12/83

| | |
|---------------|-------|
| benzene | -- |
| toluene | 1.732 |
| chlorobenzene | 0.259 |
| ethylbenzene | 0.360 |
| p-xylene | 0.264 |
| o-xylene | 0.168 |
| cumene | 0.110 |
| 1,2,4-TMB | 0.148 |
| naptalene | 0.083 |

SAMPLING POINT:

UW 10-4

Sampling date:

FIELD DATA

temp (C)
El (EV)
pH
cond. (uS)

LAB DATA

pH
cond. (uS)
hardness (CaCO3)
Ca (mg/l)
Mg
Na
K
Cl
Alk., as CaCO3
SO4
F
NO3, as N
NO2, as N
Kjeld. N, as N
NH3, as N
TOC
DOC
E
Fe (tot)
Mn
As
Cd
Cr
Cu
Ni
Pb
Se
Zn

PURGEABLE ORGANICS

Sampling Date: 12/12/83

| | |
|---------------|-------|
| benzene | -- |
| toluene | 2.119 |
| chlorobenzene | 0.162 |
| ethylbenzene | 0.585 |
| p-xylene | 0.416 |
| o-xylene | 0.077 |
| cumene | -- |
| 1,2,4-TMB | 0.045 |
| naphthalene | -- |

SAMPLING POINT:

UW10-5

Sampling date:

FIELD DATA

temp. (C)
Eh (mV)
pH
cond. (uS)

LAE DATA

pH
cond. (uS)
hardness (CaCO3)
Ca (mg/l)
Mg
Na
K
Cl
Alk., as CaCO3
SO4
F
NO3, as N
NO2, as N
Kjeld. N, as N
NH3, as N
TCC
DOC
E
Fe (tot)
Mn
As
Cd
Cr
Cu
Ni
Pb
Se
Zn

PURGEABLE ORGANICS

Sampling Date: 12/12/83

| | |
|---------------|-------|
| benzene | 0.873 |
| toluene | 2.870 |
| chlorobenzene | 0.071 |
| ethylbenzene | 0.294 |
| p-xylene | 0.350 |
| o-xylene | 0.100 |
| cumene | -- |
| 1,2,4-TMB | 0.300 |
| naphthalene | 0.124 |

SAMPLING POINT:

UW10-6

Sampling date: 31/05/83

FIELD DATA

| | |
|------------|----|
| temp (C) | NA |
| En (mV) | NA |
| pH | NA |
| cond. (uS) | NA |

LAB DATA

| | |
|------------------|--------|
| pH | 5.70 |
| cond. (uS) | 6.0 |
| hardness (CaCO3) | <0.4 |
| Ca (mg/l) | <0.1 |
| Mg | <0.10 |
| Na | 0.5 |
| K | 0.80 |
| Cl | <0.2 |
| Alk., as CaCO3 | 3.2 |
| SO4 | <1.0 |
| F | <0.01 |
| NO3, as N | <0.1 |
| NO2, as N | <0.01 |
| Kjeld. N, as N | <0.1 |
| NH3, as N | <0.1 |
| TOC | NA |
| DOC | 0.7 |
| B | NA |
| Fe (tot) | <0.010 |
| Mn | <0.005 |
| As | <0.001 |
| Cd | <0.002 |
| Cr | <0.010 |
| Cu | <0.010 |
| Ni | <0.005 |
| Pb | <0.030 |
| Se | <0.001 |
| Zn | <0.010 |

PURGEABLE ORGANICS

Sampling Date:

benzene
toluene
chlorobenzene
ethylbenzene
p-xylene
o-xylene
cumene
1,2,4-TMB
naphthalene

SAMPLING POINT:

UW11-2

Sampling date:

FIELD DATA

temp (C)
Eh (mV)
pH
cond. (uS)

LAB DATA

pH
cond. (uS)
hardness (CaCO3)
Ca (mg/l)
Mg
Na
K
Cl
Alk., as CaCO3
SO4
F
NO3, as N
NO2, as N
Kjeld. N, as N
NH3, as N
TOC
DOC
B
Fe (tot)
Mn
As
Cd
Cr
Cu
Ni
Pb
Se
Zn

PURGEABLE ORGANICS

Sampling Date: 08/12/83

| | |
|---------------|-------|
| benzene | 0.343 |
| toluene | 2.691 |
| chlorobenzene | 0.194 |
| ethylbenzene | 1.258 |
| p-xylene | 0.538 |
| o-xylene | 0.091 |
| cumene | -- |
| 1,2,4-TMB | 0.013 |
| naphthalene | 0.003 |

SAMPLING POINT:

DW 11-3

Sampling date:

FIELD DATA

temp (C)
Eh (mV)
pH
cond. (uS)

LAB DATA

pH
cond. (uS)
hardness (CaCO3)
Ca (mg/l)
Mg
Na
K
Cl
Alk., as CaCO3
SO4
F
NO3, as N
NO2, as N
Kjeld. N, as N
NH3, as N
TOC
DOC
E
Fe (tot)
Mn
As
Cd
Cr
Cu
Ni
Pb
Se
Zn

PURGEABLE ORGANICS

Sampling Date: 08/12/83

| | |
|---------------|-------|
| benzene | -- |
| toluene | 1.267 |
| chlorobenzene | 0.241 |
| ethylbenzene | 0.646 |
| p-xylene | 0.286 |
| o-xylene | -- |
| cumene | -- |
| 1,2,4-TMB | 0.094 |
| naphthalene | 0.101 |

SAMPLING POINT:

OW11-5

Sampling date:

FIELD DATA

temp (C)
Eh (mV)
pH
cond. (uS)

LAB DATA

pH
cond. (uS)
hardness (CaCO3)
Ca (mg/l)
Mg
Na
K
Cl
Alk., as CaCO3
SO4
F
NO3, as N
NO2, as N
Kjeld. N, as N
NH3, as N
TOC
DOC
E
Fe (tot)
Mn
As
Cd
Cr
Cu
Ni
Pb
Se
Zn

PURGEABLE ORGANICS

Sampling Date: 08/12/83

| | |
|---------------|-------|
| benzene | 3.089 |
| toluene | 0.273 |
| chlorobenzene | 0.097 |
| ethylbenzene | 0.079 |
| p-xylene | 0.090 |
| o-xylene | -- |
| cumene | -- |
| 1,2,4-TMB | 0.066 |
| naphthalene | 0.142 |

SAMPLING POINT:

U# 12-1

Sampling date:
FIELD DATA

temp (C)
Eh (mV)
pH
Cond. (uS)
LAB DATA

pH
Cond. (uS)
hardness (CaCO3)
Ca (mg/l)
Mg
Na
K
Cl
Alk., as CaCO3
SO4
F
NO3, as N
NO2, as N
Kjeld. N, as N
NH3, as N
TOC
DOC
B
Fe (tot)
Mn
As
Cd
Cr
Cu
Ni
Pb
Se
Zn

DISSOLVED GASES

Sampling Date:

CH4
O2

PURGEABLE ORGANICS

Sampling Date:

benzene
toluene
chlorobenzene
ethylbenzene
p-xylene
o-xylene
cumene
1,2,4-TMB
naphthalene

AQUEOUS ISOTOPES

Sampling Date: 29/08/83

Delta O-18 -10.5
Delta H-2 -72
Tritium (T.U.) NA

SAMPLING POINT:

UW 12-3

Sampling date: 29/08/83 30/08/83 29/09/83

FIELD DATA

| | | | |
|------------|----|--------|----|
| temp (C) | NA | 729.0 | NA |
| Eh (mV) | NA | NA | NA |
| pH | NA | 6.65 | NA |
| cond. (uS) | NA | >50000 | NA |

LAB DATA

| | | | |
|------------------|--------|-------|--------|
| pH | NA | 7.06 | 6.80 |
| cond. (uS) | NA | 70000 | 75000 |
| hardness (CaCO3) | NA | 22462 | 24290 |
| Ca (mg/l) | NA | 6200 | 6900 |
| Mg | NA | 1700 | 1720 |
| Na | NA | 10700 | 11200 |
| K | NA | 206.0 | 200.0 |
| Cl | NA | 30380 | 33920 |
| Alk., as CaCO3 | NA | 231.6 | 185.8 |
| SO4 | NA | 1160 | 1275 |
| F | NA | NA | NA |
| NO3, as N | NA | 0.5 | 0.7 |
| NO2, as N | NA | <0.01 | 0.70 |
| Kjeld. N, as N | NA | 14.0 | 35.0 |
| NH3, as N | NA | 25.0 | 25.0 |
| TOC | 1090 | 503 | 110 |
| DOC | NA | 970.0 | 380.0 |
| B | 1.70 | NA | 4.80 |
| Fe (tot) | 0.46 | NA | 0.50 |
| Mn | 1.23 | NA | 0.750 |
| As | <0.001 | NA | 0.005 |
| Cd | 0.002 | NA | <0.005 |
| Cr | 0.087 | NA | 0.390 |
| Cu | 0.530 | NA | 0.180 |
| Ni | 0.012 | NA | <0.005 |
| Pb | <0.030 | NA | 0.054 |
| Se | <0.001 | NA | <0.001 |
| Zn | 0.650 | NA | 0.550 |

DISSOLVED GASES

Sampling Date: 29/09/83

| | |
|-----|----|
| CH4 | ND |
| O2 | NA |

PURGEABLE ORGANICS

Sampling Date: 07/11/83

| | |
|---------------|-------|
| benzene | 1.046 |
| toluene | 1.450 |
| chlorobenzene | -- |
| ethylbenzene | 0.266 |
| p-xylene | 0.745 |
| o-xylene | 0.232 |
| cumene | -- |
| 1,2,4-TMB | 0.238 |
| naphthalene | 0.331 |

AQUEOUS ISOTOPES

Sampling Date: 29/08/83

| | |
|----------------|------|
| Delta O-18 | -8.7 |
| Delta H-2 | -64 |
| Tritium (T.U.) | 35 |

SAMPLING POINT:

UW13-1

Sampling date:

FIELD DATA

temp (C)
En (mV)
pH
cond. (uS)

LAB DATA

pH
cond. (uS)
hardness (CaCO3)
Ca (mg/l)
Mg
Na
K
Cl
Alk., as CaCO3
SO4
F
NO3, as N
NO2, as N
Kjeld. N, as N
NH3, as N
TOC
DOC
B
Fe (tot)
Mn
As
Cd
Cr
Cu
Ni
Pb
Se
Zn

DISSOLVED GASES

Sampling Date: 22/10/82

CH4 ND
C2 NA

PURGEABLE ORGANICS

Sampling Date:

benzene
toluene
chlorobenzene
ethylbenzene
p-xylene
o-xylene
cumene
1,2,4-TMB
naphthalene

AQUEOUS ISOTOPES

Sampling Date: 19/10/82

Delta C-18 -10.3
Delta H-2 NA
Tritium (T.U.) 70

SAMPLING POINT:

UW13-2

Sampling date:

FIELD DATA

temp (C)
Eh (mV)
pH
Cond. (uS)

LAB DATA

pH
cond. (uS)
hardness (CaCO3)
Ca (mg/l)
Mg
Na
K
Cl
Alk., as CaCO3
SO4
F
NO3, as N
NO2, as N
Kjeld. N, as N
NH3, as N
TOC
DOC
B
Fe (tot)
Mn
As
Cd
Cr
Cu
Ni
PL
Se
Zn

PURGEABLE ORGANICS

Sampling Date:

benzene
toluene
chlorobenzene
ethybenzene
p-xylene
o-xylene
cumene
1,2,4-TMB
naphthalene

AQUEOUS ISOTOPES

Sampling Date: 12/05/83

Delta O-18 -8.0
Delta H-2 -63
Tritium (T.U.) 18

SAMPLING POINT:

U-13-5

Sampling date:

19/10/82 04/08/83 29/09/83

FIELD DATA

| | | | |
|------------|------|------|----|
| temp (C) | NA | 19.0 | NA |
| Em (mV) | +75 | NA | NA |
| pH | 7.02 | 5.55 | NA |
| cond. (uS) | NA | NA | NA |

LAB DATA

| | | | |
|------------------|--------|--------|--------|
| pH | 7.07 | 5.80 | 5.44 |
| cond. (uS) | 52900 | 87000 | 80000 |
| hardness (CaCO3) | 11886 | 24082 | 26690 |
| Ca (mg/l) | 3000 | 6500 | 7400 |
| Mg | 1070 | 1912 | 2000 |
| Na | 7850 | 15400 | 12600 |
| K | 182.0 | 290.0 | 200.0 |
| Cl | 21480 | 40680 | 36780 |
| Alk., as CaCO3 | 257.6 | 199.6 | 140.0 |
| SO4 | 1080 | 850.0 | 638.0 |
| F | NA | NA | NA |
| NO3, as N | 0.3 | <0.1 | <0.1 |
| NO2, as N | 0.03 | 0.02 | 0.03 |
| Kjeld. N, as N | 28.5 | NA | 50.0 |
| NH3, as N | 25.1 | 35.5 | 20.0 |
| TOC | 620 | 1630 | 1330 |
| DOC | NA | 2280 | NA |
| B | 3.30 | 3.80 | 5.0 |
| Fe (tot) | <0.04 | 48.0 | 40.0 |
| Mn | 1.050 | 10.30 | 16.0 |
| As | <0.030 | 0.001 | <0.001 |
| Cd | <0.002 | <0.002 | <0.010 |
| Cr | 0.039 | 0.150 | 0.380 |
| Cu | 0.089 | 0.370 | 0.170 |
| Ni | <0.010 | 0.060 | 0.090 |
| Pb | <0.012 | 0.080 | 0.064 |
| Se | <0.030 | <0.001 | <0.001 |
| Zn | 0.054 | 0.030 | 0.026 |

DISSOLVED GASES

Sampling Date: 19/10/82

| | |
|-----|-----|
| CH4 | 700 |
| O2 | NA |

PURGEABLE ORGANICS

Sampling Date: 29/09/83 03/10/83

| | | |
|---------------|-------|-------|
| benzene | 4.218 | 8.089 |
| toluene | 1.627 | 1.530 |
| chlorobenzene | 0.047 | -- |
| ethylbenzene | 0.046 | -- |
| p-xylene | 0.138 | 0.233 |
| o-xylene | 0.012 | -- |
| cumene | -- | -- |
| 1,2,4-TMB | 0.075 | 0.023 |
| naphthalene | 0.217 | 0.183 |

AQUEOUS ISOTOPES

Sampling Date: 19/10/82 04/08/83

| | | |
|----------------|------|------|
| Delta O-18 | -8.1 | -6.7 |
| Delta H-2 | NA | -58 |
| Tritium (T.U.) | 20 | 25 |

SAMPLING POINT:

UW13-o

Sampling date: 30/08/83

FIELD DATA

| | |
|------------|--------|
| temp (C) | 226.0 |
| Eh (mV) | NA |
| pH | 6.15 |
| cond. (uS) | >50000 |

LAE DATA

| | |
|------------------|--------|
| pH | 6.0 |
| cond. (uS) | 115000 |
| hardness (CaCO3) | 38756 |
| Ca (mg/l) | 11000 |
| Mg | 2750 |
| Na | 23000 |
| K | 460.0 |
| Cl | 59520 |
| Alk., as CaCO3 | 81.6 |
| SO4 | 1120 |
| F | NA |
| NO3, as N | NA |
| NO2, as N | NA |
| Kjeld. N, as N | 23.0 |
| NH3, as N | NA |
| TOC | 1170 |
| DOC | NA |
| B | 0.97 |
| Fe (tot) | 33.0 |
| Mn | 4.90 |
| As | <0.001 |
| Cd | <0.002 |
| Cr | 0.490 |
| Cu | 0.710 |
| Ni | 0.013 |
| Pb | 0.750 |
| Se | <0.001 |
| Zn | 0.410 |

DISSOLVED GASES

Sampling Date: 22/10/82

| | |
|-----|-----|
| CH4 | 400 |
| O2 | NA |

PURGEABLE ORGANICS

Sampling Date:

benzene
toluene
chlorobenzene
ethylbenzene
p-xylene
o-xylene
cumene
1,2,4-TMB
naphthalene

AQUEOUS ISOTOPES

Sampling Date: 19/10/82 30/08/83

| | | |
|----------------|------|------|
| Delta O-18 | -8.1 | -6.1 |
| Delta H-2 | NA | -53 |
| Tritium (T.O.) | 90 | 24 |

SAMPLING POINT:

UW 14-1

Sampling date: 21/10/82 03/10/83
FIELD DATA

| | | |
|------------|------|-------|
| temp (C) | 9.0 | 019.0 |
| Eh (mV) | -136 | NA |
| pH | 6.82 | 6.85 |
| Cond. (uS) | NA | NA |

LAB DATA

| | | |
|------------------|--------|--------|
| pH | 7.04 | 6.94 |
| cond. (uS) | 8950 | 10000 |
| hardness (CaCO3) | 2733 | 3117 |
| Ca (mg/l) | 700.0 | 812.5 |
| Mg | 240.0 | 265.0 |
| Na | 980.0 | 1180 |
| K | 24.0 | 25.0 |
| Cl | 2550 | 2906 |
| Alk., as CaCO3 | 140.6 | 277.2 |
| SO4 | 860.0 | 1110 |
| F | 0.70 | 0.70 |
| NO3, as N | 0.2 | <0.1 |
| NO2, as N | <0.01 | <0.01 |
| Kjeld. N, as N | 3.7 | 12.5 |
| NH3, as N | 2.0 | 2.6 |
| TOC | 11 | 8.3 |
| DOC | NA | NA |
| E | 2.10 | 1.80 |
| Fe (tot) | 0.28 | 0.046 |
| Mn | 0.30 | 0.084 |
| As | <0.030 | 0.014 |
| Cd | <0.002 | <0.005 |
| Cr | 0.011 | <0.025 |
| Cu | 0.035 | 0.060 |
| Ni | <0.010 | 0.015 |
| Pb | <0.012 | <0.030 |
| Se | <0.030 | <0.001 |
| Zn | 0.017 | 0.025 |

DISSOLVED GASES

Sampling Date: 21/10/82 03/12/82 03/10/83

| | | | |
|-----|-----|-----|-----|
| CH4 | 300 | 185 | 110 |
| C2 | NA | NA | ND |

PURGEABLE ORGANICS

Sampling Date: 03/10/83

| | |
|---------------|-------|
| benzene | 0.118 |
| toluene | 0.126 |
| chlorobenzene | -- |
| ethylbenzene | -- |
| p-xylene | 0.055 |
| o-xylene | -- |
| cumene | -- |
| 1,2,4-TMB | 0.029 |
| naphthalene | 0.025 |

AQUEOUS ISOTOPES

Sampling Date: 21/10/82 30/11/82 04/10/83

| | | | |
|----------------|------|------|------|
| Delta O-18 | -9.8 | -9.7 | |
| Delta H-2 | NA | NA | NA |
| Tritium (T.O.) | 10 | 18 | 9(4) |

SAMPLING POINT:

UW 14-3

Sampling date: 03/10/83

FIELD DATA

| | |
|------------|----|
| temp (C) | NA |
| Eh (mV) | NA |
| pH | NA |
| cond. (uS) | NA |

LAB DATA

| | |
|------------------|--------|
| pH | 6.27 |
| cond. (uS) | 14150 |
| hardness (CaCO3) | 3451 |
| Ca (mg/l) | 988.0 |
| Mg | 240.0 |
| Na | 1910 |
| K | 53.0 |
| Cl | 5120 |
| Alk., as CaCO3 | 742.0 |
| SO4 | 60.0 |
| F | 00.40 |
| NO3, as N | 0.7 |
| NO2, as N | 0.33 |
| Kjeld. N, as N | 12.5 |
| NH3, as N | 3.4 |
| TOC | 1780 |
| DOC | 21810 |
| E | 1.10 |
| Fe (tot) | 0.340 |
| Mn | 6.50 |
| As | 0.001 |
| Cd | <0.005 |
| Cr | 0.150 |
| Cu | 0.110 |
| Ni | 0.043 |
| Pb | 0.033 |
| Se | <0.001 |
| Zn | <0.005 |

PURGEABLE ORGANICS

Sampling Date: 03/10/83

| | |
|---------------|--------|
| benzene | 16.855 |
| toluene | 1.902 |
| chlorobenzene | 0.074 |
| ethylenzene | 0.714 |
| p-xylene | 1.872 |
| o-xylene | 0.707 |
| cumene | 0.103 |
| 1,2,4-TMB | 0.084 |
| naphthalene | 0.525 |

AQUEOUS ISOTOPES

Sampling Date: 12/05/83

| | |
|----------------|------|
| Delta O-18 | -6.7 |
| Delta H-2 | -55 |
| Tritium (T.U.) | 62 |

SAMPLING POINT:

UW14-4

Sampling date:

FIELD DATA

temp (C)

En (mV)

pH

cond. (uS)

LAB DATA

pH

cond. (uS)

hardness (CaCO₃)

Ca (mg/l)

Mg

Na

K

Cl

Alk., as CaCO₃

SO₄

F

NO₃, as N

NO₂, as N

Kjeld. N, as N

NH₃, as N

TOC

DOC

B

Fe (tot)

Mn

As

Cd

Cr

Cu

Ni

Pb

Se

Zn

PURGEABLE ORGANICS

| Sampling Date: | 10/11/83 | 10/11/83 |
|----------------|----------|----------|
| | (A) | (E) |
| benzene | 5.251 | 5.196 |
| toluene | 6.451 | 10.560 |
| chlorobenzene | -- | -- |
| ethylbenzene | 0.748 | 0.801 |
| p-xylene | 2.920 | 3.033 |
| o-xylene | 1.378 | 1.354 |
| cumene | 0.038 | 0.037 |
| 1,2,4-TMB | 1.086 | 1.037 |
| naptalene | 0.345 | 0.386 |

SAMPLING POINT:

OW 14-5

Sampling date:

FIELD DATA

temp (C)
Eh (mV)
pH
cond. (uS)

LAE DATA

pH
cond. (uS)
hardness (CaCO₃)
Ca (mg/l)
Mg
Na
K
Cl
Alk., as CaCO₃
SO₄
F
NO₃, as N
NO₂, as N
Kjeld. N, as N
NH₃, as N
TOC
DOC
E
Fe (tot)
Mn
As
Cd
Cr
Cu
Ni
Pb
Se
Zn

PUROGEABLE ORGANICS

| Sampling Date: | 10/11/83 (B?) | 10/11/83 (A) |
|----------------|------------------|-----------------|
| benzene | 6.038 | 5.143 |
| toluene | 0.699 | 1.274 |
| chlorobenzene | -- | -- |
| ethylbenzene | 0.145 | 0.333 |
| p-xylene | 0.378 | 0.949 |
| o-xylene | 0.151 | 0.360 |
| cumene | -- | -- |
| 1,2,4-TMB | 0.273 | 0.495 |
| naphthalene | 0.326 | 0.134 |

SAMPLING POINT:

UW 15-1

Sampling date: 24/09/82 11/05/83 20/10/83
 FIELD DATA

| | | | |
|------------|------|------|-------|
| temp (C) | NA | 10.0 | 211.0 |
| En (mv) | NA | NA | NA |
| pH | 6.55 | 6.45 | 7.20 |
| cond. (uS) | NA | 650 | NA |

LAB DATA

| | | | |
|------------------|--------|--------|--------|
| pH | 7.44 | 7.64 | 7.34 |
| cond. (uS) | 1247 | 1020 | 1530 |
| hardness (CaCO3) | 679.9 | 559.1 | 743.8 |
| Ca (mg/l) | 182.5 | 142.5 | 186.0 |
| Mg | 54.60 | 49.50 | 68.0 |
| Na | 37.2 | 31.5 | 65.0 |
| K | 1.90 | 1.25 | 2.0 |
| Cl | 70.0 | 33.4 | 133.4 |
| Alk., as CaCO3 | 343.2 | 340.0 | 324.4 |
| SO4 | 310 | 237.5 | 330.0 |
| F | 0.65 | 0.52 | 0.70 |
| NO3, as N | <0.1 | <0.1 | <0.1 |
| NO2, as N | <0.01 | <0.01 | 0.02 |
| Kjeld. N, as N | <0.2 | 0.7 | 0.3 |
| NH3, as N | 0.1 | <0.1 | 0.2 |
| TOC | 15 | 5.5 | 7.2 |
| DOC | NA | 2.1 | 3.1 |
| B | 0.03 | <0.04 | 0.10 |
| Fe (tot) | 0.190 | <0.050 | 0.140 |
| Mn | 0.033 | 0.015 | 0.025 |
| As | <0.030 | <0.001 | <0.001 |
| Cd | 0.0009 | <0.010 | <0.005 |
| Cr | 0.007 | <0.050 | <0.025 |
| Cu | 0.028 | <0.010 | 0.016 |
| Ni | 0.007 | 0.015 | 0.012 |
| Pb | 0.013 | 0.080 | <0.030 |
| Se | <0.030 | <0.001 | <0.001 |
| Zn | 0.270 | 0.420 | 0.450 |

DISSOLVED GASES

Sampling Date: 29/06/83 02/11/83

| | | |
|-----|------|----|
| CH4 | ND | ND |
| CO2 | 0.35 | |

PURGEABLE ORGANICS

Sampling Date: 20/10/83

| | |
|---------------|-------|
| benzene | 0.176 |
| toluene | 0.503 |
| chlorobenzene | -- |
| ethylbenzene | 0.091 |
| p-xylene | 0.219 |
| o-xylene | -- |
| cumene | -- |
| 1,2,4-TMB | 0.204 |
| naphthalene | 0.105 |

AQUEOUS ISOTOPES

Sampling Date: 24/09/82 11/05/83

| | | |
|----------------|------|------|
| Delta C-18 | -8.5 | -8.9 |
| Delta H-2 | NA | -48 |
| Tritium (T.U.) | 70 | 70 |

SAMPLING POINT:

UW 15-2

Sampling date: 24/09/82 11/05/83 20/10/83
 FIELD DATA

| | 24/09/82 | 11/05/83 | 20/10/83 |
|------------|----------|----------|----------|
| temp (C) | NA | 13.0 | 13.0 |
| En (mV) | NA | NA | NA |
| pH | 6.75 | 6.80 | 7.85 |
| cond. (uS) | NA | 22000 | NA |

LAB DATA

| | 24/09/82 | 11/05/83 | 20/10/83 |
|------------------|----------|----------|----------|
| pH | 7.45 | 7.52 | 7.24 |
| cond. (uS) | 24820 | 24800 | 27700 |
| hardness (CaCO3) | 2787 | 1066 | 1611 |
| Ca (mg/l) | 850.0 | 325.0 | 490.0 |
| Mg | 162.0 | 62.0 | 94.0 |
| Na | 5500 | 5750 | 6000 |
| K | 20.0 | 17.50 | 20.30 |
| Cl | 8725 | 9420 | 10100 |
| Alk., as CaCO3 | 276.6 | 308.0 | 294.6 |
| SO4 | 780.0 | 380.0 | 920.0 |
| F | 0.47 | 0.65 | 0.70 |
| NO3, as N | 0.1 | 0.3 | 0.2 |
| NO2, as N | <0.01 | <0.01 | 0.02 |
| Kjeld. N, as N | 1.1 | 1.4 | 5.0 |
| NH3, as N | 1.5 | 0.8 | 0.5 |
| TOC | 310 | 15.9 | 16.3 |
| DOC | NA | NA | 17.0 |
| B | 0.33 | 0.32 | 0.37 |
| Fe (tot) | <0.002 | 0.140 | 0.170 |
| Mn | <0.001 | 0.120 | 0.140 |
| As | <0.030 | <0.001 | <0.001 |
| Cd | <0.0004 | 0.013 | <0.005 |
| Cr | 0.002 | <0.050 | <0.025 |
| Cu | <0.001 | 0.036 | 0.034 |
| Ni | 0.005 | 0.019 | <0.005 |
| Pb | <0.010 | 0.065 | <0.030 |
| Se | <0.030 | <0.001 | <0.001 |
| Zn | 0.001 | 0.020 | 0.028 |

DISSOLVED GASES

Sampling Date: 29/06/83 02/11/83

| | 29/06/83 | 02/11/83 |
|-----|----------|----------|
| CH4 | ND | ND |
| CO2 | 0.20 | |

PURGEABLE ORGANICS

Sampling Date: 20/10/83 20/10/83

| | (A) | (E) |
|---------------|-------|-------|
| benzene | 0.224 | 0.420 |
| toluene | 0.442 | 0.192 |
| chlorobenzene | -- | -- |
| ethylnbenzene | 0.029 | 0.023 |
| p-xylene | 0.097 | 0.063 |
| o-xylene | -- | -- |
| cumene | -- | -- |
| 1,2,4-TMB | 0.100 | 0.057 |
| napthalene | 0.025 | 0.075 |

AQUEOUS ISOTOPES

Sampling Date: 24/09/82 11/05/83

| | 24/09/82 | 11/05/83 |
|----------------|----------|----------|
| Delta O-18 | -9.7 | -9.6 |
| Delta H-2 | NA | -69 |
| Tritium (T.U.) | 80 | 167 |

SAMPLING POINT:

UM16-3

Sampling date: 16/05/83 06/10/83
 FIELD DATA

| | | |
|------------|--------|-------|
| temp (C) | 9.0 | 217.0 |
| En (mV) | NA | NA |
| pH | 5.70 | 6.55 |
| cond. (uS) | >50000 | NA |

LAB DATA

| | | |
|------------------|--------|--------|
| pH | 6.60 | 6.06 |
| cond. (uS) | 148000 | 150000 |
| hardness (CaCO3) | 59683 | 58605 |
| Ca (mg/l) | 16500 | 16400 |
| Mg | 4550 | 4300 |
| Na | 58250 | 29400 |
| K | 445.0 | 490.0 |
| Cl | 98001 | 84560 |
| Alk., as CaCO3 | NA | 45.0 |
| SO4 | 1025 | 1080 |
| F | NA | NA |
| NO3, as N | <0.1 | <0.1 |
| NO2, as N | 0.03 | 0.02 |
| Kjeld. N, as N | NA | 65.0 |
| NH3, as N | 53.5 | 51.0 |
| TOC | 14.5 | 4.2 |
| DOC | NA | NA |
| E | 5.60 | 3.20 |
| Fe (tot) | 0.850 | 0.860 |
| Mn | 1.60 | 1.10 |
| As | 0.001 | <0.001 |
| Cd | 0.001 | <0.005 |
| Cr | 0.170 | 0.042 |
| Cu | 1.30 | 0.460 |
| Ni | 0.150 | 0.008 |
| Pb | 1.10 | 0.086 |
| Se | 0.002 | <0.001 |
| Zn | 0.140 | 0.036 |

DISSOLVED GASES

Sampling Date: 06/07/83 12/10/83

| | | |
|-----|-----|----|
| CH4 | 150 | 40 |
| O2 | ND | ND |

PURGEABLE ORGANICS

Sampling Date: 06/10/83

| | |
|---------------|-------|
| benzene | 0.762 |
| toluene | 1.504 |
| chlorobenzene | -- |
| ethylbenzene | 0.103 |
| p-xylene | 0.144 |
| o-xylene | 0.090 |
| cumene | -- |
| 1,2,4-TMB | 0.102 |
| naphthalene | 0.096 |

AQUEOUS ISOTOPES

Sampling Date: 16/05/83 12/10/83

| | | |
|----------------|------|-------|
| Delta O-18 | -7.8 | |
| Delta H-2 | -66 | |
| Tritium (T.U.) | ND | 4 (2) |

SAMPLING POINT:

UW 16-4

Sampling date:

FIELD DATA

temp (C)
Eh (mV)
pH
cond. (uS)
LAB DATA

pH
cond. (uS)
hardness (CaCO3)
Ca (mg/l)
Mg
Na
K
Cl
Alk., as CaCO3
SO4
F
NO3, as N
NO2, as N
Kjeld. N, as N
NH3, as N
TOC
DOC
I
Fe (tot)
Mn
As
Cd
Cr
Cu
Ni
Pb
Se
Zn

PURGABLE ORGANICS

Sampling Date: 15/11/83

| | |
|---------------|-------|
| benzene | 0.732 |
| toluene | 4.572 |
| chlorobenzene | -- |
| ethylbenzene | 0.653 |
| p-xylene | 1.396 |
| o-xylene | 0.583 |
| cumene | -- |
| 1,2,4-TMB | 0.573 |
| naphthalene | 0.026 |

SAMPLING POINT:

UW 16-5

Sampling date:
FIELD DATA

temp (C)
Eh (mV)
pH
Cond. (uS)
LAB DATA

pH
Cond. (uS)
hardness (CaCO3)
Ca (mg/l)
Mg
Na
K
Cl
Alk., as CaCO3
SO4
F
NO3, as N
NO2, as N
Kjeld. N, as N
NH3, as N
TOC
DOC
Fe (tot)
Mn
As
Cd
Cr
Cu
Ni
Pb
Se
Zn

PURGEABLE ORGANICS

Sampling Date: 15/11/83

| | |
|---------------|-------|
| benzene | 1.017 |
| toluene | 7.817 |
| chlorobenzene | -- |
| ethylbenzene | 0.211 |
| p-xylene | 0.742 |
| o-xylene | 0.174 |
| cumene | -- |
| 1,2,4-TMB | 0.207 |
| naphthalene | 0.164 |

SAMPLING POINT:

UW17-1

Sampling date: 02/08/83 25/10/83
FIELD DATA

| | | |
|------------|------|------|
| temp (C) | 16.0 | 9.5 |
| Em (mv) | NA | NA |
| pH | 6.85 | 6.95 |
| cond. (uS) | 2580 | NA |

LAB DATA

| | | |
|-------------------------------|--------|--------|
| pH | 7.10 | 7.01 |
| cond. (uS) | 3200 | 2900 |
| hardness (CaCO ₃) | 629.9 | 698.0 |
| Ca (mg/l) | 114.0 | 128.0 |
| Mg | 84.0 | 92.0 |
| Na | 530.0 | 400.0 |
| K | 35.50 | 41.80 |
| Cl | 533.0 | 430.8 |
| Alk., as CaCO ₃ | 2614.4 | 676.8 |
| SO ₄ | 265.0 | 245.0 |
| F | 1.39 | 01.05 |
| NO ₃ , as N | <0.1 | <0.1 |
| NO ₂ , as N | 0.03 | <0.01 |
| Kjeld. N, as N | 21.1 | 25.0 |
| NH ₃ , as N | 17.2 | 20.5 |
| TOC | 52.3 | NA |
| DOC | 140.0 | 150.0 |
| E | 3.40 | 3.70 |
| Fe (tot) | 13.30 | 9.70 |
| Mn | 1.130 | 1.60 |
| As | 0.001 | 0.001 |
| Cd | <0.002 | <0.005 |
| Cr | 0.010 | <0.025 |
| Cu | 0.010 | 0.020 |
| Ni | 0.030 | 0.043 |
| Pb | 0.040 | <0.030 |
| Se | <0.001 | <0.001 |
| Zn | 0.090 | 0.033 |

DISSOLVED GASES

Sampling Date: 25/10/83

| | |
|-----------------|-----|
| CH ₄ | 390 |
| O ₂ | NA |

PURGEABLE ORGANICS

Sampling Date: 25/10/83

| | |
|---------------|-------|
| benzene | 2.425 |
| toluene | 0.151 |
| chlorobenzene | 1.454 |
| ethylbenzene | 0.151 |
| p-xylene | 0.875 |
| o-xylene | -- |
| cumene | 0.440 |
| 1,2,4-TMB | 0.108 |
| naphthalene | 0.117 |

AQUEOUS ISOTOPES

Sampling Date: 02/08/83

| | |
|----------------|------|
| Delta O-16 | -6.8 |
| Delta H-2 | -50 |
| Tritium (T.U.) | 71 |

SAMPLING POINT:

UW17-2

Sampling date: 02/08/83 25/10/83
 FIELD DATA

| | | |
|------------|------|-------|
| temp. (C) | 16.0 | 710.0 |
| En (mV) | NA | NA |
| pH | 6.85 | 6.55 |
| cond. (uS) | 5200 | NA |

LAB DATA

| | | |
|------------------|--------|--------|
| pH | 7.0 | 6.77 |
| cond. (uS) | 6400 | 4060 |
| hardness (CaCO3) | 1222 | 1157 |
| Ca (mg/l) | 160.0 | 270.0 |
| Mg | 200.0 | 117.5 |
| Na | 980.0 | 460.0 |
| K | 86.0 | 29.60 |
| Cl | 1148 | 902.0 |
| Alk., as CaCO3 | 1746 | 721.4 |
| SO4 | 170.0 | 130.0 |
| F | 1.02 | 90.60 |
| NO3, as N | <0.1 | <0.1 |
| NO2, as N | 0.03 | <0.01 |
| Kjeld. N, as N | 970.0 | 12.0 |
| NH3, as N | 56.0 | 8.5 |
| TOC | 196 | NA |
| DOC | 180.0 | 47.0 |
| B | 11.0 | 2.40 |
| Fe (tot) | 14.0 | 0.350 |
| Mn | 0.50 | 0.580 |
| As | 0.003 | <0.001 |
| Cd | <0.002 | <0.005 |
| Cr | 0.020 | <0.025 |
| Cu | 0.020 | 0.031 |
| Ni | 0.060 | 0.073 |
| Pb | <0.030 | <0.030 |
| Se | 0.001 | <0.001 |
| Zn | 0.130 | 0.021 |

DISSOLVED GASES

Sampling Date: 25/10/83

| | |
|-----|-----|
| CH4 | 520 |
| O2 | NA |

PURGEABLE ORGANICS

Sampling Date: 25/10/83 25/10/83

| | (A) | (E) |
|---------------|-------|-------|
| benzene | 1.046 | 1.057 |
| toluene | 0.163 | 0.074 |
| chlorobenzene | 0.439 | 0.362 |
| ethylbenzene | 0.105 | 0.004 |
| p-xylene | 0.382 | 0.227 |
| o-xylene | -- | -- |
| cumene | 0.161 | 0.135 |
| 1,2,4-TMB | 0.323 | 0.192 |
| naphthalene | 0.110 | 0.014 |

AQUEOUS ISOCTES

Sampling Date: 02/08/83

| | |
|----------------|------|
| Delta C-18 | -8.5 |
| Delta H-2 | -57 |
| Iritium (I.U.) | 117 |

SAMPLING POINTS:

DW 17-5

Sampling date: 24/06/83
FIELD DATA

| | |
|------------|------|
| temp (C) | 18.0 |
| Eh (mV) | NA |
| pH | 6.05 |
| cond. (uS) | 5000 |

LAB DATA

| | |
|------------------|--------|
| pH | |
| cond. (uS) | |
| hardness (CaCO3) | |
| Ca (mg/l) | |
| Mg | |
| Na | |
| K | |
| Cl | |
| Alk., as CaCO3 | |
| SO4 | |
| F | |
| NO3, as N | |
| NO2, as N | |
| Kjeld. N, as N | |
| NH3, as N | |
| IOC | |
| DOC | |
| B | 7.20 |
| Fe (tot) | |
| Mn | NA |
| As | <0.001 |
| Cd | NA |
| Cr | NA |
| Cu | NA |
| Ni | NA |
| Pb | NA |
| Se | <0.001 |
| Zn | NA |

PURGEABLE ORGANICS

Sampling Date: 25/10/83

| | |
|---------------|-------|
| benzene | 0.591 |
| toluene | 1.963 |
| chlorobenzene | -- |
| ethylbenzene | 0.272 |
| p-xylene | 0.213 |
| o-xylene | -- |
| cumene | -- |
| 1,2,4-TMB | 0.114 |
| naphthalene | 0.025 |

AQUEOUS ISOTOPES

Sampling Date: 24/06/83

| | |
|----------------|------|
| Delta O-18 | -9.7 |
| Delta H-2 | -73 |
| Tritium (T.U.) | 2 |

SAMPLING POINT:

DW18-1

Sampling date: 28/07/83 19/10/83
 FIELD DATA

| | | |
|------------|------|------|
| temp (C) | NA | 10.0 |
| Em (mV) | NA | NA |
| pH | 6.70 | 7.05 |
| cond. (uS) | 2100 | NA |

LAB DATA

| | | |
|------------------|---------|--------|
| pH | 7.50 | 7.16 |
| cond. (uS) | 1960 | 1700 |
| hardness (CaCO3) | 916.8 | 903.5 |
| Ca (mg/l) | 196.0 | 222.0 |
| Mg | 104.0 | 85.0 |
| Na | 48.5 | 25.5 |
| K | 18.25 | 15.70 |
| Cl | 227.4 | 180.4 |
| Alk., as CaCO3 | 510.2 | 453.4 |
| SO4 | 200.0 | 230.0 |
| F | 0.65 | 0.10 |
| NO3, as N | <0.1 | <0.1 |
| NO2, as N | <0.01 | 0.02 |
| Kjeld. N, as N | <0.3 | 1.8 |
| NH3, as N | 1.4 | 1.3 |
| TOC | 61.5 | 11.6 |
| DOC | 96.0 | 8.7 |
| B | 1.50 | 3.90 |
| Fe (tot) | 0.29 | 0.059 |
| Mn | 0.040 | 0.026 |
| As | 0.001 | <0.001 |
| Cd | <0.0002 | <0.005 |
| Cr | 0.017 | <0.025 |
| Cu | 0.015 | 0.021 |
| Ni | 0.017 | 0.018 |
| Pb | 0.003 | <0.030 |
| Se | <0.001 | <0.001 |
| Zn | 0.003 | 0.006 |

DISSOLVED GASES

Sampling Date: 28/07/83 19/10/83

| | | |
|-----|------|----|
| CH4 | NA | 50 |
| O2 | 0.48 | |

PURGEABLE ORGANICS

Sampling Date: 19/10/83 19/10/83

| | (A) | (B) |
|---------------|-------|-------|
| benzene | 0.467 | 0.217 |
| toluene | 1.646 | 1.009 |
| chlorobenzene | -- | -- |
| ethylbenzene | 1.146 | 0.555 |
| p-xylene | 2.473 | 1.231 |
| o-xylene | 1.115 | 0.529 |
| cumene | 0.398 | 0.185 |
| 1,2,4-IMB | 4.465 | 2.328 |
| naphthalene | 0.634 | 0.292 |

AQUEOUS ISOTOPES

Sampling Date: 28/07/83

| | |
|----------------|------|
| Delta C-16 | -9.6 |
| Delta H-2 | -60 |
| Tritium (1.U.) | 105 |

SAMPLING POINT:

UW 18-2

Sampling date: 28/07/83 20/10/83
FIELD DATA

| | | |
|------------|-------|----|
| temp (C) | 226.0 | NA |
| Eh (mV) | NA | NA |
| pH | 6.85 | NA |
| cond. (uS) | 3000 | NA |

LAB DATA

| | | |
|------------------|--------|--------|
| pH | 7.44 | |
| cond. (uS) | 3800 | |
| hardness (CaCO3) | 1562 | |
| Ca (mg/l) | 465.0 | |
| Mg | 102.5 | |
| Na | 260.0 | |
| K | 19.0 | |
| Cl | 525.2 | |
| Alk., as CaCO3 | 348.2 | |
| SO4 | 1100 | |
| F | 0.56 | |
| NO3, as N | <0.1 | |
| NO2, as N | <0.01 | |
| Kjeld. N, as N | 0.6 | |
| NH3, as N | 2.5 | |
| TOC | 67.6 | 14.9 |
| DOC | 72.0 | NA |
| E | 1.60 | 1.80 |
| Fe (tot) | <0.02 | 0.052 |
| Mn | 0.017 | 0.047 |
| As | 0.001 | 0.001 |
| Cd | 0.0002 | <0.005 |
| Cr | 0.015 | <0.025 |
| Cu | 0.022 | 0.018 |
| Ni | 0.005 | <0.005 |
| Pb | <0.003 | <0.030 |
| Se | <0.001 | <0.001 |
| Zn | 0.004 | 0.033 |

DISSOLVED GASES

Sampling Date: 28/07/83

| | |
|-----|----|
| CH4 | NA |
| C2 | ND |

PURGEABLE ORGANICS

Sampling Date: 19/10/83

| | |
|---------------|--------|
| benzene | 0.530 |
| toluene | 16.307 |
| chlorobenzene | -- |
| ethylbenzene | 0.173 |
| p-xylene | 0.530 |
| o-xylene | -- |
| cumene | -- |
| 1,2,4-TMB | 0.239 |
| naphthalene | 0.107 |

AQUEOUS ISOTOPES

Sampling Date: 28/07/83

| | |
|----------------|------|
| Delta O-18 | -9.7 |
| Delta H-2 | -67 |
| Tritium (T.U.) | 34 |

SAMPLING POINT:

UW18-3

Sampling date: 17/05/83 20/10/83

FIELD DATA

| | |
|------------|-------|
| temp (C) | 17.5 |
| Eh (mV) | NA |
| pH | 7.0 |
| cond. (uS) | 11200 |

LAB DATA

| | | |
|------------------|--------|-------|
| pH | 7.53 | 7.51 |
| cond. (uS) | 14000 | 13500 |
| hardness (CaCO3) | 5182 | 4332 |
| Ca (mg/l) | 1500 | 1250 |
| Mg | 350.0 | 295.0 |
| Na | 1630 | 1480 |
| K | 40.0 | 39.0 |
| Cl | 4288 | 4022 |
| Alk., as CaCO3 | NA | 389.4 |
| SO4 | 1438 | 1300 |
| F | 1.0 | 90.90 |
| NO3, as N | <0.1 | 0.3 |
| NO2, as N | <0.01 | 0.02 |
| Kjeld. N, as N | NA | 10.0 |
| NH3, as N | 3.5 | 2.3 |
| TOC | 72.1 | 66.8 |
| DOC | 145.0 | 224.0 |
| E | 4.20 | NA |
| Fe (tot) | 0.045 | 2.36 |
| Mn | 0.140 | 0.060 |
| As | 0.003 | |
| Cd | 0.011 | |
| Cr | 0.064 | |
| Cu | 0.140 | |
| Ni | 0.023 | |
| Pb | <0.060 | |
| Se | <0.001 | |
| Zn | <0.010 | |

DISSOLVED GASES

Sampling Date: 29/06/83

| | |
|-----|----|
| CH4 | ND |
| O2 | ND |

PURGEABLE ORGANICS

Sampling Date: 20/10/83

| | |
|---------------|-------|
| benzene | -- |
| toluene | 7.875 |
| chlorobenzene | -- |
| ethylbenzene | 0.211 |
| p-xylene | 0.426 |
| o-xylene | 0.165 |
| cumene | -- |
| 1,2,4-TMB | 0.271 |
| naphthalene | 0.206 |

AQUEOUS ISOTOPIES

Sampling Date: 17/05/83

| | |
|----------------|------|
| Delta C-18 | -9.8 |
| Delta H-2 | -69 |
| Tritium (T.U.) | 40 |

SAMPLING POINT:

UW18-5

Sampling date: 17/05/83 19/10/83

FIELD DATA

| | | |
|------------|-------|-------|
| temp (C) | 14.0 | 210.0 |
| Em (mV) | NA | NA |
| pH | 7.35 | 7.10 |
| cond. (uS) | 49000 | NA |

LAB DATA

| | | |
|------------------|--------|--------|
| pH | 6.90 | 7.25 |
| cond. (uS) | 66000 | 72000 |
| hardness (CaCO3) | 22200 | 21746 |
| Ca (mg/l) | 6000 | 5700 |
| Mg | 1760 | 1825 |
| Na | 10900 | 10500 |
| K | 507.5 | 192.0 |
| Cl | 28740 | 30940 |
| Alk., as CaCO3 | NA | 305.6 |
| SO4 | 1388 | 1480 |
| F | NA | NA |
| NO3, as N | <0.1 | 0.2 |
| NO2, as N | <0.01 | 0.02 |
| Kjeld. N, as N | NA | 25.0 |
| NH3, as N | 25.2 | 25.0 |
| IOC | NA | 12.2 |
| DOC | 120.0 | NA |
| B | 8.40 | 5.80 |
| Fe (tot) | 0.083 | 0.084 |
| Mn | 0.360 | 0.280 |
| As | 0.007 | 0.001 |
| Cd | 0.013 | <0.005 |
| Cr | 0.10 | 0.034 |
| Cu | 0.390 | 0.280 |
| Ni | 0.020 | 0.007 |
| Pb | <0.060 | <0.030 |
| Se | <0.001 | <0.001 |
| Zn | 0.066 | 0.016 |

DISSOLVED GASES

Sampling Date: 29/06/83 19/10/83

| | | |
|-----|----|----|
| CH4 | ND | ND |
| C2 | ND | |

PURGEABLE ORGANICS

Sampling Date: 19/10/83

| | |
|---------------|-------|
| benzene | 0.077 |
| toluene | 1.343 |
| chlorobenzene | -- |
| ethylbenzene | 0.029 |
| p-xylene | 0.086 |
| o-xylene | -- |
| cumene | -- |
| 1,2,4-TMB | 0.051 |
| naphthalene | 0.071 |

AQUEOUS ISOTOPES

Sampling Date: 17/05/83

| | |
|----------------|-------|
| Delta O-18 | -11.3 |
| Delta H-2 | -80 |
| Tritium (T.O.) | 20 |

SAMPLING POINT:

DW 19-1

Sampling date: 16/05/83 16/05/83 22/11/83
 FIELD DATA (A) (B)

| | (A) | (B) | |
|------------|------|-----|----|
| temp (C) | 10.0 | NA | NA |
| En (mV) | NA | NA | NA |
| pH | 6.55 | NA | NA |
| cond. (uS) | 2680 | NA | NA |

LAE DATA

| | (A) | (B) | |
|------------------|--------|--------|--------|
| pH | 7.08 | 7.15 | 7.02 |
| cond. (uS) | 3980 | 3880 | 3800 |
| hardness (CaCO3) | 1299 | 1272 | 1287 |
| Ca (mg/l) | 335.0 | 332.5 | 334.0 |
| Mg | 112.5 | 107.5 | 110.0 |
| Na | 390.0 | 370.0 | 310.0 |
| K | 18.25 | 18.0 | 19.80 |
| Cl | 612.0 | 753.0 | 710.0 |
| Alk., as CaCO3 | NA | NA | 406.8 |
| SO4 | 640.0 | 585.0 | 645.0 |
| F | 0.35 | NA | 0.36 |
| NO3, as N | 0.2 | <0.1 | <0.1 |
| NO2, as N | <0.01 | <0.01 | <0.01 |
| Kjeld. N, as N | 1.7 | 1.8 | 2.5 |
| NH3, as N | 1.5 | 1.5 | 1.2 |
| TOC | NA | NA | NA |
| DOC | NA | 85.0 | 3.4 |
| B | 0.72 | 0.04 | 0.73 |
| Fe (tot) | 2.60 | 2.50 | 2.00 |
| Mn | 0.570 | 0.550 | 0.450 |
| As | 0.001 | 0.001 | <0.001 |
| Cd | <0.010 | <0.010 | 0.0008 |
| Cr | <0.050 | <0.050 | 0.004 |
| Cu | 0.026 | 0.032 | 0.019 |
| Ni | 0.023 | 0.022 | 0.003 |
| Pb | <0.060 | <0.060 | 0.003 |
| Se | 0.001 | 0.001 | <0.001 |
| Zn | 0.110 | 0.120 | 0.150 |

DISSOLVED GASES

Sampling Date: 29/06/83

| | |
|-----|------|
| CH4 | ND |
| CO2 | 0.40 |

PURGEABLE ORGANICS

Sampling Date: 22/11/83

| | |
|---------------|-------|
| benzene | -- |
| toluene | 0.207 |
| chlorobenzene | -- |
| ethylbenzene | -- |
| p-xylene | 0.067 |
| o-xylene | -- |
| cumene | -- |
| 1,2,4-TMB | 0.027 |
| naphthalene | -- |

AQUEOUS ISOTOPES

Sampling Date: 16/05/83 16/05/83

| | (A) | (B) |
|----------------|------|------|
| Delta O-18 | -9.9 | -9.7 |
| Delta H-2 | -71 | -64 |
| Tritium (T.U.) | 62 | 88 |

SAMPLING POINT:

0-19-2

Sampling date:

FIELD DATA

temp (C)
Em (mV)
pH
cond. (uS)

LAB DATA

pH
cond. (uS)
hardness (CaCO3)
Ca (mg/l)
Mg
Na
K
Cl
Alk., as CaCO3
SO4
F
NO3, as N
NO2, as N
Kjeld. N, as N
NH3, as N
TOC
DOC
B
Fe (tot)
Mn
As
Cd
Cr
Cu
Ni
Pb
Se
Zn

PURGEABLE ORGANICS

Sampling Date: 22/11/83

| | |
|---------------|-------|
| benzene | 0.053 |
| toluene | 0.351 |
| chlorobenzene | -- |
| ethylbenzene | 0.030 |
| p-xylene | 0.137 |
| o-xylene | -- |
| cumene | -- |
| 1,2,4-TMB | 0.080 |
| naphthalene | 0.119 |

SAMPLING POINT:

U#19-3

Sampling date:

FIELD DATA

temp (C)
 Eh (mV)
 pH
 cond. (uS)

LAB DATA

pH
 cond. (uS)
 hardness (CaCO₃)
 Ca (mg/l)
 Mg
 Na
 K
 Cl
 Alk., as CaCO₃
 SO₄
 F
 NO₃, as N
 NO₂, as N
 Kjeld. N, as N
 NH₃, as N
 TOC
 DOC
 E
 Fe (tot)
 Mn
 As
 Cd
 Cr
 Cu
 Ni
 Pb
 Se
 Zn

DISSOLVED GASES

Sampling Date: 11/08/83

CH₄ NA
 O₂ ND

PURGEABLE ORGANICS

Sampling Date: 11/10/83 22/11/83

| | | |
|---------------|--------|-------|
| benzene | 17.479 | 5.649 |
| toluene | 3.656 | 3.013 |
| chlorobenzene | -- | -- |
| ethylbenzene | 0.221 | 0.296 |
| p-xylene | 1.599 | 1.127 |
| o-xylene | 0.470 | 0.238 |
| cumene | 0.028 | -- |
| 1,2,4-TMB | 0.541 | 0.286 |
| naphthalene | 0.186 | 0.149 |

AQUEOUS ISOTOPES

Sampling Date: 11/08/83

Delta O-18 -6.1
 Delta H-2 -56
 Tritium (T.U.) 8d

SAMPLING POINT:

UW 19-4

Sampling date:

FIELD DATA

temp (C)

Eh (mV)

pH

cond. (uS)

LAE DATA

pH

cond. (uS)

hardness (CaCO3)

Ca (mg/l)

Mg

Na

K

Cl

Alk., as CaCO3

SO4

F

NO3, as N

NO2, as N

Kjeld. N, as N

NH3, as N

TOC

DOC

E

Fe (tot)

Mn

As

Cd

Cr

Cu

Ni

Pb

Se

Zn

PURGEABLE ORGANICS

Sampling Date: 22/11/83

| | |
|---------------|-------|
| benzene | 7.751 |
| toluene | 8.438 |
| chlorobenzene | 0.134 |
| ethylbenzene | 0.222 |
| p-xylene | 0.821 |
| o-xylene | 0.093 |
| cumene | -- |
| 1,2,4-TMB | 0.385 |
| naphthalene | 0.489 |

SAMPLING POINT:

U# 19-5

Sampling date:

FIELD DATA

temp (C)

Em (mV)

pH

Cond. (uS)

LAB DATA

pH

Cond. (uS)

hardness (CaCO₃)

Ca (mg/l)

Mg

Na

K

Cl

Alk., as CaCO₃

SO₄

F

NO₃, as N

NO₂, as N

Kjeld. N, as N

NH₃, as N

TOC

DOC

E

Fe (tot)

Mn

As

Cd

Cr

Cu

Ni

Pb

Se

Zn

DISSOLVED GASES

Sampling Date:

CH₄

O₂

PURGEABLE ORGANICS

Sampling Date:

benzene

toluene

chlorobenzene

ethylbenzene

p-xylene

o-xylene

cumene

1,2,4-TMB

naphthalene

AQUEOUS ISOTOPES

SAMPLING DATE:

16/05/83 17/05/83

Delta C-18

-7.9

-8.1

Delta H-2

-62

-62

Iritium (1.U.)

97

53

SAMPLING POINT:

UW20-1

Sampling date: 28/07/83

FIELD DATA

| | |
|------------|-------|
| temp (C) | 230.0 |
| Eh (mV) | NA |
| pH | 7.6 |
| cond. (uS) | 2350 |

LAB DATA

| | |
|------------------|--------|
| pH | |
| cond. (uS) | |
| hardness (CaCO3) | |
| Ca (mg/l) | |
| Mg | |
| Na | |
| K | |
| Cl | |
| Alk., as CaCO3 | |
| SO4 | |
| F | |
| NO3, as N | |
| NO2, as N | |
| Kjeld. N, as N | |
| NH3, as N | |
| TOC | 341 |
| DOC | |
| B | 2.0 |
| Fe (tot) | |
| Mn | |
| As | |
| Cd | 0.002 |
| Cr | 0.040 |
| Cu | 0.110 |
| Ni | 0.150 |
| Pb | 0.020 |
| Se | <0.001 |
| Zn | 0.290 |

DISSOLVED GASES

Sampling Date: 28/07/83

| | |
|-----|------|
| CH4 | NA |
| O2 | 1.68 |

PURGEABLE ORGANICS

Sampling Date: 29/11/83

| | |
|---------------|-------|
| benzene | 0.080 |
| toluene | 0.410 |
| chlorobenzene | 0.228 |
| ethylbenzene | 0.185 |
| p-xylene | 0.284 |
| o-xylene | 0.213 |
| cumene | 0.112 |
| 1,2,4-TMB | 0.378 |
| naphthalene | 5.025 |

AQUEOUS ISOTOPES

Sampling Date: 28/07/83

| | |
|----------------|-------|
| Delta O-18 | -10.8 |
| Delta H-2 | -76 |
| Tritium (T.U.) | 31 |

SAMPLING POINT:

DW 20-4

Sampling date: 16/05/83 29/11/83

FIELD DATA

| | |
|------------|--------|
| temp (C) | 12.0 |
| En (mV) | NA |
| pH | 6.10 |
| cond. (uS) | >50000 |

LAB DATA

| | | |
|------------------|--------|---------|
| pH | 6.70 | 6.61 |
| cond. (uS) | 112000 | 108000 |
| hardness (CaCO3) | 41650 | 38275 |
| Ca (mg/l) | 11500 | 10300 |
| Mg | 3150 | 3050 |
| Na | 18400 | 15100 |
| K | 300.0 | 267.0 |
| Cl | 61400 | 52440.2 |
| Alk., as CaCO3 | NA | 107.0 |
| SO4 | 1200 | 1150 |
| F | NA | NA |
| NO3, as N | <0.1 | 1.1 |
| NO2, as N | 0.02 | 0.06 |
| Kjeld. N, as N | NA | 45.0 |
| NH3, as N | 39.3 | 37.8 |
| TOC | 36.6 | NA |
| DCC | NA | NA |
| E | 6.80 | 6.90 |
| Fe (tot) | 1.20 | 3.10 |
| Mn | 1.60 | 1.32 |
| As | <0.001 | 0.001 |
| Cd | <0.010 | <0.002 |
| Cr | 0.120 | 0.019 |
| Cu | 0.750 | 0.320 |
| Ni | 0.016 | <0.010 |
| Pb | <0.060 | <0.030 |
| Se | 0.001 | <0.001 |
| Zn | 0.075 | 0.060 |

DISSOLVED GASES

Sampling Date: 29/06/83

| | |
|-----|----|
| CH4 | ND |
| O2 | ND |

PURGEABLE ORGANICS

Sampling Date: 24/10/83

| | |
|---------------|-------|
| benzene | 0.653 |
| toluene | 2.604 |
| chlorobenzene | -- |
| ethybenzene | 0.203 |
| p-xylene | 0.665 |
| o-xylene | 0.256 |
| cumene | -- |
| 1,2,4-TMB | 0.456 |
| naphthalene | 0.274 |

AQUEOUS ISOTOPIES

Sampling Date: 16/05/83 09/11/83

| | | |
|----------------|------|------|
| Delta C-18 | -8.2 | |
| Delta H-2 | -62 | |
| Tritium (T.U.) | ND | 1(2) |

SAMPLING POINT:

UW20-5

Sampling date: 24/10/83
FIELD DATA

| | |
|------------|------|
| temp. (C) | 11.0 |
| En (mV) | NA |
| pH | 6.10 |
| cond. (uS) | NA |

LAF DATA

| | |
|------------------|--------|
| pH | 6.22 |
| cond. (uS) | 105000 |
| hardness (CaCO3) | 36730 |
| Ca (mg/l) | 10600 |
| Mg | 2500 |
| Na | 16700 |
| K | 317.0 |
| Cl | 52560 |
| alk., as CaCO3 | 118.6 |
| SO4 | 840.0 |
| F | 91.0 |
| NO3, as N | 6.2 |
| NO2, as N | 0.02 |
| Kjeld. N, as N | 70.0 |
| NH3, as N | 39.5 |
| TOC | NA |
| DOC | 3300 |
| E | 3.60 |
| Fe (tot) | 13.0 |
| Mn | 2.60 |
| As | 0.003 |
| Cd | <0.005 |
| Cr | 0.240 |
| Cu | 0.520 |
| Ni | 0.013 |
| Pb | 0.054 |
| Se | <0.001 |
| Zn | 0.030 |

PURGEABLE ORGANICS

Sampling Date: 24/10/83

| | |
|---------------|-------|
| benzene | 3.509 |
| toluene | 3.823 |
| chlorobenzene | 0.016 |
| ethylbenzene | 0.409 |
| p-xylene | 0.487 |
| o-xylene | 0.152 |
| cumene | -- |
| 1,2,4-TMB | 0.122 |
| naphthalene | 0.497 |

AQUEOUS ISOTOPES

Sampling Date: 29/07/83

| | |
|----------------|------|
| Delta O-18 | -6.4 |
| Delta H-2 | -56 |
| Tritium (T.U.) | 40 |

SAMPLING POINT:

UW21-1

Sampling date: 20/09/83
FIELD DATA

| | |
|------------|------|
| temp (C) | 25.0 |
| En (mV) | NA |
| pH | 7.0 |
| cond. (uS) | 4000 |

LAB DATA

| | |
|------------------|--------|
| pH | 7.19 |
| cond. (uS) | 5700 |
| hardness (CaCO3) | 2424 |
| Ca (mg/l) | 670.0 |
| Mg | 183.0 |
| Na | 570.0 |
| K | 15.70 |
| Cl | 1130 |
| Alk., as CaCO3 | 264.6 |
| SO4 | 1850 |
| F | 0.98 |
| NO3, as N | <0.1 |
| NO2, as N | <0.01 |
| Kjeld. N, as N | NA |
| NH3, as N | 1.7 |
| TOC | 5.4 |
| DCC | 5.1 |
| B | 0.92 |
| Fe (tot) | 0.026 |
| Mn | 0.068 |
| As | 0.060 |
| Cd | <0.005 |
| Cr | <0.025 |
| Cu | 0.079 |
| Ni | 0.014 |
| Pb | 0.053 |
| Se | <0.001 |
| Zn | 0.019 |

DISSOLVED GASES

Sampling Date: 20/09/83

| | |
|-----|-----|
| CH4 | 100 |
| O2 | ND |

PURGEABLE ORGANICS

Sampling Date: 20/09/83 20/09/83

| | (A) | (B) |
|---------------|-------|-------|
| benzene | 0.063 | 0.133 |
| toluene | 3.008 | 3.307 |
| chlorobenzene | 0.006 | -- |
| ethylbenzene | 0.014 | 0.045 |
| p-xylene | 0.061 | 0.048 |
| o-xylene | 0.011 | -- |
| cumene | 0.007 | -- |
| 1,2,4-TMB | 0.108 | 0.050 |
| naphthalene | -- | -- |

SAMPLING POINT:

DU21-2

Sampling date:

FIELD DATA

temp (C)

En (mV)

pH

cond. (uS)

LAB DATA

pH

cond. (uS)

hardness (CaCO₃)

Ca (mg/l)

Mg

Na

K

Cl

Alk., as CaCO₃

SO₄

F

NO₃, as N

NO₂, as N

Kjeld. N, as N

NH₃, as N

TOC

DOC

B

Fe (tot)

Mn

As

Cd

Cr

Cu

Ni

Pb

Se

Zn

PURGABLE ORGANICS

Sampling Date: 30/11/83

| | |
|---------------|--------|
| benzene | 0.191 |
| toluene | 93.404 |
| chlorobenzene | 0.019 |
| ethylbenzene | 4.835 |
| p-xylene | 19.608 |
| o-xylene | 9.114 |
| cumene | 0.150 |
| 1,2,4-TMB | 4.845 |
| naphthalene | 5.179 |

SAMPLING POINT:

sampling date:
FIELD DATA

02/08/83 22/09/83

temp (C)
Eh (mV)
pH
cond. (uS)
LAE DATA

724.0
NA
7.05
44800

13.0
NA
6.70
NA
>50000

PH
cond. (uS)
hardness (CaCO3)
Ca (mg/l)
Mg
Na
K
Cl
Alk., as CaCO3
SO4
F
NO3, as N
NO2, as N
Kjeld. N, as N
NH3, as N
TOC
DOC
B
Fe (tot)
Mn
As
Cd
Cr
Cu
Ni
Pb
Se
Zn

7.00
70000
22499
6100
1770
10800
198.0
31860
146.6
1190
NA
00.7
0.02
NA
25.5
2960
4000
4.60
0.45
2.20
0.001
<0.002
0.280
0.240
0.020
<0.030
<0.001
0.040

7.06
89000
30900
8100
2600
12800
212.0
42680
80.8
890.0
NA
<0.1
0.03
55.0
28.2
NA
3100
4.30
0.20
0.580
0.002
<0.005
0.760
0.430
0.011
0.044
0.002
0.039

DISSOLVED GASES

sampling Date:

23/09/83

CH4
O2

500
NA

PURGEABLE ORGANICS

sampling Date:

21/09/83 21/09/83

benzene
toluene
chlorobenzene
ethylbenzene
p-xylene
o-xylene
cumene
1,2,4-TMB
naphthalene

(h)
8.207
73.920
0.012
0.722
0.450
0.060
0.011
0.212
--

(E?)
0.407
47.740
--
6.002
0.634
0.134
--
0.131
0.199

AQUEOUS ISOTOPES

sampling Date:

02/08/83

Delta C-18
Delta H-2

-8.0
-64
20

SAMPLING POINT:

UW21-4

Sampling date: 04/08/83 22/09/83

FIELD DATA

| | | |
|------------|------|--------|
| temp (C) | 20.0 | 13.0 |
| Eh (mV) | NA | NA |
| pH | 6.15 | 6.60 |
| cond. (uS) | NA | >50000 |

LAB DATA

| | | |
|------------------|--------|--------|
| pH | 6.10 | 6.30 |
| cond. (uS) | 136000 | 142000 |
| hardness (CaCO3) | 52644 | 54900 |
| Ca (mg/l) | 15000 | 15000 |
| Mg | 3700 | 4250 |
| Na | 25000 | 26600 |
| K | 535.0 | 378.0 |
| Cl | 75160 | 82360 |
| Alk., as CaCO3 | 42.0 | 44.8 |
| SO4 | 1200 | 1010 |
| F | NA | NA |
| NO3, as N | 01.2 | <0.1 |
| NO2, as N | 0.02 | 0.03 |
| Kjeld. N, as N | NA | 55.0 |
| NH3, as N | 45.5 | 47.5 |
| TOC | 91.3 | NA |
| DOC | 375.0 | 260.0 |
| B | 4.60 | 4.80 |
| Fe (tot) | 15.20 | 8.70 |
| Mn | 1.90 | 1.20 |
| As | 0.001 | 0.003 |
| Cd | <0.002 | <0.005 |
| Cr | 0.040 | 0.037 |
| Cu | 0.50 | 0.490 |
| Ni | <0.010 | <0.005 |
| Pb | <0.030 | <0.030 |
| Se | 0.001 | <0.001 |
| Zn | 0.10 | 0.037 |

DISSOLVED GASES

Sampling Date: 21/09/83

| | |
|-----|-----|
| CH4 | 330 |
| O2 | NA |

PURGEABLE ORGANICS

| Sampling Date: | 21/09/83 | 21/09/83 | 21/09/83 | 21/09/83 |
|----------------|----------|----------|----------|----------|
| | (A) | (A?) | (E) | (B?) |
| benzene | 0.349 | 3.958 | 2.050 | 3.962 |
| toluene | 2.316 | 85.601 | 60.986 | 81.840 |
| chlorobenzene | 0.028 | -- | -- | 0.089 |
| ethylbenzene | 6.996 | -- | 0.601 | 0.235 |
| p-xylene | 0.606 | 0.170 | 0.151 | 0.380 |
| o-xylene | 0.175 | 0.012 | -- | 0.174 |
| cumene | -- | -- | -- | 0.023 |
| 1,2,4-TMB | 0.105 | 0.107 | 0.053 | 0.436 |
| naphthalene | 0.314 | -- | 0.122 | -- |

AQUEOUS ISOTOPES

Sampling Date: 04/08/83

| | |
|----------------|------|
| Delta O-18 | -6.4 |
| Delta H-2 | -55 |
| Tritium (T.U.) | 5 |

SAMPLING POINT:

UW21-5

Sampling date: 21/09/83

FIELD DATA

| | |
|------------|----|
| temp (C) | NA |
| Eh (mV) | NA |
| pH | NA |
| cond. (uS) | NA |

LAB DATA

| | |
|------------------|-------|
| pH | 6.12 |
| cond. (uS) | 15400 |
| hardness (CaCO3) | 4042 |
| Ca (mg/l) | 1150 |
| Mg | 285.0 |
| Na | 2500 |
| K | 77.0 |
| Cl | 6170 |
| Alk., as CaCO3 | 102.2 |
| SO4 | 285.0 |
| F | 90.55 |
| NO3, as N | <0.1 |
| NO2, as N | 0.03 |
| Kjeld. N, as N | 65.0 |
| NH3, as N | 14.8 |
| TOC | 10000 |
| DOC | 8600 |
| B | NA |
| Fe (tot) | 1.110 |
| Mn | 0.380 |
| As | NA |
| Cd | NA |
| Cr | NA |
| Cu | NA |
| Ni | NA |
| Pb | NA |
| Se | NA |
| Zn | NA |

PURGEABLE ORGANICS

Sampling Date: 20/12/83

| | |
|---------------|---------|
| benzene | 1.506 |
| toluene | 166.813 |
| chlorobenzene | 0.377 |
| ethylbenzene | 0.146 |
| p-xylene | 0.482 |
| o-xylene | 0.210 |
| cumene | -- |
| 1,2,4-TMB | 0.051 |
| naphthalene | 0.013 |

SAMPLING POINT:

UL22-1

Sampling date: 31/10/83 31/10/83
 FIELD DATA (A) (E)

temp (C) 13.0 13.0
 Em (mV) NA NA
 pH 6.55 6.55
 Cond. (uS) NA NA

LAE DATA

pH 6.70 6.70
 Cond. (uS) 9800 9800
 Hardness (CaCO₃) 2987 2962
 Ca (mg/l) 850.0 840.0
 Mg 210.0 210.0
 Na 985.0 1010
 K 73.40 74.0
 Cl 1507 1502
 Alk., as CaCO₃ 1686 1869
 SO₄ 2020 2020
 F 0.80 0.85
 NO₃, as N 0.2 0.2
 NO₂, as N 0.02 <0.01
 Kjeld. N, as N 190.0 195.0
 NH₃, as N 168.0 163.0
 TOC NA NA
 DOC 138.0 136.0
 E 7.40 7.20
 Fe (tot) 0.170 0.110
 Mn 0.047 0.017
 As 0.001 <0.001
 Cd <0.005 <0.005
 Cr 0.023 0.018
 Cu 0.063 0.052
 Ni 0.043 0.044
 Pb <0.030 <0.030
 Se <0.001 <0.001
 Zn 0.017 0.011

DISSOLVED GASES

Sampling Date: 31/10/83

CH₄ 590
 O₂ NA

PURGEABLE ORGANICS

Sampling Date: 31/10/83 31/10/83
 (A) (B)
 benzene 2.568 2.974
 toluene 1.004 1.179
 chlorobenzene -- --
 ethylbenzene 0.689 0.819
 p-xylene 1.553 1.830
 o-xylene 0.760 0.880
 cumene -- --
 1,2,4-TMB 0.438 0.501
 naphthalene 0.035 --

SAMPLING POINT:

UW22-2

Sampling date: 31/10/83
FIELD DATA

| | |
|------------|------|
| temp (C) | NA |
| En (mV) | NA |
| pH | 5.80 |
| cond. (uS) | NA |

LAB DATA

| | |
|------------------|--------|
| pH | 6.17 |
| cond. (uS) | 122000 |
| hardness (CaCO3) | 40789 |
| Ca (mg/l) | 10400 |
| Mg | 3600 |
| Na | 19800 |
| K | 370.0 |
| Cl | 58220 |
| Alk., as CaCO3 | 184.0 |
| SO4 | 1200 |
| F | 01.0 |
| NO3, as N | 2.0 |
| NO2, as N | 0.03 |
| Kjeld. N, as N | 75.0 |
| NH3, as N | 61.0 |
| IOC | NA |
| DOC | NA |
| B | 7.0 |
| Fe (tot) | 0.640 |
| Mn | 0.330 |
| As | 0.001 |
| Cd | <0.005 |
| Cr | 0.027 |
| Cu | 0.380 |
| Ni | <0.006 |
| Pb | 0.045 |
| Se | <0.001 |
| Zn | 0.009 |

DISSOLVED GASES

Sampling Date: 31/10/83

| | |
|-----|-----|
| CH4 | 370 |
| O2 | NA |

PURGEABLE ORGANICS

| Sampling Date: | 31/10/83 | 31/10/83 |
|----------------|----------|----------|
| | (L) | (E) |
| benzene | 5.427 | 5.075 |
| toluene | 7.408 | 8.000 |
| chlorobenzene | -- | -- |
| ethylbenzene | 0.325 | 0.327 |
| p-xylene | 0.395 | 0.359 |
| o-xylene | -- | -- |
| cumene | -- | -- |
| 1,2,4-TMB | 0.241 | 0.176 |
| naphthalene | 0.281 | 0.295 |

SAMPLING POINT:

UW22-3

Sampling date: 31/10/83

FIELD DATA

| | |
|------------|----|
| temp (C) | NA |
| Eh (mV) | NA |
| pH | NA |
| cond. (uS) | NA |

LAB DATA

| | |
|------------------|--------|
| pH | 7.11 |
| cond. (uS) | 34100 |
| hardness (CaCO3) | 7400 |
| Ca (mg/l) | 2125 |
| Mg | 510.0 |
| Na | 5000 |
| K | 193.0 |
| Cl | 13060 |
| Alk., as CaCO3 | 2228.0 |
| SO4 | 670.0 |
| F | NA |
| NO3, as N | 0.4 |
| NO2, as N | 0.02 |
| Kjeld. N, as N | 50.0 |
| NH3, as N | 39.0 |
| TOC | NA |
| DOC | NA |
| B | NA |
| Fe (tot) | 0.25 |
| Mn | 0.60 |
| As | NA |
| Cd | NA |
| Cr | NA |
| Cu | NA |
| Ni | NA |
| Pb | NA |
| Se | NA |
| Zn | NA |

PURGEABLE ORGANICS

Sampling Date: 03/11/83

| | |
|---------------|--------|
| benzene | 0.089 |
| toluene | 25.197 |
| chlorobenzene | 0.016 |
| ethylbenzene | 0.720 |
| p-xylene | 1.556 |
| o-xylene | 1.139 |
| cumene | -- |
| 1,2,4-TMB | 0.390 |
| naphthalene | 0.846 |

SAMPLING POINT:

OW 22-4

Sampling date:

FIELD DATA

temp (C)
Eh (mV)
pH
Cond. (uS)

LAB DATA

pH
Cond. (uS)
hardness (CaCO₃)
Ca (mg/l)
Mg
Na
K
Cl
Alk., as CaCO₃
SO₄
F
NO₃, as N
NO₂, as N
Kjeld. N, as N
NH₃, as N
TOC
DOC
B
Fe (tot)
Mn
As
Cd
Cr
Cu
Ni
Pb
Se
Zn

PURGEABLE ORGANICS

Sampling Date: 31/10/83

| | |
|---------------|---------|
| benzene | 5.548 |
| toluene | 179.676 |
| chlorobenzene | -- |
| ethylbenzene | 0.306 |
| p-xylene | 1.635 |
| o-xylene | 0.938 |
| cumene | 0.175 |
| 1,2,4-TMB | 0.595 |
| naphthalene | 0.441 |

SAMPLING POINT:

UW22-5

Sampling date: 03/11/83

FIELD DATA

| | |
|------------|----|
| temp (C) | NA |
| Em (mV) | NA |
| pH | NA |
| cond. (uS) | NA |

LAB DATA

| | |
|------------------|--------|
| pH | 6.88 |
| cond. (uS) | 4560 |
| hardness (CaCO3) | 709.5 |
| Ca (mg/l) | 205.0 |
| Mg | 48.0 |
| Na | 760.0 |
| K | 20.0 |
| Cl | 1316 |
| Alk., as CaCO3 | 146.8 |
| SO4 | 350.0 |
| P | 0.90 |
| NO3, as N | 0.4 |
| NO2, as N | 0.02 |
| Kjeld. N, as N | 100.0 |
| NH3, as N | 5.8 |
| TOC | NA |
| DOC | NA |
| E | 0.57 |
| Fe (tot) | 1.50 |
| Mn | 0.130 |
| As | <0.001 |
| Cd | <0.005 |
| Cr | 2.0 |
| Cu | 0.021 |
| Ni | 0.013 |
| Pb | <0.030 |
| Se | <0.001 |
| Zn | 0.060 |

PURGEABLE ORGANICS

Sampling Date: 03/11/83

| | |
|---------------|---------|
| benzene | -- |
| toluene | 264.249 |
| chlorobenzene | -- |
| ethylbenzene | 0.271 |
| p-xylene | 0.922 |
| o-xylene | 0.425 |
| cumene | -- |
| 1,2,4-IMB | 0.655 |
| naphthalene | 0.451 |

SAMPLING POINT:

UW23-1

Sampling date: 28/09/83
 FIELD DATA

temp (C) 16.0
 Eh (mV) NA
 pH 6.60
 Cond. (uS) 10500

LAB DATA

pH 6.80
 Cond. (uS) 16600
 hardness (CaCO3) 5285
 Ca (mg/l) 1500
 Mg 375.0
 Na 1820
 K 45.0
 Cl 5180
 Alk., as CaCO3 277.8
 SO4 1600
 F 0.90
 NO3, as N <0.1
 NO2, as N 0.02
 Kjeld. N, as N NA
 NH3, as N 20.0
 TOC NA
 DOC NA
 E 2.70
 Fe (tot) 0.260
 Mn 0.160
 As 0.002
 Cd <0.005
 Cr 0.120
 Cu 0.060
 Ni 0.010
 Pb <0.030
 Se <0.001
 Zn 0.020

DISSOLVED GASES

Sampling Date: 29/09/83

CH4 140
 C2 ND

PURGEABLE ORGANICS

| Sampling Date: | 28/09/83 | 28/09/83 |
|----------------|----------|----------|
| | (A) | (E) |
| benzene | 1.537 | 0.412 |
| toluene | 5.412 | 3.721 |
| chlorobenzene | -- | -- |
| ethylenzene | 0.083 | 0.057 |
| p-xylene | 0.150 | 0.082 |
| o-xylene | 0.022 | -- |
| cumene | -- | -- |
| 1,2,4-TMB | 0.108 | 0.049 |
| naphthalene | -- | 0.046 |

SAMPLING POINT:

UW23-2

Sampling date: 28/09/83 29/09/83
FIELD DATA

| | | |
|------------|------|----|
| temp (C) | 24.0 | NA |
| Eh (mV) | NA | NA |
| pH | 6.80 | NA |
| cond. (uS) | NA | NA |

LAB DATA

| | | |
|------------------|--------|--------|
| pH | NA | 6.80 |
| cond. (uS) | NA | 114000 |
| hardness (CaCO3) | NA | 43180 |
| Ca (mg/l) | NA | 10300 |
| Mg | NA | 4250 |
| Na | NA | 18800 |
| K | NA | 290.0 |
| Cl | NA | 59440 |
| Alk., as CaCO3 | NA | 95.6 |
| SO4 | NA | 1150 |
| F | NA | NA |
| NO3, as N | NA | <0.1 |
| NO2, as N | NA | 0.03 |
| Kjeld. N, as N | NA | 55.0 |
| NH3, as N | NA | 35.0 |
| TOC | 1480 | NA |
| DOC | NA | NA |
| B | 3.90 | NA |
| Fe (tot) | NA | 0.42 |
| Mn | NA | 0.490 |
| As | 0.001 | |
| Cd | <0.005 | |
| Cr | 0.420 | |
| Cu | 0.20 | |
| Ni | <0.005 | |
| Pb | 0.030 | |
| Se | <0.001 | |
| Zn | 0.033 | |

DISSOLVED GASES

Sampling Date: 29/09/83

| | |
|-----|-----|
| CH4 | 300 |
| O2 | ND |

PURGEABLE ORGANICS

Sampling Date: 28/09/83

| | |
|---------------|--------|
| benzene | NA |
| toluene | 18.842 |
| chlorobenzene | -- |
| ethylbenzene | 0.373 |
| p-xylene | 0.426 |
| o-xylene | 0.091 |
| cumene | -- |
| 1,2,4-TMB | 0.222 |
| naphthalene | 0.004 |

SAMPLING POINT:

DW 23-3

Sampling date: 28/09/83

FIELD DATA

| | |
|------------|--------|
| temp (C) | 24.0 |
| Eh (mV) | NA |
| pH | 6.40 |
| cond. (uS) | >50000 |

LAB DATA

| | |
|------------------|--------|
| pH | 6.16 |
| cond. (uS) | 110000 |
| hardness (CaCO3) | 41650 |
| Ca (mg/l) | 11500 |
| Mg | 3150 |
| Na | 17300 |
| K | 270.0 |
| Cl | 57480 |
| Alk., as CaCO3 | 71.0 |
| SO4 | 838.0 |
| F | NA |
| NO3, as N | <0.1 |
| NO2, as N | 0.02 |
| Kjeld. N, as N | 40.0 |
| NH3, as N | 32.5 |
| TOC | 31.3 |
| DOC | NA |
| B | 3.20 |
| Fe (tot) | 10.0 |
| Mn | 2.20 |
| As | 0.002 |
| Cd | <0.005 |
| Cr | 0.450 |
| Cu | 0.240 |
| Ni | 0.009 |
| Pb | 0.036 |
| Se | <0.001 |
| Zn | 0.180 |

PURGEABLE ORGANICS

Sampling Date: 28/09/83

| | |
|---------------|--------|
| benzene | 5.945 |
| toluene | 58.680 |
| chlorobenzene | -- |
| ethylbenzene | 0.216 |
| p-xylene | 0.643 |
| o-xylene | 0.234 |
| cumene | -- |
| 1,2,4-TMB | 0.324 |
| naphthalene | 0.189 |

SAMPLING POINT:

UW23-4

Sampling date: 29/09/83

FIELD DATA

| | |
|------------|----|
| temp (C) | NA |
| Eh (mV) | NA |
| pH | NA |
| cond. (uS) | NA |

LAB DATA

| | |
|------------------|--------|
| pH | 6.80 |
| cond. (uS) | 42000 |
| hardness (CaCO3) | 11530 |
| Ca (mg/l) | 3450 |
| Mg | 710.0 |
| Na | 6700 |
| K | 140.0 |
| Cl | 19400 |
| Alk., as CaCO3 | 112.0 |
| SO4 | 775.0 |
| F | 90.10 |
| NO3, as N | <0.1 |
| NO2, as N | 0.02 |
| Kjeld. N, as N | 105.0 |
| NH3, as N | 17.5 |
| TOC | 15900 |
| DCC | NA |
| E | 0.89 |
| Fe (tot) | 0.540 |
| Mn | 0.270 |
| As | 0.000 |
| Cd | <0.005 |
| Cr | 6.20 |
| Cu | 0.046 |
| Ni | 0.010 |
| Pb | 0.032 |
| Se | 0.003 |
| Zn | 2.20 |

DISSOLVED GASES

Sampling Date: 29/09/83

| | |
|-----|-----|
| CH4 | 600 |
| O2 | ND |

PURGEABLE ORGANICS

Sampling Date: 29/09/83

| | |
|---------------|---------|
| benzene | 45.188 |
| toluene | 130.611 |
| chlorobenzene | -- |
| ethylbenzene | 0.564 |
| p-xylene | 1.971 |
| o-xylene | 32.787 |
| cumene | -- |
| 1,2,4-TMB | 0.121 |
| naphthalene | 0.722 |

SAMPLING POINT:

OW24-1

Sampling date: 13/10/83

FIELD DATA

| | |
|------------|----|
| temp (C) | NA |
| Eh (mV) | NA |
| pH | NA |
| cond. (uS) | NA |

LAE DATA

| | |
|------------------|--------|
| pH | 7.18 |
| cond. (uS) | 14200 |
| hardness (CaCO3) | 4444 |
| Ca (mg/l) | 1270 |
| Mg | 310.0 |
| Na | 1475 |
| K | 39.0 |
| Cl | 4240 |
| Alk., as CaCO3 | 252.6 |
| SO4 | 1700 |
| F | -0.55 |
| NO3, as N | 0.5 |
| NO2, as N | <0.01 |
| Kjeld. N, as N | 7.5 |
| NH3, as N | 3.2 |
| TOC | NA |
| DOC | 400 |
| E | 3.60 |
| Fe (tot) | 0.12 |
| Mn | 0.20 |
| As | <0.001 |
| Cd | 0.0002 |
| Cr | 0.003 |
| Cu | 0.016 |
| Ni | 0.006 |
| Pb | 0.004 |
| Se | <0.001 |
| Zn | 0.023 |

DISSOLVED GASES

Sampling Date: 13/10/83

| | |
|-----|----|
| CH4 | 50 |
| C2 | ND |

PURGEABLE ORGANICS

Sampling Date: 13/10/83

| | |
|---------------|--------|
| benzene | 0.237 |
| toluene | 53.911 |
| chlorobenzene | -- |
| ethylbenzene | 0.383 |
| p-xylene | 0.409 |
| o-xylene | 4.759 |
| cumene | -- |
| 1,2,4-TMB | 0.154 |
| naphthalene | 0.141 |

SAMPLING POINT:

OW24-2

Sampling date: 13/10/83

FIELD DATA

| | |
|------------|----|
| temp (C) | NA |
| Eh (mV) | NA |
| pH | NA |
| Cond. (uS) | NA |

LAB DATA

| | |
|------------------|-------|
| pH | |
| Cond. (uS) | |
| hardness (CaCO3) | |
| Ca (mg/l) | |
| Mg | |
| Na | |
| K | |
| Cl | |
| Alk., as CaCO3 | |
| SO4 | |
| F | |
| NO3, as N | |
| NO2, as N | |
| Kjeld. N, as N | |
| NH3, as N | |
| TOC | |
| DOC | |
| E | 4.40 |
| Fe (tot) | 0.80 |
| Mn | 0.610 |
| As | 0.009 |
| Cd | 0.007 |
| Cr | 0.110 |
| Cu | 0.440 |
| Ni | 0.026 |
| Pb | 0.190 |
| Se | 0.002 |
| Zn | 0.190 |

PURGEABLE ORGANICS

Sampling Date:

benzene
toluene
chlorobenzene
ethylbenzene
p-xylene
o-xylene
cumene
1,2,4-IMs
naphthalene

SAMPLING POINT:

UW24-4

Sampling date: 17/10/83 19/10/83
FIELD DATA

| | |
|------------|----|
| temp (C) | NA |
| En (mV) | NA |
| pH | NA |
| cond. (uS) | NA |

LAB DATA

| | |
|------------------|--------|
| pH | 6.78 |
| cond. (uS) | 122000 |
| hardness (CaCO3) | 48139 |
| Ca (mg/l) | 12700 |
| Mg | 4000 |
| Na | 19900 |
| K | 310.0 |
| Cl | 62120 |
| Alk., as CaCO3 | 115.4 |
| SO4 | 1080 |
| F | NA |
| NO3, as N | 1.8 |
| NO2, as N | 0.02 |
| NH4, as N | 55.0 |
| NH3, as N | 42.8 |
| TOC | 876 |
| DOC | 1420 |
| B | 3.30 |
| Fe (tot) | 0.140 |
| Mn | 0.750 |
| As | 0.001 |
| Cd | <0.005 |
| Cr | 0.130 |
| Cu | 0.390 |
| Ni | 0.006 |
| Pb | 0.056 |
| Se | <0.001 |
| Zn | 0.053 |

DISSOLVED GASES

Sampling Date: 19/10/83

| | |
|-----|-----|
| CH4 | 750 |
| C2 | NA |

PURGEABLE ORGANICS

Sampling Date: 19/10/83

| | |
|---------------|--------|
| benzene | -- |
| toluene | 85.582 |
| chlorobenzene | -- |
| ethylbenzene | 0.122 |
| p-xylene | 0.229 |
| o-xylene | 4.369 |
| cumene | -- |
| 1,2,4-IMB | 0.050 |
| naphthalene | -- |

SAMPLING POINT:

UW26-1

Sampling date:

FIELD DATA

temp (C)
Em (mV)
pH
cond. (uS)

LAB DATA

pH
cond. (uS)
hardness (CaCO3)
Ca (mg/l)
Mg
Na
K
Cl
Alk., as CaCO3
SO4
F
NO3, as N
NO2, as N
Kjeld. N, as N
NH3, as N
TOC
DOC
E
Fe (tot)
Mn
As
Cd
Cr
Cu
Ni
Pb
Se
Zn

PURGABLE ORGANICS

Sampling Date: 14/12/83

| | |
|---------------|---------|
| benzene | 14.213 |
| toluene | 269.215 |
| chlorobenzene | 107.358 |
| ethylbenzene | 75.688 |
| p-xylene | 76.332 |
| o-xylene | 30.753 |
| cumene | 2.755 |
| 1,2,4-TMB | 18.391 |
| naphthalene | 131.670 |

SAMPLING POINT:

UW27-1

Sampling date: 08/09/83 26/09/83

FIELD DATA

| | | |
|------------|-------|------|
| temp (C) | 234.0 | 20.0 |
| En (mV) | NA | NA |
| pH | 6.60 | 6.35 |
| cond. (uS) | 5900 | 6000 |

LAB DATA

| | | |
|------------------|--------|--------|
| pH | 6.78 | 6.60 |
| cond. (uS) | 9200 | 9400 |
| hardness (CaCO3) | 2611 | 3359 |
| Ca (mg/l) | 725.0 | 1000 |
| Mg | 195.0 | 210.0 |
| Na | 1125 | 1050 |
| K | 151.0 | 160.0 |
| Cl | 1544 | 1598 |
| Alk., as CaCO3 | 1291 | 1341 |
| SO4 | 1875 | 1938 |
| F | 20.72 | 20.90 |
| NO3, as N | <0.1 | <0.1 |
| NO2, as N | 0.02 | <0.01 |
| Kjeld. N, as N | NA | 145.0 |
| NH3, as N | 126.0 | 120.0 |
| TOC | 96.0 | 99.3 |
| DOC | 90.0 | ?120.0 |
| B | 6.70 | 5.80 |
| Fe (tot) | 1.40 | 0.490 |
| Mn | 0.260 | 0.180 |
| As | 0.001 | <0.001 |
| Cd | <0.005 | <0.005 |
| Cr | <0.025 | <0.025 |
| Cu | 0.071 | 0.030 |
| Ni | 0.032 | 0.030 |
| Pb | <0.030 | <0.030 |
| Se | 0.008 | <0.001 |
| Zn | 0.019 | 0.008 |

DISSOLVED GASES

Sampling Date: 08/09/83 27/09/83

| | | |
|-----|----|-----|
| CH4 | NA | 360 |
| O2 | ND | ND |

PURGEABLE ORGANICS

Sampling Date: 27/09/83 27/09/83

| | (A) | (B) |
|---------------|-------|-------|
| benzene | 1.686 | 1.932 |
| toluene | 0.650 | 0.662 |
| chlorobenzene | 0.038 | -- |
| ethylbenzene | 0.902 | 1.719 |
| p-xylene | 1.466 | 1.615 |
| o-xylene | 0.622 | 0.689 |
| cumene | 0.064 | 0.138 |
| 1,2,4-TMB | 1.002 | 1.304 |
| naphthalene | 0.192 | 0.098 |

SAMPLING POINT:

UW27-2

Sampling date: 08/09/83 26/09/83 27/09/83

FIELD DATA

| | | | |
|------------|----|----|----|
| temp (C) | NA | NA | NA |
| Eh (mV) | NA | NA | NA |
| pH | NA | NA | NA |
| cond. (uS) | NA | NA | NA |

LAB DATA

| | | | |
|------------------|--------|--------|--------|
| pH | 6.46 | NA | 6.70 |
| cond. (uS) | 136000 | NA | 139000 |
| hardness (CaCO3) | 52206 | NA | 56250 |
| Ca (mg/l) | 14000 | NA | 15600 |
| Mg | 4200 | NA | 4700 |
| Na | 25750 | NA | 20000 |
| K | 310.0 | NA | 430.0 |
| Cl | 73680 | NA | 72840 |
| Alk., as CaCO3 | 55.8 | NA | 55.8 |
| SO4 | 730.0 | NA | 800.0 |
| F | NA | NA | NA |
| NO3, as N | 01.3 | NA | <0.1 |
| NO2, as N | 0.02 | NA | 0.02 |
| Kjeld. N, as N | NA | NA | 50.0 |
| NH3, as N | 51.0 | NA | 45.0 |
| TOC | 0.35 | 1.4 | 0.7 |
| DOC | NA | NA | NA |
| C | 5.80 | 4.80 | NA |
| Fe (tot) | 3.70 | NA | 0.58 |
| Mn | 1.90 | NA | 1.130 |
| As | 0.001 | 0.001 | |
| Cd | <0.005 | <0.005 | |
| Cr | 0.090 | 0.420 | |
| Cu | 0.40 | 0.230 | |
| Ni | 0.020 | <0.005 | |
| Pb | 0.087 | <0.030 | |
| Se | 0.006 | <0.001 | |
| Zn | 0.052 | 0.013 | |

PURGEABLE ORGANICS

| Sampling Date: | 26/09/83 | 26/09/83 |
|----------------|----------|----------|
| | (A) | (B) |
| benzene | 0.241 | 0.093 |
| toluene | 0.188 | 0.103 |
| chlorobenzene | -- | -- |
| ethylbenzene | 0.140 | 0.028 |
| p-xylene | 0.374 | 0.096 |
| o-xylene | 0.304 | -- |
| cumene | 0.221 | -- |
| 1,2,4-TMB | 11.770 | 0.002 |
| naphthalene | 0.245 | 0.143 |

SAMPLING POINT:

UW27-3

Sampling date: 27/09/83

FIELD DATA

| | |
|------------|-------|
| temp (C) | 224.0 |
| Em (mV) | NA |
| pH | 6.65 |
| cond. (uS) | NA |

LAB DATA

| | |
|------------------|--------|
| pH | 6.66 |
| cond. (uS) | 136000 |
| hardness (CaCO3) | 55510 |
| Ca (mg/l) | 14500 |
| Mg | 4700 |
| Na | 22800 |
| K | 420.0 |
| Cl | 74080 |
| Alk., as CaCO3 | 75.6 |
| SO4 | 1113 |
| F | NA |
| NO3, as N | <0.1 |
| NO2, as N | 0.03 |
| Kjeld. N, as N | 60.0 |
| NH3, as N | 40.0 |
| TOC | 36.9 |
| DOC | NA |
| E | 3.60 |
| Fe (tot) | 0.550 |
| Mn | 0.760 |
| As | 0.005 |
| Cd | <0.005 |
| Cr | 0.440 |
| Cu | 0.240 |
| Ni | <0.005 |
| Pb | 0.053 |
| Se | <0.001 |
| Zn | 0.150 |

DISSOLVED GASES

Sampling Date: 27/09/83

| | |
|-----|-----|
| CH4 | 620 |
| O2 | ND |

PURGEABLE ORGANICS

Sampling Date: 27/09/83

| | |
|---------------|-------|
| benzene | 0.846 |
| toluene | 0.201 |
| chlorobenzene | -- |
| ethylbenzene | 0.211 |
| p-xylene | 0.055 |
| o-xylene | 0.056 |
| cumene | 0.005 |
| 1,2,4-THB | -- |
| naphthalene | 0.827 |

SAMPLING POINT:

U#27-4

Sampling date: 27/09/83

FIELD DATA

| | |
|------------|----|
| temp (C) | NA |
| En (mV) | NA |
| pH | NA |
| Cond. (uS) | NA |

LAB DATA

| | |
|------------------|--------|
| pH | 4.66 |
| Cond. (uS) | 122000 |
| hardness (CaCO3) | 47450 |
| Ca (mg/l) | 13000 |
| Mg | 3650 |
| Na | 20000 |
| K | 440.0 |
| Cl | 63200 |
| Alk., as CaCO3 | <0.2 |
| SO4 | 725.0 |
| F | NA |
| NO3, as N | <0.1 |
| NO2, as N | 0.03 |
| Kjeld. N, as N | 60.0 |
| NH3, as N | 42.5 |
| TOC | 39.9 |
| DOC | NA |
| r | 3.0 |
| Fe (tot) | 12.0 |
| Mn | 1.70 |
| As | <0.001 |
| Cd | <0.005 |
| Cr | 0.440 |
| Cu | 0.620 |
| Ni | 0.010 |
| Pb | 0.30 |
| Se | <0.001 |
| Zn | 1.50 |

DISSOLVED GASES

Sampling Date: 28/09/83

| | |
|-----|-----|
| CH4 | 330 |
| O2 | ND |

PURGEABLE ORGANICS

| Sampling Date: | 27/09/83 | 28/09/83 | 28/09/83 |
|----------------|----------|----------|----------|
| | (A?) | (E) | (C) |
| benzene | 4.535 | 2.052 | 5.136 |
| toluene | 1.105 | 0.714 | 0.995 |
| chlorobenzene | -- | -- | -- |
| ethylbenzene | 0.039 | 0.051 | 0.012 |
| p-xylene | 0.271 | 0.136 | 0.232 |
| o-xylene | 0.076 | -- | 0.092 |
| cumene | -- | -- | -- |
| 1,2,4-TMB | 0.135 | 0.071 | 0.130 |
| naphthalene | -- | 0.036 | -- |

SAMPLING POINT:

UW 27-6

Sampling date: 27/09/83 27/09/83
 FIELD DATA (A) (B)

temp (C) NA NA
 Eh (mV) NA NA
 pH NA NA
 cond. (uS) NA NA
 LAB DATA

pH 5.83 6.02
 cond. (uS) 90000 98000
 hardness (CaCO3) 34350 27937
 Ca (mg/l) 9400 7900
 Mg 2650 2000
 Na 14600 16100
 K 365.0 300.0
 Cl 45000 46640
 Alk., as CaCO3 27.4 37.4
 SO4 900.0 963.0
 F NA NA
 NO3, as N <0.1 <0.1
 NO2, as N 0.03 0.03
 Kjeld. N, as N 50.0 50.0
 NH3, as N 35.0 35.0
 TOC 39.2 39.2
 DOC NA NA
 B 2.90 2.70
 Fe (tot) 6.70 7.80
 Mn 1.60 1.70
 As <0.001 <0.001
 Cd <0.005 <0.005
 Cr 0.40 0.40
 Cu 0.560 0.260
 Ni 0.010 0.014
 Pb 0.056 0.110
 Se <0.001 <0.001
 Zn 0.560 0.250

PURGEABLE ORGANICS

Sampling Date: 07/11/83 07/11/83 04/01/83
 (A) (B)

benzene 0.727 1.000 2.042
 toluene 16.665 9.398 2.670
 chlorobenzene -- 0.031 0.173
 ethylbenzene 0.189 0.143 0.441
 p-xylene 0.640 0.524 0.405
 o-xylene 0.366 0.175 0.227
 cumene -- -- --
 1,2,4-TMB 0.240 0.010 0.251
 naphthalene 0.307 0.351 0.262

SAMPLING POINT:

UW28-1

Sampling date:

FIELD DATA

temp (C)
Eh (mV)
pH
cond. (uS)

LAB DATA

pH
cond. (uS)
hardness (CaCO3)
Ca (mg/l)
Mg
Na
K
Cl
Alk., as CaCO3
SO4
F
NO3, as N
NO2, as N
Kjeld. N, as N
NH3, as N
TOC
DOC
E
Fe (tot)
Mn
As
Cd
Cr
Cu
Ni
Pb
Se
Zn

PURGEABLE ORGANICS

Sampling Date: 24/11/83

| | |
|---------------|-------|
| benzene | 0.055 |
| toluene | 2.549 |
| chlorobenzene | -- |
| ethylbenzene | 0.703 |
| p-xylene | 2.236 |
| o-xylene | 1.177 |
| cumene | 0.023 |
| 1,2,4-TdB | 0.450 |
| naphthalene | 0.076 |

SAMPLING POINT:

OW28-2

Sampling date: 01/11/83
FIELD DATA

temp (C) 34.0
Eh (mV) NA
pH 7.50
cond. (uS) NA
LAB DATA

pH 7.86
cond. (uS) 25900
hardness (CaCO3) 401.5
Ca (mg/l) 19.0
Mg 86.0
Na 4700
K 135.0
Cl 4362
Alk., as CaCO3 9130
SO4 130.0
F 96.60
NO3, as N 0.5
NO2, as N 0.41
Kjeld. N, as N 1600
NH3, as N 1040
TOC NA
DOC 4600
B 120.0
Fe (tot) 7.10
Mn 0.160
As 0.029
Cd <0.010
Cr 0.820
Cu 0.150
Ni 0.40
Pb 0.097
Se 0.004
Zn 0.470

PURGABLE ORGANICS

Sampling Date: 11/11/83

benzene 26.961
toluene 241.922
chlorobenzene --
ethylenzene 74.045
p-xylene 191.121
o-xylene 123.173
cumene 4.182
1,2,4-TMB 50.750
naphthalene 60.329

SAMPLING POINT:

SEEP NEAR UW-7 (UW29-1)

Sampling date: 27/10/83

FIELD DATA

| | |
|------------|----|
| temp (C) | NA |
| Eh (mV) | NA |
| pH | NA |
| Cond. (uS) | NA |

LAB DATA

| | |
|------------------|--------|
| pH | 7.67 |
| Cond. (uS) | 13100 |
| hardness (CaCO3) | 1660 |
| Ca (mg/l) | 87.5 |
| Mg | 355.0 |
| Na | 2120 |
| K | 408.0 |
| Cl | 3185 |
| Alk., as CaCO3 | 3543 |
| SO4 | 40.0 |
| F | 01.30 |
| NO3, as N | 0.3 |
| NO2, as N | 0.03 |
| Kjeld. N, as N | 380.0 |
| NH3, as N | 340.0 |
| TOC | NA |
| DOC | 294.0 |
| E | 24.0 |
| Fe (tot) | 3.20 |
| Mn | 0.20 |
| As | 0.003 |
| Cd | <0.005 |
| Cr | 0.043 |
| Cu | 0.015 |
| Ni | 0.150 |
| Pb | 0.032 |
| Se | 0.001 |
| Zn | 0.028 |

DISSOLVED GASES

Sampling Date: 30/11/82

| | |
|-----|-----|
| CH4 | 150 |
| C2 | NA |

PURGEABLE ORGANICS

Sampling Date: 27/10/83 27/10/83

| | (C) | (D) |
|---------------|--------|--------|
| benzene | 6.913 | 8.892 |
| toluene | 0.991 | 1.613 |
| chlorobenzene | 2.830 | 5.208 |
| ethylbenzene | 0.315 | 18.057 |
| p-xylene | 3.487 | 12.521 |
| o-xylene | 45.845 | 53.055 |
| cumene | 0.294 | 2.303 |
| 1,2,4-TMB | 1.828 | 2.291 |
| naphthalene | 4.349 | 10.736 |

AQUEOUS ISOTOPES

Sampling Date: 01/12/82

| | |
|----------------|-------|
| Delta O-18 | -10.1 |
| Delta H-2 | NA |
| Tritium (T.U.) | 129 |

APPENDIX D. Report of Trace Organic Analyses - Ministry of the Environment



248-3031

Laboratory Services and Applied Research Branch
125 Resources Road, Rexdale

March 5, 1984

MEMORANDUM

TO: J. Mayes
Hamilton Office
West Central Region

FROM: M. G. Foster
Chief, Mass Spectrometry Systems
Organic Characterization Section

RE: GC/MS ANALYSIS OF GROUNDWATER FROM UPPER OTTAWA
ST. LANDFILL SITE (SUBMISSION NO. WC 12515)

Two samples were submitted for mass spectrometry analysis in this submission. Unfortunately, on close inspection the two bottles received, although assigned different lab sample numbers both were the same field sample number - UW 24-4. Both bottles were analysed for volatile organics and the results indicated that the samples were indeed duplicates and the lab reference numbers had been assigned incorrectly. We attempted to recover the other sample prior to its analysis by the Pesticide Section but unfortunately it had already been extracted without their noticing the discrepancy. The results from the Pesticides Section would therefore be assumed to be two duplicates of UW 20-4. Only one bottle was analysed for extractable organics and the data is presented here along with the volatiles data. The sample from UW 24-4 was assigned lab sample number MY49-0004.

The sample was subjected to GC/MS analysis. It was first analysed by a purge and trap technique followed by GC/MS to separate, identify and quantitate the volatile organics. The compounds found and their concentrations are indicated in the attached Table 1. Many of the components isolated have only an approximate concentration marked. This approximation is based on three major assumptions which are:

1. The purging efficiency of the compound is identical to that of the internal standard added to each sample.
2. The GC behaviour of the compound is identical to that of the internal standard.
3. The MS response of the compound is identical to that of the internal standard.

These assumptions may not hold, and any deviation will affect the estimate of concentration.

The sample was also extracted under both basic and acid conditions and the extracts concentrated prior to capillary GC/MS analysis of the extractable fractions. Internal standards were added to the sample prior to extraction and similar assumptions apply for the estimates made of the concentrations of components. Table 11 indicates the individual compounds and compound classes observed in the sample. The sample showed several compounds that were isomeric or were from the same compound class and these are also indicated in the tables.

The major volatile organics seen were tetrahydrofuran (THF), methyl ethyl ketone (MEK), toluene. The THF and MEK are often found as a result of the use of adhesives in the construction of wells. Toluene is also a commonly used solvent and may also derive from a glue. Methylene chloride and trichloroethane are also commonly used industrial solvents, the latter having many applications in degreasing and cleaning of metals. The sulfur-containing compounds may be present as a result of bacterial degradation.

The major components seen in the extractable fraction include molecular sulfur, an alkene, diethylene glycol - a widely used antifreeze, and mercapto benzothiazole - used in rubber manufacturing.

The other prominent components are a series of carboxylic acids which are likely degradation products of organic material, and polyethylene glycol derivatives which are commonly used as solvents and lubricants. The two phthalate esters are widely used plasticizers.

The organics seen in this sample include compounds which are normal degradation products of domestic waste as well as some compounds which are used industrially. These latter compounds, however, also have application in household products.

M. G. Foster

M. G. Foster

MGF:mm

c.c.

O. Meresz

J. Barker

J. Barbash

J. Cherry

LIS



Ontario

Ministry
of the
Environment

Hamilton L/F

Components Found & Their Concentration in ug/L

Date Sampled: 831201

Date Analyzed: 840119

Sample MY49-0004

[illegible]

NOTES

ND - not detected

ND† - not detected

~~tr - trace~~

* - approximate

- less 05 ug/litre

- less than 5 ug/litre

~~less than 0.1 ug/litre~~

- response of standard not determined

Ministry
of the
Environment

Hamilton L/F

Components Found & Their Concentration in $\mu\text{g/L}$

Date Sampled: 83 1201

Date Analyzed: 840119

Sample NY49-0004

| Compound | | UW 24-4 | | | |
|-----------------------------------|----------|---------|--|--|--|
| | MY49 | - 0004 | | | |
| Acetone | * | 1.7 | | | |
| Carbon Disulfide | * | 2.2 | | | |
| Internal Std. | | ✓ | | | |
| Tetrahydrofuran | * | > 271 | | | |
| Methyl ethyl ketone | * | 121 | | | |
| n pentanol | * | 0.8 | | | |
| Dimethyl disulfide | * | 0.6 | | | |
| n C ₇ H ₁₆ | * | 1.4 | | | |
| Pioidine | * | 1.3 | | | |
| Internal Std. | | ✓ | | | |
| n C ₁₀ H ₂₂ | * 305 | 7.8 | | | |
| n C ₁₀ H ₂₂ | * 322 | 5.1 | | | |
| n C ₁₀ H ₂₂ | * 342 | 4.9 | | | |

| | | |
|------|-----------------------|---------------------------------------|
| | ND - not detected | - less than 0.5 ug/litre |
| OTES | ND† - not detected | - less than 5 ug/litre |
| | tr - trace | - less than 0.1 ug/litre |
| | * - approximate | - response of standard not determined |

TABLE II
GC/MS OF EXTRACTABLE ORGANICS AND
ESTIMATED CONCENTRATION LEVELS (ug/L)

| | | MY49-0004 |
|----------------------------|-----------------|---------------|
| Carboxylic acids: | C ₅ | 25 |
| | C ₆ | 3 |
| | C ₇ | 2 |
| | C ₈ | 3 |
| | C ₁₀ | 5 |
| | C ₁₂ | 3 |
| Alkenes - C ₇ | | 71 |
| Aliphatic ethers | | 3 |
| Aliphatic alcohols | | 1 |
| 1-(2-Butoxyethoxy) ethanol | | 19 |
| Diethylene glycol | | 118 |
| Polyethyleneglycol derivs. | | 5; 1; 1; 1; 2 |
| Benzothiazole | | 11 |
| Mercaptobenzothiazole | | 61 |
| Sulfur | | 176 |
| Diethylphthalate | | 2 |
| Di isooctyl phthalate | | 8 |
| Aliphatic amide | | 1 |

The LIS final report appears to have
been sent out without this attachment.

MG Foster



248-3031

Laboratory Services & Applied Research Branch
125 Resources Road, Rexdale

March 6, 1984

MEMORANDUM

TO: Mr. J. Mayes
Hamilton Office
West Central Region

FROM: Ms. M. G. Foster
Chief, Mass Spectrometry Systems

RE: GC/MS ANALYSIS OF TEST WELLS IN
UPPER OTTAWA ST. LANDFILL SITE
(SUBMISSION NO. WC 12514)

Three samples were received in this submission for GC/MS analysis of organics present. They were assigned the following lab sample numbers:

| | |
|---------|-----------|
| UW19-1 | MY47-0147 |
| UW28-ST | MY47-0148 |
| UW22-2 | MY47-0149 |

The samples were subjected to GC/MS analysis. They were first analysed by a purge and trap technique followed by GC/MS to separate, identify and quantitate the volatile organics. The compounds found and their concentrations are indicated in the attached Table 1. Many of the components isolated have only an approximate concentration marked. This approximation is based on three major assumptions which are:

1. The purging efficiency of the compound is identical to that of the internal standard added to each sample.
2. The GC behaviour of the compound is identical to that of the internal standard.
3. The MS response of the compound is identical to that of the internal standard.

These assumptions may not hold, and any deviation will affect the estimate of concentration.

The samples were also extracted under both basic and acid conditions and the extracts concentrated prior to capillary GC/MS analysis of the extractable fractions. Internal standards were added to the sample prior to extraction and similar assumptions apply for the estimates made of

the concentrations of components. Table 11 indicates the individual compounds and compound classes observed in the samples and estimated to be at levels of 1 ug/L or greater. The samples showed several compounds that were isomeric or were from the same compound class and these are also indicated in the tables.

The extractable organics in samples MY47-0148 and MY47-0149 were so numerous and the sample matrix was so complex that the internal standard was not observed. The estimate of concentration levels in these two samples is based on our experiences of recoveries of the internal standard in other samples and an evaluation of the area expected to be found at the sample dilution used. This estimate should enable comparative concentration levels to be assessed but must be used with extreme caution.

The major volatile organics seen in well UW19-1 were toluene, tetrahydrofuran, acetone, methyl ethyl ketone and two aliphatic hydrocarbons. The first four of these could be associated with adhesives used in the well construction or with equipment cleaning. All were present at low ug/L levels. The major extractable organics seen in this well included polypropylene glycol derivatives, terpenes, hydroxybenzothiazole, resin acids, bis phenols and alkyl substituted benzenes. Lower levels were also seen of PAH, phthalates, aliphatic hydrocarbons and phenolics. The range of organics seen would suggest the source as being more than one industry.

Well UW28-ST contained high levels of aromatic hydrocarbons in the volatile fraction. Other prominent components were a series of oxygenated solvents, terpenoids and a 1,2-dichloroethylene. The oxygenated solvents, which included tetrahydrofuran, several ketones, dioxane and dioxolane derivatives could be associated with well construction techniques and the adhesives used. The major extractable organics included oxathiolane, alcohols, aromatic and aliphatic hydrocarbons, polypropylene glycol derivatives, alkyl phenols, terpenes, carboxylic acids, dioxolane and dioxane derivatives, cyclic alcohols and ketones, hydroxybenzothiazole, bis phenols, resin acids and PAH. The only chlorinated organics seen in the extractable fraction were two PCB congeners. The concentration levels of all extractable organics in this sample were given only a rough estimate because of the complexity. Some of the organics such as fenchone, α, α -dimethyl benzyl alcohol, terpineols and phenylacetic acid are widely used in perfumery. The sulfur-containing compounds could be present as a result of natural degradation. Many of the carboxylic acids seen are probably present as a result of the normal degradation process of organic material. The bis-phenols are associated with epoxy resin manufacture and the solvent mix seen in the volatiles fraction could also be linked with this type of industrial source. The trimethyl cyclohexanone and trimethyl cyclohexanol could be used as solvents or they may also be used as starting materials in plastics manufacturing. The presence of the substituted phenols together with trioxane could suggest a source as phenol-formaldehyde resin. They could also be found in foundry sand along with the PAH, cresols and indane derivatives. These latter compounds could also be derived from coal tar or from wood preservatives. The phthalates are widely used plasticizers, benzothiazole derivatives are used in rubber manufacturing while

polypropylene glycol derivatives are used as lubricants. The organics seen in this sample could derive from a wide variety of sources, some industrial but some may be domestic as many household products contain a range of organics which will be released over time.

The final sample in this submission UW22-2 contained generally lower concentrations of organics than the other two samples. In the volatile fraction, the major compounds seen were tetrahydrofuran and toluene - both being organics previously linked to well construction. Low levels of other aromatics were also seen along with oxygenated solvents, aliphatic hydrocarbons and sulfur-containing compounds. The latter compounds are likely biological degradation products. The major compound seen in the extractable fraction was molecular sulfur. Prominent organics seen included phthalate esters, carboxylic acids and mercaptobenzothiazole. The phthalates are used as plasticizers, the acids are probably derived from the general degradation of organic matter in the landfill while mercaptobenzothiazole is used in rubber manufacturing.

?
The samples analysed here from the Upper Ottawa St. landfill site are extremely complex and the organics identified indicate a variety of sources. Few chlorinated organics were observed, the ones being seen were minor components in all samples. Of note was the presence of PCBs in two of the samples - the quantitation of these would be better handled by the GC/ECD analysis which I believe has also been requested on these samples.

If you have any questions, please feel free to contact me.

MG Foster

M. G. Foster

MGF:mm

c.c.

O. Meresz
LIS
J. Barbash
J. Barker
J. Cherry

Environment
 Date Sampled: 831123
 Date Analyzed: 840118

Sample MY47-0147 to 149

| Compound | | UW 19-1 | | UW 28-ST | | UW 22-2 |
|---|---------|---------|--|----------|--|---------|
| | MY47 | -0147 | | -0148 | | -0149 |
| Acetone | * | 2.0 | | 1.4 | | 1.2 |
| Acetaldehyde | * | ND | | 1.0 | | ND |
| Ethyl cyanide | * | ND | | 1.1 | | ND |
| 1,3-dioxolane | * | ND | | 3.8 | | ND |
| Diethyl ether | * | ND | | 0.6 | | ND |
| Carbon disulfide | * | ND | | ND | | 0.7 |
| Internal Std. | | ✓ | | ✓ | | ✓ |
| t-Butanol | * | ND | | 29.0 | | ND |
| Tetrahydrofuran | * | 6.0 | | 23.9 | | 166 |
| Methyl ethyl ketone MEK | * | 1.1 | | 2.6 | | ND |
| 1,3-dioxane | * | ND | | 1.0 | | ND |
| 1,4-dioxane | * | ND | | 26.6 | | 0.8 |
| Methyl isopropyl ketone | * | ND | | 50.3 | | ND |
| 3-oxathiolane | * | ND | | 14.3 | | ND |
| 2-dimethoxy-2-propanol | * | ND | | 16.0 | | ND |
| Acetaldehyde | * | ND | | 1.0 | | ND |
| C ₇ H ₁₄ | (38) * | ND | | 9.2 | | ND |
| C ₇ H ₁₆ | (148) * | 1.6 | | 37.0 | | 2.3 |
| Methyl isobutyl ketone MIBK | * | ND | | 10.2 | | ND |
| C ₇ H ₁₆ | (161) * | ND | | 8.1 | | ND |
| 1,5-dimethyl-1,4-dioxane | * | ND | | 2.5 | | ND |
| Internal Std. | | ✓ | | ✓ | | ✓ |
| Acetoxy-but-2-ene | * | ND | | 5.3 | | ND |
| C ₈ H ₁₈ | (140) * | 1.6 | | 5.9 | | ND |
| Heptanone | * | ND | | 88.8 | | ND |
| Amphene | * | ND | | 67.3 | | ND |
| C ₉ H ₁₂ | (247) * | ND | | 23.1 | | ND |
| Pinchone | * | ND | | 44.1 | | ND |
| C ₉ H ₁₂ | (315) * | ND | | 60.9 | | ND |
| C ₈ H ₁₂ O ₂ | * | ND | | 17.2 | | ND |

ND - not detected - less than 0.5 ug/litre
 ND+ - not detected - less than 25 ug/litre
~~tr - trace~~ - ~~less than 0.1 ug/litre~~
 * - approximate - response of standard not determined

TABLE II

GC/MS ANALYSIS OF EXTRACTABLE ORGANICS AND
ESTIMATED CONCENTRATIONS LEVELS (ug/L)

Upper Ottawa Street Landfill Site

| | MY47-0147 (UW 19-1) | MY47-0148 (UW 28-ST) * | MY47-0149 (UW 22-2) * |
|---|---------------------------------|--|-----------------------------|
| Aliphatic hydrocarbons | 5;3;3;2;2;2; 10;11;10;2;2;15 | 31;8;36;36;50; 22;24;176;200; 16;75;421;35; 7;100;38;23 | 2;2 |
| Alicyclic hydrocarbons | 1 | 23;17;108;4154; 436 | 2 |
| Terpene | 8 | 42 | |
| Alkyl substituted benzenes | 8;4;2;25;15;3; 1;3;7;25 | 50;52;16;98;59; 36;11;109;43;13 | |
| Indane | # | | |
| Naphthalene | | # | |
| Acenaphthene | 2 | 24 | |
| Fluorene | 17 | | |
| Phenanthrene | | 26 | |
| Methyl phenanthrene | | 4154 | |
| Pyrene | | 19 | |
| Fluoranthene | | 4260 | |
| Alcohols | 20;8 | 100;4200 | 3 |
| Polypropylene glycol(s) | #;40;1;8;1;7 | 7;580;56;11 | 2;13 |
| Polyethylene glycol(s) | 2 | | 3;7 |
| 3,3,5-Trimethyl cyclohexanol | 27 | 202 | |
| α,α -dimethylbenzyl alcohol | | 890 | |
| Methyltetrahydrofuranmethanol | | 87 | |
| Cyclohexanol derivative | | 1,800 | |

Table II (cont'd.)

Upper Ottawa Street Landfill Site

| | | MY47-0147 (UW 19-1) | MY47-0148 (UW 28-ST) * | MY47-0149 (UW 22-2) * |
|---|-----------------|------------------------|------------------------------|-----------------------------|
| Polyglycol type alcohol | | | 160 | |
| Acids: | C ₆ | | | 30;1 |
| | C ₈ | | | 1;12 |
| | C ₉ | | | 6 |
| | C ₁₀ | 8 | | 5 |
| | C ₁₂ | | | 5 |
| | C ₁₄ | | | 1 |
| | C ₁₆ | | | 1 |
| | C ₁₈ | | 6 | 1 |
| Cyclohexaneacetic acid | | | 170 | |
| Methylbenzoic acid | | | 200 | |
| Dimethyl benzoic acid | | | 37 | |
| α -Ethylbenzeneacetic acid | | | 190 | |
| Benzene propanoic acid | | | 1,110 | |
| Benzene butanoic acid | | | 38;120;752 | |
| Ethylbenzenebutanoic acid | | | <880 | |
| C ₄ Benzoic acid | | | | <8 |
| Resin acids | | 4;12;230 | <36;89;58;239; 36;38 | |
| Phenol | | 3 | 92 | |
| Cresol(s) | | | 89;45 | |
| Xylenol(s) | | 7 | 16;486;74 | |
| Phenol(s)C ₃ alkyl substituted | | 6;13 | 104;110 | |
| Hydroxybiphenyl | | 9 | | |
| Butylatedhydroxy toluene | | | 49 | |
| Methylene bis dimethyl phenol | | | <65 | |
| 2,2'-Methylene bis phenol | | 25 | 390 | |

Table II (cont'd.)

Upper Ottawa Street Landfill Site

| | MY47-0147 (UW 19-1) | MY47-0148 (UW 28-ST) * | MY47-0149 (UW 22-2) * |
|---|------------------------|------------------------------|-----------------------------|
| 4,4'-Methylene bis phenol | 29 | | |
| 4,4'-(1-Methylethylidene) bis phenol | 12 | | |
| Methylene bis phenol | < 3 | 350;100 | |
| Sulphur | 47 | 1,000 | 2,044 |
| Dimethyl trisulfide | | | 1 |
| Hexathiepane | | | 7 |
| 3-(1-Methylethyl)thio-1-propene | | 150 | |
| Benzothiazole | # | | 10 |
| Methyl benzothiazole | 1 | | |
| Hydroxybenzothiazole | 127 | 990 | |
| Mercapto benzothiazole | | | 51 |
| Polychlorinated biphenyls | Cl ₂ | 32 | |
| | Cl ₃ | <2 | |
| | | <36 | |
| Di butyl phthalate | <5 | | 35;5 |
| Di (2-ethyl hexyl) phthalate | 20 | 350 | 100 |
| Di (n-octyl) phthalate | | 73 | 5 |
| Oxathiolane | 15 | 200 | |
| Dimethyl dioxane | 4 | 15 | |
| Methyl pyridine | 3 | 11 | |
| Ketone | | 30 | |
| Hexamethylcyclotrisiloxane | 1 | | |

Table II (cont'd.)

Upper Ottawa Street Landfill Site

| | MY47-0147 (UW 19-1) | MY47-0148 (UW 28-ST) * | MY47-0149 (UW 22-2) * |
|--------------------------------------|------------------------|------------------------------|-----------------------------|
| 1,3,5 Trioxane | | 43 | |
| Aniline | # | | |
| Dichlorobenzene(s) | 9 | | |
| 3,3,5-Trimethylcyclohexanone | 78 | 660 | |
| 1,1'-oxybis (2-ethoxy) ethane | 100 | | |
| Camphor | 41 | 331 | |
| α -Terpineol (& isomers) | 97 | 39;800 | |
| Dioxolane derivative(s) | | 1,300 | |
| Dioxane derivative(s) | | 700 | |
| Unknown E1 | | <140 | |
| 1-H-Phenylene | | <140 | |
| Octahydromethyl indene derivative | 6 | | |
| 1-Phenoxy-3-phenoxy benzene | 1 | | |
| Octahydromethylnaphthalenone | | 200 | |
| Trimethylbenzenesulfonamide | | 17 | |
| Phenylmethyl-benzene methanol deriv. | | 59 | |
| 4H-Cyclopenta-d,e,f-phenanthrene | | 17 | |
| Long chain alcohol acetates | 1 | | 5;1 |
| Vitavax | <3 | | |
| Phenyl-p-tolyl-2-pyrazoline | | 36;38 | |

Table II (cont'd.)

Upper Ottawa Street Landfill Site

| | MY47-0147 (UW 19-1) | MY47-0148 (UW 28-ST) * | MY47-0149 (UW 22-2) * |
|---|------------------------|------------------------------|-----------------------------|
| N-(9,10-Dihydro-2-phenanthryl) acetamide | 3 | | |
| Benzaldehyde derivative | | < 26 | |
| Isoquinoline derivative | | < 26 | |
| Tetrahydrofuranyl indole | | < 26 | |

* Very approximate value

not quantitated

248-3031

Laboratory Services & Applied Research Branch
125 Resources Road, Rexdale

March 8, 1984

MEMORANDUM

TO: J. Mayes
Hamilton Office
West Central Region

FROM: M. G. Foster
Chief, Mass Spectrometry Systems
Organic Characterization Section

RE: GC/MS ANALYSIS OF SAMPLE FROM UPPER
OTTAWA ST. LANDFILL SITE (SUB.# WC 12516)

One sample was received in this submission. Its reference number was UW27-6 and it was assigned lab number MY50-0147.

The sample was subjected to GC/MS analysis. It was first analysed by a purge and trap technique followed by GC/MS to separate, identify and quantitate the volatile organics. The compounds found and their concentrations are indicated in the attached Table 1. Many of the components isolated have only an approximate concentration marked. This approximation is based on three major assumptions which are:

1. The purging efficiency of the compound is identical to that of the internal standard added to each sample.
2. The GC behaviour of the compound is identical to that of the internal standard.
3. The MS response of the compound is identical to that of the internal standard.

These assumptions may not hold, and any deviation will affect the estimate of concentration.

The sample was also extracted under both basic and acid conditions and the extracts concentrated prior to capillary GC/MS analysis of the extractable fractions. Internal standards were added to the sample prior to extraction and similar assumptions apply for the estimates made of the concentrations of components. Table 11 indicates the individual compounds and compound classes observed in the sample. The sample showed several compounds that were isomeric or were from the same compound class and these are also indicated in the tables.

The major volatile organics seen in this sample were two alcohols. A number of other oxygenated solvents and aliphatic hydrocarbons were also seen but at much lower levels. The major extractable organics seen were diethylene glycol and butyl carbitol. These were associated with lower levels of other oxygenated solvents such as the polyethylene glycol derivatives. Other compounds seen included rubber additives - benzothiazole and plastic additives - the phthalate esters. The mixture of organics seen here suggest a polar industrial solvent mix which may have antifreeze properties. It could be a solution used for special applications. The presence of the additives of rubber and plastic may be explained by their dissolution from the original materials by the action of this strong solvent. The carboxylic acids are associated with the natural degradation of organic materials and are generally found in landfill sites.

MG Foster

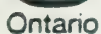
M. G. Foster

MGF:mm
c.c.

O. Meresz
LIS
J. Barbash
J. Barker
J. Cherry

TABLE II
GC/MS ANALYSIS OF EXTRACTABLE ORGANICS AND
ESTIMATED CONCENTRATION LEVELS (ug/L)

| | MY50-0147 |
|--------------------------------------|---------------|
| Benzothiazole | >238 |
| Methylmercaptobenzothiazole | 8 |
| Sulfur | 262 |
| Polyethylene glycol derivatives | 78; 57 |
| Diethylene glycol | >5479 |
| Butyl carbitol | >678 |
| Ethers | 52; 12 |
| Aliphatic alcohol | 24 |
| Dioxolane derivative | 26 |
| Carboxylic acids C ₆ | 220 |
| Miscellaneous | 4; 9; 18; 126 |
| Di n-butyl phthalate | 6 |
| Di isooctyl phthalate | >10 |



Components Found & Their Concentration in ug/L

Date Sampled: 831213

Date Analyzed: 840124

Sample MY 50-0147

[illegible]

NOTES

ND - not detected

ND† - not detected

~~tr~~ trace

* - approximate

- less 0.5 ug/litre

- less than 25 ug/litre

~~less than 0.1 ug/litre~~

- response of standard not determined

ND - not detected - less than 0.5 ug/litre
 ND† - not detected - less than 25 ug/litre
~~tr - trace - less than 0.1 ug/litre~~
 * - approximate - response of standard not determined

APPENDIX E. Report of Trace Organic Analyses - Department of Civil
Engineering, Stanford University

Draft
June 1983

ORGANIC CONTAMINATION OF GROUNDWATER
AT THE UPPER OTTAWA STREET SITE

Naomi Goodman
Department of Civil Engineering
Stanford, CA 94305

FOR INTERNAL DISTRIBUTION ONLY

relatively simple analyses as monitoring tools; nearby groundwaters also contain naturally high levels of heavy metals and other inorganic constituents. The fractured nature of the underlying rock would tend to disperse the leachate, and there are indications that the landfill forms a water table mound from which flow proceeds radially. These factors make it difficult to establish the extent of contamination. In this study we attempt to identify specific organic compounds originating in the landfill that are indicative of the presence of leachate.

Sampling and Analysis

Samples were collected by the Department of Earth Sciences, University of Waterloo, and shipped to Stanford in cooled containers. Samples were taken from seven monitoring wells in the vicinity of the site and from surface seepage from the face of the landfill. The wells were furnished with multi-level bundle piezometers that extended as much as 50 meters below the surface. Details of the construction, placement, and operation of these wells have been reported elsewhere [2]. Sampling tubes were purged for a month before collecting samples to avoid contamination with water used in drilling the wells. Two liter glass bottles and two 50-ml hypovials were collected from each sample point. The hypovials were used for analysis of volatile halogenated organics (VOA) by pentane extraction and gas chromatography. The liter samples were used for closed-loop stripping analysis (CLSA) and solvent extract analysis (SEA). The CLS procedure allows reproducible extraction of neutral nonpolar, volatile compounds while the SEA method is effective for organic acids and bases. VOA extracts were analyzed on a Tracor GC equipped with a 2-m packed column of 10% Squalane on Chromosorb W and quantified with a Spectra-Physics data system. CLS extracts were analyzed on a Finnigan GC-MS

equipped with a 30-m SE-52 fused silica capillary column, and quantified automatically by comparison of compound and internal standard single-ion peak areas. The SEA procedure was as follows: one or two-liter samples were extracted with methylene chloride using a continuous liquid-liquid extractor. Extraction was begun at pH 11 for 24 hours, the pH was lowered to 2, and the process was continued for another 24 hours. The extract was then concentrated to 1 ml and separated into two fractions on 15% w/w deactivated silica gel (80-200 mesh). The first fraction contained basic, neutral and phenolic compounds, and the second contained acidic components. The acid fraction was methylated with diazomethane and both fractions were analyzed by GC-MS. Quantification was based on peak-height comparison between single characteristic ions of the compounds and internal standards. Because these calculations were not corrected for extraction efficiency or detector response, the given values may differ by as much as an order of magnitude from the true concentrations. However, these semiquantitative data are adequate for determining patterns of removal.

Results and Discussion

Preliminary analysis of oily leachate from within the landfill, conducted by the Stanford Water Quality Laboratory in September 1982, identified primarily compounds characteristic of mineral oil contamination: n-alkanes, aromatic and polyaromatic hydrocarbons (Table 1). Industrial solvents and other miscellaneous chemicals were also detected. It was expected that leachate from the landfill would contain some but not all of the major components of the oily leachate, certain classes of compounds being selectively retained or biodegraded within the landfill. This is in fact observed in the seepage from the streamside face of the mound. Certain compounds that were major com-

ponents of the oily leachate are reduced or absent in the seepage. These include the n-alkanes, a homologous series of alkyl ketones, and all polyaromatic hydrocarbons with more than two rings. The removal of these hydrophobic species is probably due to adsorption by the soil of the landfill cover, but biodegradation may also play a part [3]. N-alkanes with more than 7 carbons are aerobically degraded by a variety of soil bacteria. The ground water beneath the site is anaerobic, as evidenced by the presence of H_2S and methane, however zones of aerobic decomposition probably exist within the landfill.

Of the seven wells that were sampled, five lie along the course of the stream that borders the landfill to the north, and two lie approximately 500 meters to the southeast. Well UW-10 is located upstream from the site, and is therefore the most likely to be uncontaminated. All samples were analyzed for VOA, CLSA and SEA compounds. Method detection limits for many of these compounds have been established and are approximately $0.1 \mu\text{g/l}$ for the VOA, $.05$ for CLS compounds and $0.3 \mu\text{g/l}$ for SEA [4]. The precision of measurement is proportional to the concentration, having a standard deviation of approx. $0.1C + .05 \mu\text{g/l}$ for VOA and 0.2 to $0.9C + .01 \mu\text{g/l}$ for CLS, where C is the concentration. These values do not include the error contributed by the well sampling technique, for which no estimate is available.

Volatiles (VOA) were present only at low concentrations ($<1 \mu\text{g/l}$) in all samples, and variability between duplicate samples was higher than differences between wells (Table 2). It is possible that loss of volatile solvents to the air accounts for the low levels, however on-site monitoring of the air also failed to detect these compounds.

Low levels of purgeable compounds were detected in all wells with the exception of UW-10, however the only well which showed clear evidence of contamination was UW-7. Even in this well, closest to the landfill, concentrations of most purgeables were below 1 µg/L. These results indicate that, although some contamination may be present, these compounds are not useful as tracers.

Examining the solvent-extract compounds, it is necessary to first discount contributions from the natural groundwater, as well as contamination from sampling devices, solvents and glassware. Well casings, piezometer linings and screens are made of various plastics, which could contaminate the sample. These materials were soaked in water in a laboratory test to determine their leaching potential. The result was a clear, extremely viscous solution. The sample could not be analyzed for CLS compounds due to extreme foaming problems, however pentane extraction detected a large peak corresponding in GC retention time to 1,1,1-trichloroethane. Solvent extract analysis identified a large number of compounds, the major ones being diethylene glycol, methyl carbitol^(R), benzothiazolethione, benzothiazole, bis(2-ethylhexyl)phthalate, octanoic, decanoic and benzoic acids. Other compounds were present but could not be identified at the high dilution necessary for the major components. Table 3 lists those compounds that have been tentatively identified by computer matching of MS spectra. Some of these appear in samples from all wells, and are therefore likely to have leached from the well materials. Benzothiazolone, benzothiazole and the phthalates fall into this category.

In addition to the aromatic hydrocarbons found in the CLS extracts, the major compounds apparently contributed by the aquifer materials were numerous organic polysulfides and molecular sulfur. These were the largest peaks in

the basic/neutral fraction of all well samples, and in some cases were present in concentrations high enough to seriously interfere with detection of other components. Future analytical work at the Upper Ottawa Street site will probably require a modification of the SEA method to remove these compounds.

Listed in Table 4 are those SEA compounds which appeared in the landfill leachate and were also present in one or more of the well samples. Several patterns are apparent from the data; first, only wells UW-7, GL-9, and UW-3 appear to contain compounds identified in the landfill seepage, and second, the concentrations appear to decrease between wells in the order given. Well UW-6, which is located along the creek between UW-7 and GL-9, did not contain these compounds. The fact that the sample from this well contained higher levels of the piezometer-lining compounds implies that either this well had not been completely purged of drilling water, or that some leakage had occurred. Therefore, this sample may not be representative of the ground water at this point. Wells UW-14, GL-11, and UW-10 contained essentially no extractable organics except the sulfur compounds.

The generally low concentrations of organics found in the wells make interpretation difficult. Studies of other landfills have commonly found high (mg/l) levels of organics, particularly carboxylic acids, near the source of the plume [5]. Their absence at this site may be due to any of several factors: the fractured rock of the aquifer may be impermeable enough that leachate is conducted through relatively few channels and the existing wells have not intercepted a zone of high contamination. Alternatively, the high organic content of the aquifer may result in organic contaminants being adsorbed onto the soil particles and effectively removed from the leachate. The data can be seen as giving some support to this second hypothesis. Of those compounds that appear to be mobile in the ground water, all are similar

in being moderately polar and water-soluble. Although none of these are extensively ionized at neutral pH, several are capable of hydrogen-bonding with water, which would lead to reduced interaction with the organic material of the aquifer. None of the neutral polyaromatic hydrocarbons are found in the wells sampled. The absence of organic acids is puzzling, but may signify that biological degradation is not a major factor under the highly reducing conditions found in the ground water.

Conclusions

The results presented in this report have several implications for future work on the Upper Ottawa Street Site. It is apparent that the analytical methodology can be changed and simplified to fit the needs of this project. The volatiles' analysis is unnecessary, and an acid-base separation step in the SEA method can also be eliminated. Unfortunately, the procedures which show the most promise in identifying tracer compounds are also the most time-consuming and expensive. It is possible that if a sulfur-removal step were added that a GC method could be substituted for GC-MS. A Total Organic Halogen (TOX) assay may be of use as a screening technique for identifying contamination, as there should be little interference from aquifer materials.

Regarding the plume of leachate from this site, it appears that the extent of organic contamination may be less than anticipated. The measured concentrations of those compounds that were found to migrate from the landfill were low, implying either failure to locate the streamline of the plume or an extremely high adsorptive capacity for organics within the aquifer. If the first alternative is to be examined further, additional samples will be needed; pooling samples from several depths within a well would increase the chance of detecting contamination.

Table 1

TENTATIVELY IDENTIFIED COMPOUNDS IN EXTRACTS

Solvent extract of GL-3-2 oily leachate

Alkyl (R)-Benzenes R=1-5 carbons
Dichlorobenzenes
Naphthalene
Alkyl(R-) Naphthalenes R=1-3 carbons
Anthracene, Phenanthrene
Alkyl Anthracenes and Phenanthrenes
Acenaphthene
Fluorene
Fluoranthene
Pyrene
Benz(a)anthracene
Chrysene
Biphenyl
Terpenes (camphor, pinene, etc.)
Tributyl phosphate
n-alkanes C10-C35+
2-methyl-alkanes
Alkylphenol polyethoxylate (3 EtO)

CLS extract of GL-2-2 standpipe leachate

| | |
|---------------------------------|-----------------------------|
| 4-Pentanone | Tetrachloroethylene (trace) |
| 4-Methyl-2-pentanone | Chlorobenzene |
| 2-Pentanone | Dichlorobenzenes |
| 2-Hexanone | Naphthalene |
| Dimethyl pentanone | Alkyl Naphthalenes |
| 2,2,4,4 tetramethyl-3-pentanone | Methyl benzonitrile |
| Trimethyl cyclohexanone | Terpenes |

Table 2

VOLATILE (VOA) AND PURGABLE (CLS) COMPOUNDS

| | Concentration $\mu\text{g/l}$ | | | | | | | | |
|---------------------|-------------------------------|-------------------------|------------|------------|------------|-------------|-------------|-------------|--------------------|
| | Seep ¹ | UW-7 ² -1 | UW-6 -1 | GL-9 -1 | UW-3 -1 | UW-14 -4 | GL-11 -1 | UW-10 -1 | Leach ³ |
| nd les roform | 0.2 - | 0.3 P | 0.1 - | 0.2 0.2 | P - | 0.4 0.4 | ND 0.3 | P P | 0.4 0.4 |
| 1 TC Ethane | 0.1 - | 0.1 P | 0.1 - | 0.2 0.1 | P - | 0.2 0.1 | P 0.1 | P P | 14.3 11.9 |
| | P - | P ND | ND - | P P | ND - | P P | ND 0.2 | ND ND | ND ND |
| 2 TC Ethane | P - | 0.1 0.2 | ND - | 0.1 P | P - | P P | 0.1 P | ND ND | P P |
| 4 | P - | P P | P - | P P | P - | P P | P P | P P | 0.1 P |
| oform | 0.3 - | ND ND | 0.1 - | ND ND | P - | P ND | P 0.1 | 0.1 P | 0.1 ND |
| les | | | | | | | | | Blank ⁴ |
| ene | ND | .43 | .92 | .21 | .37 | .61 | .21 | .31 | P |
| CCl ₂ | ND | .20 | P | .06 | ND | ND | ND | ND | ND |
| ene | 1.3 | 2.0 | .86 | .53 | .79 | .66 | .35 | P | P |
| robenzene | 4.0 | .08 | P | .07 | P | .31 | P | P | ND |
| lbenzene | 24.1 | 1.3 | .08 | .51 | .06 | .20 | .08 | P | ND |
| xylenes | 137 | 5.1 | .21 | 1.4 | .24 | .89 | .58 | .09 | P |
| ene | 2.6 | .07 | P | .05 | P | .13 | .05 | P | P |
| lene | 27.3 | 1.9 | .10 | .51 | .09 | .39 | .21 | P | ND |
| opylbenzene | 20.5 | .07 | P | P | P | .05 | P | P | ND |
| 5 Trimebenz. | 153 | .16 | P | .05 | P | .16 | .08 | P | ND |
| 4 TMB | 840 | 3.0 | .24 | .45 | .10 | .65 | .36 | P | ND |
| 3 TMB | 382 | .51 | .19 | .11 | P | .33 | .18 | P | ND |
| Dichlorobenz. | 4.0 | P | P | P | ND | .10 | P | ND | ND |
| OCB | 9.0 | .04 | .08 | P | P | .43 | P | P | ND |
| OCB | 8.3 | P | P | P | ND | .15 | P | ND | ND |
| thalene | 382 | .54 | .76 | .07 | P | .50 | .37 | .07 | .19 |
| -naphthalene | 24.9 | .15 | .17 | P | P | .17 | .06 | P | P |
| -naphthalene | 52.3 | .36 | .30 | P | P | .38 | .21 | P | P |

ot detected

resent below method detection limit

e from landfill seepage face

digit identifies depth of piezometer tube, i.e., UW-7-1 was taken from the topmost

[1] of well UW-7

meter lining leaching experiment

d blank

Table 3

COMPOUNDS LEACHED FROM PIEZOMETER
LINING MATERIALS

Phenol
Cresol
Benzaldehyde
2-(2-chloroethoxy)ethanol
Octanoic acid*
Decanoic acid*
Benzoic acid*
Benzothiazolone*
Benzothiazolethione*
2-methylthiobenzothiazole
Tributyl phosphate
Phenyl ether
BHT (butylated hydroxytoluene)
Bis(2-ethylhexyl) phthalate
Isocyanato benzene
Thiocyanic acid, ethyl ester
1,2,4 trithiolane
5-butylidihydrofuranone
Diethylene glycol**
Methyl Carbitol (2-(2-methoxyethoxy)ethanol)*
Salicylic acid
1,1,1-Trichloroethane

*major component

Table 4

SOLVENT EXTRACT COMPOUNDS

| Compound | Concentration $\mu\text{g/l}$ | | | | | | | | |
|-------------------|-------------------------------|------|------|------|------|-------|-------|-------|-------|
| | Seep | UW-7 | UW-6 | GL-9 | UW-3 | UW-14 | GL-11 | UW-10 | Leach |
| | | -1 | -1 | -1 | -4 | -1 | -1 | -1 | |
| line | 72.8 | ND | 0.5 | 0.5 | 5.6 | ND | ND | ND | ND |
| thyl aniline | 117 | 0.7 | ND | 1.8 | 4.0 | ND | ND | ND | ND |
| ime.aniline | 109 | 18.1 | ND | 4.2 | 5.8 | ND | ND | ND | ND |
| ol | 12.3 | 10.4 | 1.5 | 2.3 | 0.5 | 14.5 | 4.9 | ND | ND |
| thyl phenol | 40.8 | 16.2 | ND | ND | ND | ND | ND | ND | ND |
| yl alcohol 1', | | | | | | | | | |
| ' dimethyl- | 184 | 22.6 | ND | 25.9 | 7.1 | ND | ND | ND | ND |
| thyl phosphate | 17.4 | 15.8 | ND | 15.4 | 7.7 | ND | ND | ND | ND |
| thyl benzoic acid | 2.4 | 6.2 | ND | 1.6 | ND | ND | ND | ND | ND |
| quinolinone | 3.4 | 1.4 | ND | 1.7 | ND | ND | ND | ND | ND |
| aphthene | 8.1 | ND | ND | ND | ND | ND | ND | ND | ND |
| ic acid | 0.4 | 4.9 | 0.8 | 1.2 | P | 0.1 | P | P | 85.2 |
| yl phthalate | 7.5 | 2.0 | 5.3 | 2.3 | 0.4 | 0.5 | 2.0 | 1.8 | 2.6 |
| thiazole | 24.5 | 4.9 | 94.3 | 5.4 | P | 1.4 | 0.5 | 4.9 | SAT. |
| anthene | 2.6 | ND | ND | ND | ND | ND | ND | ND | ND |
| -butyl phthal. | 85.6 | 2.9 | 17.3 | 12.3 | 8.7 | 2.7 | 5.1 | 4.8 | 9.6 |
| thiazolone | 356 | 11.1 | 47.1 | 16.6 | 1.1 | 0.5 | 0.9 | 0.3 | 19.6 |

not detected

present below detection limit

Bibliography

1. Report on Hamilton Project, Univ. of Waterloo, draft, 1983.
2. Pickens, J. F., J. A. Cherry, G. E. Grisak, W. F. Merrit, and B. A. Risto, "A Multilevel Device for Groundwater Sampling and Piezometric Monitoring," Groundwater, 16(5):322-327, 1978.
3. Goring, C., and J. Hamaker, Eds., Organic Chemicals in the Soil Environment, Vol. 1, M. Dekker Inc., N.Y., 1972.
4. McCarty, P.L., et al., "Advanced Treatment for Wastewater Reclamation at Water Factory 21", Technical Report No. 236, Department of Civil Engineering, Stanford University, January 1980.
5. Chian, E. S., "Characterization of Soluble Organic Matter in Leachate," Environ. Sci. & Tech., 10, 158-163, 1977.

Hydraulic Conductivity Investigations of a groundwater zone
in shallow

fractured dolomite and limestone

Appendix G

by

R.A. Blackport and J.A. Cherry

Institute for Groundwater Research
University of Waterloo
Waterloo, Ontario N2L 3G1

November, 1984

INTRODUCTION

A major hydrogeologic investigation was performed in fractured bedrock at the Upper Ottawa Street Landfill situated near the top of the Niagara escarpment, Hamilton, Ontario (figure 1). The purpose of this study was to determine the extent of migration of the landfill-derived contaminants in the groundwater zone in the bedrock. As part of this overall investigation, a small site within the general study area was selected for more detailed studies of the hydraulic conductivity and fracture conductivity within the shallow bedrock units. The results of this site specific investigation are reported on in this paper with emphasis on comparison of the various hydraulic conductivity results from several types of tests at different scales. Pumping tests were used to determine the bulk hydraulic conductivity and fracture conductivity at the larger scale. Packer tests at various levels within boreholes and response tests of piezometers were used to determine hydraulic conductivity and vertical fracture conductivity at the smaller scale.

The study area is situated on a thin deposit of glacial till that overlies fractured dolomite and shale. The water table exists within the surficial glacial deposits. Horizontal or near horizontal fractures are evident in core samples and vertical or near vertical fractures are seen in the

small outcrop areas of the bedrock that exists in the vicinity of the study site. It was expected, therefore, that the dolomite and shale would display hydraulic conductivity in both vertical and horizontal directions. The various field tests provide a means of quantifying these hydraulic conductivities and of gaining insight into the influences of the fracture features as perceived from the various scales of tests.

SITE SETTING

The area chosen for the detailed study of hydraulic conductivity testing of the fractured rock is located east of the Upper Ottawa Street landfill (Figure 2). Regionally the shallow groundwater flow is from the west to the east. Seven boreholes equipped with multilevel monitoring devices were used for observation during the pumping tests. These devices were installed as part of an extensive groundwater monitoring program at the landfill. A central location was chosen for a pumping well (UW251) to utilize the existing monitoring well network. The multilevel device enables water level monitoring of several zones within one borehole (Cherry et al. 1984).

The rock units that directly underlie the Niagara Peninsula form part of the Michigan Basin sequence of sedimentary rocks, ranging in age from Ordovician to Devonian. The strata dip gently towards the south at approximately five metres per kilometre (Morris and White, 1975).

The study area is overlain by a one to three metres thick glacial till and glaciolacustrine clay which rests on nearly horizontal beds of fractured dolomite, shale and limestone. These rocks are, from the bottom up, the Queenston Formation (Late Ordovician), The Cataract Group (Early Silurian), the Clinton Group, and the Guelph Lockport Forma-

tion (Middle Silurian) (Morris and White, 1975). Only the upper two units are penetrated by the boreholes at the test site.

The highest stratigraphic unit is the Goat Island Member of the Guelph Lockport Formation which is a massive, irregularly bedded, fine grained dolomite. It is referred to as cherty dolomite in the geologic cross sections in Figure 4. The next unit includes two formations which are difficult to differentiate in the core logs. The Gasport Member of the Guelph Lockport Formation, and the lower Decew Formation are both highly variable, consisting of alternating thinly bedded semicrystalline dolomite and shale. The lowest unit is the Rochester shale which is a dark calcareous shale and siltstone with some interbedded limestone. The Gasport Member, the Decew Formation, and the Rochester shale are referred to as dolomitic shale and shale in this study.

The strata may be divided generally into two hydrogeological units. The shallow cherty dolomite is a high hydraulic conductivity zone while the deeper dolomitic shale and other shale units generally have lower hydraulic conductivities. The study concentrated on the shallow high hydraulic conductivity zone and the upper portion of the underlying low hydraulic conductivity to determine variations in hydraulic conductivity and connectivity on both a localized and a large scale.

Pollard (1959) considered all three components to affect head differentials during very early times, however as time increased the only component of flow would be from the matrix or micro fracture system into the main fracture system. As a result, the shape of response curves depend on the magnitude of each components of flow. For example, if there was little disturbance around the well, and there was a non-existent or poorly connected fracture system, then the only real component of water flow would be from the rock matrix or micro fractures along bedding planes and the response curve would essentially be a straight line as in Figure 6a. This can be analysed by the Hvorslev method as the system is treated as a reasonably homogeneous porous medium with flow primarily through the rock matrix.

If some well disturbance was encountered, and there was no connected fracture system, then a response curve similar to Figure 6b might be expected. It is also possible that the fracture system is well connected and resulting curves could be similar to Figure 6a and 6b if the recovery of the water level to equilibrium is relatively rapid. The component of flow from the rock matrix would then be negligible compared to the flow of water from the fracture system during this time period.

If flow through the fracture system and matrix system is occurring in the vicinity of the piezometer intake zone, a response similar to Figure 6c might be expected, whether

METHODS OF INVESTIGATION

Water level response tests in individual piezometers in the multilevel monitoring devices were performed using either the rising head or the falling head methods. The rising head method was applied to most of the piezometers. These tests were performed by evacuating much of the water column from each piezometer using the triple tube pump developed by Robin et al., (1982). Immediately after the water column in each piezometer was expelled, the tubing of the pump was withdrawn and the water levels were measured with sufficient frequency to define the rate of water level recovery.

The rates of water level recovery in some of the piezometers were too rapid for this test method to yield useful results. In these rapidly responding piezometers, therefore, falling head response tests were then conducted. These tests were accomplished by coupling a large diameter reservoir to the top of the piezometer tubing. Before each test was conducted this reservoir was filled with water pumped from the piezometer to be tested and then the water level in the piezometer was allowed to reach equilibrium before testing. The water level in the reservoir was allowed to decline rapidly when a valve was opened and the rate of decline was monitored visually in the reservoir rel-

ative to a graduated scale with readings noted at various times. The piezometers tested in this manner were generally at shallow depth where the hydraulic conductivity is highest and the water table is near ground surface.

The primary purpose of the piezometer response tests described above was to obtain values of hydraulic conductivity for each of the borehole intervals in which piezometers were installed. A secondary purpose of these tests was to obtain information on the degree of vertical hydraulic connection between each piezometer zone and the ones above and below. Thus when some of the piezometer response tests were done, water level measurements were made in the piezometers above and below the piezometer being response-tested. This type of monitoring in an individual multilevel device provides information on the degree of vertical hydraulic connection that exists at a very local scale. Information on the extent of vertical hydraulic connection at a much larger scale was obtained from the pumping tests described below.

At site UW25-1 where an open borehole exists to a depth of 20 metres with casing in the top 2 metres, constant head injection tests were conducted to obtain values of hydraulic conductivity. The test intervals in the borehole were isolated using double packers inflated with nitrogen. Water was injected into each test zone under conditions of constant head in the above-ground reservoir and conditions of

essentially constant flow rate under steady state conditions. The test system is illustrated schematically in Figure 2. The test system includes several reservoirs of different diameter so that injection rates could be adjusted to suit the hydraulic conductivity of the zone being tested. The zones with highest hydraulic conductivity were not successfully tested because of the excessively large volume of water needed to maintain the constant head in the reservoir.

The pumping tests were conducted by pumping the borehole at site UW25-1 and measuring water level declines in various piezometers in the multilevel devices and in two open shallow boreholes near the pumping hole. These boreholes are designated UW2-2 which extends to a depth of 4.2 metres and UW3-2 which has a depth of 4.5 metres. Cross-sections of the pumping test site showing the geology and location of multilevel monitors and open boreholes are shown in Figure 4. Locations of the cross-sections are displayed in Figure 2.

Four pumping tests using the borehole at UW25-1 were performed. In the first test the entire borehole was left open for pumping. In the other three tests, different segments of the borehole were pumped when the borehole segments were isolated using the inflatable packers. By conducting pumping tests using different vertical segments of the borehole information on the vertical hydraulic connection provided by the fractured rock was obtained.

Information on the nature of the fractured rock at the study site was also obtained by monitoring static water levels in the multilevel devices. The differentials in water levels observed in each multilevel device under static conditions provided qualitative insight into the continuity of zones of highest hydraulic conductivity in the rock.

RESULTS AND DISCUSSION

Response Testing

Response tests for hydraulic conductivities were analysed by the method of Hvorslev (1951). To determine hydraulic conductivities using the Hvorslev method, the rate of water level recovery and the shape of the piezometer intake are utilized in the following equation:

$$K = r^2 \ln (L/R)/(2LT_0)$$

where r is the radius of the piezometer [L], L is the length of the intake zone [L], R is the radius of the intake zone [L], and T_0 is the basic time lag [T]. The basic time lag is defined as the time that would be taken for complete water level recovery to occur in a piezometer if the initial rate of water inflow were maintained. This is the length of time required to achieve 63% of the complete water level recovery.

To determine T_0 , the data are plotted on a semi-logarithmic scale of time versus relative water level recovery, as shown in Figure 6. In theory, the data should represent a straight line passing through the origin. This is based on several assumptions which are, that radial flow occurs into the test section and is governed by Darcy's law, and the zone is a homogeneous porous medium. However, the nature of the fractured rock being investigated in this

study would imply a varying degree of homogeneity within each rock type depending on the degree of fracturing, fracture connection, size of fractures and roughness of fractures. As a result a number of response curves were not straight lines and exhibited varying non-linear responses on semi-logarithmic plot.

Figures 6b, 6c, and 6d show examples of these responses. Before discussing these diagrams, a brief description of the hydraulic head response in a fractured porous medium will give a better understanding of the behaviour of these curves. Pollard (1959) and Schwartz (1975) give a more detailed description of the hydraulic head response in fractured porous medium. Three possible components or stages of water flow can occur when water is removed from a piezometer where the water level or hydraulic head is at equilibrium.

The first possible stage is a rapid decrease in hydraulic head in the disturbed zone (i.e. the disturbed zone as a result of drilling) in the vicinity of the piezometer intake. The second stage is when hydraulic head within the zone is equalizing, water movement occurs in the fracture system connected to the piezometer intake zone. The third stage is when the hydraulic gradients (i.e. water levels) within the fracture system equalize with time, flow occurs from within the rock matrix or micro fractures to the main fracture system due to the head differentials between the two systems.

well disturbance is present or not. Schwartz (1975) describes how resistance to flow by disturbance around the well or resistance to flow by the fracture system is determined for the early portion of the curve and this will not be discussed here.

If the fracture system is connected for some distance around the piezometer intake but gradually decreases in fracture size or number of fractures connected, then a long declining curve as in Figure 6d might be expected where an equilibrium head within the fracture system is attained very slowly relative to the response time and it is difficult to separate the components of fracture flow and matrix flow.

Hydraulic conductivities of response tests showing curves similar to Figure 6b and 6c can be determined by a method developed by Pollard (1959) which has the same theoretical basis as Hvorslev (1951). The slope of the straight line portion of the response curve can be used to determine the equilibrium time as in the Hvorslev method, and matrix hydraulic conductivity can be determined. If the slope of this straight line is subtracted from the values in the early part of the curve, then the component of water flow from the fractures only, can be determined and an equilibrium time from the slope of this line can be used to determine fracture hydraulic conductivity in the vicinity of the well.

Results of response testing of monitoring zones in the study area are shown in Table 1. Results indicate two gen-

eral trends. In the shallow groundwater zone where the rock unit is the cherty dolomite of the Goat Island Member the hydraulic conductivities were generally high, on the order of 1.5×10^{-3} cm/sec. Some recoveries (i.e. UW3-2, UW1-4) were too fast to obtain an accurate value of hydraulic conductivity by the rising head method. However, based on the maximum time taken to obtain the initial water level after pumping, which was already back to an equilibrium level, the minimum value of hydraulic conductivity was 6.1×10^{-4} cm/sec for these monitoring zones. Some of the monitoring zones in the cherty dolomite exhibited a lower hydraulic conductivity than the median value. These values were on the order of 1×10^{-5} to 1×10^{-6} cm/sec.

The majority of the high hydraulic conductivity zones exhibited a linear water level recovery as in Figure 6a. Some of the lower hydraulic conductivity monitoring zones in the cherty dolomite exhibited a non-linear response similar to Figures 6c and 6d indicating that the fracture network near the monitoring zone has a higher hydraulic conductivity than the fractures away from the monitoring zone.

In the rock units below the cherty dolomite the values of hydraulic conductivity determined from response tests were generally low, on the order of 10^{-6} - 10^{-8} cm/sec.

There was one very high hydraulic conductivity (UW3-4) of 2.6×10^{-3} cm/sec found in the Rochester shale indicating that the shale does have high hydraulic conductivity zones.

This monitoring zone was pumped and zones above and below it as well as the centre column of the multilevel monitoring device were monitored for any changes in water levels to determine if a possible leak may have been the reason for high hydraulic conductivity.

Water level recoveries in the lower hydraulic conductivity rock units generally exhibited a non-linear response similar to Figures 6c and 6d indicating the decreasing fracture hydraulic conductivity away from the monitoring zone.

Packer Testing

In determining hydraulic conductivity from the packer test method used in this study, it was assumed that laminar flow occurs between the vertical test section and surrounding rock. It was also assumed the rock is a homogeneous isotropic porous medium. The above assumptions are standard practice as outlined by Zeigler (1976).

A number of methods are available to determine hydraulic conductivity by this test method, and under most situations many of them yield identical results. The equation used for this study was derived by Hvorslev (1951) and is;

$$K = Q \ln(R/r_o) / Ls h_o$$

where K = hydraulic conductivity [L/T]

h_o = excess pressure head [L] at the centre
of the test section

R = radius of influence [L]; i.e. the radial

distance from the test section
corresponding to a 100 percent loss in
excess head, H_o .

L_s = length of the test section [L]

r_o = radius of the borehole [L]

Q = volume flow rate [L^3/T]

The volume flow rate Q was obtained from calibrated flow reservoirs at ground surface and averaged over time. The length of each test was determined by the consistency of flow rate under a given pressure, the more consistent the rate the shorter the duration of each test. The excess pressure head, H_o , at the centre of the test section was calculated from the following equation:

$$H_o = h_i + H_c - s_h$$

where h_i is the induced head, taken as a pressure reading from the pressure gauge at a ground surface and converted to head, H_c is the excess head in the borehole, above the static water level of the test zone, and s_h is the head loss due to friction in the pipe. The s_h term was assumed to be negligible for this study because of the low flow rates and shallow testing depths.

The radius of influence R must be estimated. It is generally quite small and often assumed to be equal to or less than the length of the test zone. A rough estimate of R is normally adequate since large variations in R generally produce only small variations in the calculated hydraulic

conductivity. Studies conducted by Zeigler (1976) indicate that changing the radius of influence from 1.0 ft (0.3 m) to 1×10^{-6} ft (3×10^5 m) for a test conducted in the same size borehole used in this study, resulted in the hydraulic conductivity changing by only a factor of 7.5.

Hydraulic conductivity was calculated for the range of observed values of excess pressure head and corresponding values of flow rates for each zone tested. Results did not always yield similar values for each zone as deviations could occur as a result of hydro fracturing of the rock mass under high pressures or the loss of a packer seal. Tests were performed by increasing the pressure at each test interval to a reasonable point and lowering the pressure to attempt to duplicate results. A reasonable number of tests were performed on each test section in borehole UW25I and the average value reported as shown in Table 2.

Results were difficult to obtain in the cherty dolomite due to the high hydraulic conductivity. Results indicated hydraulic conductivities of at least 1.0×10^{-3} cm/sec except for one zone towards the base, which was slightly lower (1.0×10^{-4} cm/sec). The underlying Gasport dolomite and upper Rochester shale had a hydraulic conductivity of around 8.5×10^{-6} cm/sec. A zone of high hydraulic conductivity was found in the Rochester shale at 11.6 - 12.8 m and was $> 1.0 \times 10^{-3}$ cm/sec. This zone is the same elevation as Uw3-4 and compares favorably with the hydraulic conductivity

of 3.6×10^{-3} cm/sec determined from response testing. The remainder of the tests indicated hydraulic conductivities to range from 9.4×10^{-7} cm/sec to 1.0×10^{-8} cm/sec in the Rochester shale, the same range as determined from response testing. Results of packer testing indicate that although the test zone was longer than the test zones in response tests the hydraulic conductivities obtained were similar for the various rock units.

Pumping Test Results

Analyses of pumping test data can be performed using numerous methods depending on the geologic setting and hydrogeologic conditions. Kruseman and De Ritter, 1979 give one of the most comprehensive description of methods of analyses available in the literature, and methods will only be briefly discussed here.

Most data are plotted in some form of time-drawdown curves on either single logarithmic scale or double logarithmic scale. The shape of the resulting curve often determines which method of analyses are most applicable, but information on the geology of the site is also necessary to determine the method most suitable.

The methods of analyses used in this study were restricted to relatively simple methods. Although the behavior of water movement in fractured rock is complex, the basic methods of analyses should give reasonable estimates

of hydraulic characteristics. Generally, several methods were employed to determine if results were in reasonable agreement to each other.

The methods of Theis, Jacob and Boulton were the most commonly used in this study. Theis and Jacob methods are used to determine the hydraulic conductivity in either a confined or unconfined aquifer, The Boulton method is used to determine the hydraulic conductivity yield from either a semi-confined (leaky) aquifer or unconfined aquifer with delayed yield.

The first pumping test (PT1) was performed on September 30 and October 1, 1983 with the entire length of UW25-1 left open and pumped. The pumping rate was initially set at 28.5 lpm, however the water level response was less than anticipated and was increased to a pumping rate of 39 lpm after approximately 300 minutes. The duration of the pumping was 1500 minutes. Water level recoveries were monitored for 1440 minutes after pumping was stopped. Results of analyses of hydraulic properties for PT1 are shown in Table 3.

Sufficient water level response data were obtained at 14 locations to determine hydraulic characteristics at those locations. All locations but one showing water level responses were in the cherty dolomite (Lockport dolomite), which was to be expected based on results of response tests. The only zone showing a water level response below this dolomite was UW3-4, located in the Rochester shale. This

zone also had a very high hydraulic conductivity from the response tests.

Results indicate the hydraulic conductivity in the cherty dolomite ranges from 3.2×10^{-2} cm/sec to 1.1×10^{-3} cm/sec for 40 analyses performed on drawdown data in 13 locations in the Lockport dolomite. Most analyses were done using the Theis and Jacob method as data generally fit the Theis drawdown curve for a confined or unconfined aquifer. Early and later portions of the drawdown curves were analysed as two different pumping rates were used. Water level recovery data was also analysed. Figure 7 shows examples of Jacob plots of drawdown versus time on a semi logarithmic scale. Figure 8 shows examples of Theis plots of drawdown versus time on a logarithmic scale.

Results agreed quite well in most cases for different methods of analyses used. For example UW3-2 had hydraulic conductivities of 2.2×10^{-3} cm/sec for Theis (early part), 2.7×10^{-3} cm/sec for Jacob (early part), 1.3×10^{-3} cm/sec for Jacob (later part) and 1.1×10^{-3} cm/sec for the Theis recovery method.

Analyses of early drawdowns at a low pumping rate and later drawdowns at a high pumping rate using the Jacob method indicate a decrease in hydraulic conductivity at later times of generally a factor of three to four. For example the hydraulic conductivity of UW25II-2 decreased from 8.2×10^{-3} cm/sec to 2.6×10^{-3} cm/sec and UW25II-3 decreased from

6.6×10^{-3} cm/sec to 1.7×10^{-3} cm/sec. This could be the result of several factors. The increased pumping rate could be drawing a greater percentage of water out of the shallow zones than during to lower pumping rate, or the drawdown cone caused by the pumping could be extending to a lower hydraulic conductivity zone than was encountered in the vicinity of the pumping well.

Hydraulic conductivities appeared to show a slight decrease with depth in the Lockport dolomite based on results from PT1. However these decreases are small, a factor of two to three and are not considered significant based on this pumping test alone.

The hydraulic conductivity of the only zone showing a water level response not located in the Lockport dolomite was UW3-4 which is in the Rochester shale. The hydraulic conductivity of this zone ranged from 1.0×10^{-3} cm/sec to 2.0×10^{-3} cm/sec. It should be noted that this zone is the same elevation as a high hydraulic conductivity zone found in the pumping well.

The second pumping test (PT2) was performed at UW251 on October 18, 1983 by pumping the zone from 11.6 - 12.8 m located in the Rochester shale. The duration of the test was 3 hours, the pumping level was found to be too great as degassing occurred in the pumping line and it appeared that the amount of water available from the pumping zone had decreased significantly (probably the result of dewatering

the fracture zone). Pumping was ceased and water level recovery monitored.

Results of analyses for hydraulic conductivities in the few monitoring zones to respond during PT2 are shown in Table 3. Figure 19 shows the time-drawdown curves for UW3-4 and UW3-2. The drawdown curve for UW3-4 was analysed by the Theis and Jacob methods with the hydraulic conductivity determined to be 2.3×10^{-3} cm/sec and 2.5×10^{-3} cm/sec respectively.

A more complex analysis was performed utilizing drawdown curves for both UW3-4 and UW3-2. The method was developed by Neuman and Witherspoon, 1969 and in the case of UW3, assumes the lower zone (UW3-4) being pumped is an aquifer and the upper zone (UW3-2) is also an aquifer but is not pumped. These two aquifers are separated by an aquitard through which vertical leakage occurs. Results of analyses indicate the hydraulic conductivity of UW3-4 in the Rochester shale to be 8.8×10^{-4} cm/sec. The aquitard, or upper zone of the Rochester shale and the Decew Formation had a calculated vertical hydraulic conductivity of 2.4×10^{-6} cm/sec. Packer tests conducted in the same zone at UW251 had a hydraulic conductivity of 8.5×10^{-6} cm/sec.

The third pumping test (PT3) commenced on October 27, 1983 with the upper 7.6 m (cherty dolomite) sealed off and pumped at a rate of 39 Lpm for 1600 min. Results of analyses for hydraulic conductivity are shown in Table 3. Examples of time-drawdown curves are shown in Figure 10.

tion (i.e. vertical interconnection) of the base of this dolomite to dolomite in the upper part of the Lockport formation. The duration of FT4 was 270 min. at a pumping rate of 6.3 Lpm.

Results of analyses of the hydraulic properties are shown in Table 3. Few monitoring zones responded during the pumping and as a result only three hydraulic conductivities were determined at two zones, both of which were the same elevation as the pumping zone. Figure 11 shows the time-drawdown curves for UW2-2 and UW3-2. UW3-2 showed hydraulic conductivity results of 5.2×10^{-3} cm/sec by the Theis method and 1×10^{-3} cm/sec by the Glover, Woody and Tap method. The hydraulic conductivity at UW2-2 was determined to be 5.4×10^{-3} cm/sec using the Theis method. It should be noted that rapid response occurred at UW25-III-3 during the first 2 minutes of pumping and quickly stabilized. No early data were obtained and as a result no analyses could be performed.

A vertical hydraulic conductivity was determined above the monitoring zone at UW3-2 using the Glover, Woody and Tap method. Results indicate the vertical hydraulic conductivity to be on the order of 6.9×10^{-6} cm/sec in this portion of the Lockport dolomite.

In summarizing the quantitative results of the hydraulic characteristics of zones pumped in the previously described tests it can be seen from Table 3 that results

generally agreed quite well between tests and methods used to analyse the results. The prime water bearing zone was the Lockport dolomite, the upper most rock unit, upon which the Upper Ottawa Street landfill lies. Fifteen zones were analysed from the four pumping tests using 7 different methods or analyses to obtain 51 values of hydraulic conductivities. These values ranged from 2.6×10^{-2} cm/sec to 1.1×10^{-3} cm/sec, showing a relatively consistent value of hydraulic conductivity within the Lockport dolomite, as well as consistent values between different methods of analyses.

Two hydraulic conductivity determinations were made in the vertical direction within the Lockport dolomite. One test, in the zone above UW25111-3 in P13, indicates a vertical hydraulic conductivity of 2×10^{-4} cm/sec while the other test made in the zone above UW3-2 indicates a vertical hydraulic conductivity of 6.9×10^{-5} cm/sec. Although there is limited data for vertical hydraulic conductivity the results would indicate that it is lower than the horizontal hydraulic conductivity by one to three orders of magnitude.

Hydraulic conductivities determined for the only water bearing zone found below the Lockport dolomite, at UW3-4 in the Rochester shale ranged from 8.3×10^{-4} to 2.5×10^{-3} cm/sec for six analyses. A vertical hydraulic conductivity in the zone of Rochester shale and Decew Formation between UW3-4 and UW5-2 was determined to be 2.4×10^{-7} cm/sec.

CONCLUSIONS

Results of several methods of determining hydraulic conductivities in fractured dolomite and shale indicate that small scale and large scale tests yield similar results and that the water level recovery data from response tests may give a reasonable idea of the degree of fracturing within a rock unit.

Results of response tests of 0.6 m - 1.0 m intervals in the high hydraulic conductivity cherty dolomite of the Goat Island Member of the Lockport Formation indicate that the hydraulic conductivity is approximately 1.5×10^{-3} cm/sec with some values as low as 1×10^{-6} cm/sec. Response tests in the lower hydraulic conductivity shales and shaly dolomites were on the order of 10^{-6} - 10^{-8} cm/sec, with one value of 1.6×10^{-3} cm/sec.

Many of the low hydraulic conductivity zones exhibited non-linear water level recoveries on a semi-logarithmic plot, while most of the high hydraulic conductivity zones exhibited a linear response. This would indicate that the rock units with high hydraulic conductivities show well connected fractures while the lower hydraulic conductivity units show a varying degree of fracture connection, often decreasing with distance from the monitoring zone.

Results of packer testing 1.5 m intervals on the open borehole at UW251 show similar hydraulic conductivity results to the response tests. Values of hydraulic conductivity in the cherty dolomite was at least 1.0×10^{-3} cm/sec in 2 of the 3 intervals tested, similar to the values of response tests. Hydraulic conductivities in the shale units generally ranged 10^{-6} - 10^{-8} cm/sec. One high value of $> 1.0 \times 10^{-3}$ cm was determined at 11.6 - 12.8 m and this corresponds with the zone at UW3-4 in the shale which had a hydraulic conductivity of 2.0×10^{-3} cm/sec from response tests.

Results of pumping tests utilizing simple analyses on a relatively complex hydrogeologic system (i.e. fractured rock) yielded a generally good agreement between methods of analyses and between pumping tests. Fifteen monitoring zones from the cherty dolomite were analysed from four pumping tests using seven methods of analyses. Fifty-one values of hydraulic conductivity were obtained and ranged from 2.6×10^{-2} cm/sec to 1.1×10^{-3} cm/sec. This shows a general consistency both in the unit studied and methods of analyses used.

The results also compare well with the response tests and packer tests in the high hydraulic conductivity zones. Even though the rock is fractured, the high hydraulic conductivity values agree well from intervals as small as 0.6 m long and pumping tests showing drawdowns several hundred

metres away from the pumping well. No response was exhibited in any of the monitoring zones showing a low hydraulic conductivity. Since most of these zones exhibited a non-linear response than it is assumed that the fractures are not well-connected over sufficient distances to be important pathways to groundwater movement. However, the good comparison of hydraulic conductivity between different test methods in the high hydraulic zone in the generally low hydraulic conductivity Rochester shale as well as a good horizontal connection indicates that a low hydraulic conductivity unit may contain sufficient permeable zones to be an important pathway for groundwater movement.

List of Figures

- Figure 1. Location Map
- Figure 2. Site Setting
- Figure 3. Multilevel Monitoring Device
- Figure 4. Geologic Cross Sections
- Figure 5. Schematic representation of the borehole packer testing system (after Gale et al. 1975)
- Figure 6. Types of water level response curves
- Figure 7. Time-Drawdown Curves for UW3 (PT1)
- Figure 8. Theis Plots for PT1
- Figure 9. Time-Drawdown Curves PT2
- Figure 10. Time-Drawdown Curves PT3
- Figure 11. Time-Drawdown Curves PT4

List of Tables

Table 1. Hydraulic conductivity results from response
testing.

Table 2. Hydraulic conductivity results from packer testing.

Table 3. Hydraulic conductivity results from pumping tests.

References

- Hvorslev, M.J., 1951. Time Lag and Soil Permeability in Groundwater Observations, U.S. Corps. Eng. Waterways Exp. Stn. Bull. No. 36.
- Morris, P.G. and C.L. White, 1975. Engineering Geology of the Niagara Peninsula, G.A.C., M.A.C., G.S.A. Field Trip, No. 9.
- Neuman, S.P. and P.A. Witherspoon, 1969. Applicability of Current Theories of Flow in Leaky Aquifers, Water. Resources Research, Vol. 5.
- Pollard, P., 1959. Evaluation of Acid Treatments from Pressure Building Analysis. Petrol. Trans. Am. Inst. Min. Eng. 216 pp. 38-43.
- Robin, J.J.L., D.J. Dytynyshyn, and S.J. Sweeney, 1982. Two Gas-Driven Sampling Devices for Deep narrow Piezometers. Groundwater Monitoring Review, Vol. 2, no. 1, pp. 63-66.
- Schwartz, F.W., 1975. Response Testing of Piezometers in Fractured Porous Media, Can. Geotech. J., Vol. 12.
- Zeigler, F.W., 1976. Determination of Rock Mass Permeability. Vicksburg, U.S. Army Engineer Waterways Experimental Station.

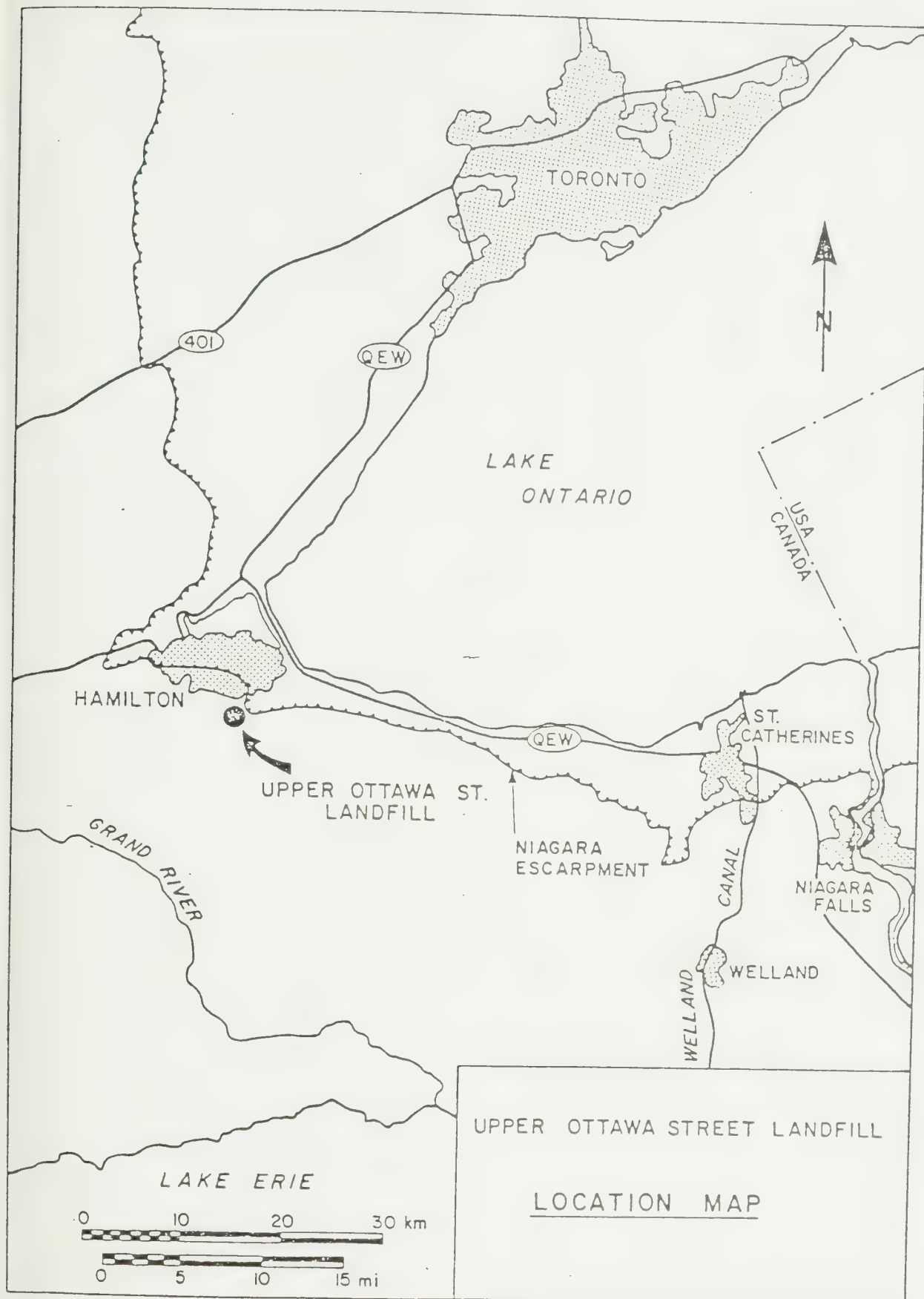
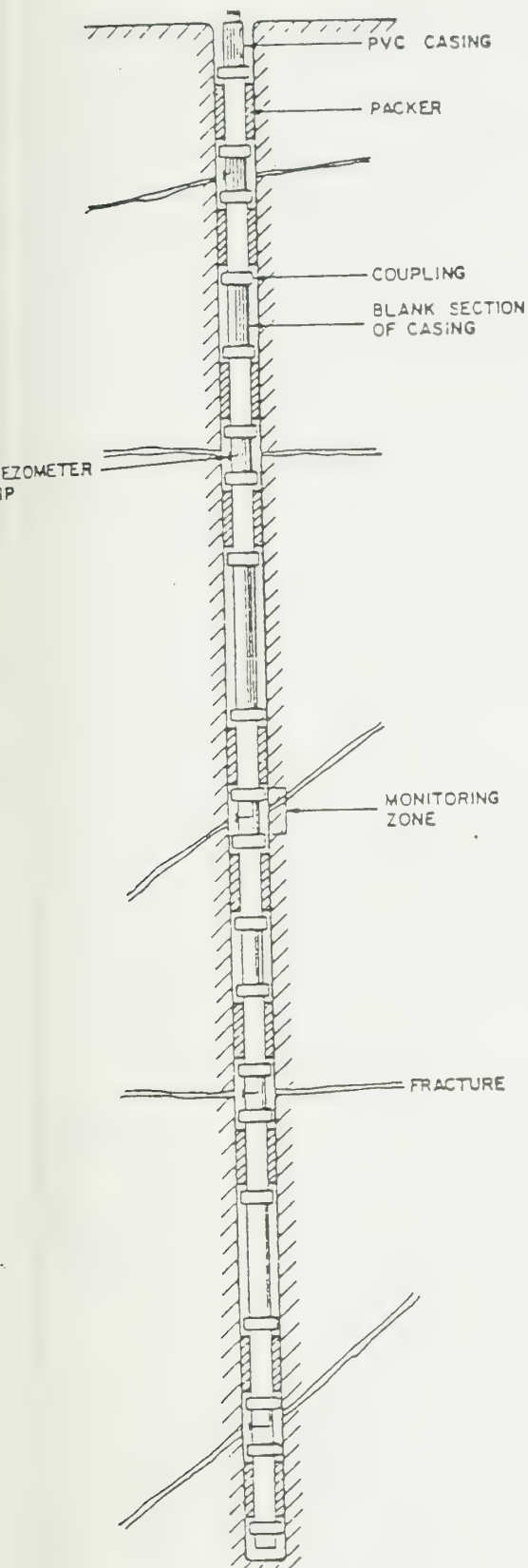


Figure 1. Location of the Upper Ottawa Street Landfill

Figure 2. Site setting



DISCREET ZONE MONITORING



SEGMENTED BOREHOLE MONITORING

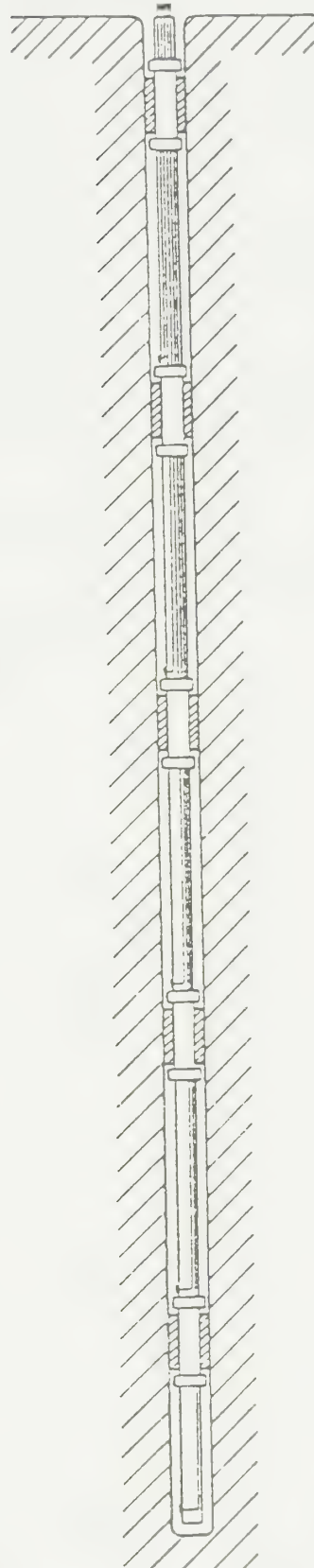


Figure 3. Schematic illustration of the multilevel device

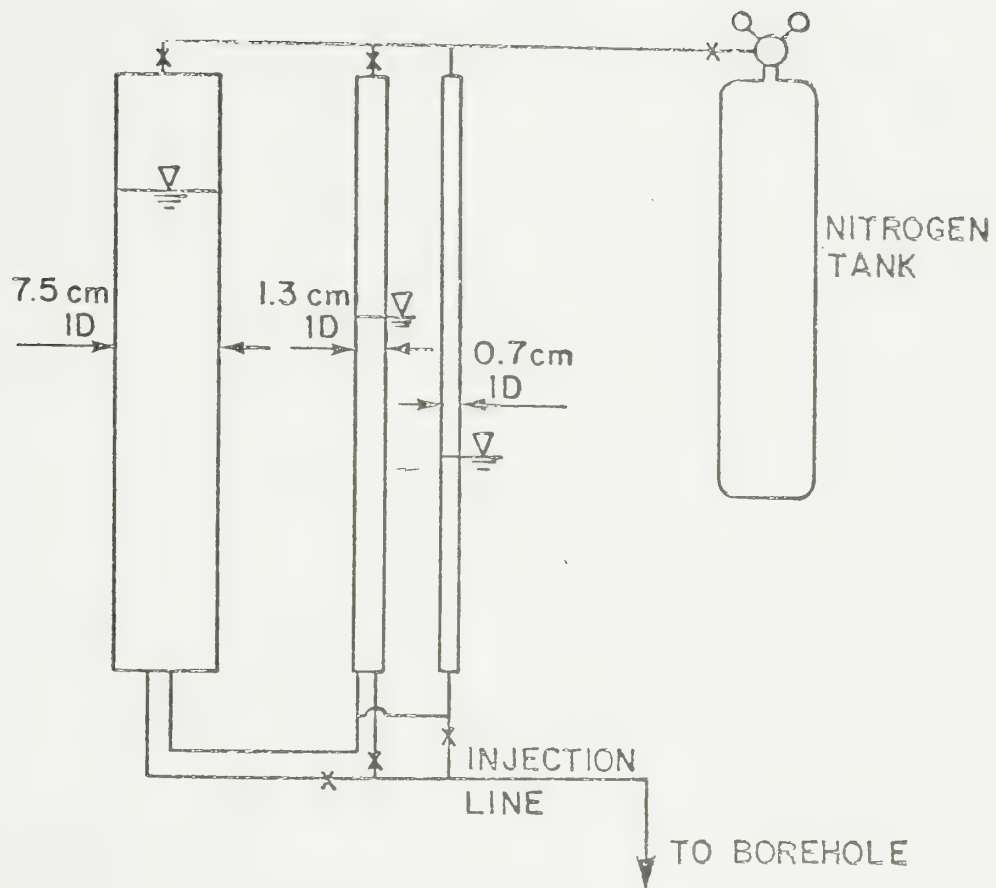


Figure 5. Schematic representation of the borehole packer testing systems .
(after Gale et al. 1979).

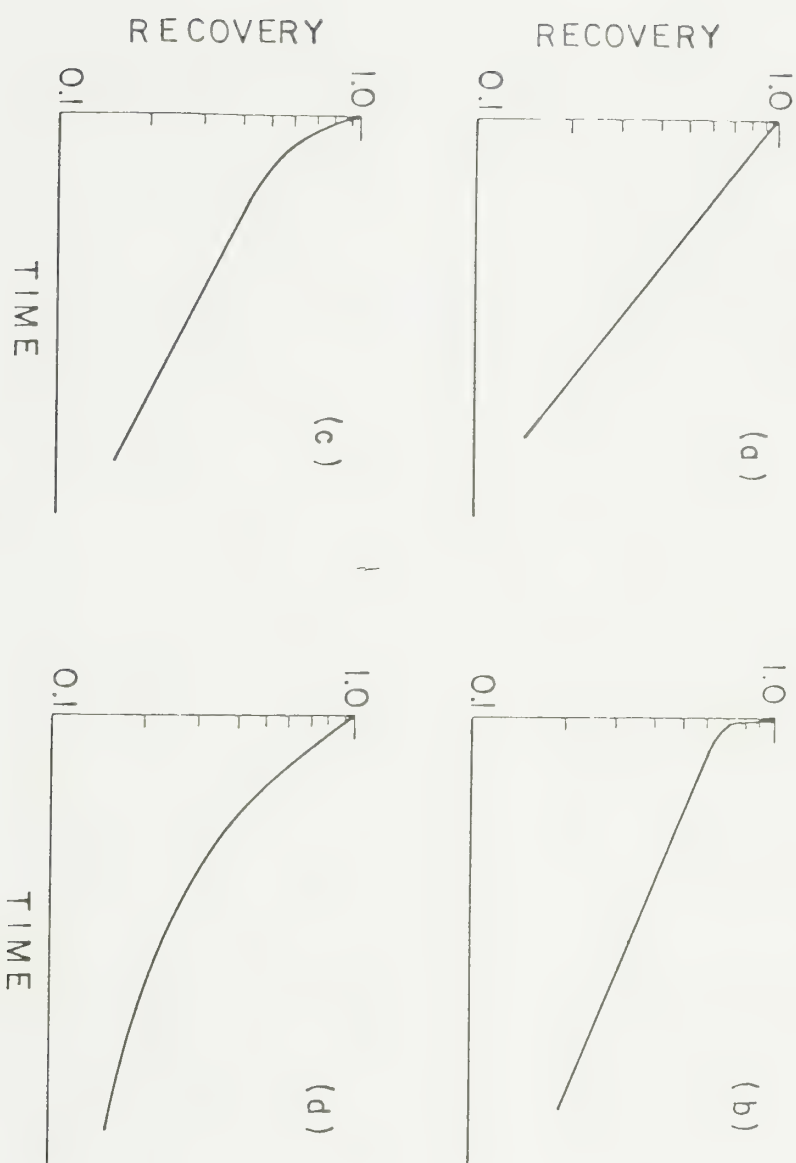
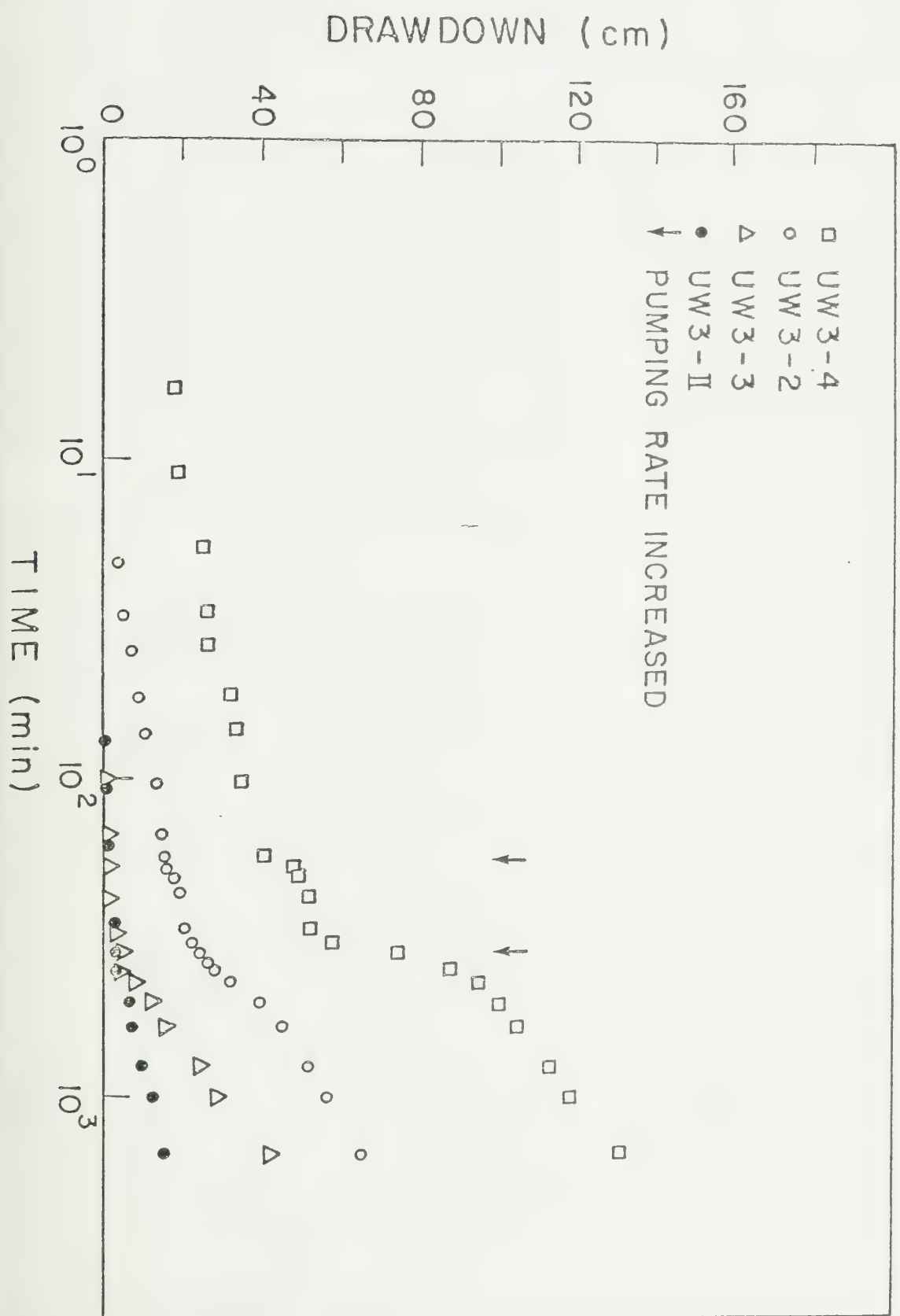
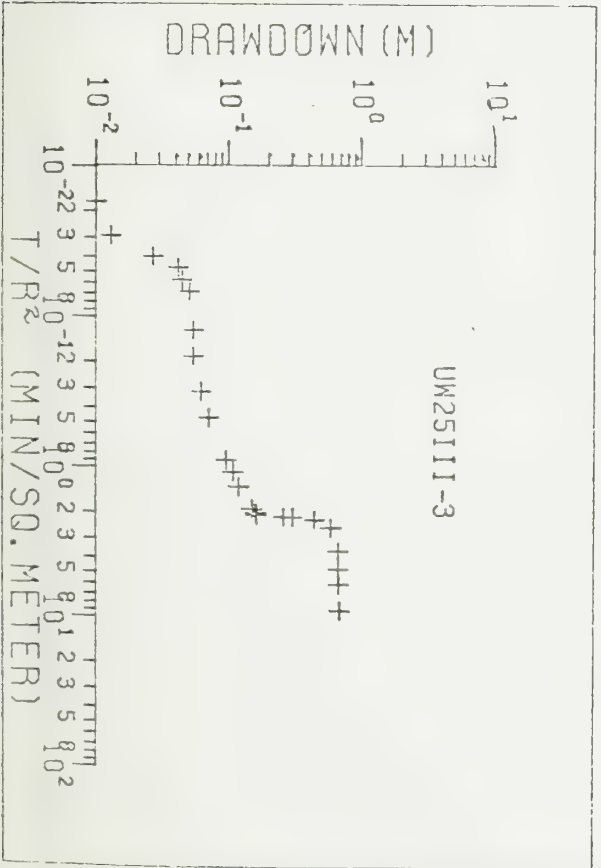
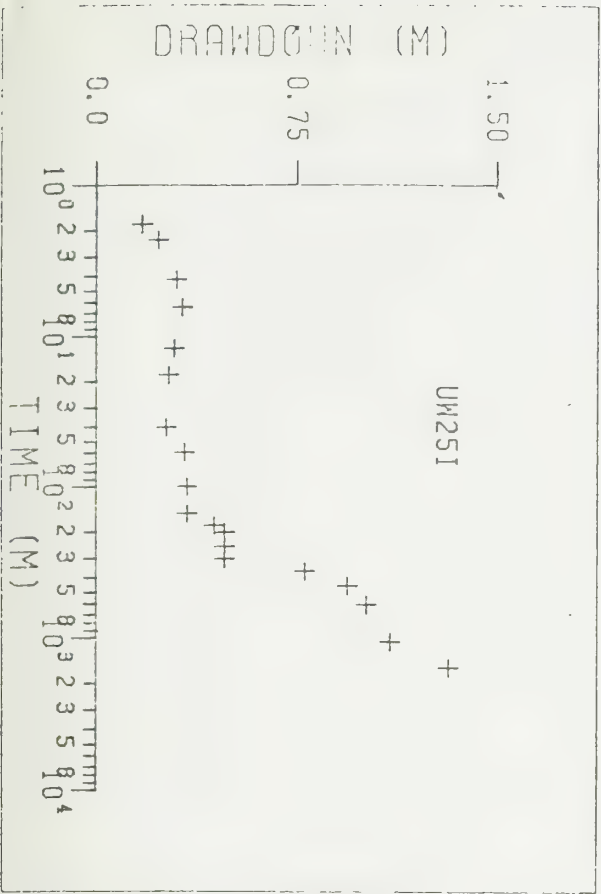
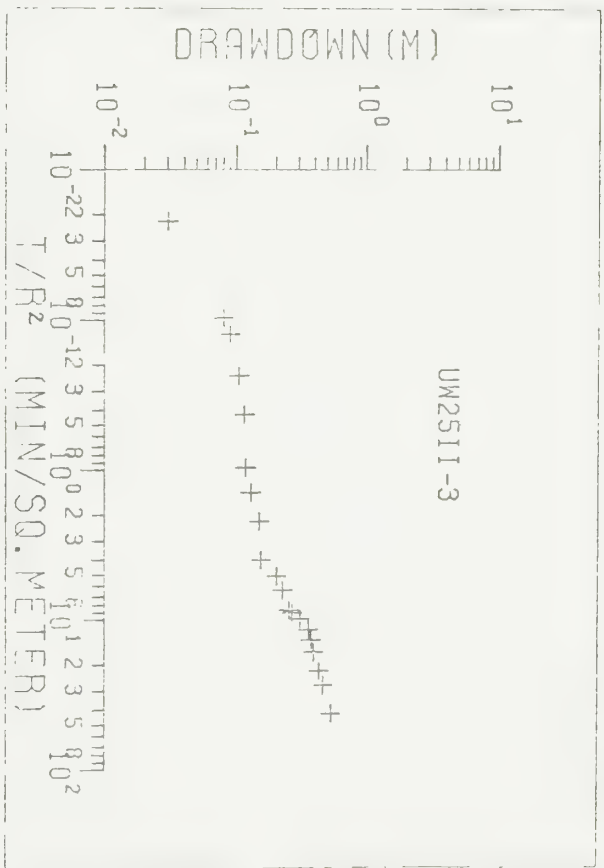
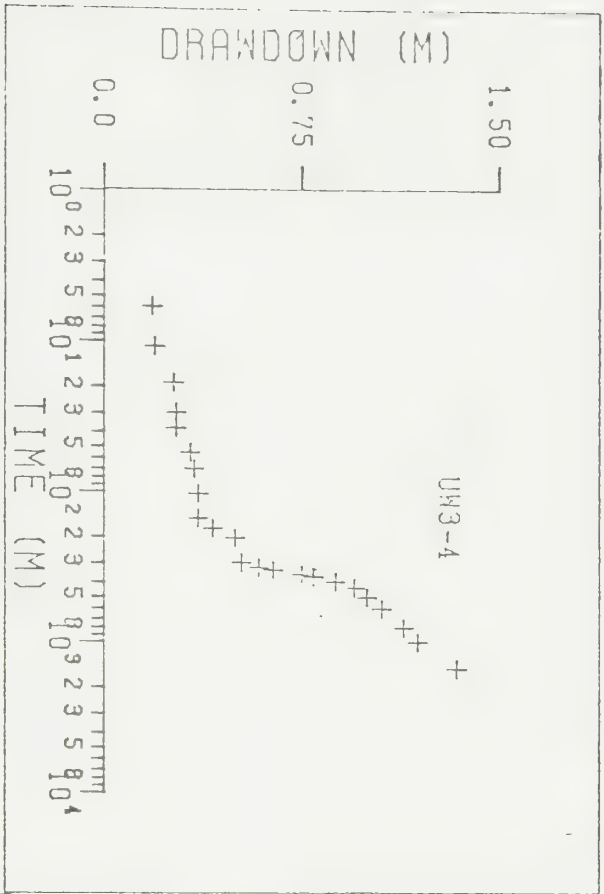
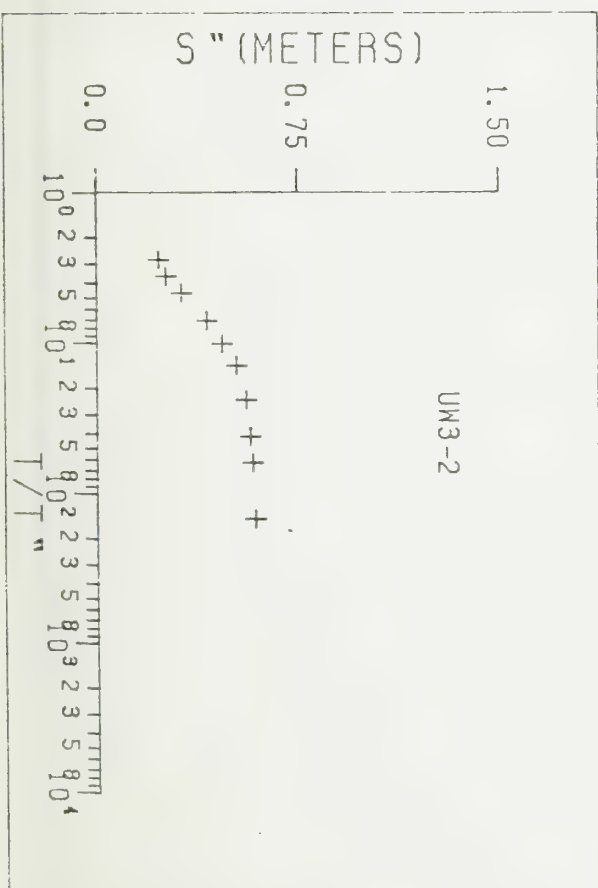
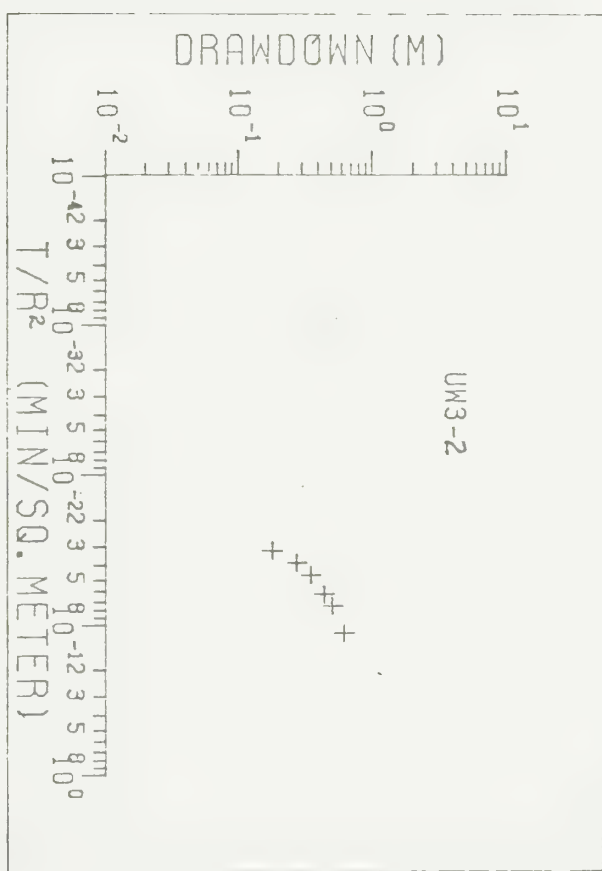
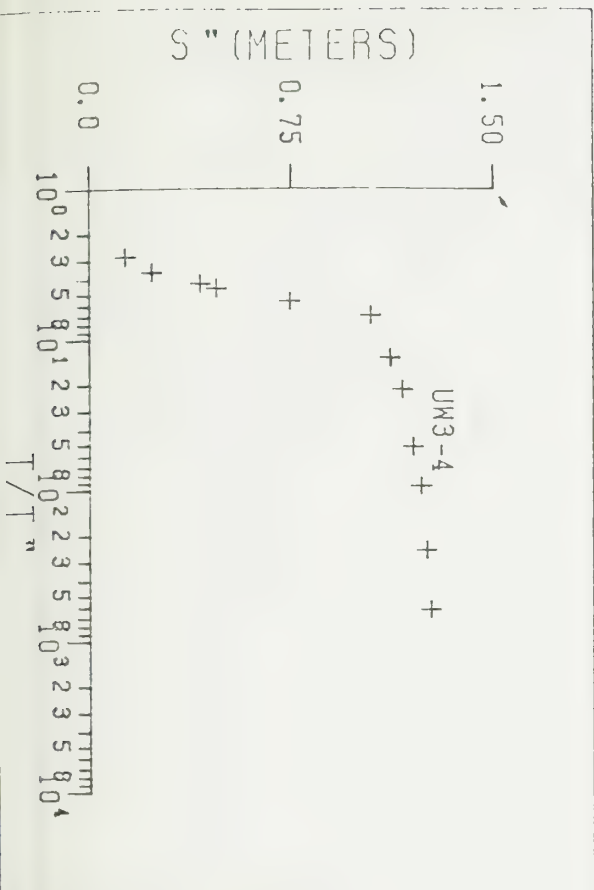
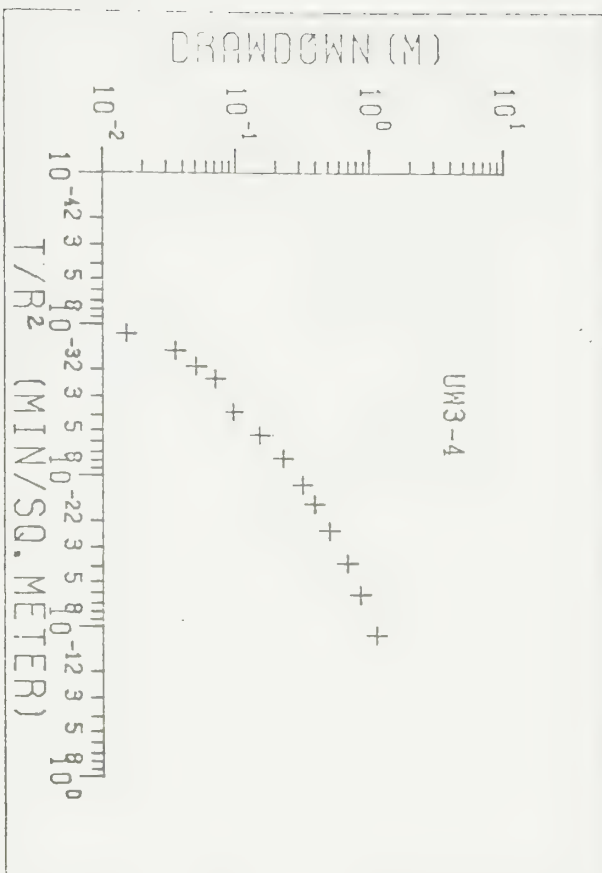
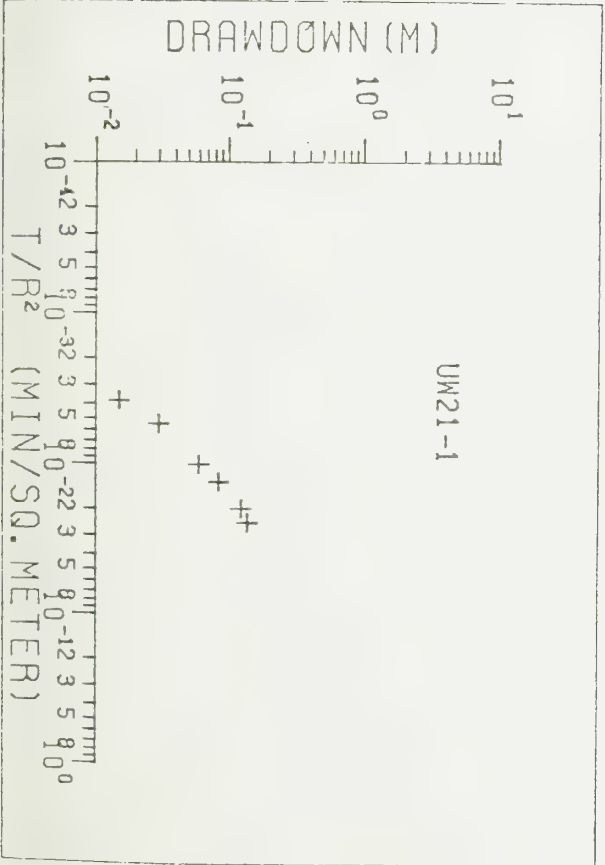
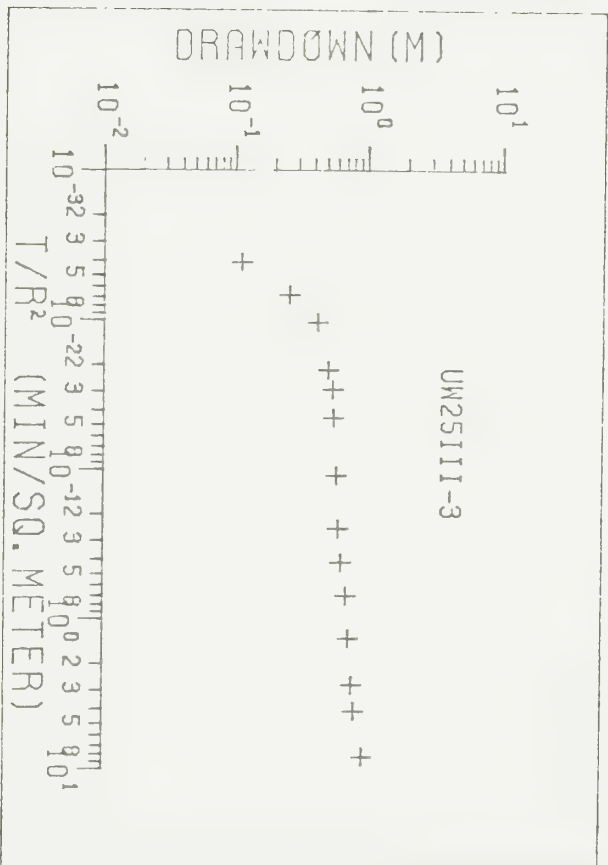
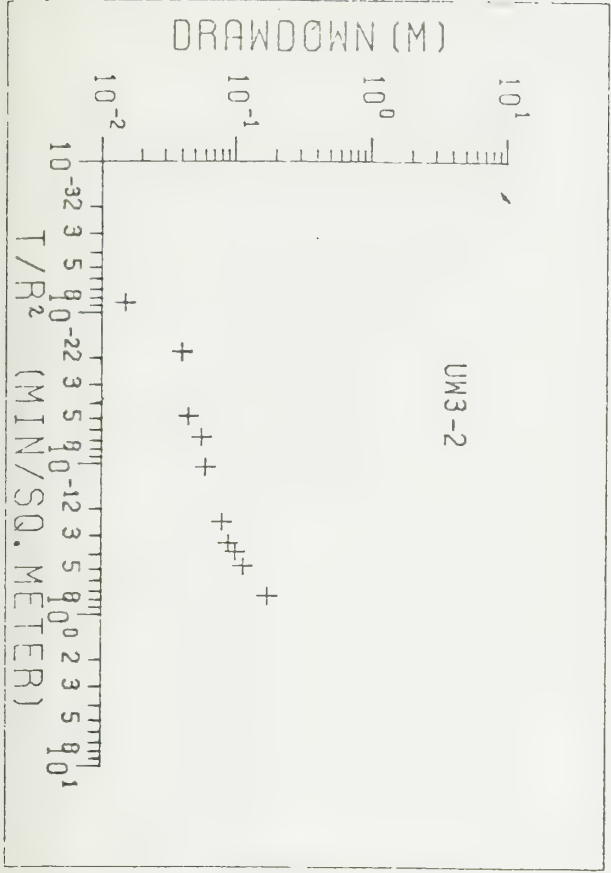
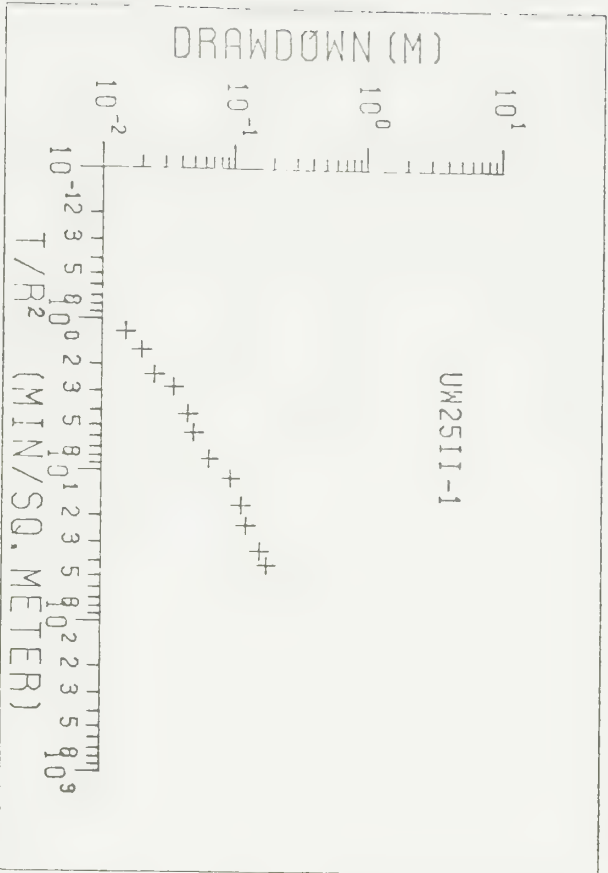


Figure 6. Types of water level response curves.









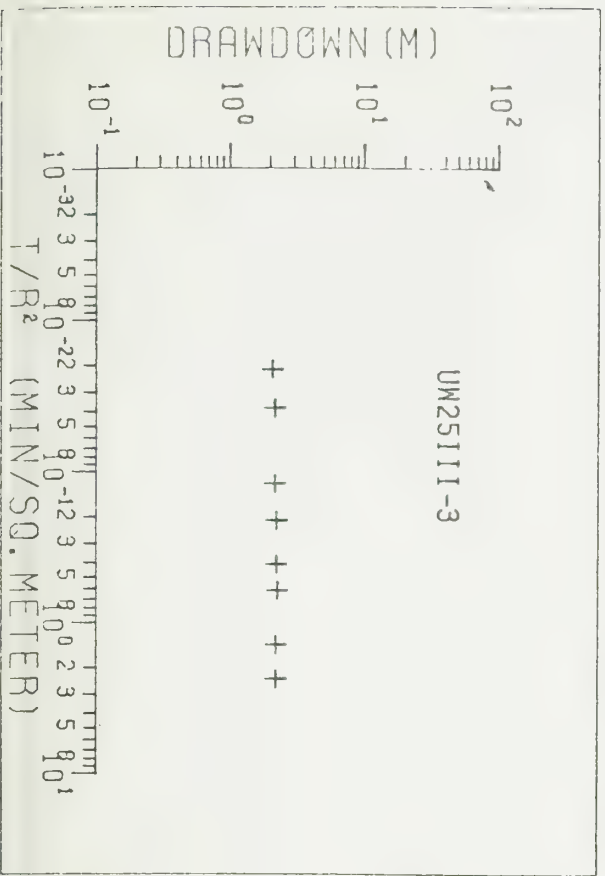
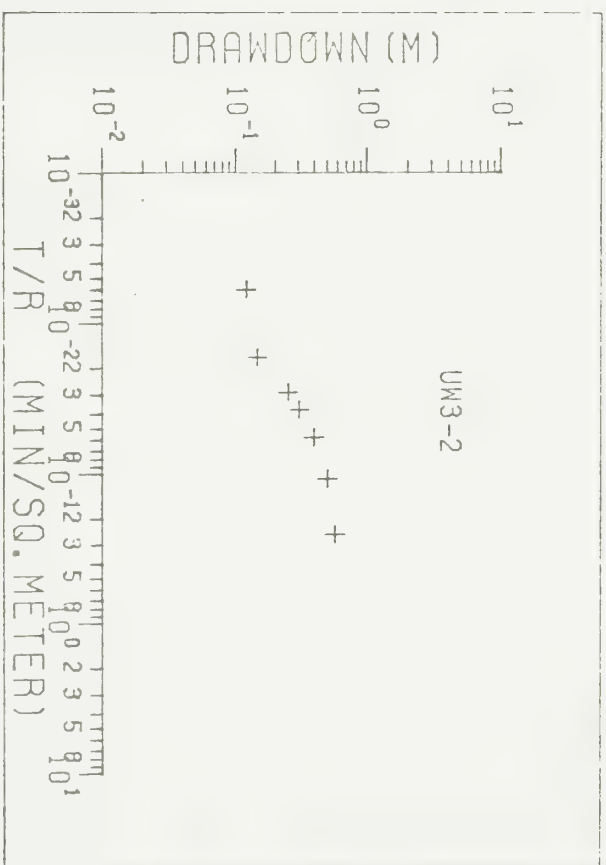
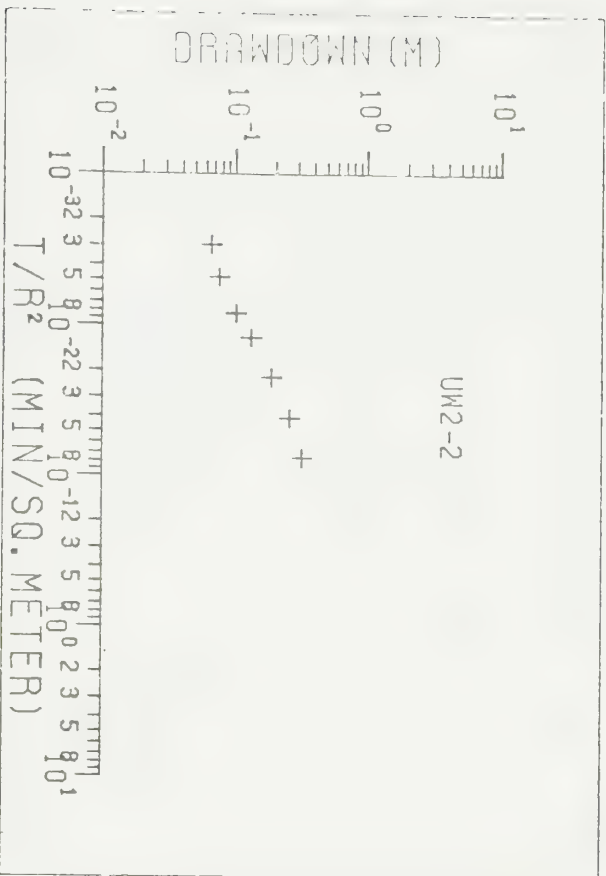


Figure 11: Drawdown curves for test 4

Table 1. Hydraulic conductivity results from response testing

| ZOMETER | DEPTH (m) | ELEVATION | ROCK TYPE | K_1 (cm/sec) | K_2 (cm/sec) |
|---------|--------------|-----------|---------------------------------------|-----------------------|----------------------|
| 1-2 | 4.3 | 178.1 | cherty dolomite | $>6.1 \times 10^{-4}$ | |
| 3 | 7.0 | 175.4 | cherty dolomite | | 1.9×10^{-6} |
| 4 | 8.1 | 174.3 | cherty dolomite | $>6.1 \times 10^{-4}$ | |
| 5 | 9.6 | 172.8 | massive dolomite | | 2.3×10^{-8} |
| 6 | 14.0 | 168.3 | shaly dolomite | | 7.6×10^{-8} |
| 2-1 | 4.1 | 177.3 | cherty dolomite | $>9.6 \times 10^{-6}$ | |
| 2 | 8.0 | 173.5 | cherty dolomite | $>1.0 \times 10^{-4}$ | 3.0×10^{-6} |
| 3 | 10.1 | 171.3 | dolomite | | |
| 4 | 18.1 | 163.3 | shale | | 1.4×10^{-7} |
| 5 | 21.3 | 160.1 | limestone | | 1.5×10^{-8} |
| 3-1 | 4.4 | 177.1 | cherty dolomite (possible massive) | $>6.1 \times 10^{-4}$ | |
| 2 | 8.4 | 173.2 | cherty dolomite | 1.1×10^{-5} | |
| 3 | 10.6 | 171.0 | shaly dolomite | | 6.5×10^{-6} |
| 4 | 12.6 | 169.0 | shaly dolomite | 2.6×10^{-3} | |
| 5 | 16.3 | 165.3 | shaly dolomite | 1.2×10^{-7} | 5.5×10^{-9} |
| 1-3 | 23.5 | 162.6 | shale | | 9.8×10^{-7} |
| 5 | 32.9 | 153.2 | siltstone (shale | | 8.0×10^{-7} |
| 5-II-1 | 1.7-2.9 | 179.1 | cherty dolomite | 1.2×10^{-3} | |
| II-2 | 3.4-4.6 | 177.4 | cherty dolomite | 1.6×10^{-3} | |
| II-3 | 5.0-6.2 | 175.8 | cherty dolomite | 1.2×10^{-3} | |
| 5III-1 | 1.6-2.8 | 179.2 | cherty dolomite | 1.4×10^{-3} | |
| III-2 | 3.7-4.9 | 177.1 | cherty dolomite | 2.2×10^{-3} | |
| III-3 | 5.8-7.0 | 175.0 | cherty dolomite | 1.6×10^{-4} | |

Table 2. Hydraulic conductivity results from packer tests

| TEST INTERVAL (depth in metres) | HYDRAULIC CONDUCTIVITY (cm/sec) | ROCK TYPE |
|------------------------------------|------------------------------------|--------------------|
| 5.8 - 6.7 | $>1.0 \times 10^{-3}$ | cherty dolomite |
| 6.7 - 7.9 | 1×10^{-4} | cherty dolomite |
| 7.9 - 9.1 | $>1.0 \times 10^{-3}$ | cherty dolomite |
| 9.1 - 10.3 | 1.0×10^{-5} | dolomite (Gasport) |
| 10.3 - 11.6 | 8.5×10^{-6} | Rochester shale |
| 11.6 - 12.8 | $>1.0 \times 10^{-3}$ | Rochester shale |
| 12.8 - 14.0 | 4.2×10^{-8} | Rochester shale |
| 14.0 - 15.2 | 1×10^{-8} | Rochester shale |
| 15.2 - 16.5 | 4.2×10^{-7} | Rochester shale |
| 16.5 - 17.7 | 9.4×10^{-7} | Rochester shale |

Table 3. Hydraulic conductivity results from pumping tes

| WELL | DEPTH (m) | ROCK TYPE | THEIS | TEST ONE | | RECOVERY THEIS | TEST TWO | |
|---------|--------------|-----------------|----------------------|----------------------|----------------------|----------------------|----------------------|------------|
| | | | | JACOB PART 1 | JACOB PART 2 | | THEIS AND JACOB | NEU WIT |
| 25 11-1 | 1.7 - 2.9 | cherty dolomite | - | - | - | - | - | - |
| 25 11-2 | 3.4 - 4.6 | cherty dolomite | 7.5×10^{-3} | 8.2×10^{-3} | 2.6×10^{-3} | 7.9×10^{-3} | - | - |
| 25 11-3 | 5.0 - 6.2 | cherty dolomite | - | 6.6×10^{-3} | 1.7×10^{-3} | 4.2×10^{-3} | - | - |
| 25 11-2 | 3.7 - 4.9 | cherty dolomite | - | 1.1×10^{-2} | 3.1×10^{-3} | 9.1×10^{-3} | - | - |
| 25 11-3 | 5.8 - 7.0 | cherty dolomite | - | 8.2×10^{-3} | 2.6×10^{-2} | - | - | - |
| 3-11 | 0 - 5.0 | cherty dolomite | - | - | - | - | - | - |
| 3-2 | 8.4 | dolomite | 2.2×10^{-3} | 2.7×10^{-3} | 1.3×10^{-3} | 2.0×10^{-2} | 2.5×10^{-3} | - |
| 3-3 | 10.6 | shale | - | - | - | 1.1×10^{-3} | - | 2.1 |
| 3-4 | 12.6 | shale | 1.1×10^{-3} | 2.0×10^{-3} | 1.0×10^{-3} | - | 2.4×10^{-3} | 8.1 |
| 2-11 | 0 - 5.0 | cherty dolomite | 1.0×10^{-2} | 6.6×10^{-3} | 3.8×10^{-3} | 2.0×10^{-2} | - | - |
| 2-2 | 8.0 | cherty dolomite | 6.8×10^{-3} | 8.2×10^{-3} | 1.8×10^{-2} | 2.5×10^{-3} | - | - |
| 2-3 | 10.1 | dolomite | - | - | - | - | - | - |
| 1-2 | 4.3 | cherty dolomite | - | 4.3×10^{-3} | 3.8×10^{-3} | 9.9×10^{-3} | - | - |
| 1-3 | 7.0 | cherty dolomite | - | - | - | - | - | - |
| 1-4 | 8.1 | cherty dolomite | - | - | - | 4.4×10^{-3} | - | - |
| 1-5 | 9.6 | dolomite | - | - | - | 4.6×10^{-3} | - | - |
| 21-1 | 9.0 | cherty dolomite | 3.0×10^{-3} | - | - | 4.0×10^{-3} | - | - |
| 21-2 | 11.5 | cherty dolomite | 2.5×10^{-3} | - | - | 4.1×10^{-3} | - | - |

APPENDIX H

~

**SIMULATING FLOW AND ADVECTIVE-DISPERSIVE TRANSPORT
IN STOCHASTICALLY-GENERATED FRACTURE NETWORKS**

by

Alice Lynn Roberts

A thesis
presented to the University of Waterloo
in fulfillment of the
thesis requirement for the degree of
Master of Science
in
Earth Sciences

Waterloo, Ontario, 1984

(c) Alice Lynn Roberts, 1984

I hereby declare that I am the sole author of this thesis. I authorize the University of Waterloo to lend this thesis to other institutions or individuals for the purpose of scholarly research.

Alice Lynn Roberts

Alice Lynn Roberts

I further authorize the University of Waterloo to reproduce this thesis by photocopying or by other means, in total or in part, at the request of other institutions or individuals for the purpose of scholarly research.

Alice Lynn Roberts

Alice Lynn Roberts

The University of Waterloo requires the signatures of all persons using or photocopying this thesis. Please sign below, and give address and date.

ABSTRACT

Purely deterministic modeling of contaminant transport in fractured media is rarely feasible for problems of practical significance owing to difficulties involved in specifying fracture locations and parameters governing the details of hydraulic characteristics. Three alternative models are available: stochastically-generated discrete fracture models, continuum models, and dual-porosity models. The first technique is limited to small problems on the order of a few hundreds of fractures. Although the other two techniques are forced to sacrifice an accurate representation of the physical system in order to address regional- or field-scale problems, they remain the only methods currently available for studying problems at these scales. Some of the simplifications that are often made with these techniques are that fractures are extensive rather than finite, either do not interact or meet at some consistent angle, or that apertures are constant either within a set or within an individual fracture. These assumptions, by neglecting or simplifying the interactions between individual fractures, may falsely represent the hydraulics of the network as well as the effect of potentially important attenuation mechanisms on the transport of contaminants within a real fracture system. Continuum approaches commonly also invoke a Fickian model for the description of macroscopic dispersion. The applicability of such a model to fractured media has not, however, been established.

The present study assesses the limitations of current conceptual models through a sensitivity analysis, examining the response of a few realizations of a stochastically-generated, two-dimensional network of discrete fractures within a

small region. Flow and advective-dispersive transport within the fractures are simulated using finite element techniques.

The effect of changes in the fracture geometry, represented by the variability of the fracture apertures and the degree of interconnection of fractures in the network, is studied in detail. The simulations demonstrate that on a local scale, flow and transport in fractured media are very sensitive to uncertainties in the statistical parameters describing the geometry of a fracture network. The single most important parameter may be the network connectivity. Vagaries of interconnection can produce preferred pathways, which may occupy the medium- to large-sized fractures rather than the largest features. The common wisdom that flow is governed by the largest fractures may be a fallacy in the case of a network of finite fractures.

For the limited number of realizations tested, macroscopic transport appeared relatively insensitive to changes in fracture network geometry, at least for a conservative tracer. Variations in fracture aperture proved more significant when coupled with ion-exchange or sorption reactions, however. For a reactive tracer, the mean residence time observed was less than the value expected for the mean aperture but more than that predicted for the largest fractures.

Although observed macroscopic dispersion was not strictly Fickian, such a model may still provide an approximate indication of the averaged response of a fracture network. The macroscopic dispersion was somewhat enhanced by retardation. Diffusion to deadend fracture regions decreased the observed macroscopic dispersion coefficient, and delayed the tracer velocity roughly in proportion to the volume occupied by deadend regions.

The study points out several limitations of current conceptual models for problems pertinent to contaminant hydrogeology. Selection of appropriate input

parameters and boundary conditions is at best tenuous. Computed mean apertures may be an order of magnitude smaller than the true value, influencing the predicted retardation due to sorption and matrix diffusion. Attenuation via matrix diffusion may also be affected by control of transport by a few preferred pathways rather than transport being uniformly distributed throughout the fracture network. Care should be taken in selecting appropriate input parameters to avoid overestimating solute attenuation. As with any model, stochastic-discrete models, continuum models, and dual-porosity models should only be applied with a clear understanding of their limitations.

ACKNOWLEDGEMENTS

This thesis is dedicated to my husband, David Schneider, a remarkable soul who selflessly tolerated two years of mutually agonizing separation with unflagging patience. Without his wholehearted emotional backing, nothing I have accomplished would have had any meaning. The assistance of both our families was of inestimable value in surviving this long-distance relationship.

I am deeply grateful to Dr. E. O. Frind and Dr. J. A. Cherry for their invaluable counsel, for the mental stimulation they have provided throughout this study, and especially for their determined encouragement of my academic pursuits. Together with Drs. R. W. Gillham and E. J. Reardon, their efforts have ensured that the time I have spent at the University of Waterloo has been as thoroughly pleasant as it has been intellectually rewarding.

My greatest source of learning has been through my fellow graduate students and the staff associated with the Groundwater Research Institute. I would particularly like to thank Gary Hokkanen, Carol Ptacek, and Martha Weaver for their friendship and for each of the innumerable discussions. That I do not single out other names is a measure of the large number of people from whose kindly assistance I have benefited. Finally, aid was also provided by Mrs. Olsen, without whom this thesis never would have been completed.

Funding for this research was provided through the Upper Ottawa Street Landfill Study directed by Dr. J. A. Cherry and through an NSERC grant to Dr. E. O. Frind.

CONTENTS

| | |
|--|-----|
| Abstract | iv |
| Acknowledgements | vii |
| Chapter I: INTRODUCTION | 1 |
| Modeling Approaches | 1 |
| Study Objectives | 4 |
| Chapter II: TRANSPORT CONCEPTS FOR FRACTURED MEDIA | 7 |
| Flow and Transport Relationships for a Single Fracture | 7 |
| Flow in a Single Fracture | 7 |
| Dispersion in a Single Fracture | 3 |
| Macroscopic Flow and Transport Concepts | 11 |
| Relevance to Dual-Porosity Models | 12 |
| Relevance to Continuum Approach: Applicability of Fickian Model | 12 |
| Chapter III: SIMULATION TECHNIQUES | 16 |
| Fracture Network Model | 16 |
| Flow Model | 22 |
| Transport Model | 26 |
| Parameter Estimation | 32 |
| Velocities | 32 |
| Macroscopic Dispersion | 35 |
| Chapter IV: IMPACT OF FRACTURE GEOMETRY ON SOLUTE TRANSPORT | 42 |
| Effect of Variable Fracture Apertures | 42 |
| Hydraulic Properties | 45 |
| Transport Properties | 58 |
| Effect of Fracture Connectivity | 70 |
| Hydraulic Properties | 75 |
| Transport Properties | 87 |

| | | |
|------------|---|----|
| Chapter V: | IMPACT OF ATTENUATION MECHANISMS ON SOLUTE TRANSPORT | 97 |
|------------|---|----|

| | |
|---|-----|
| Effect of Sorption/Ion Exchange | 97 |
| Effect of Diffusion to Deadend Fracture Segments | 109 |
| Scale-Dependence of Dispersion in Fracture Networks | 122 |
| Matrix Diffusion in Fracture Networks | 128 |

| | | |
|-------------|-------------------------------|-----|
| Chapter VI: | IMPLICATIONS OF RESULTS | 131 |
|-------------|-------------------------------|-----|

| | |
|---|-----|
| Sensitivity of Stochastic-Discrete Fracture Model to Changes in Geometric Parameters | 131 |
| Applicability of Dual-Porosity Models | 134 |
| Applicability of Continuum Models | 135 |
| Areas for Future Research | 137 |

| | |
|------------------|-----|
| REFERENCES | 140 |
|------------------|-----|

| | |
|--|-----|
| APPENDIX A: FRACTURE GENERATION, FLOW, AND TRANSPORT MODELS | 145 |
| Fracture Generation Program | 145 |
| Fracture Flow Program | 146 |
| Fracture Rediscretization Program | 146 |
| Fracture Transport Program | 147 |

TABLES

| | | |
|----|---|-----|
| 1. | Input parameters used to simulate fracture network shown on Figure 1 (a) | 21 |
| 2. | Effect of increasing variability in fracture aperture on macroscopic transport parameters | 68 |
| 3. | Effect of increasing fracture connectivity on macroscopic transport parameters | 93 |
| 4. | Effect of increasing variability in fracture aperture on macroscopic transport for a reactive solute | 108 |
| 5. | Comparison of macroscopic transport parameters for different values of $\sigma_{ln} z_b$ without deadend fracture segments | 117 |
| 6. | Comparison of macroscopic transport parameters for different connectivities without deadend fractures | 119 |
| 7. | Change in macroscopic transport parameters with distance from the source within a single fracture network | 126 |

FIGURES

| | | |
|-----|--|----|
| 1. | Example of two-dimensional fracture network | 19 |
| 2. | Boundary conditions used for flow simulation | 25 |
| 3. | Boundary conditions for transport simulation | 29 |
| 4. | Example of a macroscopic breakthrough curve | 31 |
| 5. | Comparison of moment results to analytical solution | 39 |
| 6. | Comparison of ordinary and weighted methods of moments | 41 |
| 7. | Histograms showing aperture distributions for three cases of $\sigma_{ln} 2b$ | 44 |
| 8. | Comparison of hydraulic conductivity of finite and infinite networks with changing $\sigma_{ln} 2b$ | 47 |
| 9. | Control of flow within largest fractures with changing $\sigma_{ln} 2b$ | 48 |
| 10. | Hydraulic head and velocity distribution with changing $\sigma_{ln} 2b$ | 52 |
| 11. | Hydraulic head profiles with changing $\sigma_{ln} 2b$ | 53 |
| 12. | Comparison of discharge distribution with position of largest fractures | 55 |
| 13. | Histograms showing velocity distributions for three values of $\sigma_{ln} 2b$ | 57 |
| 14. | Concentration distributions with changing $\sigma_{ln} 2b$ | 61 |
| 15. | Macroscopic breakthrough curves for three values of $\sigma_{ln} 2b$ | 63 |
| 16. | Comparison of macroscopic breakthrough curve with dispersion model | 65 |
| 17. | Comparison of velocities obtained using several approaches for different values of $\sigma_{ln} 2b$ | 66 |
| 18. | Effect of variability in fracture aperture on macroscopic dispersion and average transport velocity. | 69 |
| 19. | Fracture networks showing changes in connectivity | 74 |
| 20. | Change in bulk hydraulic conductivity of fracture network with increasing connectivity | 76 |
| 21. | Hydraulic head contours and velocity plots for three different connectivities | 79 |

| | | |
|-----|---|-----|
| 22. | Hydraulic head profiles at $x = 5.0$ cm for three different connectivities | 30 |
| 23. | Discharge distributions for two different connectivities | 83 |
| 24. | Impact of connectivity on domination of flow by largest fractures | 85 |
| 25. | Histograms showing velocity distribution with changing connectivity | 86 |
| 26. | Concentration distributions for three different connectivities | 90 |
| 27. | Macroscopic breakthrough curves for three different fracture connectivities | 92 |
| 28. | Effect of increasing connectivity on macroscopic dispersion and transport velocity. | 94 |
| 29. | Comparison of velocities obtained using different approaches for several connectivities | 96 |
| 30. | Histograms comparing effective velocity v/R distributions for a nonretarded and a retarded case | 101 |
| 31. | Concentration distributions for retarded solute ($K_a = 1.8 \times 10^{-5}$ m) | 105 |
| 32. | Macroscopic breakthrough curves for retarded solute. | 106 |
| 33. | Fracture network with deadend fractures 'trimmed' | 111 |
| 34. | Concentration contours for 'trimmed' grid systems | 114 |
| 35. | Macroscopic breakthrough curves for cases in which deadend fractures have been 'trimmed' | 116 |
| 36. | Breakthrough curves for two connectivity values showing relative importance of diffusion to deadend fractures | 121 |
| 37. | Macroscopic breakthrough curves for four different locations within a single fracture network | 125 |
| 38. | Results of investigation of scale-dependence of dispersion | 127 |

Chapter I

INTRODUCTION

The geometric characteristics of natural fracture systems are notoriously complex; even within a single fracture, the small-scale hydraulic properties will vary with location in a manner difficult to quantify. Yet if the bulk hydraulic properties of an individual fracture were accurately determined, this may have little relevance to the prediction of solute transport in fractured media, as transport processes are noted for their sensitivity to deviations from average flow properties. When difficulties in predicting transport within a single fracture are compounded by extending the problem to a network of intersecting features of finite length and variable roughness, orientation, spacing, and aperture, it becomes apparent that purely deterministic modeling of contaminant transport is infeasible for virtually all situations of practical significance.

1.1 Modeling Approaches

Three alternative approaches have been used in simulating transport in fractured media. One technique is to ignore the effect of individual fractures or to lump them into a hypothetical equivalent porous medium; this is referred to as the continuum approach. Much attention has been directed towards techniques for determining the effective hydraulic conductivity of such a medium (e.g., Snow, 1965, 1969; Parsons, 1966; Long et al., 1982), and recent progress is being made in studying its dispersive characteristics (Smith and Schwartz, 1984). At

present, however, little is known about the relationship between the geometrical characteristics of a particular fracture system and the effective average velocity and dispersion coefficient that would be appropriate to use in simulating transport in an equivalent continuum, let alone whether such an approach is valid.

A second technique is to couple the presence of advective transport in fractures with the capacitance effect introduced by diffusion into the intact matrix blocks. This is commonly referred to as a double-continuum or dual-porosity approach, and requires a simple geometry for the matrix blocks. Analytical solutions are available for flow and transport in a single fracture with diffusion to the matrix (e.g., Tang et al., 1981; Rasmusson and Neretnieks, 1981) or in a system of parallel, noninteracting fractures (Sudicky and Frind, 1982). Numerical solutions have thus far been limited to systems of parallel fractures (Grisak and Pickens, 1980; Bibby, 1981; Noorishad and Mehran, 1982) or to systems of suborthogonal fractures in which the matrix blocks can be represented by simple structures such as prisms or spheres (Huyakorn et al., 1983a,b). The ability of matrix diffusion to safely attenuate contaminants in fractured media is sensitive to the rate of fluid advection and to the ratio of the volume of the contaminant within fractures to the surface area it contacts; in a network of finite fractures, these parameters are dictated in part by interactions between individual features. Because dual-porosity models neglect or greatly simplify such interactions, specification of hydraulic parameters that adequately represent those that would govern transport in a real system is again problematic.

The third approach to simulation of transport in fractured media is to try to incorporate as much information as possible concerning the statistical or probabilistic distribution of geometrical characteristics in a discrete-fracture approach, and simulate networks of fractures using stochastic techniques. Much progress

has been made in recent years in the characterization of the statistical geometrical characteristics of fractured media. This information has been used in stochastic-discrete fracture simulations of flow (Long et al. 1982; Rouleau and Gale, 1984) and transport (Schwartz et al. 1982, 1983; Smith and Schwartz, 1984) in two-dimensional networks of fractures. Such an approach represents a distinct improvement over early studies of flow or transport in discrete fractures (Wilson and Witherspoon, 1970; Castillo et al., 1972a,b; Krizek et al., 1972), which assumed that fracture networks were perfectly interconnected and that fractures were evenly spaced, meeting at a constant angle. The principal advantage of stochastic-discrete network models is their superior ability to represent flow within a fracture system. Equivalent porous medium models or dual-porosity models assume either a single flow velocity within the fractures or at best a simple distribution of velocities. Stochastic-discrete fracture network models predict a continuous distribution of flow velocities over a wide range, and allow contaminants to preferentially follow certain pathways. Because of their more accurate representation of real fracture systems, they can be an invaluable tool in developing insight into physical processes governing flow and transport in real systems.

Despite the enhanced ability of these models to represent flow processes, these stochastic-discrete fracture models suffer from several major limitations. Most important is their present inability to incorporate the diffusive transfer of solutes to the matrix regions. Unless fracture orientations are assumed constant, characterization of the geometry of intrablock regions is difficult even in two dimensions. Without some specification of the geometry of these regions, however, transient diffusion to the matrix cannot be incorporated in a rigorous manner.

Application of stochastic-discrete fracture models requires an understanding of the structure of the probabilistic distributions describing fracture spacing, orientations, lengths, and apertures, at a minimum. In spite of the rapid progress in the statistical characterization of these geometrical parameters, particularly for crystalline rock, little information is available to indicate whether distributions observed in one rock type have any relationship to those which may occur in other lithologies. Acquisition of the information required for the characterization of the geometry of a fracture network can be extremely costly or even virtually impossible, and the reliability of the results is sensitive to several sources of bias introduced during the sampling program. The applicability of any stochastic-discrete fracture model to real problems is limited by the high degree of uncertainty associated with the input parameters.

A further disadvantage of this approach is that, depending on the density of the fractures, computational limitations may restrict their application to areas less than a few tens of meters square. At present, simulation of most problems requires applying either a continuum approach or a dual-porosity approach. Such approaches may be acceptable for problems related to groundwater or petroleum reservoir evaluation in fractured media or possibly for transport on a regional scale. Their applicability to field-scale problems, however, in which the region of concern is in relative proximity to a contaminant source, is of considerable uncertainty.

1.2 Study Objectives

The present study has two primary objectives. The first is to address the impact that some of the statistical input parameters can have on the hydraulic behavior and transport characteristics of a fracture network through testing the

response of a stochastic-discrete fracture model. The results may be useful in assessing errors associated with any model predictions of flow and transport in fractured media, but are especially suited to extending our understanding of the relative importance of the various parameters that govern these processes.

The second objective is to provide insight into limitations that may be associated with applying a continuum or dual-porosity approach to the simulation of transport in field-scale problems. Particular attention is devoted to the examination of macroscopic, or averaged, flow and transport characteristics, and their relationship to hydraulic parameters on a local scale. If either approach is deemed valid to apply to a particular problem, the present study may assist in determining values of flow velocities or macroscopic dispersion characteristics that may be appropriate as input to continuum or dual-porosity models.

These objectives are addressed by performing a series of simulations of flow and transport in fractured media, using a stochastic-discrete fracture model. The sensitivity of flow and transport processes to changes in variability in fracture aperture and fracture connectivity is examined both in terms of the simulation results on a local scale within the network and in terms of the macroscopic results. In addition to these geometric parameters, the effect of attenuation mechanisms such as ion exchange or sorption reactions and diffusion to deadend fracture regions is also studied. Particular emphasis is placed on the interaction of the geometric parameters with the attenuation mechanisms.

To assess the applicability of a continuum concept for transport in fractured media, the macroscopic results are studied in detail to determine whether any relationship can be discerned between transport parameters on the scale of an individual fracture and parameters averaged over an entire network. Factors affecting both mean travel velocity and macroscopic dispersion are investigated,

as well as the validity of a Fickian model of dispersion to macroscopic transport in fractured media.

The remainder of this thesis is divided into five sections. The next section (Chapter II) sets forth the conceptual framework by examining processes governing transport in fractured media. Chapter III describes the techniques employed for generating a network of fractures and for simulating flow and transport. Techniques used to analyze the results are also described. The computer models developed as part of this study are presented in the Appendix. Chapter IV presents the results of the sensitivity analysis with respect to the variability of fracture apertures and degree of interconnection of fractures within the network. Chapter V tests the response of the system to attenuation mechanisms, and includes a study of the scale-dependence of macroscopic dispersion. Finally, Chapter VI critically assesses dual-porosity and continuum approaches in light of the simulation results.

Chapter II

TRANSPORT CONCEPTS FOR FRACTURED MEDIA

2.1 Flow and Transport Relationships for a Single Fracture

2.1.1 Flow in a Single Fracture

Considerable research effort has been devoted to the study of flow in fractured media within the last twenty-five to thirty years. Much of this research has been summarized by Wilson and Witherspoon (1970) and will not be reiterated here.

Most studies of flow in fractured media idealize an individual fracture as an opening between two smooth parallel plates. With this analogy, the hydraulic conductivity K_f of a single fracture can be given as :

$$K_f = (\rho g / 12 \mu) (2b)^2 \quad (1)$$

where K_f is the hydraulic conductivity of the fracture, ρ is the fluid density, g is the gravitational constant, μ is the dynamic viscosity, and $2b$ is the fracture aperture. The volumetric discharge Q per unit thickness of the fractured medium can be shown to be equal to :

$$Q = (K_f)(2b)\nabla h \quad (2)$$

where ∇h is the hydraulic gradient. From this it can be seen that the volumetric discharge through a fracture is related to the cube of the fracture aperture, whence the 'cubic law' for flow. If a fracture has a rough surface, the parameter

(2b) is interpreted as the effective hydraulic aperture. Because of wall roughness and because of the finite nature of real fractures, effective apertures calculated from flow rates and pressure gradients tend to be smaller than real fracture apertures (Gale, 1982). If a fracture has a variable rather than a constant aperture and the aperture variation is small, flow can still be approximated by a parallel plate analogy with an opening equal to the mean flow path aperture. The relationship between effective fracture aperture and mean aperture becomes less simple as the topology of the fracture becomes more complex. The validity of the cubic law to the description of flow in a real fracture is discussed by Iwai (1976), among others.

2.1.2 Dispersion in a Single Fracture

Much less attention has been directed to the study of transport within a single fracture. Because the focus of the present study is on transport rather than flow in fractured media, it is pertinent to examine some of the relevant theory in detail.

Analyses of tracer experiments in real fractures is complicated by the sensitivity of the results to channeling produced by variations in fracture aperture, to diffusion into microfractures and the rock matrix, and to sorption both on the fracture surface and in the matrix (Neretnieks et al., 1982). As in the case of flow within a single fracture, transport becomes much easier to describe if actual fracture geometry is simplified using a parallel-plate analogy.

In the absence of geochemical reactions or diffusion to the rock matrix, transport within such an idealized fracture can be described in terms of the familiar one-dimensional advection-dispersion model, as described by Taylor (1953, 1954) and Aris (1956):

$$\partial c / \partial t = D_L \partial^2 c / \partial x^2 - v \partial c / \partial x \quad (3)$$

where, for transport between two parallel plates, D_L , the hydrodynamic dispersion coefficient, can be given (Turner, 1959; Philip, 1963) as:

$$D_L = D_0 + (1/210)v^2(2b)^2/D_0 \quad (4)$$

where D_0 is the free-solution diffusion coefficient and v is the average velocity across the width of the channel.

This model expresses the importance of molecular diffusion to the transport process. In the absence of molecular diffusion, the parabolic velocity profile developed during laminar flow would theoretically result in the presence of infinitely large dispersion, as the concentration measured at a distant point would never quite attain the concentration of the injected tracer. The center of mass of the solute would travel at an apparent velocity less than the mean velocity across the channel. Taylor's work showed that, because of radial transfer of solute via molecular diffusion across the concentration gradient produced by the parabolic velocity profile, the center of mass of the injected solute will (after sufficient time has elapsed) travel at the average flow velocity.

The second term in equation (4), as pointed out by Nunge and Gill (1970), provides a great deal of physical insight into the nature of the dispersion process within a single fracture if the numerator is interpreted to be a measure of axial advection and the denominator to reflect the intensity of transverse mixing rather than just transverse molecular diffusion. Any mechanism which increases transverse mixing, such as turbulence, reduces the hydrodynamic dispersion coefficient within an individual fracture. The dispersion coefficient is enhanced by features that increase the concentration gradient across the channel or distribute the gradient over a greater area, such as large differences in velocity across the flow or a large channel width. A capacitance effect produced by roughness on

the fracture wall increases the concentration gradient across the channel by producing pockets of stagnant flow, increasing the dispersion coefficient. Such an effect could also be produced by diffusion to deadend fracture segments and regions of slow flow; this is analagous to the situation discussed by Coats and Smith (1964) for porous media containing regions to which transport is controlled by molecular diffusion. The effect is similar in concept to the capacitance effect produced by diffusion to the matrix, discussed by Neretnieks (1980) and by Tang et al. (1981), among others. In the case of diffusion to the matrix, the effect on the macroscopically-observed dispersion coefficient can be so pronounced that in many cases purely hydrodynamic dispersion can be neglected within an extensive fracture in a porous rock mass in comparison to the effect of diffusion to the rock matrix.

Most authors who have studied transport in networks of fractures in the absence of diffusion to the matrix have assumed that hydrodynamic dispersion and molecular diffusion can be neglected (Castillo et al., 1972a; Krizek et al., 1972; Schwartz et al., 1983). Whether this assumption is valid in the presence of a potential capacitance effect introduced by the presence of deadend fracture segments and regions of essentially stagnant but slow-moving flow is subject to question.

Equation (4) shows that the hydrodynamic dispersion coefficient observed within an individual smooth fracture of constant aperture should vary with the second power of the flow velocity. As discussed by Perkins and Johnston (1963), dispersion in porous media is more likely to vary as v^n with n ranging from 1.0 to 1.2. The reason for this discrepancy lies in the difference between the mechanism of mixing in a uniform simple structure and in a system of interconnected capillaries. The linear or near-linear relationship of the dispersion coef-

ficient to the flow velocity has encouraged the introduction of the concept of dispersivity as a constant geometrical characteristic of a porous medium:

$$\alpha_L = D_L/v \quad (5)$$

Neretnieks et al. (1982) observed an approximately linear relationship between the flow velocity and the dispersion coefficient for transport within a single natural fracture, with a dispersivity α_L of 25 mm. This implies that mixing produced by variations in aperture within a real fracture has an important effect on transport processes. Little information is available concerning the range of validity of equation (5) for transport within a single fracture.

2.2 Macroscopic Flow and Transport Concepts

Flow and transport within a network of fractures obeys the same physical laws that characterize these processes within an individual fracture. If it were feasible to apply stochastic-discrete models to field-scale problems, there would be little point in investigating macroscopic flow and transport concepts. For the purpose of assessing the validity of dual-porosity or continuum approaches, however, the averaged or macroscopic response of a fracture system is of great interest. As used in this study, 'macroscopic' refers to results averaged over the simulation domain. This usage conflicts with that of Bear (1972), in which the term is applied over a representative elementary volume or REV that usually only comprises a small portion of the simulation domain in the case of porous media. For the present study, the REV for transport was considered to consist of the entire fracture network rather than a small subsection of it. The term 'macroscopic' has been applied to the description of dispersion on the scale of a simulation domain by Schwartz (1977) and by Gelhar and Axness (1983), among others.

2.2.1 Relevance to Dual-Porosity Models

If a dual-porosity model is used to describe transport in fractured media, some manner of determining the appropriate fracture aperture(s) or velocity distribution is needed. These models assume individual fractures are infinitely long; such an extensive network may be hydraulically quite different from a network of finite fractures. Insight into the relationship between the actual complex velocity distribution within a real fracture network and the effective velocity of a tracer is required, as well as an appreciation of the errors that may be introduced by simplifying the interactions between fractures by assuming a simple geometry.

2.2.2 Relevance to Continuum Approach: Applicability of Fickian Model

If there is any attenuation of contaminants owing to diffusion to the matrix, dispersion, geochemical interaction with the rock, or diffusion to regions of relatively stagnant flow, the effective transport velocity may bear little resemblance to the flow velocity even within an individual fracture. In turn, the relationship between the rate at which the center of mass of a plume of contamination moves through a fracture network and the magnitude of the flow velocities within individual fractures may be even more ambiguous.

If a continuum model is used to represent transport within a fracture network, it is necessary to specify both an appropriate velocity field and the dispersive characteristics of the medium. Not only does this involve finding the relationship between the complex distribution of velocities within an actual fracture system and the hypothetical 'effective' velocity distribution within the equivalent porous medium, but it also requires determining the impact that the complex geometry of a fractured medium will have on the spread of a tracer. Transport within porous media has traditionally involved the advection-dispersion model, which assumes that dispersion can be described as a Fickian (diffusive)

process with a constant dispersivity or dispersion coefficient. This implies that dispersion is random, eventually producing a Gaussian distribution of contaminants in which the spatial variance is proportional to the time elapsed:

$$\sigma_x^2 = 2D_L t \quad (6)$$

The model is not in general valid for heterogeneous media, in which contrasts in hydraulic conductivity result in a macroscopically-observed dispersion coefficient that increases with residence time. Under certain conditions, the dispersion coefficient may asymptotically attain a constant value (Gelhar and Axness, 1983; Sudicky, 1983). Although the diffusional model of dispersion may then be applied using the asymptotic dispersion coefficient, many kilometers of travel may be required to achieve a constant macroscopic dispersion coefficient, and the question of how to treat transport in the near-field remains.

The applicability of the diffusional model of dispersion to the description of transport within a network of intersecting fractures has not been established. Many mechanisms contribute to macroscopically-observed dispersion in fractured media, principally matrix diffusion, mixing of fluid at intersections, diffusion to relatively stagnant flow regions, velocity variations within a single fracture, and velocity variations between fractures. Neretnieks (1983) considered macroscopic dispersion produced by velocity variations between parallel, noninteracting fractures of differing size, concluding that the observed dispersion coefficient will increase without bound with increasing time. This is similar to Mercado's (1967) results for stratified media in the absence of interactions between layers. Neretnieks showed that for such a system of parallel fractures, the temporal variance σ_t^2 of the tracer mass can be related to the average residence time t_r and the log standard deviation σ_l of the fracture aperture distribution:

$$(\sigma_t/t_r)^2 = \exp\{4(\ln 10\sigma_l)^2\} - 1 \quad (7)$$

Because the effective dispersion coefficient of the system of parallel fractures can be related to the temporal variance of the tracer mass at a given distance by

$$D_L = 1/2 v x (\sigma_t/t_r)^2 \quad (8)$$

it is possible to estimate the effective macroscopic dispersion coefficient at any distance x in the absence of mixing between fractures or diffusion to the matrix.

Just as molecular diffusion within a capillary tube produces a finite rather than an infinite longitudinal dispersion coefficient (Taylor, 1953), and just as incorporating transfer of solute between layers in porous media may with time produce a finite rather than an infinite dispersion coefficient (Gelhar and Axness, 1983; Sudicky, 1983), it might be argued that incorporating interactions between fractures could result in a dispersion coefficient that asymptotically approaches a constant value with time. Saffman (1960) applied a Lagrangian correlation function technique to the study of dispersion in a statistically isotropic network of straight capillaries of constant length and radius, and showed that the distribution of a tracer is asymptotically Gaussian. Whether this is also true of macroscopically-observed dispersion in a geometrically complex network of fractures has not been demonstrated.

If a diffusional model of dispersion is used to represent transport in fractured media via a continuum approach, it is necessary to demonstrate whether macroscopic dispersion in a fracture network is Fickian and whether the effective dispersion coefficient is constant or increases according to some clearly-defined function. Both of these questions are addressed in the present study. Schwartz et al. (1983) examined aspects of this issue for the special case of a network of orthogonal fractures of equal aperture. The authors concluded that a Gaussian distribution of mass was only observed when the expected value of velocity was

the same in each fracture set, and the spatial variance of the tracer did not in general increase in a consistent fashion with time. The authors related non-Fickian behavior to large standard deviations in the flow velocity distribution. Their study involved a relatively simple fracture geometry, and simplified the transport process by neglecting the effect of hydrodynamic dispersion along a single fracture. Although this process may be relatively unimportant compared to the dispersion introduced by mixing at intersections, neglecting the transfer of solute to slow-flowing regions of fluid via molecular diffusion may be unrealistic. Matrix diffusion, which may well be the most important dispersive mechanism in real systems, was also neglected.

Chapter III

SIMULATION TECHNIQUES

3.1 Fracture Network Model

For the purposes of the present study, a fractured medium is considered to consist of one or more distinct sets of smooth planar features, a set being defined on the basis of similar but variable orientations, lengths, and apertures. The fractures are all oriented at right angles to some reference plane; although the extent of each feature is finite within the reference plane, fractures are infinite in extent perpendicular to this plane. As the hydraulic aperture of each individual fracture is assumed constant, flow is two-dimensional within the network of fractures along the reference plane.

Such a conceptual model, of course, represents a significant simplification of the geometry of a real fracture network, one which may have a profound impact on the hydraulic and transport properties of the medium. Real fractures are not smooth planar features, nor do they have a constant hydraulic aperture. The assumption that flow is two-dimensional is invalid for most lithologic units. Many rock types contain three or more sets of fractures dipping at different angles; in such units, it is impossible to define any plane in which flow is restricted. Incorporating variations in aperture along individual fractures or three-dimensional networks of fractures in any numerical scheme while maintaining the finite characteristics of fractures and variability in orientations within a set is, however, a

complex problem that has not yet been successfully solved for networks containing a large number of fractures. Nonetheless, the applicability of two-dimensional models to real problems is limited.

Some lithologic units do appear to possess a two-dimensional network of fractures. Observations of fractured till at a number of locations in Canada suggest that fractures are predominantly vertical features; horizontal or sub-horizontal features are rare or virtually absent (Grisak and Cherry, 1975; Grisak et al., 1976). In such a system of fractures, the assumption that flow and transport are two-dimensional processes may be justifiable, although limitations imposed by other assumptions remain.

Numerical simulation of a two-dimensional fracture network was accomplished using a stochastic-discrete fracture generator. This generator, which produces a network of intersecting fractures represented by lines, is similar to those described by Long et al. (1982) and Rouleau and Gale (1984). It differs from that described by Schwartz et al. (1983) in that fractures need not be orthogonal. The source code, including a description of input parameters, is included in the Appendix.

Any number of sets of fractures can be generated. The geometry of each individual fracture is described in terms of the location of its centroid within the generation region, and its orientation, length, and effective hydraulic aperture. These parameters are determined by random sampling of a population characterized by some designated probability distribution function.

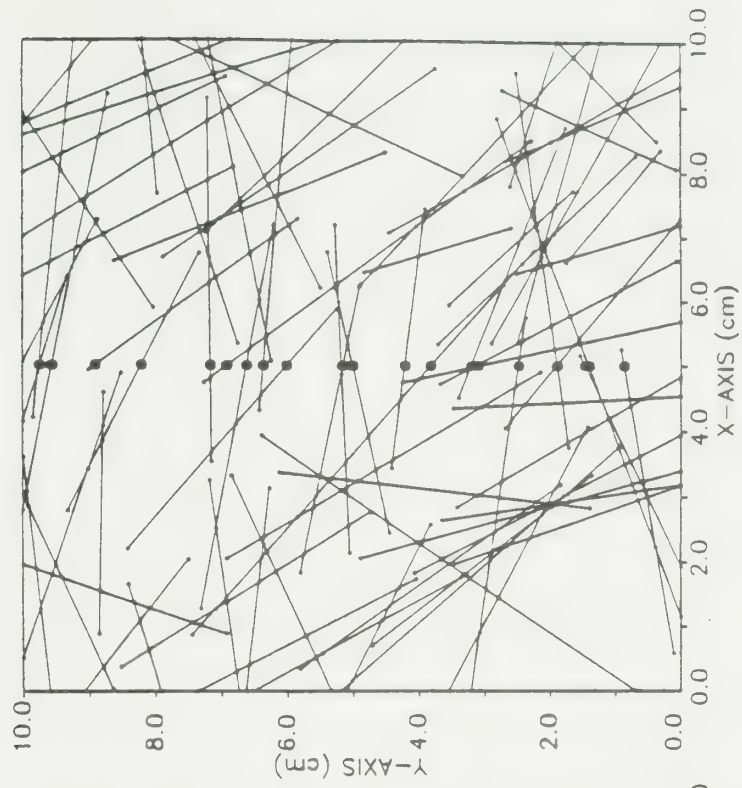
For each set, the locations of the fracture centroids are generated first. Factors influencing fracture location distributions are described by Priest and Hudson (1976). Fracture centroids are assumed to be randomly distributed within the generation region; thus, the presence of one fracture does not affect the chance of another occurring in its neighborhood.

Once the locations of the fracture centroids are determined, values of fracture orientations are selected. Field observations of fractured till in southern Ontario suggest that orientations of individual fractures within a set follow a normal distribution, which can be described in terms of a mean μ_{or} and a standard deviation σ_{or} (D. E. Desautniers, 1983, personal communication). Fractures in other rock types have been observed to obey a similar distribution. An orientation is assigned to each fracture by random sampling of a normally-distributed population with a value of μ_{or} and σ_{or} specified for each set.

Fracture lengths have been described as following either a lognormal distribution or a negative exponential distribution (Rouleau and Gale, 1984; Cruden, 1977). There currently does not appear to be any compelling evidence demonstrating which distribution would be more appropriate for the present study. For simplicity, it was assumed that the lengths of individual fractures within a set can be characterized in terms of a lognormal distribution. Parameters are said to be lognormally distributed with a mean (in the case of fracture lengths) $\mu_{ln L}$ and a standard deviation $\sigma_{ln L}$ when their logarithms are normally distributed.

Finally, apertures are selected for each fracture. Direct measurements of fracture apertures in outcrops and estimates of effective hydraulic apertures of equivalent parallel- plate openings from hydraulic testing in boreholes have been shown to follow a lognormal distribution (Snow, 1970). For the present study, the fractures are assumed to be hydraulically smooth with a constant aperture: thus, the actual fracture aperture is equivalent to the effective hydraulic aperture. The apertures of each of the fractures in a set are determined by randomly sampling a lognormally distributed population with a mean aperture $\mu_{ln 2b}$ and a standard deviation $\sigma_{ln 2b}$. An example of a fracture network generated in this manner is shown in Figure 1(a).

REALIZATION NO. 1-A1
GRID SYSTEM



REALIZATION NO. 1-A1
FRACTURE SYSTEM

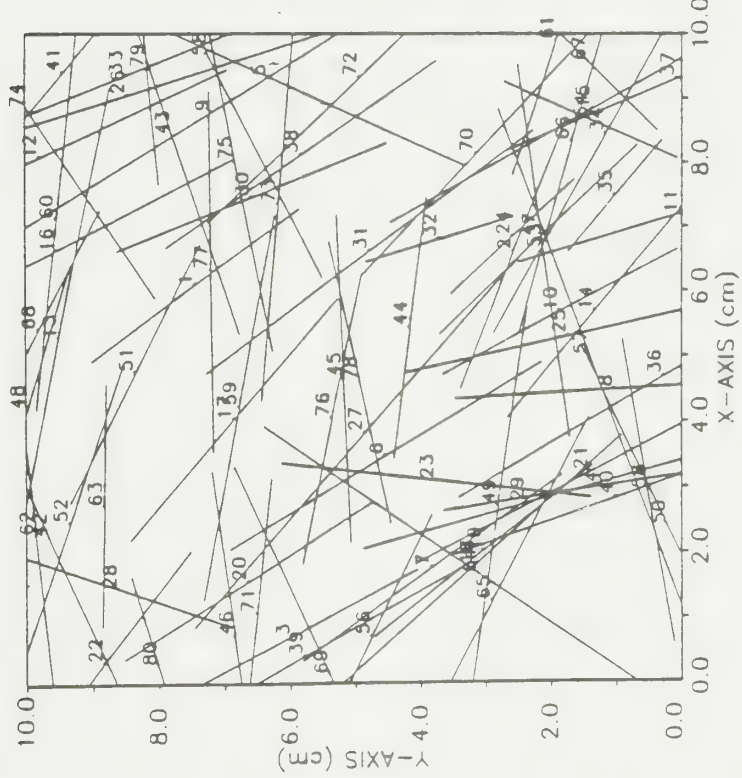


Figure 1: Example of two-dimensional fracture network. (a) Stochastically-generated network. (b) Example of grid system used in numerical simulation of flow

Required input to the fracture network generator thus includes the dimensions of the generation region, the number of fracture sets, the number of fractures within each set, and several statistical parameters describing the geometry of the fracture network (μ_{or} , σ_{or} , $\mu_{ln L}$, $\sigma_{ln L}$, $\mu_{ln 2b}$, and $\sigma_{ln 2b}$). The parameters used to generate Figure 1(a) are listed in Table 1. As previously discussed, determination of appropriate values for these parameters is at best a tenuous procedure. For some media, many parameters may even be impossible to measure. This introduces considerable uncertainty into the ability of a stochastic-discrete fracture model to simulate processes in a real fracture system.

The effect of this uncertainty on flow and transport within the system can be examined through successive realizations in which all network parameters generated in an initial realization are held constant except for one, and examining the impact on both the average and local flow and transport processes. This is the approach that was followed in the present study. Special efforts were taken in generating fracture networks to minimize the number of factors that might change between one realization and the next. For this purpose, once the values of the parameter being tested are randomly selected, they can be assigned to the fractures in a designated sequence. As an example, in studying the effect of progressive changes in $\sigma_{ln 2b}$ on the transport of solutes in the network, the values of fracture aperture generated were sorted by magnitude before being assigned to the fractures so that the largest fractures always occupied the same relative position within the network. In effect, this constitutes a greatly simplified Monte Carlo analysis. Although conventional Monte Carlo techniques can be invaluable in quantifying the uncertainty associated with the prediction of contaminant transport for a given set of conditions, it can be difficult to extrapolate results to a different set of conditions. The present technique is more useful in developing

Table 1

Input parameters used to simulate fracture network shown on
Figure 1 (a)

| Input Parameter | Value |
|---|--------------------|
| Number of fracture sets | 2 |
| Number of fractures in each set N_1, N_2 | 40, 40 |
| Mean orientation of each set $\mu_{or 1}, \mu_{or 2}$ (degrees) | 124, 7 |
| Standard deviation of orientation of each set $\sigma_{or 1}, \sigma_{or 2}$ (degrees) | 25, 25 |
| Ln mean length of each set $\mu_{ln L 1}, \mu_{ln L 2}$ (m) | -3.00, -3.00 |
| Ln standard deviation of length of each set $\sigma_{ln L 1}, \sigma_{ln L 2}$ (m) | 0.25, 0.25 |
| Ln mean fracture aperture of each set $\mu_{ln 2b 1}, \mu_{ln 2b 2}$ (cm) | -7.824, -7.824 |
| Ln standard deviation of aperture of each set $\sigma_{ln 2b 1}, \sigma_{ln 2b 2}$ (cm) | variable; see text |

insight into the actual mechanisms through which uncertainty in the input parameters may affect the transport of contaminants in a fracture system. After an understanding is obtained of which parameters may have a crucial impact on contaminant transport in a fracture network, complete Monte Carlo simulations can be employed to estimate the uncertainty in contaminant transport associated with possible errors in the different statistical geometrical parameters.

Once the fracture network has been generated, a grid system must be established to permit numerical simulation of flow and transport. This is accomplished

by algebraically determining the coordinates of the intersections of each of the fractures. A node is assigned to each intersection. In contrast with the practice adopted by other investigators (Schwartz et al., 1983; Rouleau and Gale, 1984), nodes may optionally also be assigned to the endpoints of the fractures. This was done in order to study the importance of diffusion into deadend fracture segments as an attenuation mechanism. Nodes can also be assigned to locations wherever fractures cross an imaginary line at a specified position. These nodes are used as observation points in the examination of macroscopic dispersion during solute transport within the fracture network.

During early tests of the flow simulation model, it was noted that poor fluid mass balances occurred whenever three fractures happened to intersect at almost the same point. The error was apparently introduced by the presence of very large numbers in the coefficient matrix used in the direct solution of the flow equations. The problem was rectified by modifying the grid system to 'collapse' such near-intersections to a single point.

Having determined the coordinates of all the nodes lying within the flow regime, node numbers are assigned in such a manner as to minimize the bandwidth of the coefficient matrix. This numbering is performed using an algorithm described by Collins (1973). An example of the resulting grid system which can then be used in subsequent flow simulations is shown in Figure 1(b).

3.2 Flow Model

Flow and transport are both simulated within the fracture network using conventional finite element techniques in which the fracture network is treated as a two-dimensional array of one-dimensional line elements. The elements represent

the fracture segments bounded by intersections (nodes). This approach was introduced to the study of flow in fractured rocks by Wilson and Witherspoon (1970). The hydraulic conductivity of each element is related to the fracture aperture by the cubic law (equation 1). In the present study, flow is assumed to be steady-state and laminar; head losses at intersections are neglected; changes in fracture aperture resulting from imposition of different hydraulic heads at the boundaries of the flow region are assumed negligible. The rock matrix is considered to be impermeable in comparison to the secondary permeability imparted by the fracture network.

Application of the standard Galerkin technique (Pinder and Gray, 1977) results in a system of simultaneous equations involving the unknown heads at each fracture intersection. These are solved using the Cholesky algorithm. To reduce matrix storage requirements and computational effort, specified-head nodes and deadend nodes lying at the end of fractures are eliminated from the coefficient matrix prior to solution. The deadend nodes are then assigned the hydraulic head value computed for the adjacent intersection. This has the added advantage of eliminating small spurious hydraulic gradients along deadend fracture segments introduced by numerical error. Following solution, hydraulic heads are differentiated to obtain the average velocity across the width of each fracture. The source code for the flow model is included in the Appendix.

Selection of appropriate boundary conditions for flow simulations proved problematic. If the primary focus of this study had been on the impact of changes in the statistical geometrical parameters on the overall hydraulic behavior of the fractured rock system or the distribution of velocities within the system, specified-head boundary conditions at all boundaries such as those used by Long et al. (1982) would have been appropriate. Such boundary conditions would have

permitted flux through any of the sides of the flow domain, which would have greatly complicated the analysis of transport and macroscopic dispersion through the fracture network. For this reason, the boundary conditions selected for all flow simulations were of the Dirichlet type ($h = h(y)$) at the left and right boundaries and zero flux ($\partial h / \partial y = 0$) at the top and bottom boundaries. This is illustrated on Figure 2. These boundary conditions would produce a unidirectional flow field from left to right in an idealized isotropic medium. Unless otherwise specified, the hydraulic gradient used was 0.04.

It should be noted that the boundary conditions will affect the calculated effective hydraulic conductivity values presented in later sections as well as the distribution of flow velocities within the fracture network and regions of the network in which flow is concentrated. Flow within the fracture networks generated in the present study may well be sensitive to the orientation of the fracture network with respect to the hydraulic gradient as studied by Long et al. (1982); this phenomenon was not addressed. The flow field within any fractured medium which does not behave as an equivalent porous medium will be affected by the boundary conditions imposed, and smooth hydraulic gradients are generally absent in real systems with sparse fractures. Yet computational limitations may prevent modeling of solute transport within discrete fracture networks in regions large enough so that the flow field is unaffected by the proximity of the boundaries. Because of these factors, difficulties involved in the selection of appropriate boundary conditions for modeling transport in real fracture networks may rank of equal importance with specification of statistical geometrical parameters. The concept of an appropriate representative elemental volume (REV) for transport in fractured media represents an important area for future research.

REALIZATION NO. 1-A1
BOUNDARY CONDITIONS

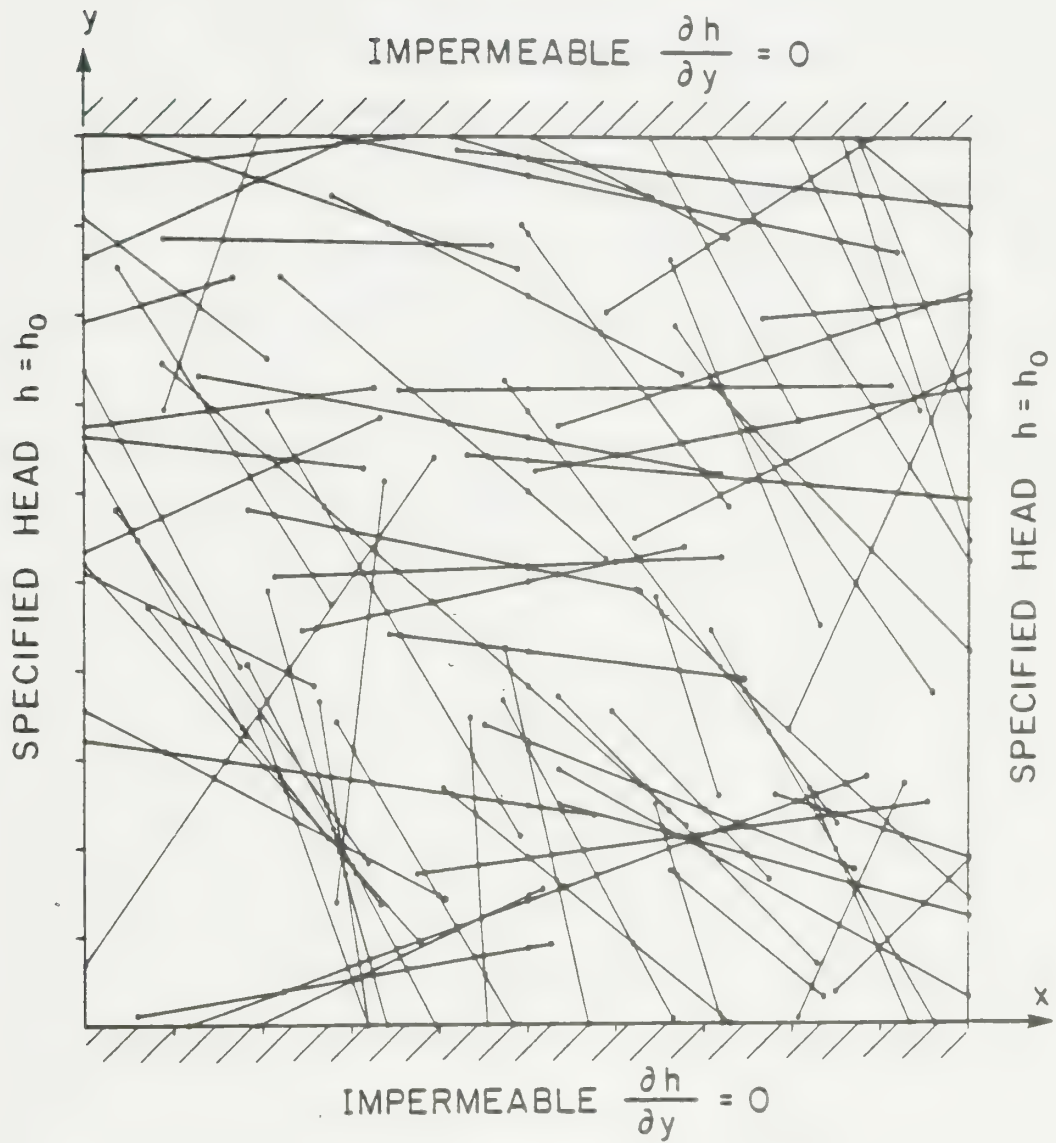


Figure 2: Boundary conditions used for flow simulation

3.3 Transport Model

Solute transport within the fracture network was simulated using conventional finite-element methods. The model developed is included in the Appendix. Application of the Galerkin technique to the partial differential equation governing transport within each fracture (equation (3)) results in a system of simultaneous linear equations that can be solved by a Gaussian elimination technique. The finite element technique assumes perfect mixing at fracture intersections: experimental data supporting such an assumption is provided by Krizek et al. (1972).

The principal advantage of the finite element technique is its flexibility. Physical and chemical processes, such as diffusion into deadend fracture segments or virtually stagnant regions of flow and attenuation via ion exchange or other chemical reactions, can be readily incorporated. Were it possible to describe the geometry of the matrix blocks, diffusion to these regions could also be included. The technique can also easily handle the irregular geometry of the discrete fracture networks generated during this study. Other techniques have been used for simulating transport in discrete fractures. Schwartz et al. (1983) simulated contaminant transport in fracture networks using a particle-tracking approach. These authors noted that their transport simulation technique is limited to systems of orthogonal fractures. This may represent a shortcoming of their solution algorithm rather than an inherent limitation of particle tracking. Difficulties in incorporating diffusion to the matrix and to regions of stagnant fluid may comprise a more serious drawback to particle-tracking techniques.

Finite element techniques are, however, susceptible to numerical dispersion unless special precautions are taken. To minimize numerical dispersion, the grid system must be discretized and the time-stepping scheme maintained to satisfy the grid Peclet and Courant numbers (Daus et al., 1983):

$$(Pe)_{\text{grid}} = v\Delta x/D_L \leq 2 \quad (9)$$

and

$$C = v\Delta t/\Delta x \leq 1 \quad (10)$$

Before solving the transport equation (3) for the fracture network, the hydrodynamic dispersion coefficient for each fracture was calculated using equation (4) with values of v determined by the flow simulation program, known values of (2b), and a free-solution diffusion coefficient of $2.0 \times 10^{-9} \text{ m}^2/\text{sec}$. For the flow velocities and the fracture apertures simulated in the present study, the hydrodynamic dispersion coefficient D_L was essentially equal to the free-solution diffusion coefficient D_0 . The maximum permissible length of each fracture segment, Δx , was then determined using equation (9), and the grid system re-discretized to satisfy the grid Peclet number criterion. The necessity of satisfying this criterion represents a major limitation of the conventional finite element technique for simulating transport within a fracture network. Although transport can be readily simulated within a highly complex network, as shown in Figure 1(a), computer storage restrictions impose an upper limit on the physical dimensions of the system that can be simulated. For the present study, it was felt that this disadvantage was outweighed by the more accurate representation of the physics of the transport process. Constraints on the physical dimensions of the simulation region for transport may be less restrictive if the fractures are conceptualized other than via a smooth parallel-plate analogy. Variations in aperture within an individual fracture or rough fracture walls may increase the longitudinal dispersion coefficient, thus permitting greater spacing between nodes and enabling simulations over a larger area.

Once the grid system was rediscrctized, the maximum time step that could be used was determined using equation (10). It was observed that this time step was largely dictated by the presence of small elements in regions where fracture intersections were clustered. The advective Peclet number (Daus et al., 1983):

$$(Pe)_{adv} = (Pe)_{grid} \cdot C = v^2 \Delta t / D_L \quad (11)$$

was less than 0.01 for each element in the network after satisfying equations (9) and (10). Although the constraint imposed by equation (10) tends to dictate conditions required to reduce numerical dispersion at early times, recent work (Daus et al., 1983) indicates that at later times an error-free solution can be obtained even if the advective Peclet number is increased to a value greater than 2. In keeping with this concept, the value of Δt used in the numerical simulations of transport was determined on the basis of equation (10) for early times, and was increased at later time. No evidence of oscillatory behavior in the solution, the usual result of violating the constraint expressed by equation (10), was noted. Accuracy of the solution was further enhanced by using a central-difference temporal approximation. Although Daus et al. (1983) show that a consistent representation produces more accurate results for a one-dimensional flow system with a uniform value of Δx , experiments during the present study showed a lumped representation to behave better for transport in a network. Boundary conditions used for transport were of the Dirichlet type ($c = c_0$) at the left (inflow) boundary and of the Neumann type ($\partial c / \partial n = 0$) at all other boundaries, as shown on Figure 3.

The concentrations determined at each of the 'observation' nodes, located at a designated distance from the inflow boundary, were used to develop a breakthrough curve that represents the macroscopic response of the fracture network

REALIZATION NO. 1-A1 BOUNDARY CONDITIONS

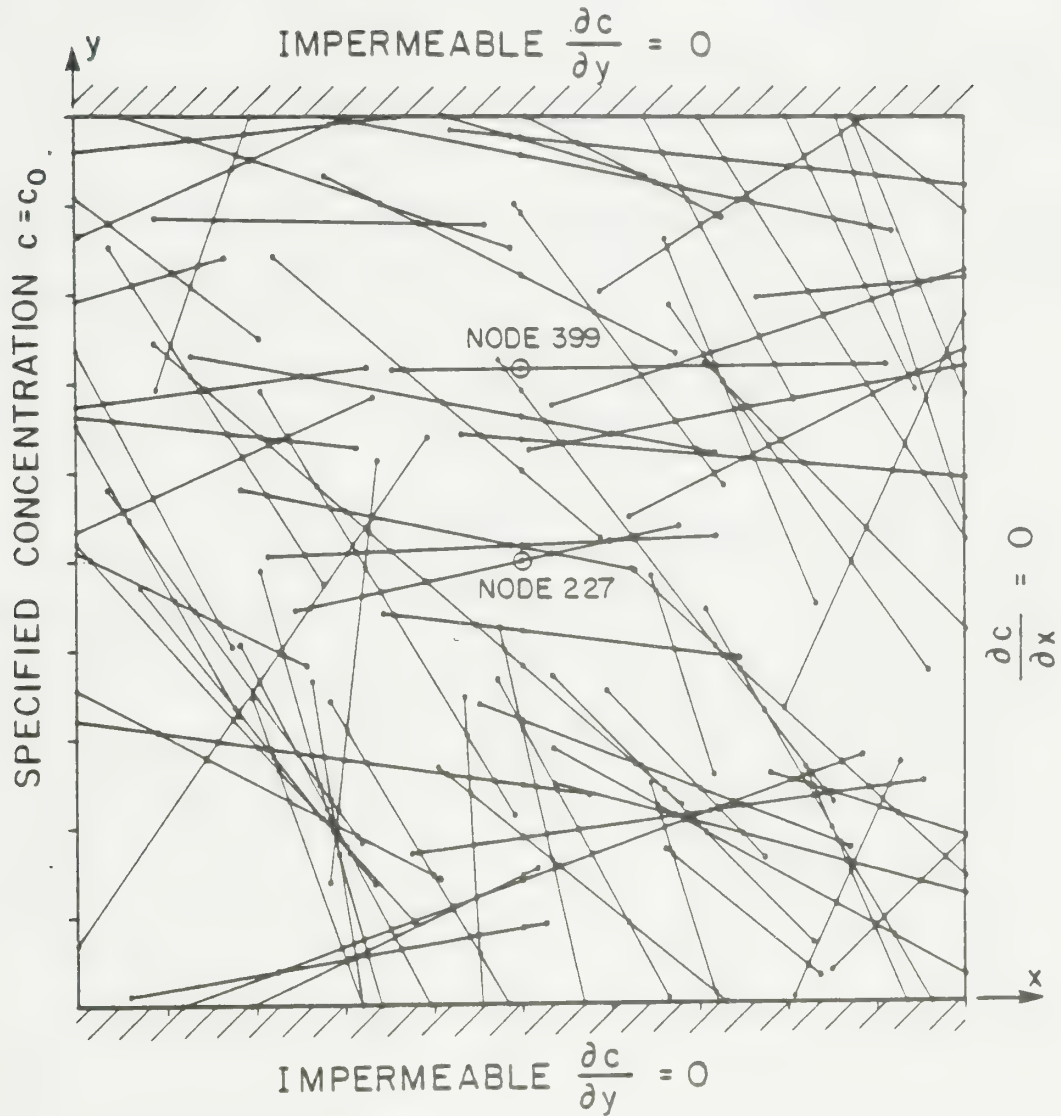


Figure 3: Boundary conditions for transport simulation

to dispersion within an individual fracture, mixing at fracture intersections, and diffusion to deadend fracture segments and relatively immobile regions. The macroscopic concentration at this distance as a function of time, $c/c_0(t)$, was determined from the relationship:

$$c/c_0(t) = \sum c_i(t)q_i / \sum q_i \quad (12)$$

where the $c_i(t)$ are the calculated concentrations at each observation node and the $q_i(t)$ are the discharges through each fracture segment containing observation node i :

$$q_i = v_i \cdot (2b) \quad (13)$$

This concentration versus time distribution was used to quantify the macroscopic dispersion characteristics of the fracture network, as described in Section 3.4.2. An example of a breakthrough curve determined in this manner is shown on Figure 4; also shown are microscopic results for two individual 'observation' nodes in the simulation. The location of these nodes is shown on Figure 3.

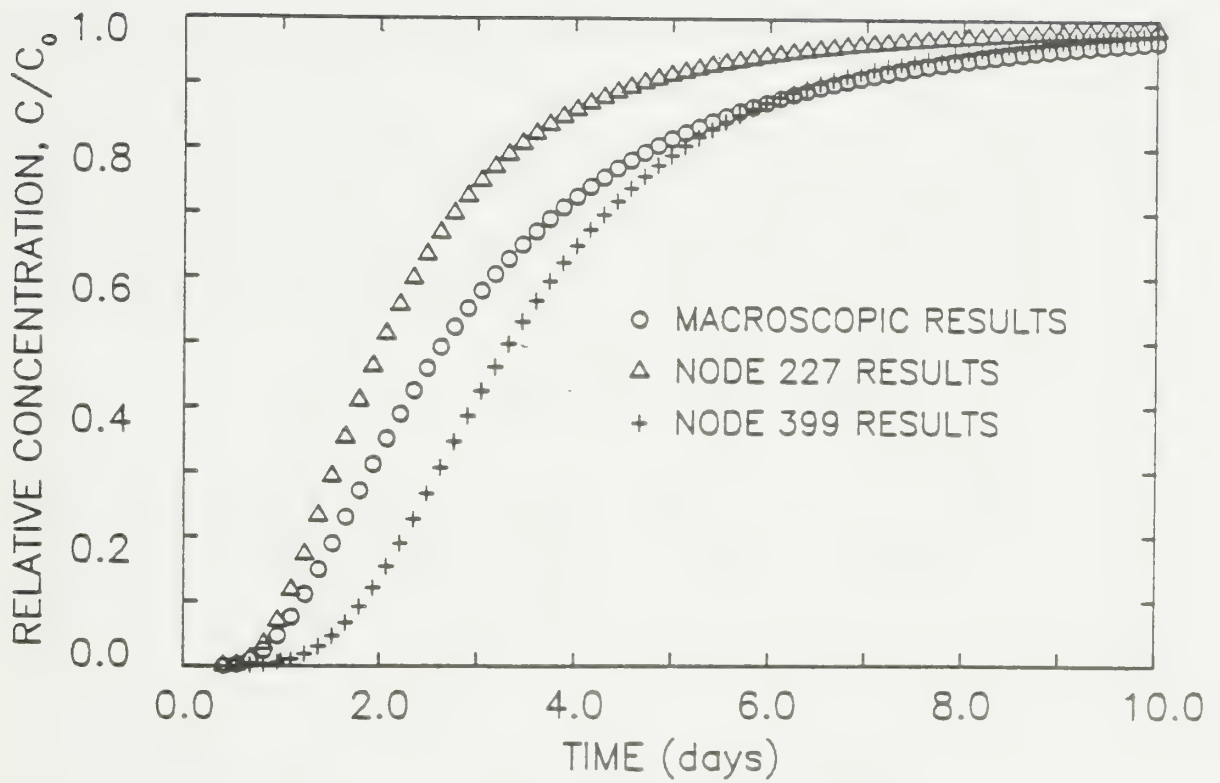


Figure 4: Example of a macroscopic breakthrough curve. Also shown are results for two individual nodes in the network: locations of these nodes are shown on Figure 3.

3.4 Parameter Estimation

3.4.1 Velocities

Depending on the manner in which it is defined, the 'average' flow or transport velocity may have very different meanings. Several techniques were used in the present study to estimate or predict the effective velocity within the fracture network.

Snow (1969) related the effective hydraulic conductivity of an equivalent anisotropic continuum to the density, apertures, and orientations of fractures within a rock mass. This technique assumes that fractures are infinitely long, i.e. that the network of fractures is perfectly interconnected; his expression, which equates the overall hydraulic conductivity of the rock to the sum of the contributions of each fracture, can be given as:

$$K_{ij} = \frac{2}{3} \frac{\phi g}{\mu} \sum (b^3 / |n_i D_i|) (\delta_{ij} - n_i n_j) \quad (14)$$

where the summation is taken over all members of a joint set intersected by a sampling line D_i , the n_i are the direction cosines of the normal to the fracture plane, and δ_{ij} is the Kroneker delta function, equal to 0 when $i \neq j$ and 1 when $i = j$.

The hydraulic conductivity of a network of finite fractures is less than that of a network of infinite fractures, as discussed by Long et al. (1982). Equation (14) thus sets an upper limit on the equivalent hydraulic conductivity of a network of fractures. For each fracture network generated, the theoretical upper limit to K_x , called $(K_x)_t$, was calculated using equation (14).

This value was compared to the effective hydraulic conductivity of the network, $(K_x)_e$, by examining the output from the flow simulation model. The total flow Q_x through the network was noted; application of Darcy's equation leads to:

$$(K_x)_e = Q_x / (\nabla h \cdot A) \quad (15)$$

where A is the cross-sectional area of flow. The comparison is useful in that an accurate estimation of the effective hydraulic conductivity of a fracture network may be a critical parameter in predicting the flux of a contaminant from a source.

If the hydraulic gradient and effective fracture porosity n_e are known, the theoretical velocity at which a conservative tracer might be expected to travel in an equivalent porous medium can be estimated:

$$(v_x)_t = (K_x)_t \nabla h / n_e \quad (16)$$

Similarly, equation (16) can be used to predict the effective velocity $(v_x)_e$ for an equivalent porous medium by using $(K_x)_e$ instead of $(K_x)_t$. This is the technique most commonly applied when the bulk rock hydraulic conductivity is known and some estimate is available of the effective porosity n_e .

Determination of n_e for a real fractured medium is not a straightforward procedure. Effective porosity has been estimated by combining effective aperture data computed from borehole tests with statistical information concerning trace length and fracture spacing (Gale et al., 1982). For the present study, the effective porosity was computed by summing the volume of the individual fracture segments, exclusive of deadend regions.

The average flow velocity within each fracture segment can be obtained by applying Darcy's equation, using equation (1) to determine K_f . Although the resulting set of velocities determined in this manner for the network as a whole do not follow any particular distribution, some measure of their variability can be demonstrated by computing the mean, the standard deviation, the skewness, and the coefficient of variation. These values were computed for all fracture segments exclusive of those deadend segments in which the flow velocity was zero, i.e.

$$\langle v \rangle = \sum_{i=1}^N v_i / N \quad v_i \neq 0 \quad (17)$$

where N is the number of non-deadend fracture segments (elements in the finite-element program).

The arithmetic mean fluid velocity may in some cases be a very poor estimate of the rate at which fluid actually moves through a fracture network, however. Once fluid enters a fracture, its velocity and direction are constrained until another fracture is intercepted. Although the average flow velocity within an individual fracture may or may not be affected by the number of times the fracture is intercepted by other fractures, the arithmetic mean velocity computed for a network may be strongly influenced by the number of fracture segments along the preferred flow paths. A macroscopic velocity that might be a better analogy to the average linear groundwater velocity within a porous medium can be obtained by weighting the velocities within each fracture segment based on the length and orientation of the fracture segment:

$$\langle v_x \rangle_w = \sum l_{xi} v_{xi} / \sum l_{xi} \quad v_{xi} \neq 0 \quad (18)$$

where v_{xi} represents the x -component of the velocity vector within each fracture segment and l_{xi} represents the projection of the length of the fracture segment in the x direction.

Finally, the effective velocity at which the center of mass of a solute injected into the flow system, $\langle v_x \rangle_{tr}$, will travel can be determined by computing the first moment of the macroscopic breakthrough curve as described in Section 3.4.2.

3.4.2 Macroscopic Dispersion

A relatively simple technique for calculating an effective dispersion coefficient from a breakthrough curve is to apply the method of moments. This technique does not imply that spreading is a Fickian process; it is simply a way of quantifying the spreading. A continuous-input macroscopic breakthrough curve, such as the one shown on Figure 4, can be converted to an instantaneous (Dirac) response by differentiating the observed results to obtain the function:

$$c'(t)/c_0 = d/dt (c/c_0) \quad (19)$$

(Levenspiel, 1962; Kreft and Zuber, 1978). The 0th moment of this instantaneous response is defined as

$$M_0 = \int_0^{\infty} c'/c_0 dt \quad (20)$$

It is apparent that this value should equal 1 if there is no loss of mass from the system. The kth moment about the origin is defined as

$$M_k = (\int_0^{\infty} t^k c'/c_0 dt) / M_0 \quad (21)$$

For $k \geq 2$, it is more useful to consider the moment about the mean rather than about the origin:

$$M_2 = \{ \int_0^{\infty} (t - M_1)^2 c'/c_0 dt \} / M_0 = \sigma_t^2 \quad (22)$$

The third and higher-order moments about the origin can be defined in a similar fashion. The principal advantage of this technique is that it provides a method of quantifying the spreading of an observed breakthrough curve without relying on any assumptions concerning the processes that produced this spreading. Several useful parameters can be obtained from the different moments. The first

moment, M_1 , is equal to the average residence time t_r of the center of mass of the tracer. From this, the effective travel velocity, $(v_x)_{tr}$, of the solute can be calculated knowing the distance of the 'observation' nodes from the source. The average tracer residence time t_r can be compared to the average residence time of the fluid t_f , defined as

$$t_f = V_f/Q \quad (23)$$

where V_f is the volume of the fractures participating in flow (equal to the total volume of the fractures minus the volume of deadend segments).

The effective dispersion coefficient can be determined from the first and second moments by rearranging equation (8) as

$$D_L = -1/2 (x^2/M_1^3) \sigma_t^2 \quad (24)$$

and the coefficient of skewness, S_k , can be computed from the third moment about the origin M_3 as:

$$S_k = M_3/\sigma_t^3 \quad (25)$$

Distributions with a positive value of S_k have a tail extending to the right of the mean (positively skewed), and distributions with a negative value of S_k have a tail extending to the left of the mean.

The principal disadvantage of the method of moments is its extreme sensitivity to the tail of the curve at large values of time, particularly for second or higher-order moments. Such a tail may result from measurement errors in laboratory or field experiments; alternatively, it may genuinely represent physical processes. Neretnieks (1983) has shown that if there is any diffusion to the matrix and if the penetration depth is small in comparison to the distance to the

next fracture, slow diffusion of solute from the matrix back into the fracture will produce an apparently infinite observed dispersion coefficient. The computed value of the dispersion coefficient in such a system may be entirely dependent on the analytical detection limit if the method of moments is applied to the data. The same may be true in the presence of diffusion to zones of essentially stagnant fluid, or if macroscopically-observed dispersion in porous media is related to diffusion to fine-grained units in keeping with the advection-diffusion concept (Gillham et al., 1984).

A theoretically-infinite dispersion coefficient or one whose measured value is arbitrarily dependent on analytical precision does not, however, provide a very useful means of characterizing solute transport. To provide a more objective means of quantifying the spreading of a tracer, the ordinary method of moments can be modified by incorporating a weighting factor to diminish the sensitivity of the results to the tail of the breakthrough curve. This weighted method of moments was introduced by Mixon et al. (1967) and is described in detail by Anderssen and White (1971). Using a weighting factor

$$w_k(t) = t^k e^{-st} \quad (26)$$

the weighted moment about the origin M can be defined as:

$$M_k(s) = \int_0^{\infty} t^k e^{-st} c'/c_0 dt \quad (27)$$

Appropriate values for s can be selected as described by Anderssen and White (1971). Just as with ordinary moments, the first weighted moment about the origin can be used to estimate $(v_x)_{tr}$ and the second weighted moment can be used to estimate D_L .

The two methods of moments were compared against an analytical solution (Ogata and Banks, 1961), truncated at different values of c/c_0 . This test showed that the ordinary method of moments was slightly more accurate than the weighted method of moments at calculating the effective velocity, but the weighted method of moments produced estimates of D_L that were much more accurate and much less sensitive to truncation of the breakthrough curve for small Peclet numbers (asymmetric breakthrough curves). An example of such a comparison is shown on Figure 5. The discrepancy between the moment results and the analytical solution is due to truncation of the breakthrough curve at a relative concentration of c/c_0 of 0.95; the results converged to the correct values in both cases at $c/c_0 = 1$. This figure shows that for this truncation value, the difference between the ordinary moment results and the weighted moment results is relatively minor.

For the present study, it was found that the weighted method of moments provided significant advantages over the ordinary method of moments in objectively determining the macroscopic dispersion coefficient from the breakthrough curves obtained for the fracture networks. This factor, rather than its better accuracy, was the main motivation for using the weighted moment method for calculating dispersion coefficients. As shown on Figure 4, the macroscopic breakthrough curves tended to be highly tailed, asymptotically approaching a relative concentration of 1. Most of this is probably the result of the averaging technique used, reflecting the slow nature of transport in part of the network. Evidence presented later suggests that at least part of the skewness may be due to slow diffusion to relatively stagnant regions of flow. Although the ordinary and weighted moments eventually converge to the same answer when tested against an analytical solution, this is not true for the fracture network model

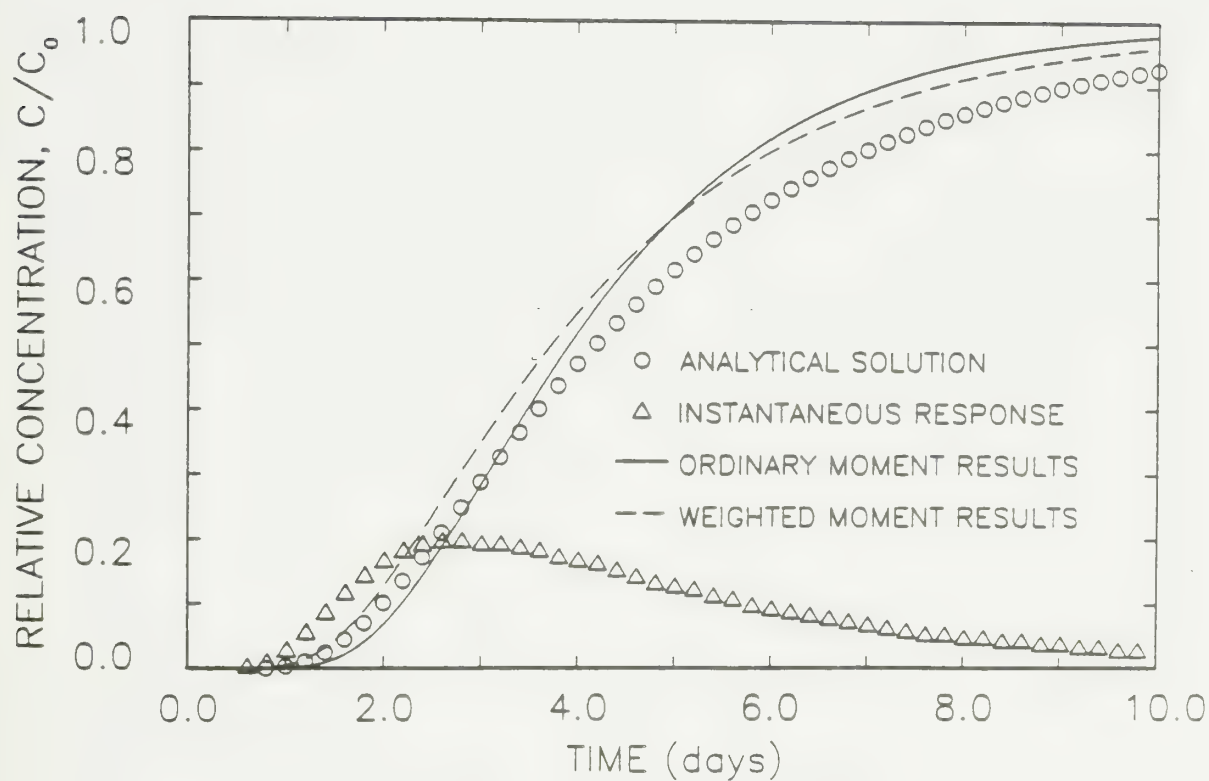


Figure 5: Comparison of moment results to analytical solution. Velocities in both cases were calculated using ordinary method of moments. Breakthrough curve was truncated at a relative concentration of 0.95 for computations.

results. In the case of the macroscopic breakthrough curves obtained from the observation nodes, the dispersion coefficient determined from the ordinary moments method increased without bound depending on the point of the breakthrough curve at which calculations were discontinued, whereas the weighted moment results were essentially constant. This is illustrated in Figure 6. For the remainder of the study, the ordinary method of moments was used to calculate the average tracer velocity and coefficient of skewness, and the weighted method of moments was used to calculate the dispersion coefficient. The breakthrough curves were consistently truncated at a relative concentration of 0.95; the computed values of S_k should thus be considered as approximate values only. The comparison shown on Figure 6 suggests that the weighted method of moments may provide significant advantages over the ordinary method of moments in obtaining estimates of the effective dispersion coefficient for situations that are strongly affected by slow diffusion processes or analytical detection limits.

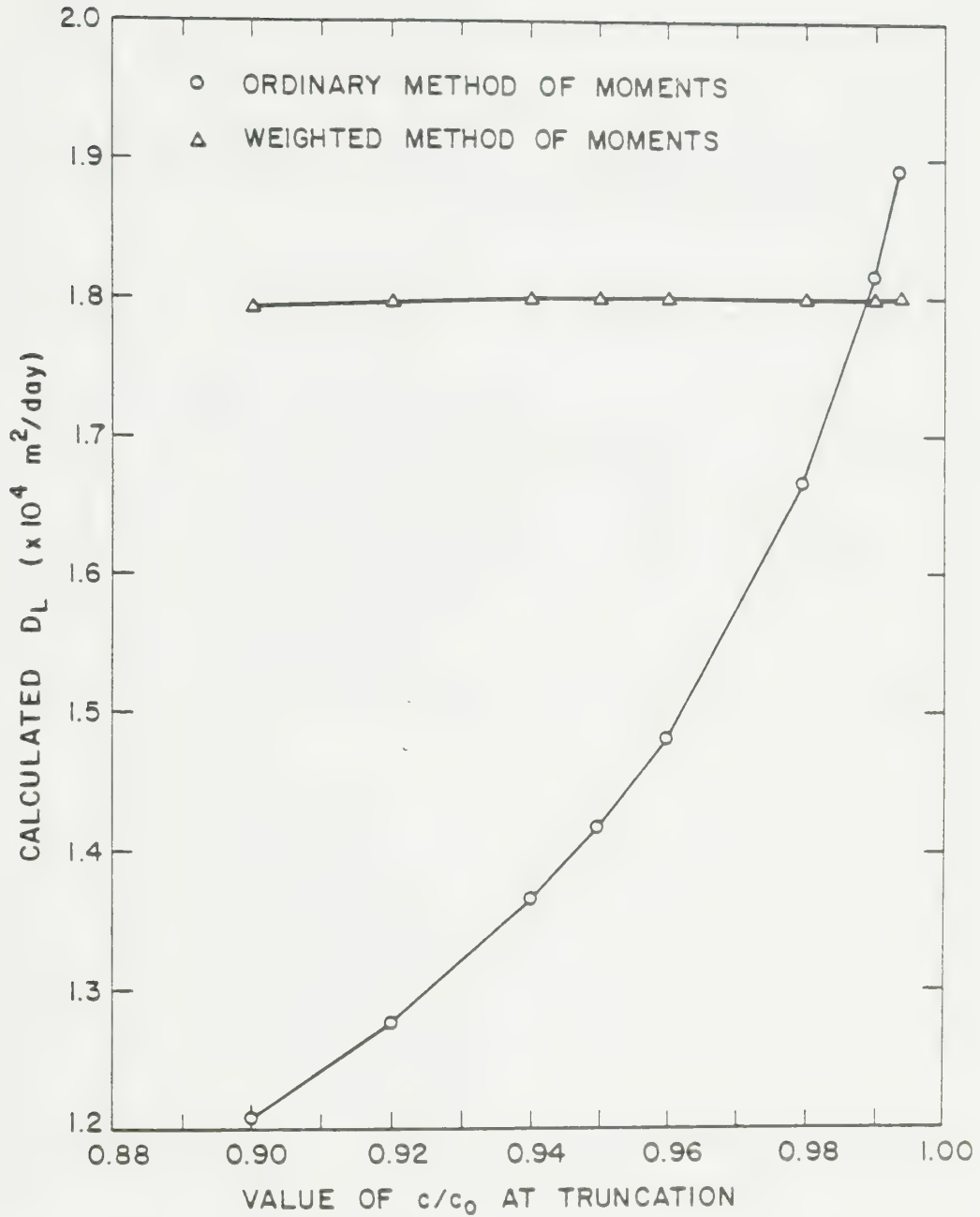


Figure 6:

Comparison of ordinary and weighted methods of moments. Dispersion coefficients were calculated by applying ordinary method of moments and weighted method of moments to numerical results for fracture network.

Chapter IV

IMPACT OF FRACTURE GEOMETRY ON SOLUTE TRANSPORT

4.1 Effect of Variable Fracture Apertures

One of the most difficult parameters to determine for a rock is the standard deviation of the fracture aperture distribution, $\sigma_{\ln b}$. For many units, this parameter may even be virtually impossible to evaluate. Variations in aperture may have a significant impact on flow and transport within a fractured medium, however, as the permeability of a fracture varies with the square of its aperture (equation 1).

Based on direct measurement of apertures in granite and estimation of effective hydraulic apertures from pressure-test data from a variety of rock types, Snow (1970) found an average value of σ_1 of approximately 0.221, with values ranging from 0.058 to 0.39 ($\sigma_{\ln b} = 0.13$ to 0.90). Whether a particular range of values is likely to characterize any given rock type is not well known, but it seems likely that different rocks will have different values of $\sigma_{\ln b}$ depending on the mode of origin of the fractures and subsequent changes introduced by geochemical reactions or deformation. Neuzil and Tracy (1981) suggest that the log-normal distribution is probably no longer a good approximation of any fracture aperture frequency distribution for a value of $\sigma_{\ln b}$ greater than about 0.83.

To test the sensitivity of flow and transport in a fracture network to the variability of apertures, five simulations were conducted using values of $\sigma_{\ln b}$

ranging from 0.0 to 0.8. The value of $\sigma_{\ln z_b}$ for each simulation was the same for both sets of fractures. The network generated is the one shown on Figure 1(a); only the values of the apertures associated with each fracture were changed from one simulation to another. Figure 7 shows the simulated aperture distributions for three of these cases. In each case, the mean aperture $\mu_{\ln z_b}$ is the same: only the standard deviation $\sigma_{\ln z_b}$ is varied. When $\sigma_{\ln z_b}$ is equal to zero, all fractures have an identical aperture. When $\sigma_{\ln z_b}$ is equal to 0.4, the largest fracture has an aperture that is six times that of the smallest, and with $\sigma_{\ln z_b}$ equal to 0.8, the largest fracture is forty times the size of the smallest.

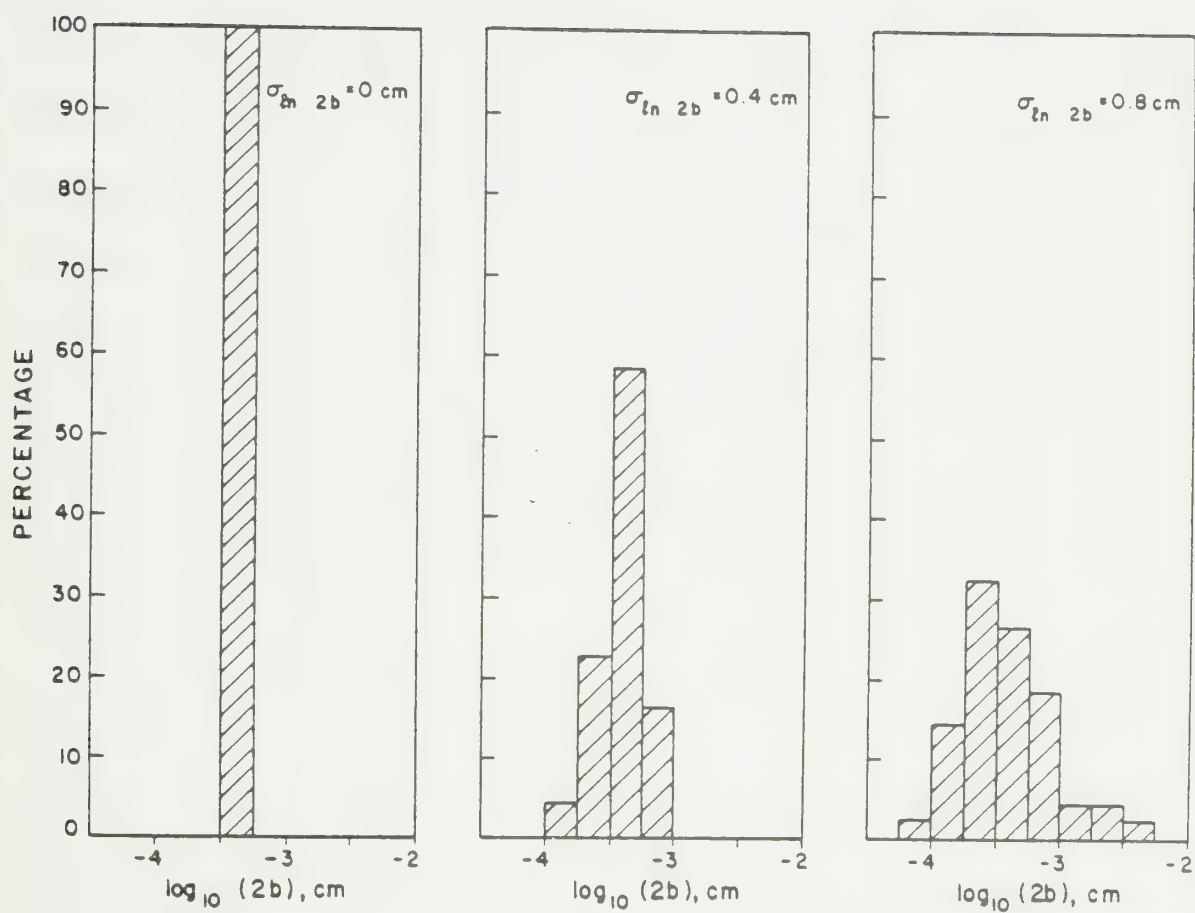


Figure 7: Histograms showing aperture distributions for three cases of $\sigma_{\ln 2b}$. Mean fracture aperture for each case = 4×10^{-2} cm.

4.1.1 Hydraulic Properties

Because of the form of the lognormal distribution, increasing the value of $\sigma_{\ln 2b}$ from 0 to 0.2 causes close to half of the fractures to become larger than the mean aperture and the other half to be smaller. Further increases in $\sigma_{\ln 2b}$ increases the frequency of small fractures relative to large fractures. The difference between the largest aperture and the mean aperture is greater than the difference between the mean aperture and the smallest aperture. If the fractures were of infinite length, flow would be dominated by the largest fracture and the permeability of the network would increase with increasing $\sigma_{\ln 2b}$. In a network of finite fractures, some of the flow must occur within the smaller fractures. For this reason, the tendency toward increasing permeability caused by increasing the size of the largest fractures can be counterbalanced to a greater or lesser extent by the increase in frequency of the smaller fractures. Thus, as $\sigma_{\ln 2b}$ increases in a network of finite fractures, the hydraulic conductivity can either increase or decrease.

This effect is shown on Figure 8, which compares the effective hydraulic conductivity $(K_x)_e$ calculated using equation (15) for the network shown on Figure 1(a) with the theoretical hydraulic conductivity $(K_x)_t$ for a network of infinite fractures calculated using Snow's model (equation 14). As shown, the hydraulic conductivity of a network can be much less than that of a system of infinite fractures. Thus, if the mean fracture aperture is estimated based on measured fracture spacing and bulk rock conductivity, and assuming perfect interconnection as described by Snow (1968), the mean fracture aperture is likely to be underestimated. The overall effect on the bulk hydraulic conductivity of increasing the size of the largest apertures is surprisingly small in comparison to what might have been expected for a well-interconnected network. The smaller fractures are

apparently capable of exerting a significant effect on the gross hydraulic behavior of a poorly-interconnected network.

Just as the hydraulic conductivity is not necessarily dominated by the largest aperture in a network of finite fractures, the volumetric flow may not be controlled by the largest fractures. The proportion of the total discharge Q_x through the network occurring within the largest 10% of the fractures was determined; the results are shown on Figure 9. For the $\sigma_{ln} 2b = 0$ case, the value shown is the proportion of the total discharge through the same fractures that represented the largest 10% in the $\sigma_{ln} 2b = 0.2$ case. If the flow had been evenly distributed in the network, approximately 10% of the flow should have occurred in these fractures; the smaller value obtained reflects the effect of preferred pathways formed in the absence of perfect interconnection and in the presence of fractures oriented in a favorable direction with respect to the boundary conditions imposed.

As $\sigma_{ln} 2b$ is increased, a progressively larger fraction of the total flow should occur within the largest fractures if the fractures were infinite. Because the discharge is proportional to the cube of the aperture, virtually all the flow should have occurred within the largest fractures for $\sigma_{ln} 2b = 0.8$. This is clearly not the case. Although the proportion of discharge contained within the largest fractures increases with the aperture variability, indicating that the flow may be contained in fewer fractures, the results shown in Figure 9 suggest that the largest fractures do not totally dominate the flow. The common wisdom that flow is controlled by the largest fracture may be a fallacy in the more realistic situation of a network of finite features.

Variations in fracture aperture have a significant effect on the local hydraulic head. Hydraulic head distributions within the network for the cases of $\sigma_{ln} 2b = 0.0$, 0.4 , and 0.8 are shown on Figure 9 (a),(b), and (c), respectively. These

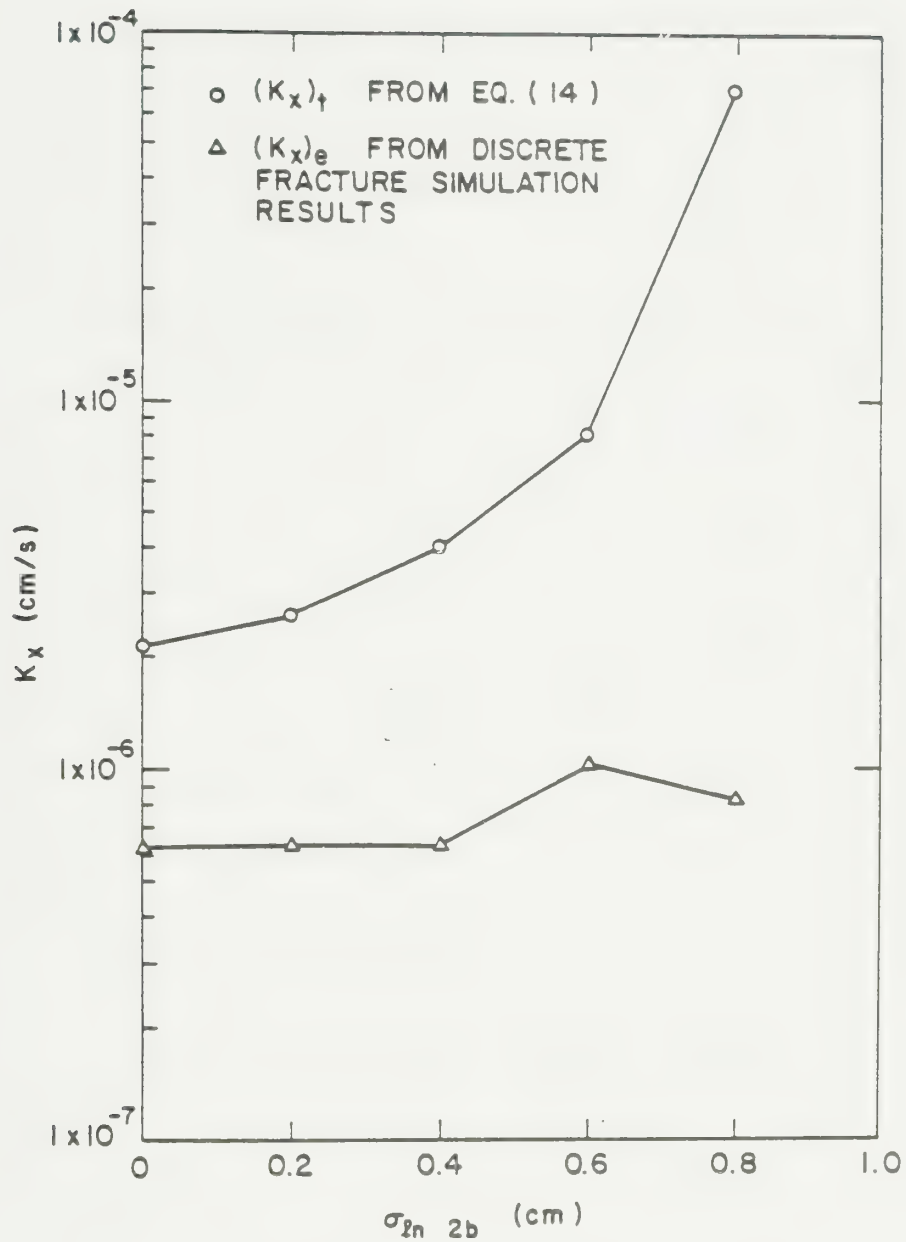


Figure 8: Comparison of hydraulic conductivity of finite and infinite networks with changing $\sigma_{ln} 2b$. Fracture connectivity ratio = 0.22

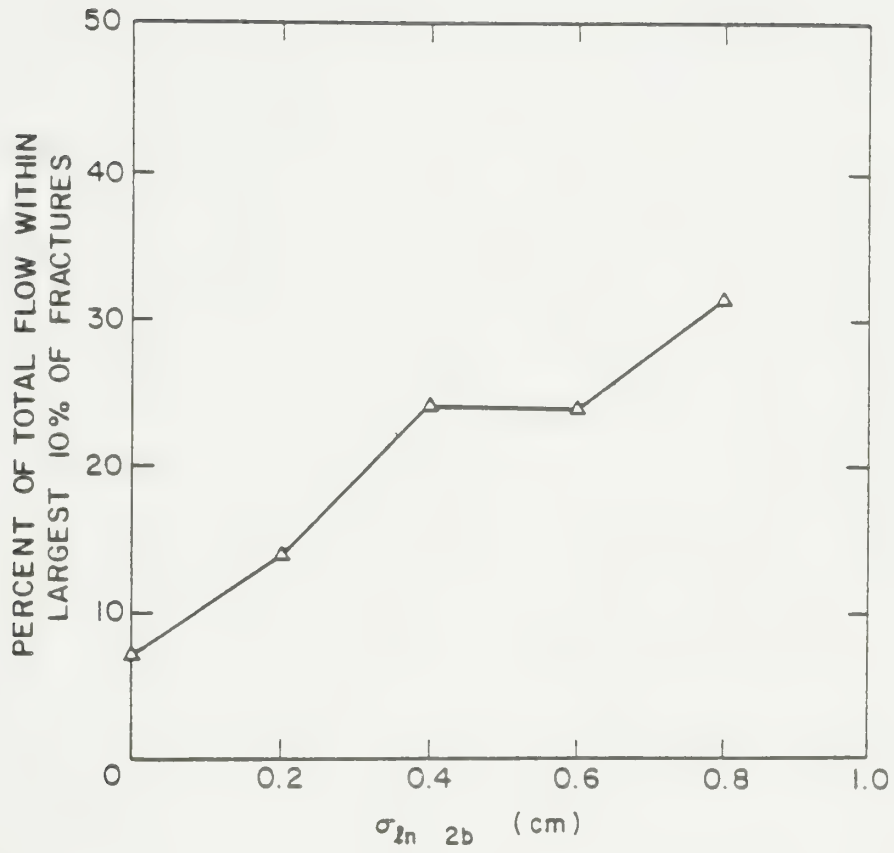


Figure 9: Control of flow within largest fractures with changing $\sigma_{ln 2b}$

equipotentials were prepared using a spatial interpolation technique (Sampson, 1978) that assumes that point values represent a continuous system. Thus, it does not account for the connection or lack of connection in the fracture system; as a result, some of the details shown (such as contour lines crossing deadend fracture segments) are physically unrealistic, although the overall visual pattern is useful in demonstrating the major features of the hydraulic head distribution. The contour lines, of course, have no physical significance as applied to the rock matrix which is assumed impermeable. Similarly, the low spots have no physical significance but are merely an artifact of the interpolation procedure.

For a system of non-orthogonal fractures of infinite length and equal aperture, Snow (1969) showed that the network would behave as an anisotropic equivalent porous medium. For the boundary conditions imposed, this would have produced parallel, equally spaced equipotentials. That this is not the case for Figure 9 (a) reflects the importance of the finite length of the fractures in the system. The irregularity of the hydraulic head distribution suggests that the fracture network is not behaving as an equivalent porous medium, although this conclusion was not rigorously tested. Increasing the variability of the fracture apertures greatly increased the irregularity of the hydraulic head distribution, as shown in Figure 10(b) and (c). This indicates that the fracture networks are deviating further from equivalent porous medium behavior as the variability of the fracture apertures increases, similar to the results of Long et al. (1982). As further evidence of the absence of equivalent porous medium behavior, hydraulic head profiles were prepared for the observation nodes, as shown on Figure 11. Were the network to behave as an equivalent porous medium, the hydraulic head values should have been equal to the $h = 0.2$ cm line on the diagram. Deviations from this value are more pronounced as $\sigma_{\ln 2b}$ increases, but are apparent even for the uniform aperture case.

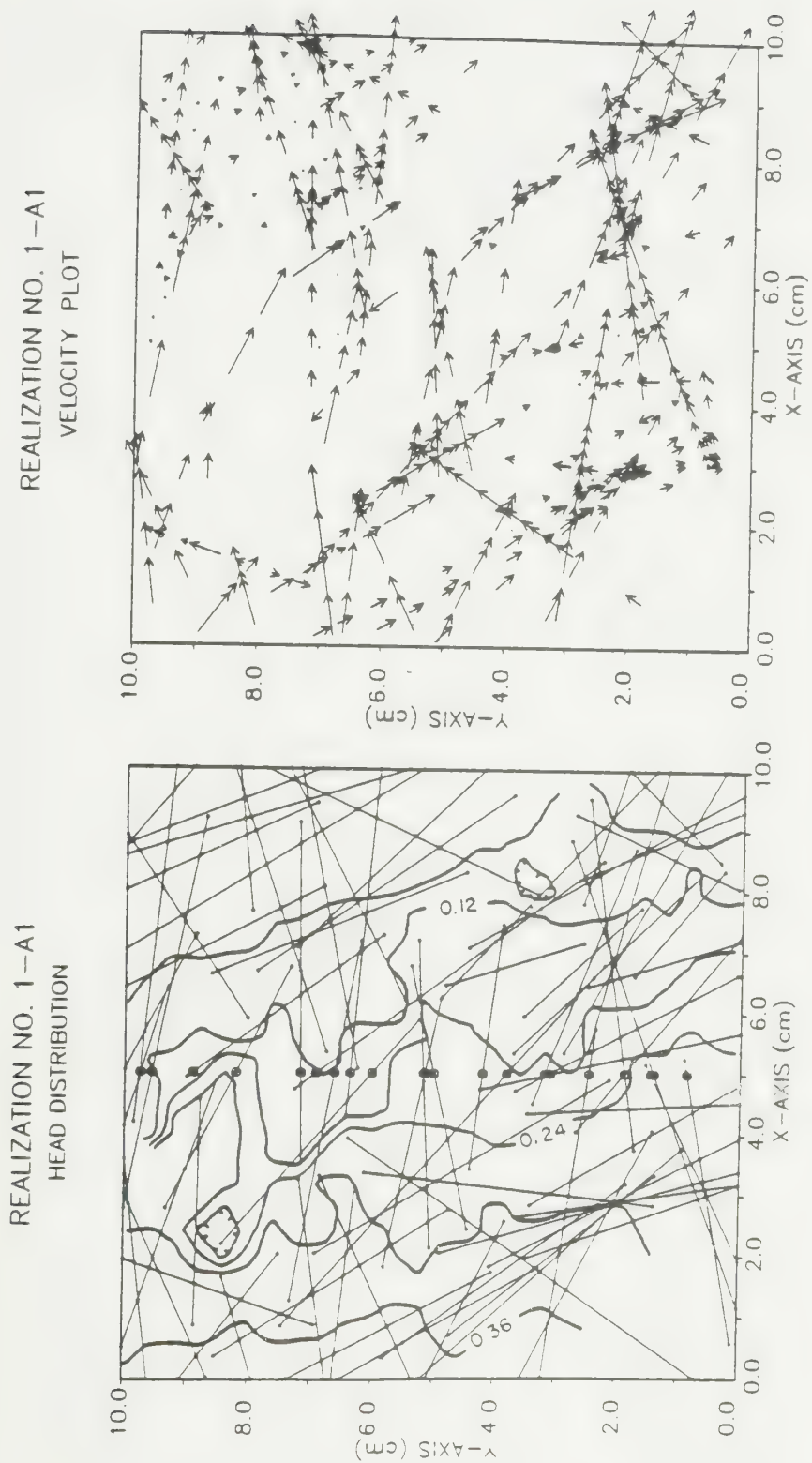
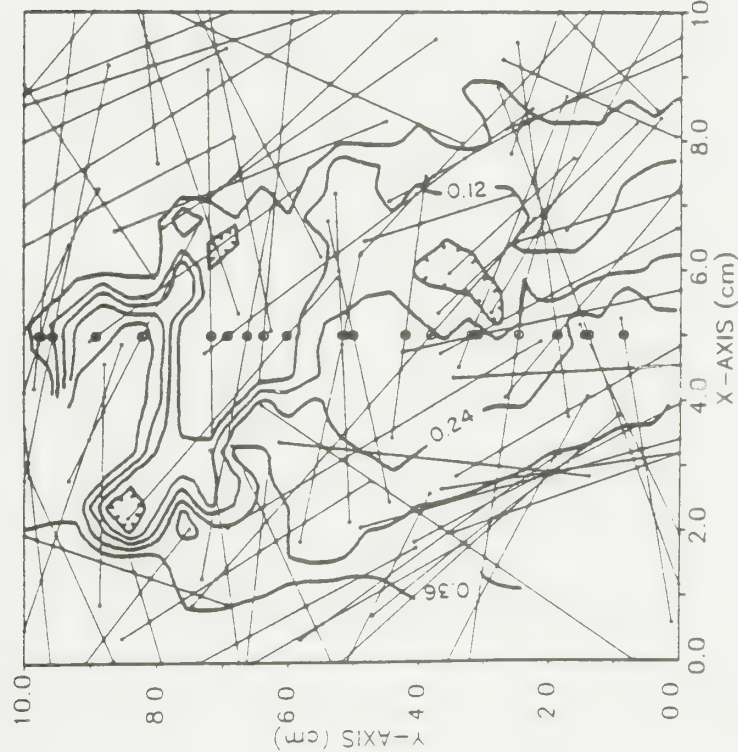


Figure 10: Hydraulic head and velocity distribution with changing $\sigma_{ln} 2b$.

(a) $\sigma_{ln} 2b_7 = 0.0$ case. 1 unit on the velocity plot represents 8.4×10^{-7} m/s

REALIZATION NO. 1-C1
HEAD DISTRIBUTION



REALIZATION NO. 1-C1
VELOCITY PLOT

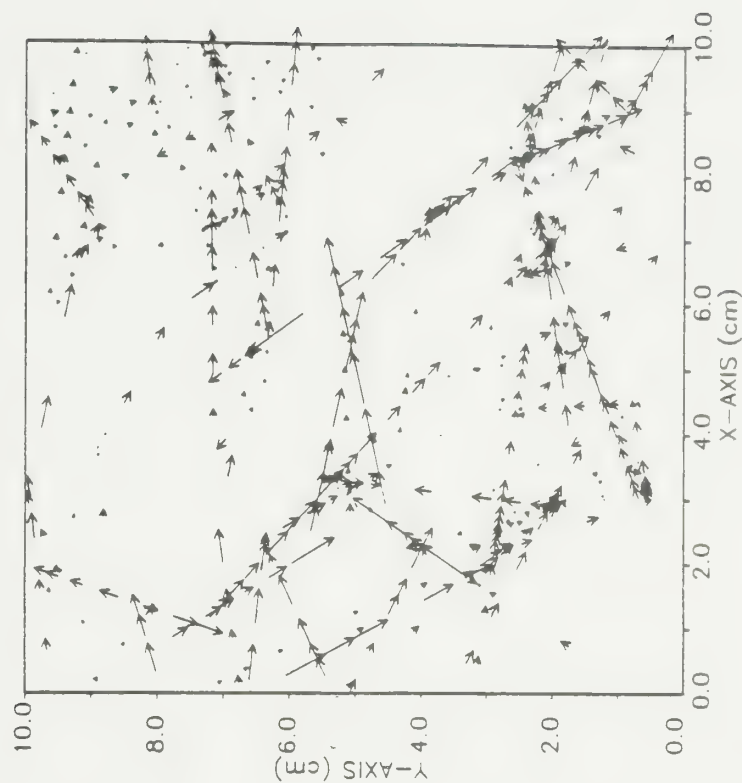


Figure 10: Hydraulic head and velocity distribution with changing $\sigma_{ln} 2b$.

(b) $\sigma_{ln} 2b = 0.4$ case. 1 unit on the velocity plot represents 1.3×10^{-6} m/s

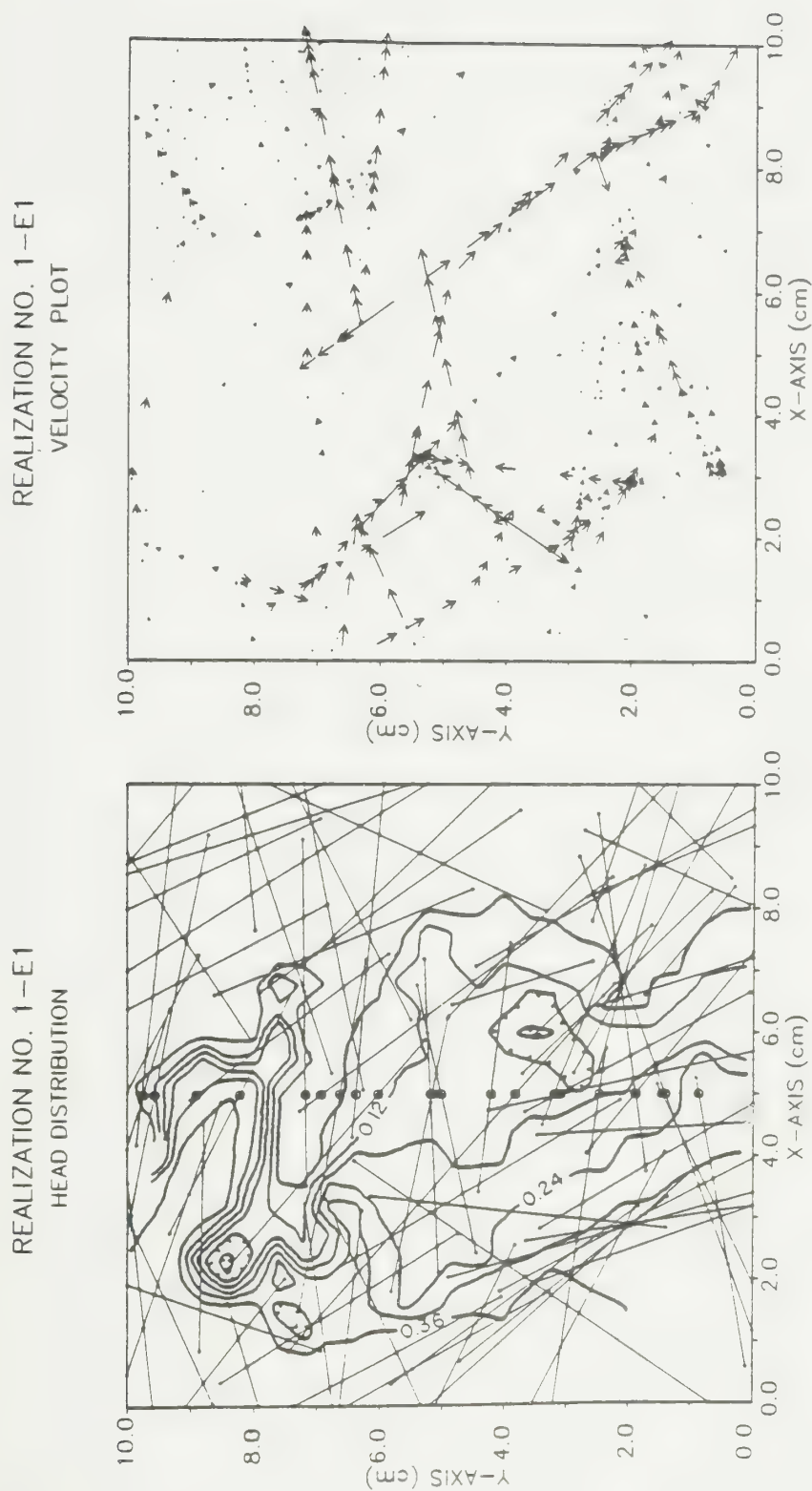


Figure 10: Hydraulic head and velocity distribution with changing $\sigma_{\ln 2b}$.
 (c) $\sigma_{\ln 2b} = 0.8$ case. 1 unit on the velocity plot represents 2.4×10^{-6} m/s

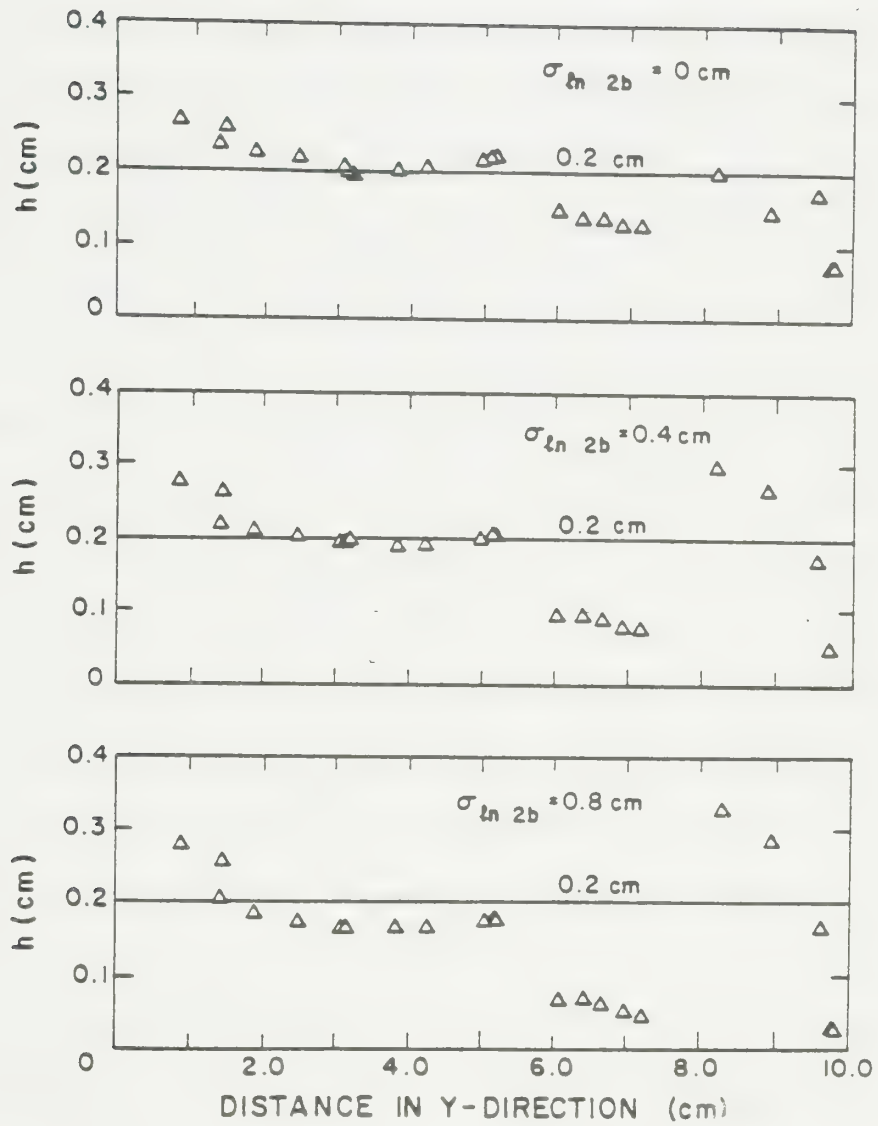


Figure 11: Hydraulic head profiles with changing $\sigma_{\ln 2b}$. Values are all at a distance $x = 5.0$ cm

Figure 10 (a), (b), and (c) also shows the spatial distribution of velocities within the fracture network. Comparison of the head plots with the velocity plots shows that head values are closest to the equivalent porous medium value where the flow paths are most continuous (i.e., around $y = 4$ to 5 cm) (the low spot at $x = 2$, $y = 8$ on Figure 10 is a result of the contouring technique).

In the case of uniform fracture apertures, the flow velocities tend to be relatively uniformly distributed. No preferred flowpath can be identified. As the variability of fracture apertures increases, however, the larger flow velocities tend to occur within fewer and fewer fractures. The highest velocities need not occur within the largest fractures, which may have limited accessibility if flow can only reach them through small fractures. Similarly, the largest discharges need not occur within the largest fractures. This is shown on Figure 12, which illustrates the distribution of discharges within the network for $\sigma_{\ln 2b} = 0.8$. The distribution of discharges is similar, but not identical to, the distribution of velocities shown in Figure 10(c). It bears only a weak relationship to the location of the largest fractures. The relationship between fracture aperture and velocity or discharge may not be simple in a network of finite features.

Histograms illustrating the distribution of flow velocities within fracture segments are presented on Figure 13. As can be seen, the arithmetic mean velocity decreases as the variability in the fracture apertures increases, although the maximum velocity within the network increases. The increasing abundance of relatively small fractures doubtlessly accounts for this decrease in the arithmetic mean velocity. The range over which the velocities are distributed increases with increasing $\sigma_{\ln 2b}$, as shown by the increasing sample standard deviation S_v for the three cases. The coefficient of skewness decreases with increasing $\sigma_{\ln 2b}$, and the velocities more nearly approach a lognormal distribution in the case of $\sigma_{\ln 2b}$.

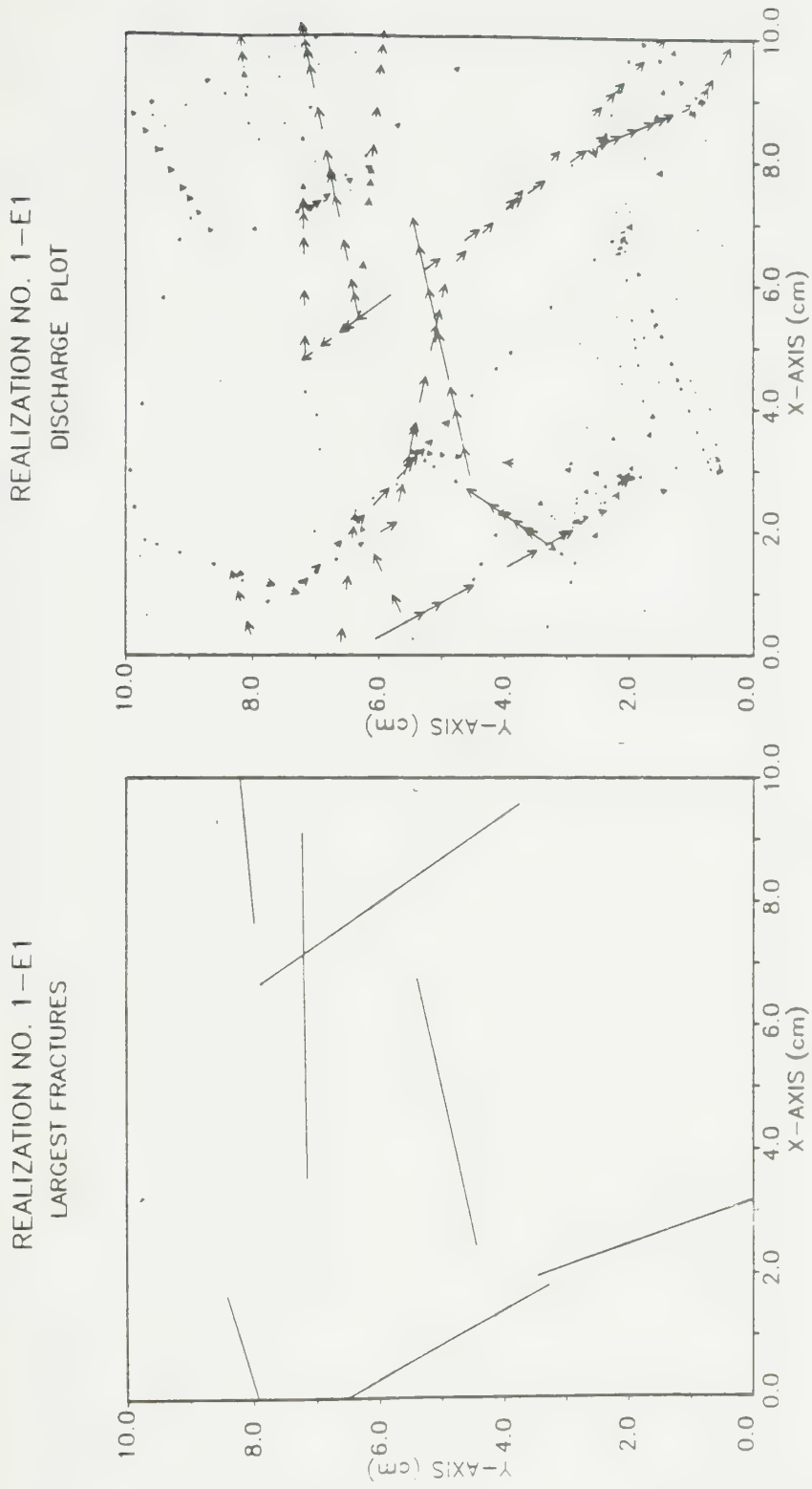


Figure 12: Comparison of discharge distribution with position of largest fractures. Fractures shown comprise largest 10% in network based on their aperture. Largest vector represents a discharge of 2.3×10^{-8} l/sec.

= 0.8. Schwartz et al. (1983) found that longitudinal macroscopic dispersion increases as the standard deviation in the velocity increases. If this is true for the present network of non-orthogonal fractures, the longitudinal macroscopic dispersion coefficient D_L should increase with $\sigma_{1n}^2 b$.

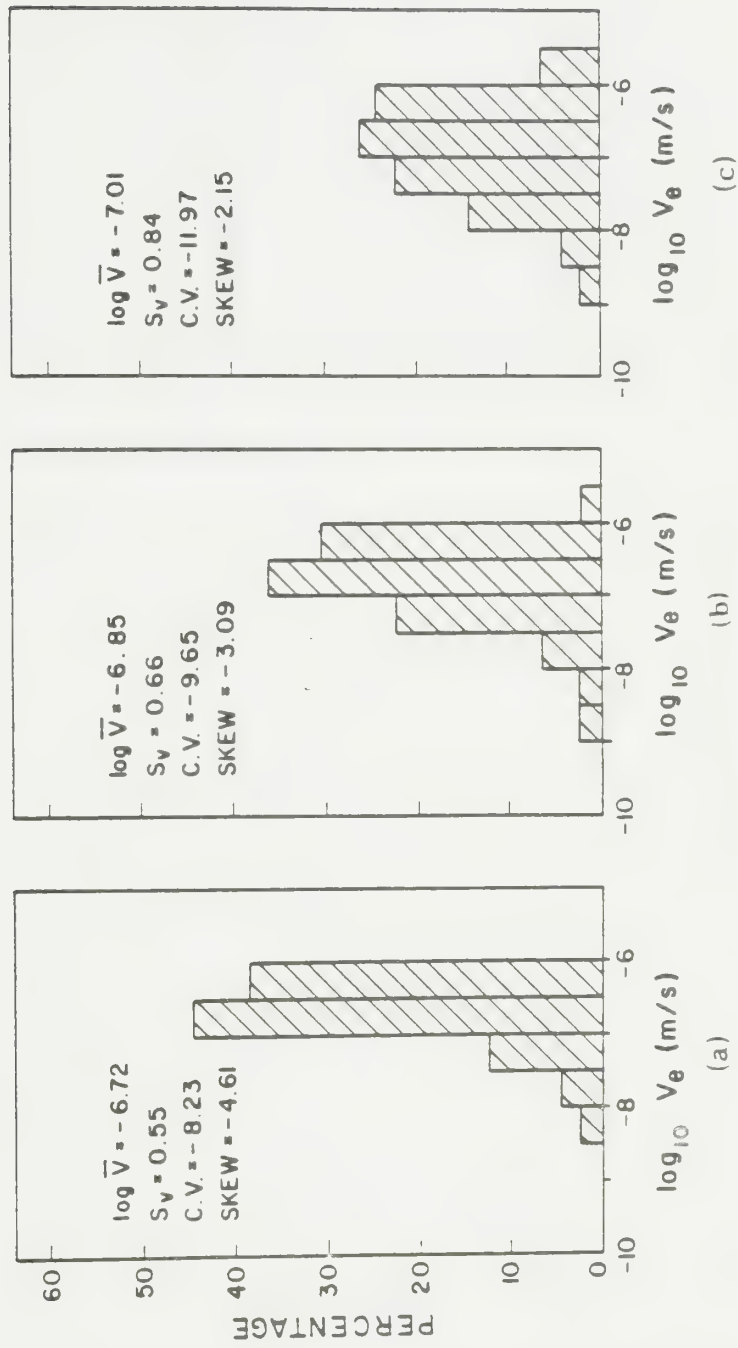


Figure 13: Histograms showing velocity distributions for three values of $\sigma_{\ln 2b}$. (a) $\sigma_{\ln 2b} = 0.8$; (b) $\sigma_{\ln 2b} = 0.4$; (c) $\sigma_{\ln 2b} = 0.0$.

4.1.2 Transport Properties

Although increasing the variability in the fracture apertures had a relatively minor effect on the overall hydraulic conductivity of the network, as shown on Figure 8, it can have a major impact on the spatial distribution of a tracer during transport through the network. Contour plots showing the distribution of the tracer in the network at three different times are shown on Figure 14 (a), (b), and (c). Again, contours shown within the intact blocks have no physical significance since the transport simulation does not include diffusion to the matrix. For the equal aperture case (Figure 14(a)), the tracer appears to be moving through the network at a relatively uniform rate.

In the non-uniform aperture cases, however, transport becomes increasingly dominated by a few high-velocity pathways which, however, do not necessarily occupy the largest fractures (Figures 14(b) and (c)). Clearly it would be difficult to accurately predict the spatial distribution of contaminants in such a system using a continuum approach unless the location of the pathways were already known. These diagrams serve as a graphical illustration of difficulties that may be encountered in groundwater monitoring in fractured media; the results suggest that sampling points should not just be confined to the largest fractures, but should also be installed in medium-sized features to increase the likelihood of intercepting contaminants.

Macroscopic breakthrough curves developed from the 'observation' points are shown on Figure 15. These curves might represent the averaged concentration that would be observed in a fully-screened well in the absence of pumping. As shown, these breakthrough curves are surprisingly similar; despite the preferential travel of the tracer in a few pathways, the lack of domination of the discharge by those fractures creates an averaging effect that counterbalances the spatial

REALIZATION NO. 1-A1
CONCENTRATION DISTRIBUTION

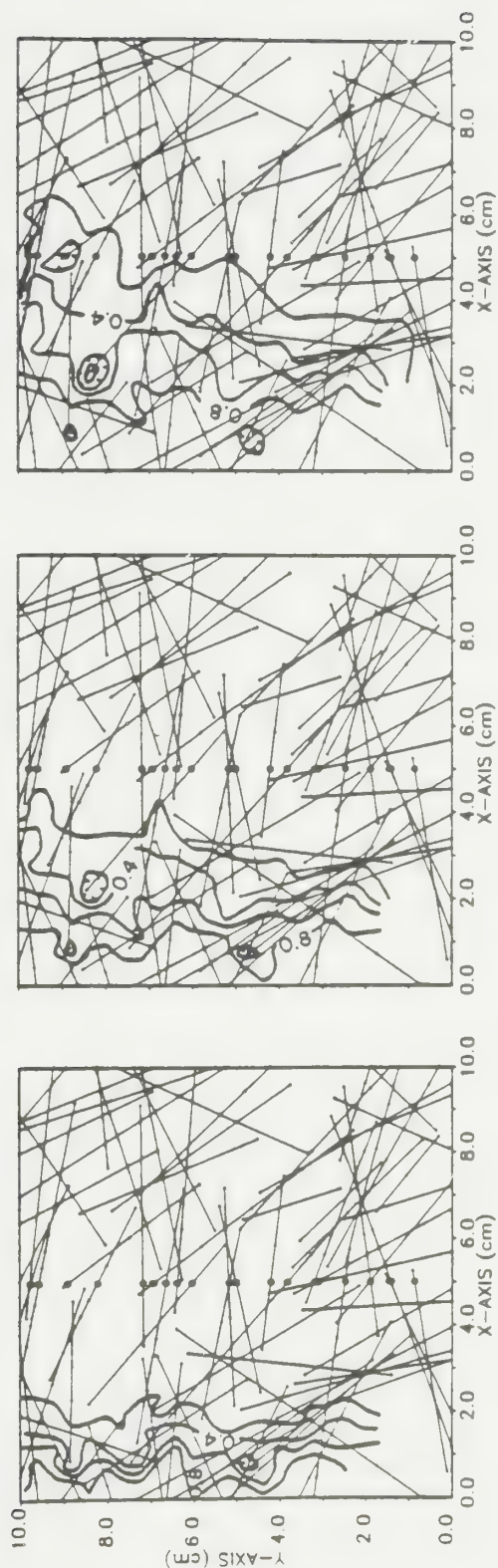


Figure 14:

Concentration distributions with changing $\sigma_{ln} 2b$.

(a) $\sigma_{ln} 2b = 0.0$ case. Results are shown at 0.5, 1.0, and 1.5 days

REALIZATION NO. 1-C1
CONCENTRATION DISTRIBUTION

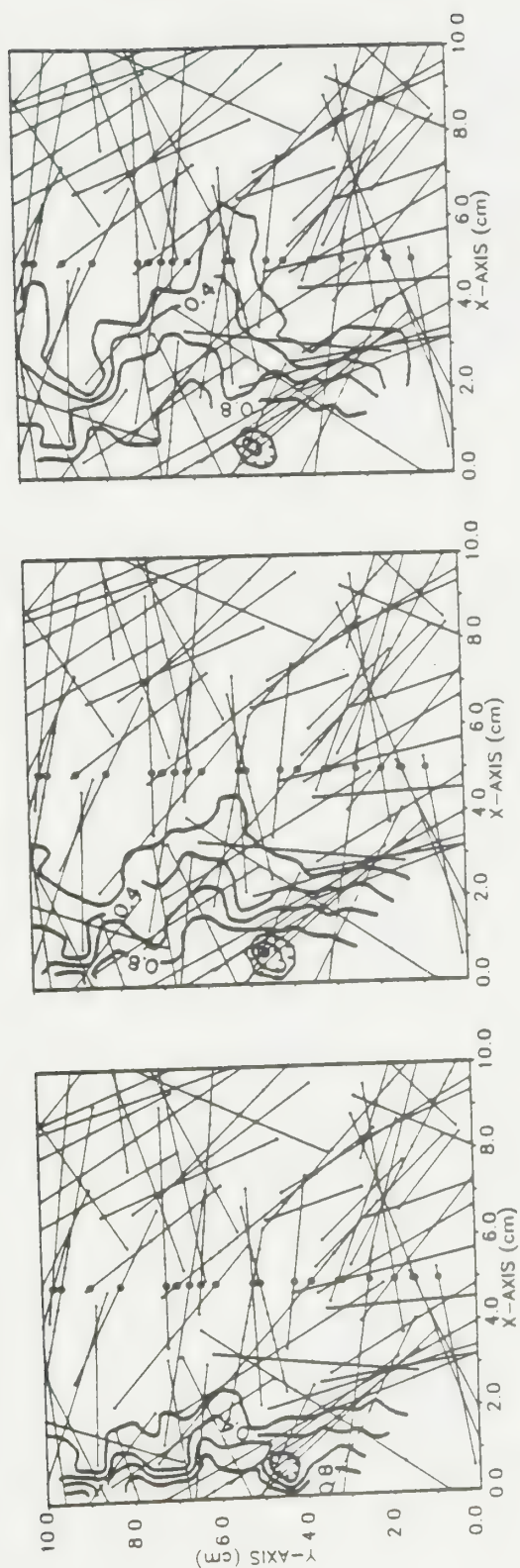


Figure 14: Concentration distributions with changing $\sigma_{\ln 2b}$
(b) $\sigma_{\ln 2b} = 0.4$ case. Results are shown at 0.5, 1.0, and 1.5 days

REALIZATION NO. 1-E1
CONCENTRATION DISTRIBUTION

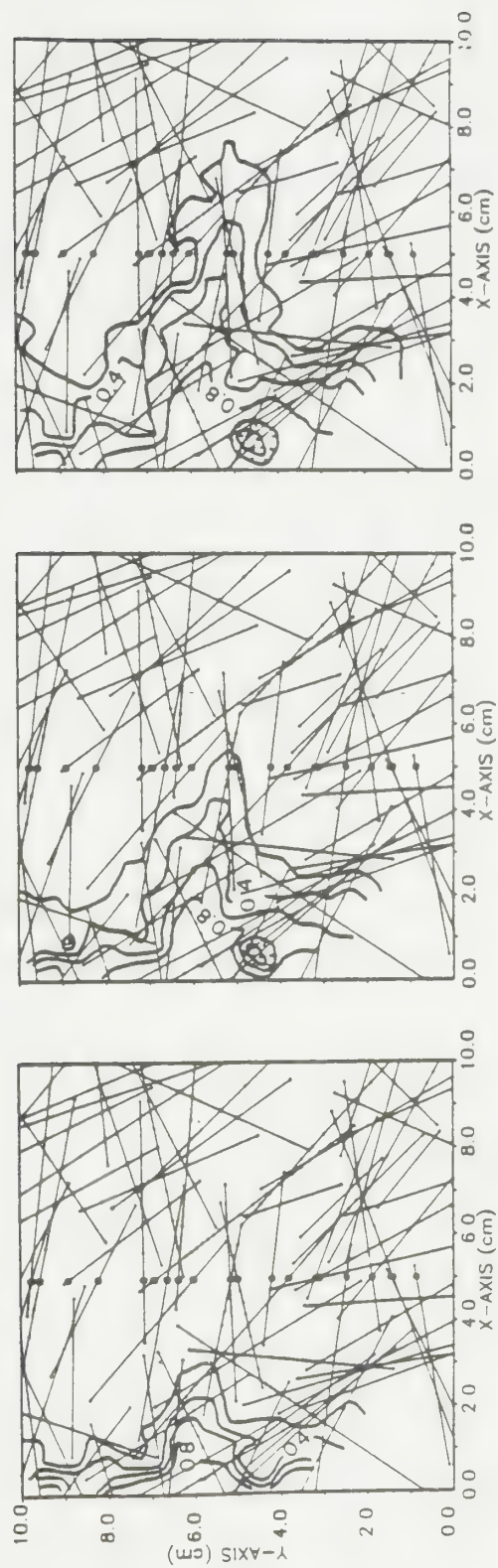


Figure 14:

Concentration distributions with changing $\sigma_{ln} 2b$

(c) $\sigma_{ln} 2b = 0.8$ case. Results are shown at 0.5, 1.0 and 1.5 days

localization of the tracer zone. Smith and Schwartz (1984) also found that introducing a variable fracture aperture had very little impact on the mean arrival time distribution of a tracer in a fracture network. Apparently the variability of fracture apertures has a secondary effect with respect to the macroscopic dispersion parameter, although it can influence the hydraulic behavior of the fracture network and the local distribution of contaminants in the system.

The breakthrough curves shown are asymmetrical, with long tails asymptotically approaching a relative concentration of 1. Part of this is undoubtedly due to the averaging technique used. Part may also be the result of mass being transferred through the network at late times by diffusion to deadend fracture segments and relatively immobile fluid regions (regions in which the fracture discharges are insignificant). Using the ordinary and weighted methods of moments previously described, the average travel time and effective macroscopic dispersion coefficient were calculated. Figure 16 compares the numerical results obtained for $\sigma_{ln} 2b = 0.40$ with the instantaneous response obtained by differentiating the breakthrough curve, and also shows results obtained from an analytical solution (Ogata and Banks, 1961) using the calculated value of $(v_x)_{tr}$ and D_L . The fit is not perfect, particularly in the tail of the data, but neither is it much worse than the fit to an analytical solution to the dispersion model shown in Figure 5. These results suggest that it may in fact be possible to at least approximate macroscopic dispersion in fractured media as a Fickian process under certain conditions. Whether the appropriate dispersion coefficient is constant or varies with distance remains to be demonstrated, and uncertainties introduced in actually predicting the location of zones of contamination may impose severe restrictions on the applicability of a continuum concept to the transport of contaminants in fractured media. Comparison of Figure 15 with the concentra-

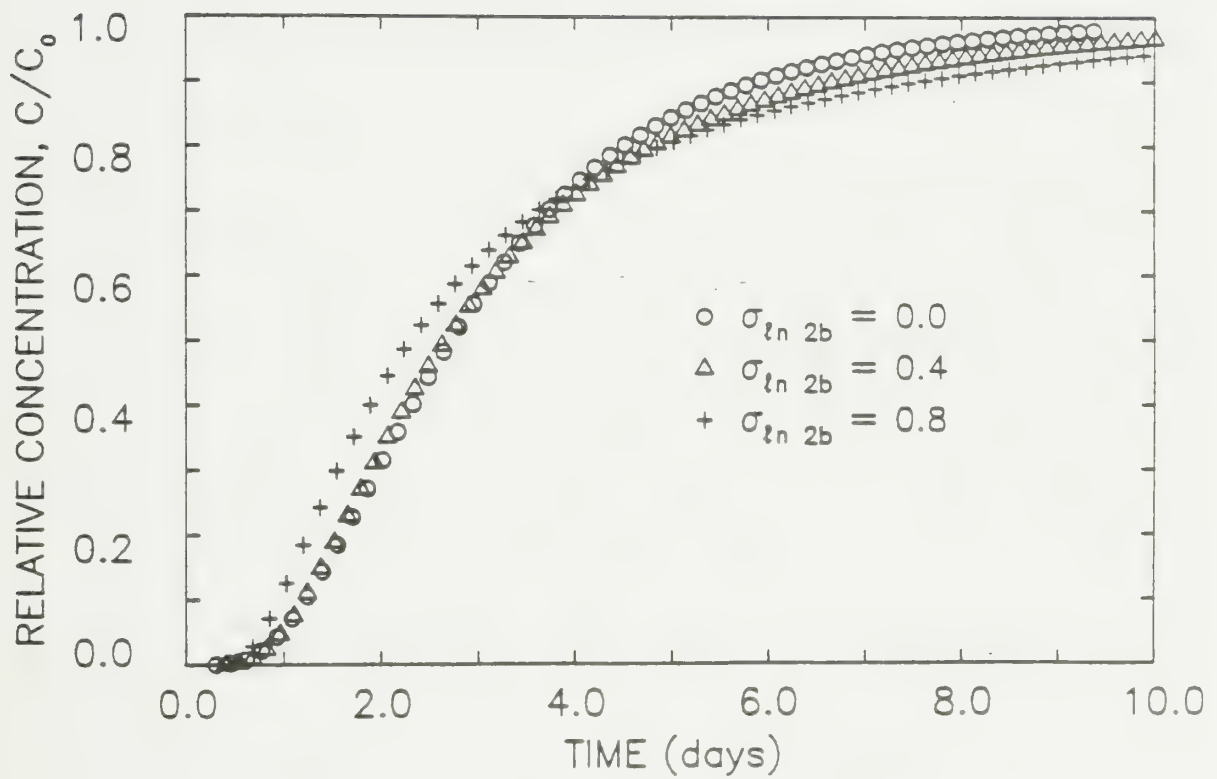


Figure 15: Macroscopic breakthrough curves for three values of $\sigma_{\ln 2b}$

tion contours shown on Figure 14 demonstrates that a contaminant may reach a relative concentration of 1 on a local scale long before it reaches a high relative concentration on a macroscopic scale. Fully-screened wells may give an overly optimistic picture of the extent of spread of a contaminant at a site.

The problem of how to actually predict the correct velocity and dispersion coefficient to use as input to a continuum model still remains. Figure 17 presents a comparison of the velocities calculated using the different approaches previously described with the actual velocity of the center of mass of the tracer. As shown, all of the predicted techniques overestimated the actual rate of travel of the center of mass of the tracer except for the arithmetic mean velocity, which underestimated it. Both the weighted approach and the effective velocity approach predicted on the basis of the known bulk hydraulic conductivity and known effective porosity were able to correctly predict changes in the actual travel time with changing aperture variability, and seemed to be closely related to the tracer velocity. The effective velocity approach may be severely limited owing to difficulties involved in accurately determining the effective porosity.

The weighted approach may be infeasible to apply to a real situation owing to the necessity for accurate values for the statistical parameters describing the geometry of the fracture network. In addition, the reproducibility of values determined with either the weighted or the effective velocity approach with changes in the details of fracture interconnection has not been established. Although Schwartz et al. (1983) found a relatively small variation in the equivalent hydraulic conductivity of a fracture network with successive realizations, this may be a result of assuming uniform apertures; Parsons (1966) found that the larger the standard deviation of the aperture distribution, the larger the standard deviation in the equivalent hydraulic conductivity for different realizations.

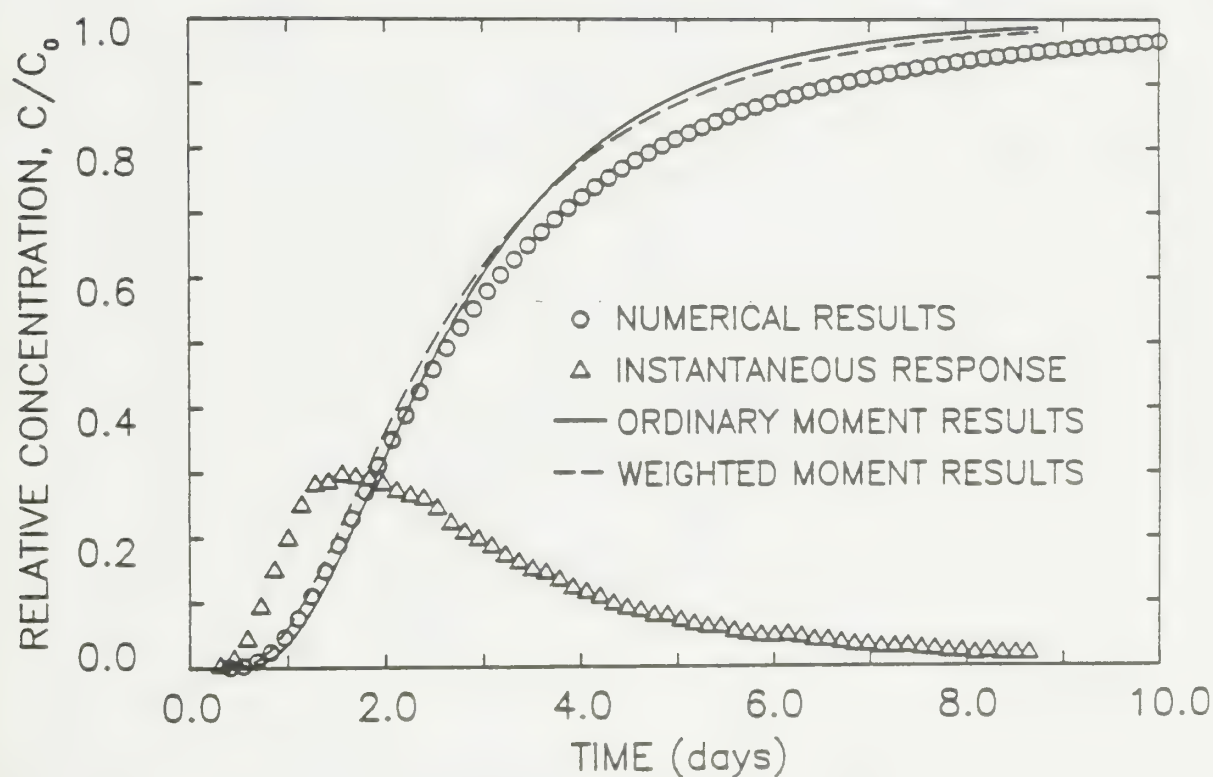


Figure 16:

Comparison of macroscopic breakthrough curve with dispersion model. $\sigma_{\ln 2b} = 0.4$. Breakthrough curve was truncated at a relative concentration of 0.95 for moment calculations.

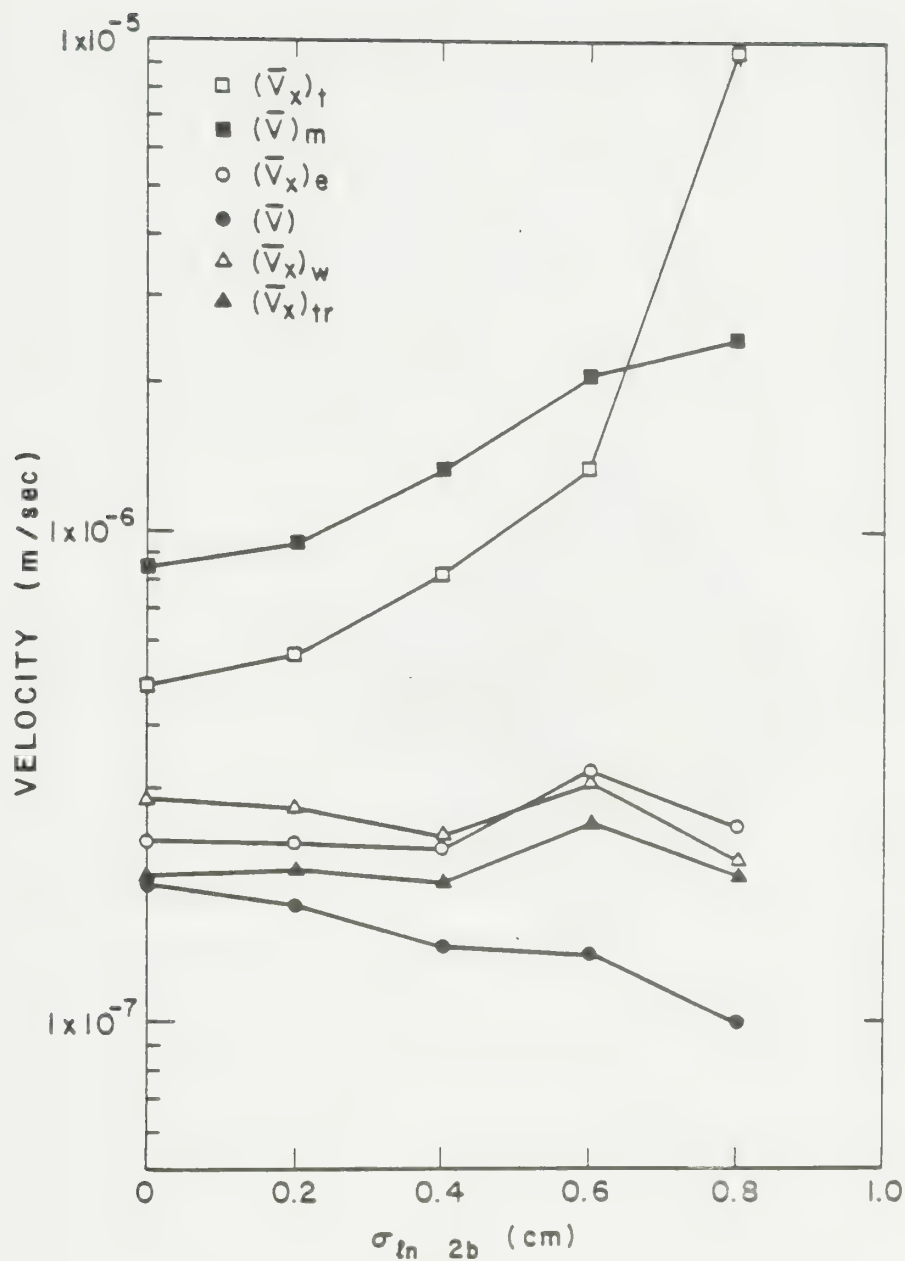


Figure 17:

Comparison of velocities obtained using several approaches for different values of $\sigma_{\ln 2b}$. $(v_x)_t$ calculated from equation (16); $(v)_m$ is maximum velocity in network; $(v_x)_e$ is calculated from bulk $(K_x)_e$ and n_e ; (v) is arithmetic mean; $(v_x)_w$ is weighted average; $(v_x)_{tr}$ is travel velocity of center of mass.

Comparisons made on the basis of a large number of realizations may be very useful in indicating the relationship between either the effective or the weighted velocity and the mean residence time of a tracer.

Table 2 shows a comparison of the macroscopic transport parameters for different values of $\sigma_{\ln 2b}$. The effective velocity does not show any consistent trend with increasing fracture aperture variability, nor does the effective longitudinal dispersion coefficient. This is demonstrated on Figure 18. The skewness of the arrival time distribution S_k increases with increasing $\sigma_{\ln 2b}$, paralleling the trend in the standard deviation of the velocity distribution. This increasing skewness suggests that a Fickian model of dispersion may become somewhat less appropriate with larger values of $\sigma_{\ln 2b}$.

The dispersion coefficient predicted for parallel, noninteracting fractures increases without bound according to equations (7) and (8). This was not observed for the present case of intersecting fractures. Apparently, similar to the manner in which interactions between strata in porous media prevent the dispersion coefficient from reaching an infinite value and similar to the manner in which mixing introduced by molecular diffusion within a tube can actually diminish dispersion by decreasing the concentration difference over the channel, mixing introduced by interactions between fractures can limit macroscopically-observed dispersion. The observed macroscopic dispersion coefficient does not show any readily discernible relationship to the tracer velocity, as shown in Figure 18. It is not clear from these results whether the concept of dispersivity is applicable to transport in fractured media within this range of Peclet numbers. A better test might be to simulate flow through the same network under different hydraulic gradients, and observe the relationship between the dispersion coefficient and the tracer velocity.

Table 2

Effect of increasing variability in fracture aperture on macro-
scopic transport parameters

$(v_x)_{tr}$ and S_k computed using ordinary method of moments; D_L calculated using weighted method of moments. Breakthrough curve truncated at a relative concentration of 0.95 for computations.

| Computed value of parameter | Ln standard deviation of fracture aperture distribution | | | | |
|---|---|-----------------------|-----------------------|-----------------------|-----------------------|
| | 0.0 | 0.2 | 0.4 | 0.6 | 0.8 |
| $(v_x)_{tr}$ (m/day) | 1.72×10^{-2} | 1.76×10^{-2} | 1.66×10^{-2} | 2.22×10^{-2} | 1.72×10^{-2} |
| t_r/t_f | 1.2250 | 1.2138 | 1.2564 | 1.3284 | 1.2695 |
| D_L (m ² /day) | 1.92×10^{-4} | 1.71×10^{-4} | 1.80×10^{-4} | 2.41×10^{-4} | 2.26×10^{-4} |
| Predicted* D_L for parallel fractures | 0.0 | 7.66×10^{-5} | 3.72×10^{-4} | 1.79×10^{-3} | 5.14×10^{-3} |
| S_k | 0.7582 | 0.8757 | 1.0711 | 1.3060 | 1.4466 |

* Neretnieks (1983).

Finally, Table 2 shows the ratio of the tracer residence time to the residence time of the fluid determined by equation (23). If transport occurred uniformly through all the fractures, this ratio should be equal to 1 (or, more precisely, to 0.95 owing to truncation of the breakthrough curve). If transport only occurred within a small fraction of the fractures, with no transfer of solute via diffusion to other fractures, this value should have been less than 1. Estimation of the tracer residence time t_r may be sensitive to errors in the calculation of the first moment; still, the results suggest that there is significant transfer of the tracer at late times by some mechanism. This is more pronounced in the cases with a higher value of $\sigma_{ln} 2b$, which were characterized by greater skewness, by a

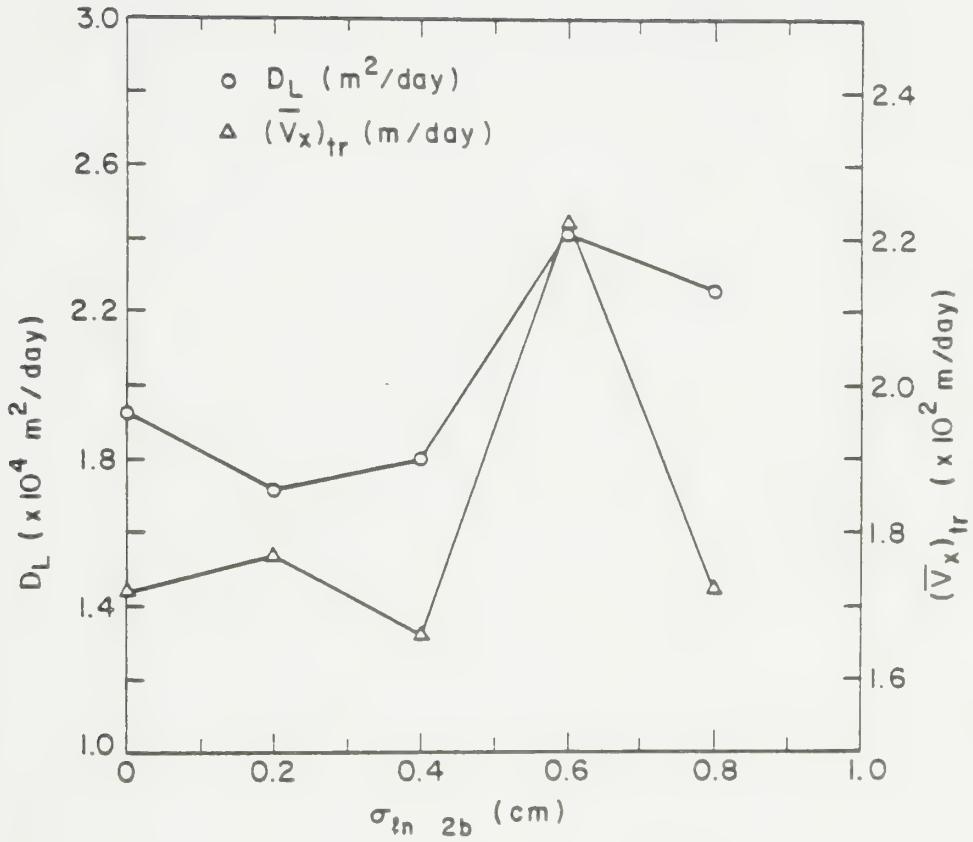


Figure 18: Effect of variability in fracture aperture on macroscopic dispersion and average transport velocity.

greater standard deviation in the velocity distribution and by a greater tendency of the tracer to occupy a few paths within the network.

4.2 Effect of Fracture Connectivity

The connectivity of a system of fractures depends on the length of the fracture, the fracture density, the size of the domain under consideration, and fracture orientation. None of these parameters alone can be used to uniquely define fracture connectivity. Because it depends on the interaction of several parameters, it is a difficult concept to quantify for natural systems, yet it may have a major impact on the hydraulic characteristics of a fractured medium.

For the present study, the connectivity of a fracture network was expressed as a 'fracture connectivity ratio', defined as the number of actual fracture intersections present within the simulation domain divided by the number of intersections that would have been present had the fractures all been of infinite length in comparison to the size of the domain. This ratio varies from zero, for parallel or otherwise nonintersecting fractures, to one for a perfectly interconnected network, and is computed by the fracture generation program.

To test the sensitivity of a fracture network to changes in fracture connectivity, five simulations were performed with different connectivity ratios. To minimize the number of variables between simulations, a network was initially generated in which the fracture lengths were assigned to the different fractures in increasing magnitude. Successive simulations used the same fracture locations, orientations, and apertures, but fracture lengths with a progressively greater mean value were generated to increase the connectivity ratio. So that flow paths established during one simulation would also be present for a greater degree of interconnection, fracture lengths were assigned each time in order of their mag-

nitude. Three of the networks are shown on Figure 19 (a), (b), and (c). The input parameters and boundary conditions were the same as those used in the previous simulations, with minor modifications. The fracture aperture standard deviation $\sigma_{ln 2b}$ was 0.6; to reduce computing costs associated with a large number of nodes, only 25 fractures were generated for each set instead of 40, and the hydraulic gradient was reduced from 0.04 to 0.004. The connectivity ratios for the five simulations varied from 0.24 to 0.86. For comparison, the connectivity ratio for the simulations described in Section 4.1 was 0.22.

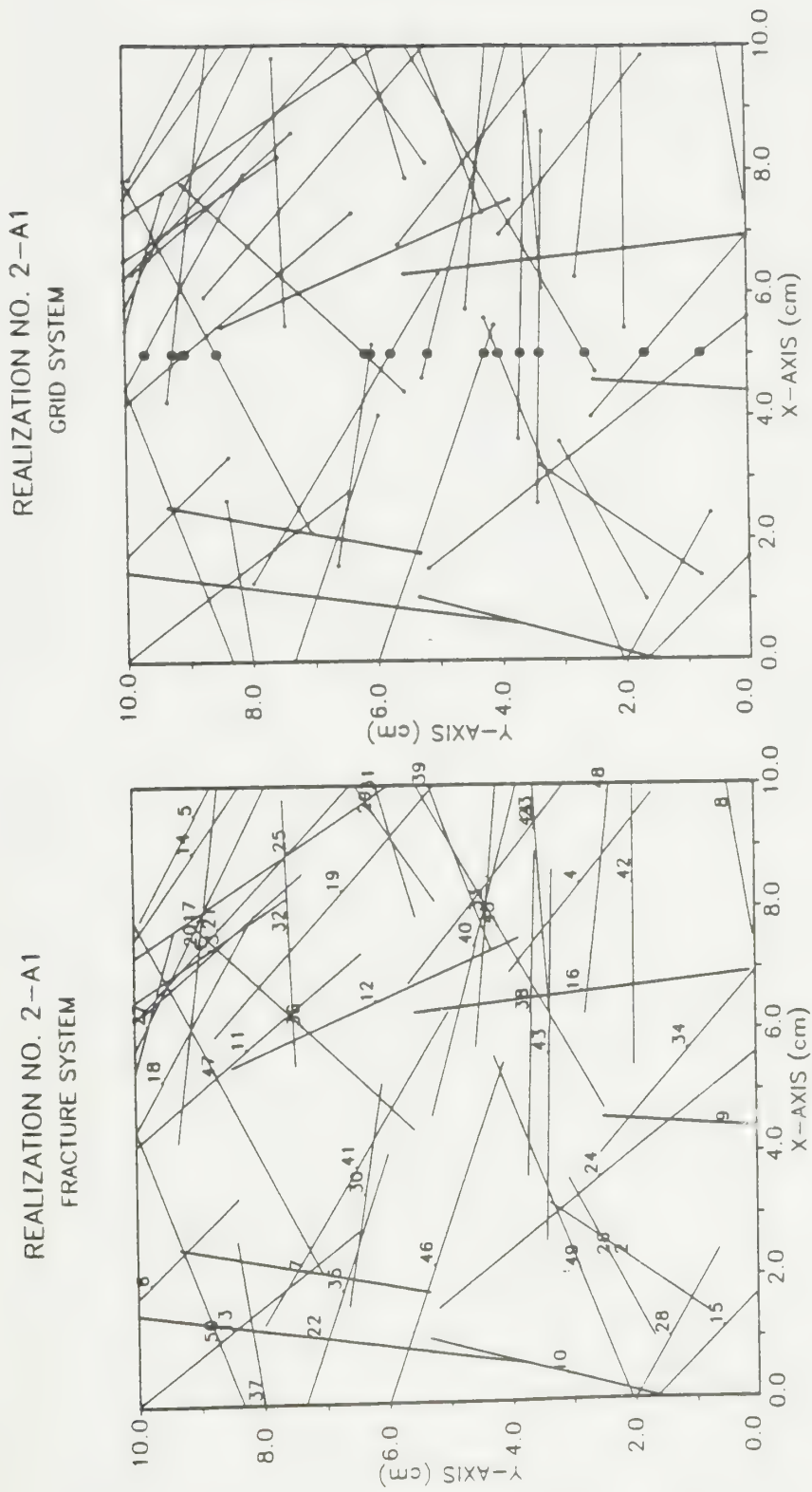


Figure 19: Fracture networks showing changes in connectivity.

(a) Fracture connectivity ratio = 0.24

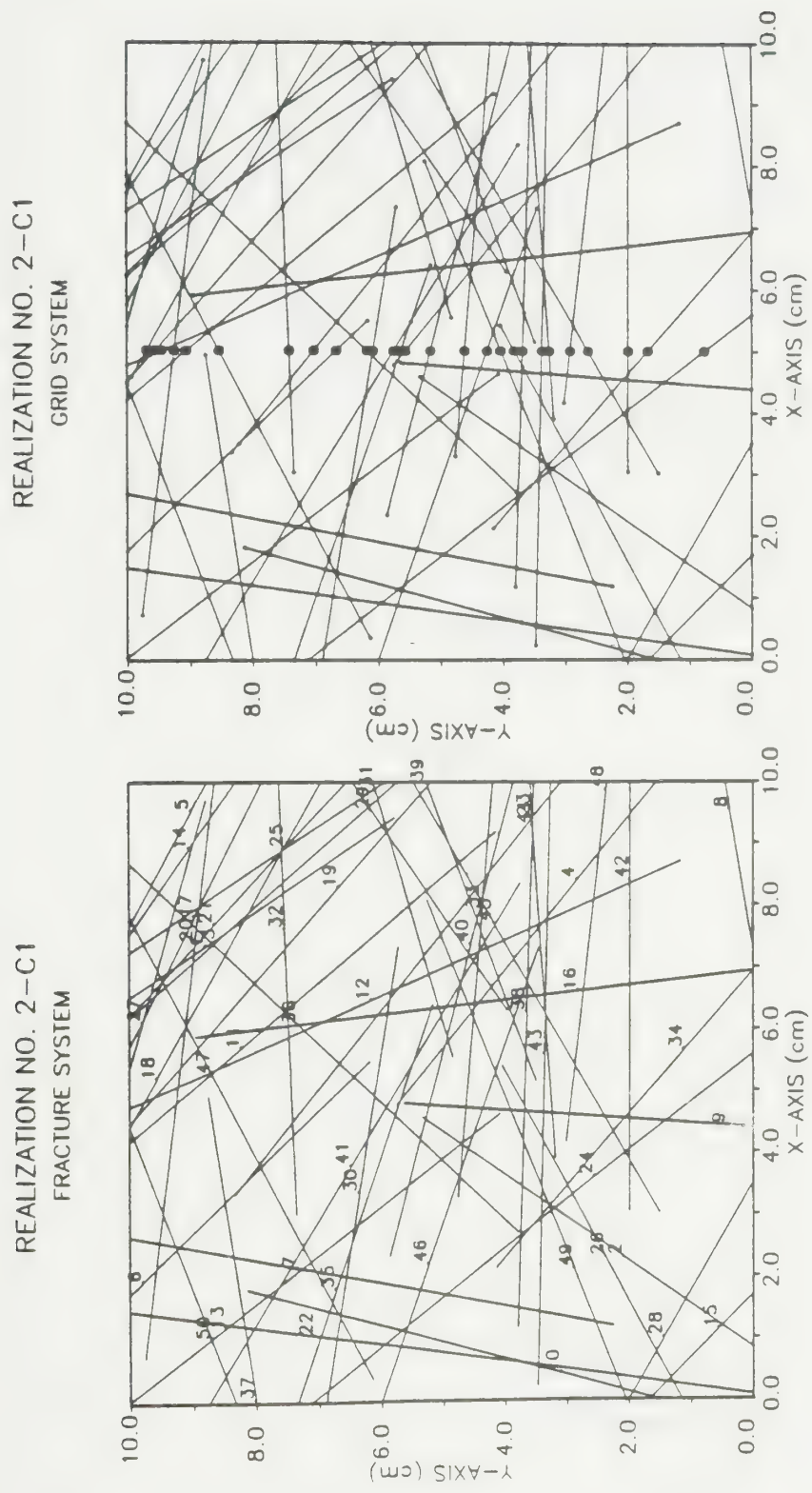
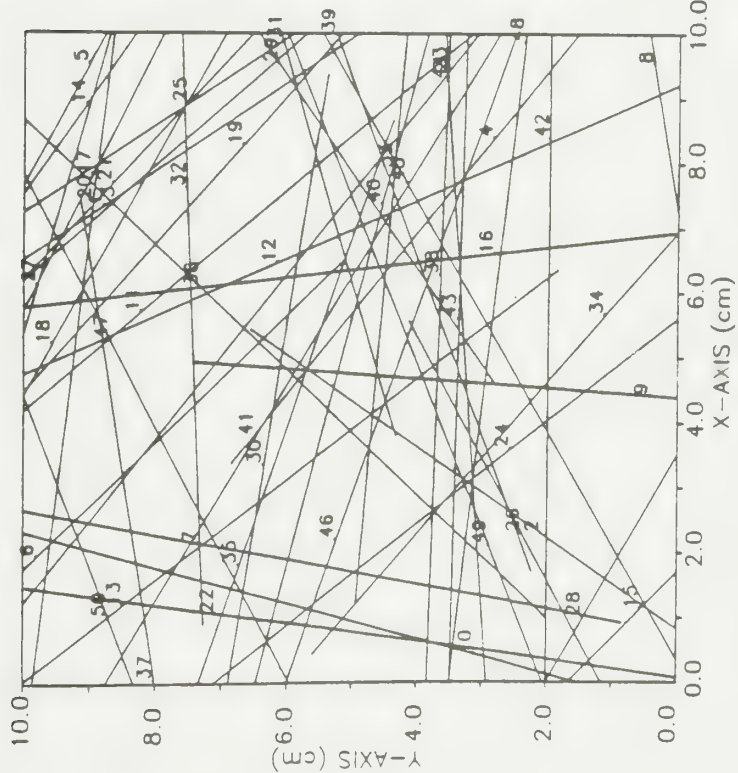


Figure 19: Fracture networks showing changes in connectivity.

(b) Fracture connectivity ratio = 0.56

REALIZATION NO. 2-E1
FRACTURE SYSTEM



REALIZATION NO. 2-E1
GRID SYSTEM

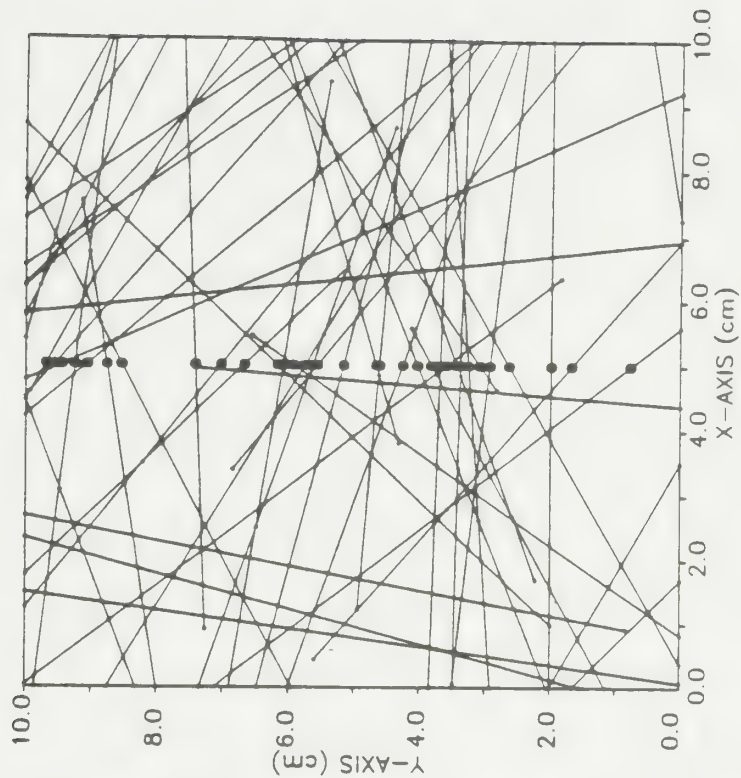


Figure 19: Fracture networks showing changes in connectivity.

(c) Fracture connectivity ratio = 0.86

4.2.1 Hydraulic Properties

The hydraulic conductivity of a network of finite fractures is less than that of a network of infinite fractures; in the limiting case, a fracture which neither intersects any other fracture nor the boundaries of the flow domain does not contribute to flow. Thus, as the degree of interconnection in a fracture network increases, the effective hydraulic conductivity should increase. This effect is shown in Figure 20. With the network with the least degree of interconnection, the bulk hydraulic conductivity is nearly two orders of magnitude less than that predicted by Snow's relationship (equation 14); as the degree of interconnection increases, the effective hydraulic conductivity rapidly approaches the theoretical value. The results shown in Figure 20 emphasize the errors that could result from estimating the mean aperture of fractures in a poorly-connected system using models developed on the assumption of perfect interconnection.

As in the case of variations in fracture aperture, variations in fracture connectivity significantly influence the hydraulic head distribution within a fracture network. Figure 21 (a), (b), and (c) illustrates hydraulic head contours for three cases with different connectivity ratios; the hydraulic head distribution becomes markedly more uniform as the degree of interconnection increases. This is also shown on Figure 22, which presents hydraulic head profiles for the same three cases at a constant distance from the inflow boundary. The extent to which a fractured medium can be represented as an equivalent porous medium is clearly sensitive to the degree of interconnection, as suggested by Long et al. (1982).

Figure 21 (a), (b), and (c) also illustrates the velocity profiles within the three networks. In none of the cases are the velocity vectors evenly distributed throughout the network; rather, there is a tendency for flow to occupy a few preferred pathways. These pathways become much better-defined as the degree of

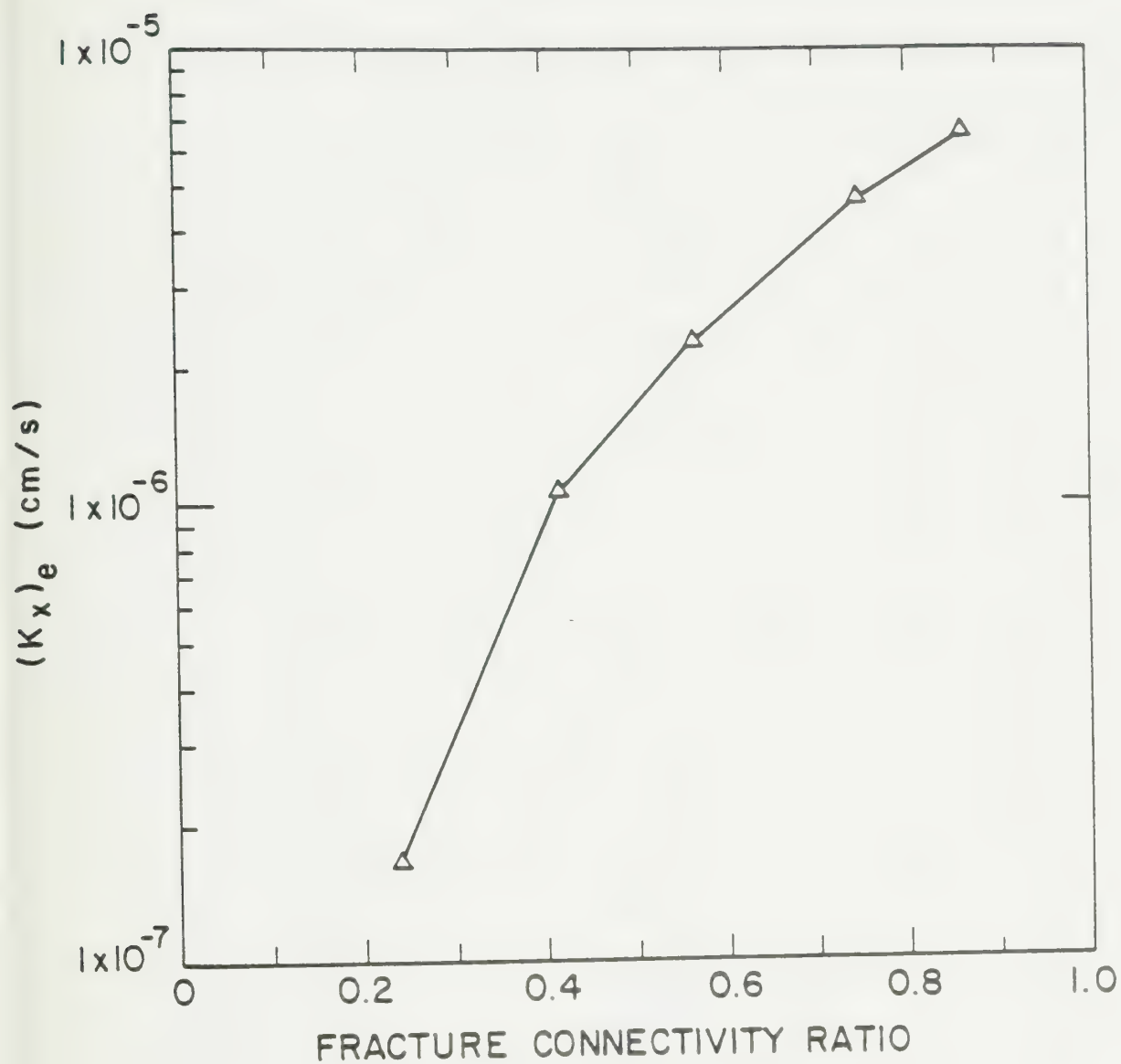
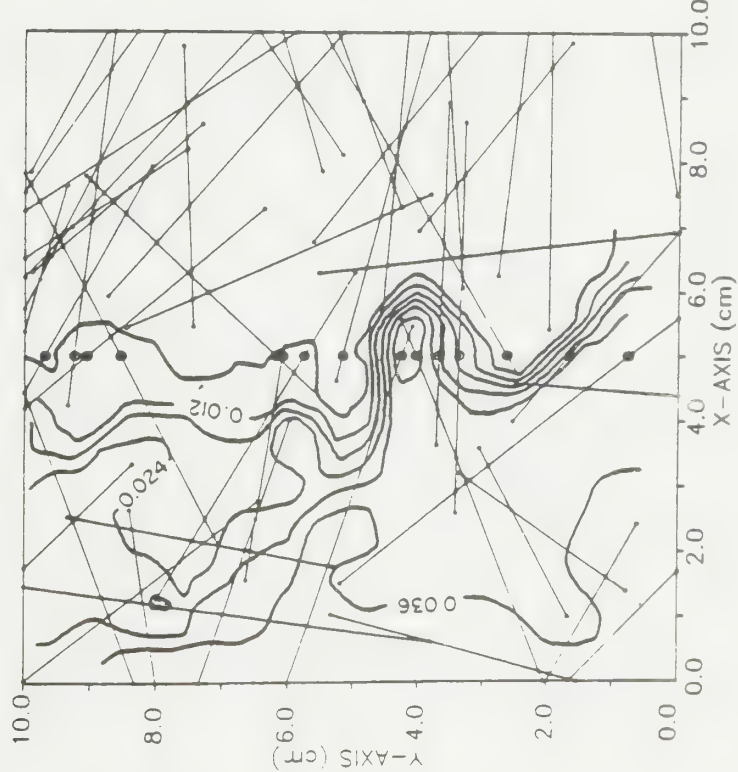


Figure 20:

Change in bulk hydraulic conductivity of fracture network with increasing connectivity. $(K_x)_t$ calculated from equation (14) for perfectly interconnected network = 8.92×10^{-6} cm/s.

REALIZATION NO. 2-A1
HEAD DISTRIBUTION



REALIZATION NO. 2-A1
VELOCITY PLOT

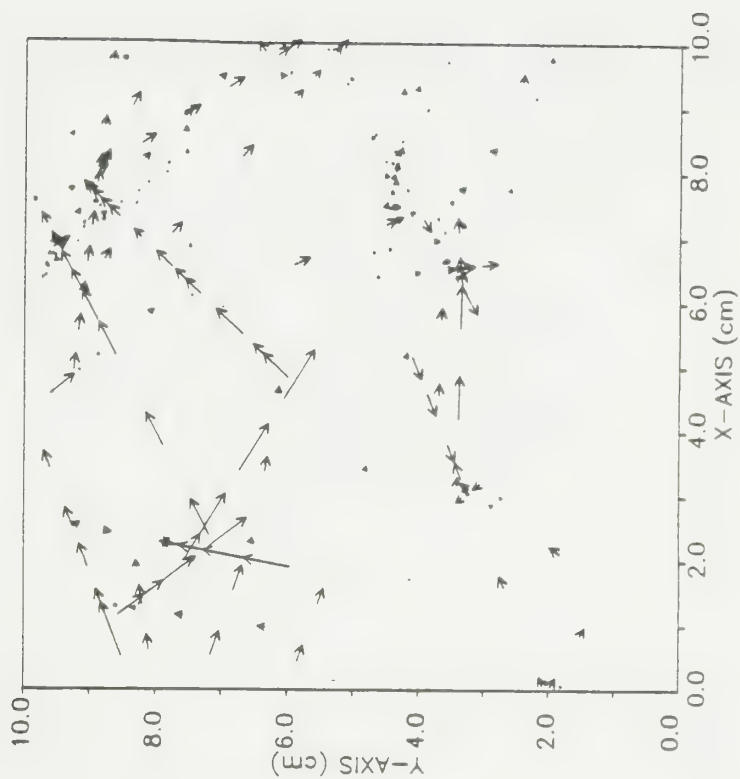
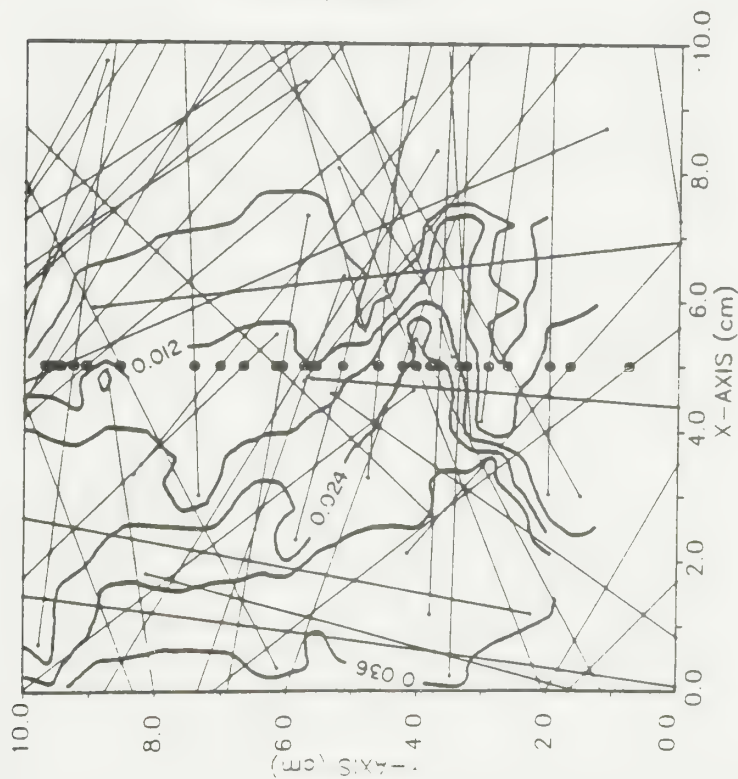


Figure 21: Hydraulic head contours and velocity plots for three different connectivities.

(a) Fracture connectivity ratio = 0.24. One unit on the velocity plot represents 8.0×10^{-3} m/s

REALIZATION NO. 2-C1
HEAD DISTRIBUTION



REALIZATION NO. 2-C1
VELOCITY PLOT

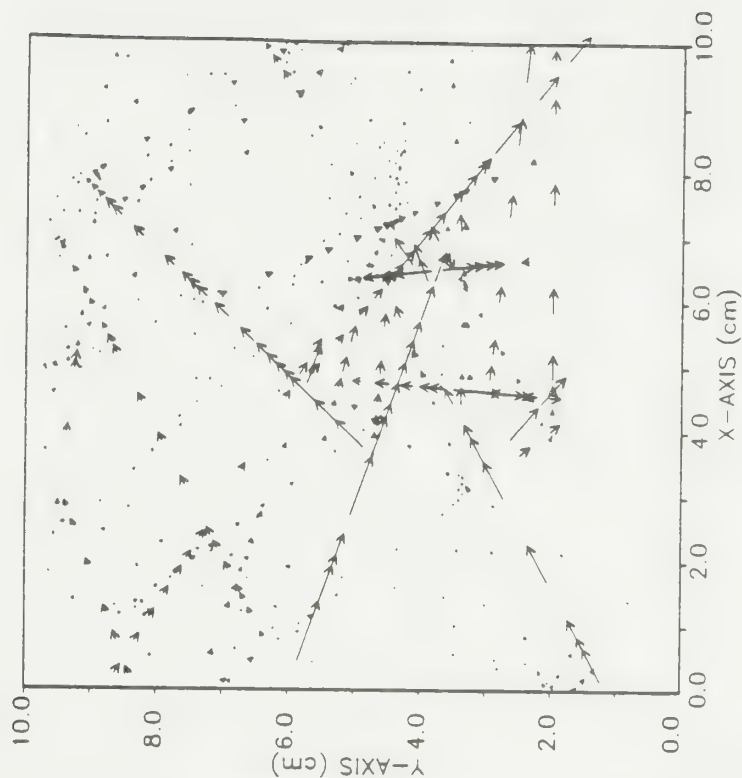


Figure 21: Hydraulic head contours and velocity plots for three different connectivities.
(b) Fracture connectivity ratio ≈ 0.56 . One unit on the velocity plot represents 4.2×10^{-7} m/s

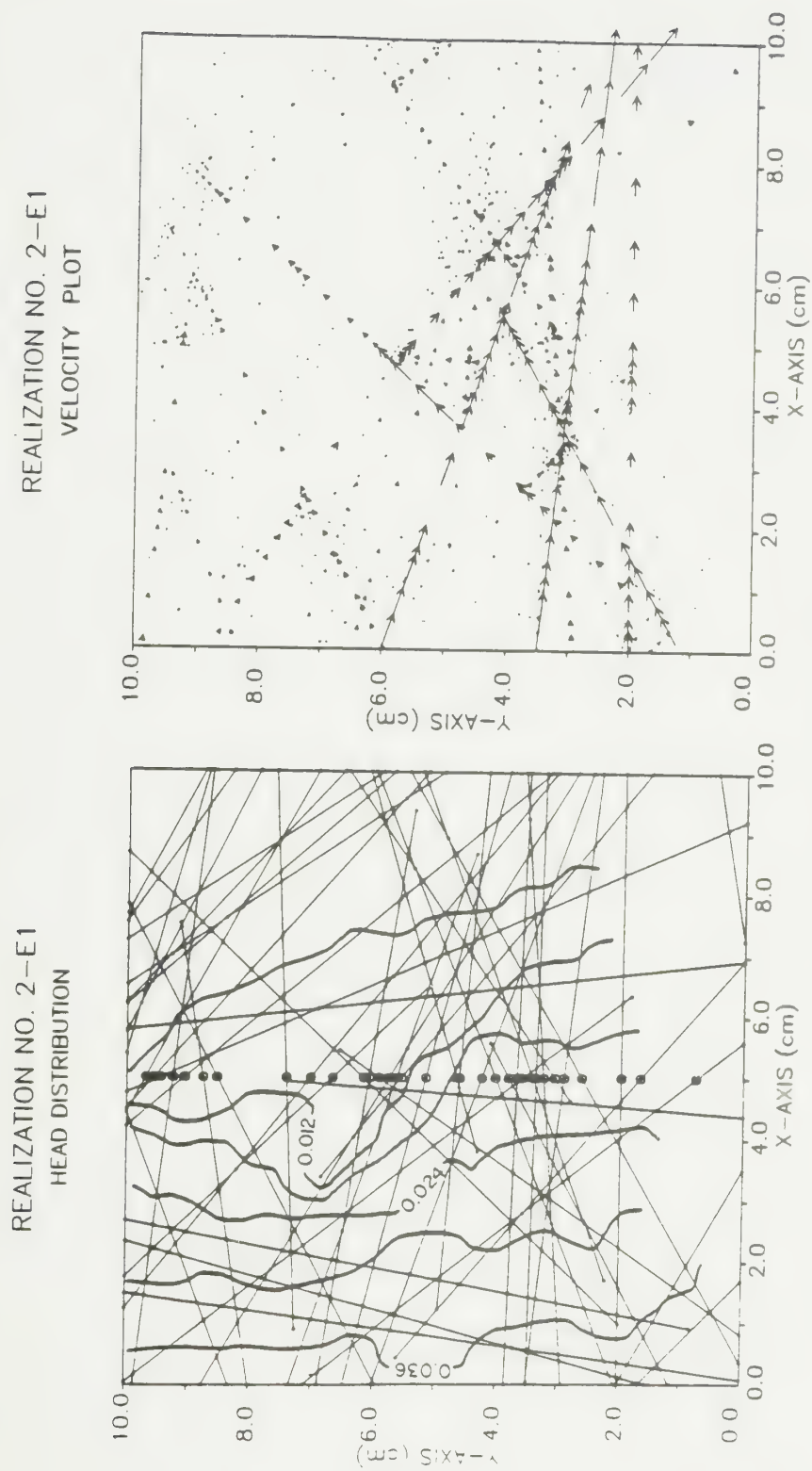


Figure 21: Hydraulic head contours and velocity plots for three different connectivities.
(c) Fracture connectivity ratio ≈ 0.86 . One unit on the velocity plot represents 7.8×10^{-7} m/s

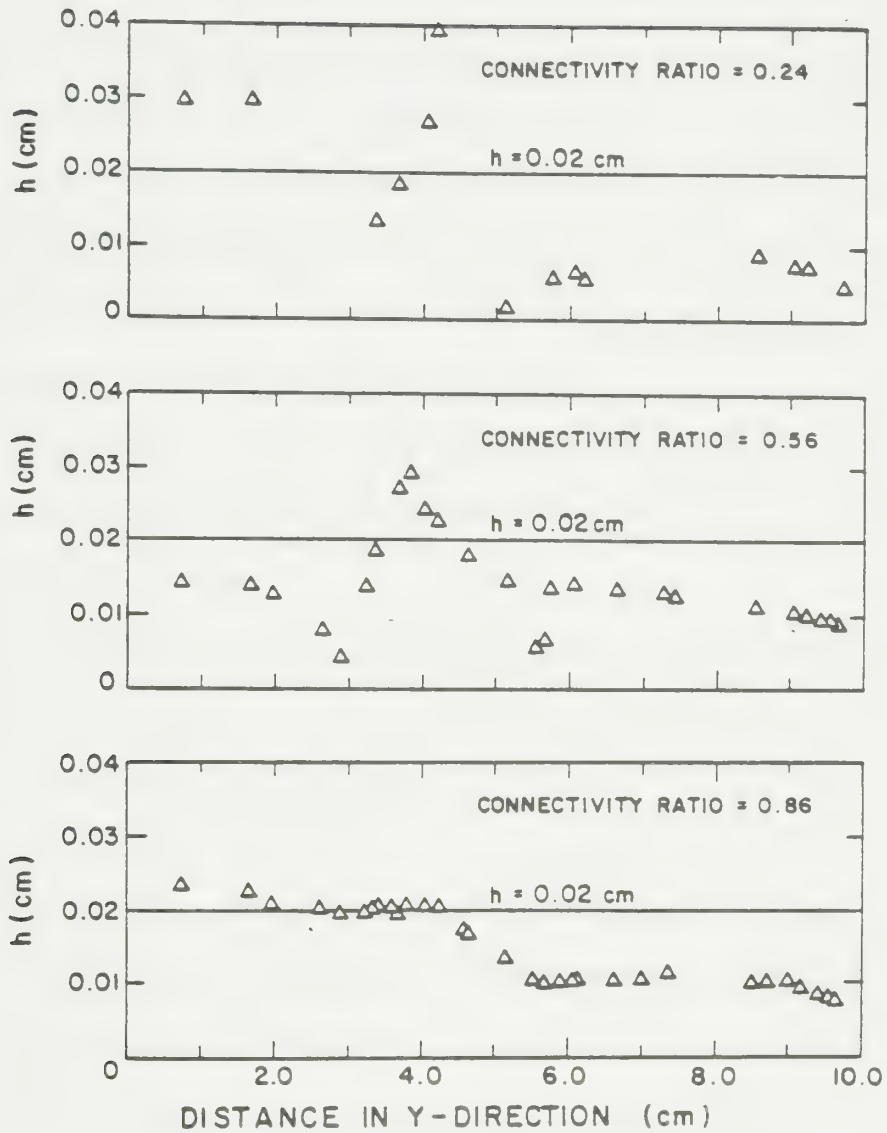


Figure 22: Hydraulic head profiles at $x = 5.0$ cm for three different connectivities

interconnection increases. For the least-interconnected case (Figure 21(a)), these pathways are markedly different from the best-interconnected case (Figure 21(c)). In the latter case, high-velocity regions are associated with the largest fractures. The highest velocities are not associated with the largest fractures in Figure 21(a), however. Rather, they are associated with the medium- to large-sized fractures that happen to lie within the pathway that is least choked off by flow being forced through small fractures. The same observation - that the highest velocities may occur in medium-sized features and not necessarily in the large features - was noted by Simon and Kelsey (1971) in miscible-displacement simulations performed using a capillary tube network model. There does not appear to be any unique correlation between flow velocity and aperture size in a network of finite fractures.

Figure 23 (a) and (b) further depicts this point by comparing the distribution of discharges for two of these cases with the position of the largest fractures. In the poorly-interconnected case, there is little relationship between the fracture aperture and the flow contained within it, whereas in Figure 23 (b), there is a close correspondence between the largest apertures and the preferred flow paths.

As the degree of interconnection increases, the largest fractures demonstrate a progressive tendency to dominate the flow in the system. Figure 24 illustrates the fraction of the total flow contained within the largest 10% of the fractures. The values increase from 12% for the poorly-interconnected case to 82% of the total flow for the well-interconnected case. In the last set of simulations, it was shown that the degree of domination of flow in a network by the largest fractures is only moderately sensitive to changes in $\sigma_{ln} \ 2b$; clearly this result is also dependent on the degree of interconnection. The sensitivity of the results to the vagaries of interconnection suggest that there may be a great deal of uncertainty

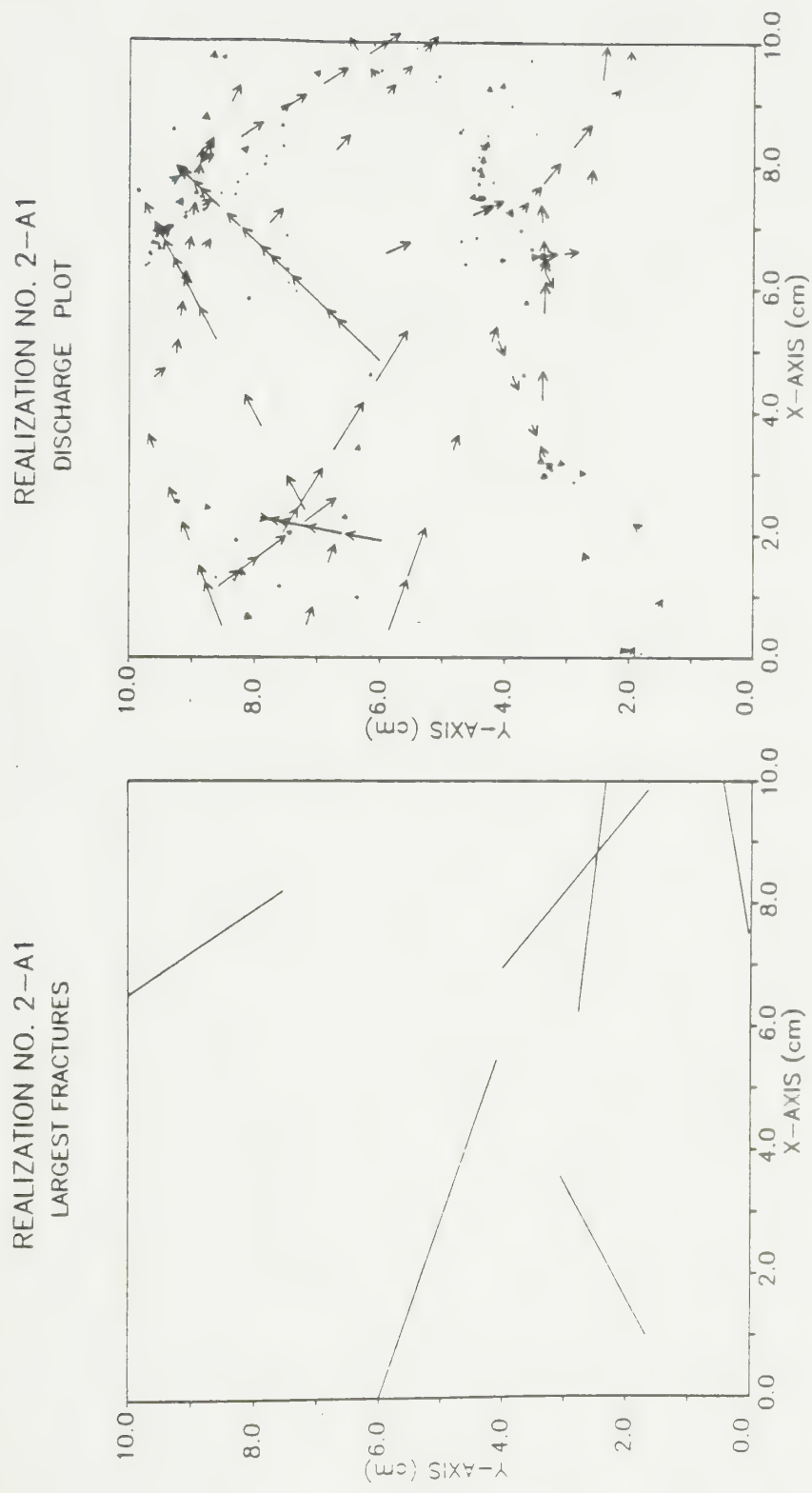
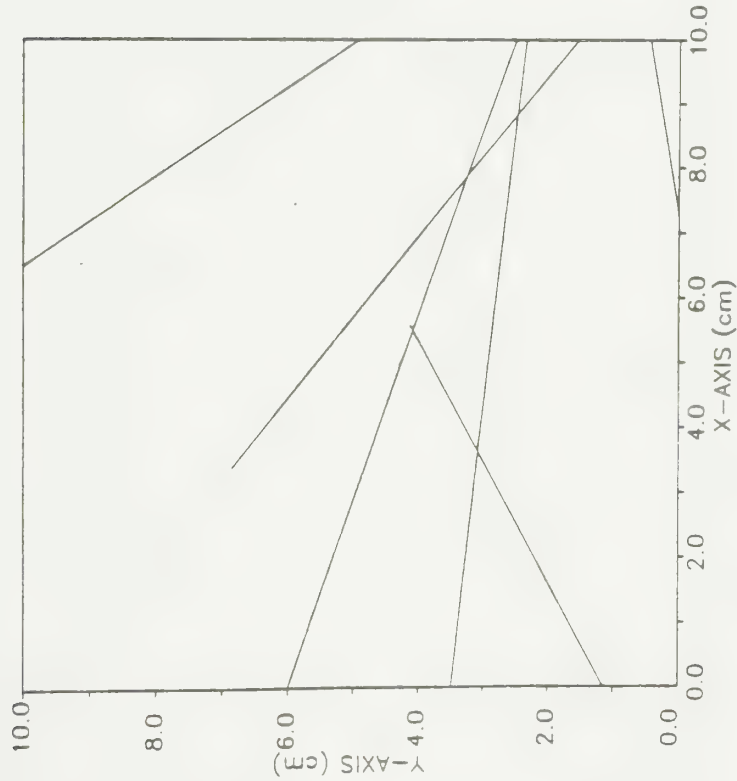


Figure 23: Discharge distributions for two different connectivities. Fractures shown comprise largest 10% in network based on their aperture

(a) Fracture connectivity ratio = 0.24; largest vector on the discharge plot represents 3.0×10^{-10} l/s

REALIZATION NO. 2-E1
LARGEST FRACTURES



REALIZATION NO. 2-E1
DISCHARGE PLOT

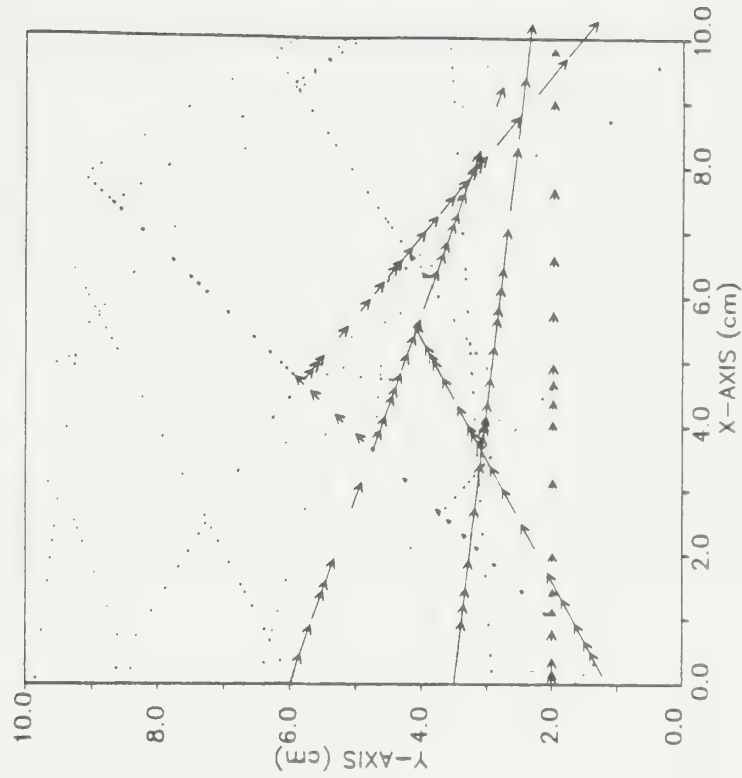


Figure 23:

Discharge distributions for two different connectivities.
Fractures shown comprise largest 10% in network based on their aperture

(b) Fracture connectivity ratio = 0.86; largest vector on the discharge plot represents $1.2 \times 10^{-8} \text{ l/s}$

surrounding the extent to which the largest fractures dominate flow in a real system. The results suggest that connectivity may be the most important single parameter controlling flow in discrete fracture networks.

Figure 25 presents histograms showing the distribution of flow velocities within fracture segments. The mean velocity increases by more than half an order of magnitude as the connectivity increases; the maximum velocity exhibits an even greater increase. The variability in flow velocity between adjacent fractures decreases as the network becomes better-interconnected as denoted by the decreasing standard deviation and decreasing absolute value of the coefficient of variation; if Schwartz et al.'s (1983) hypothesis is correct, this should cause the macroscopic dispersion coefficient to decrease with increasing connectivity.

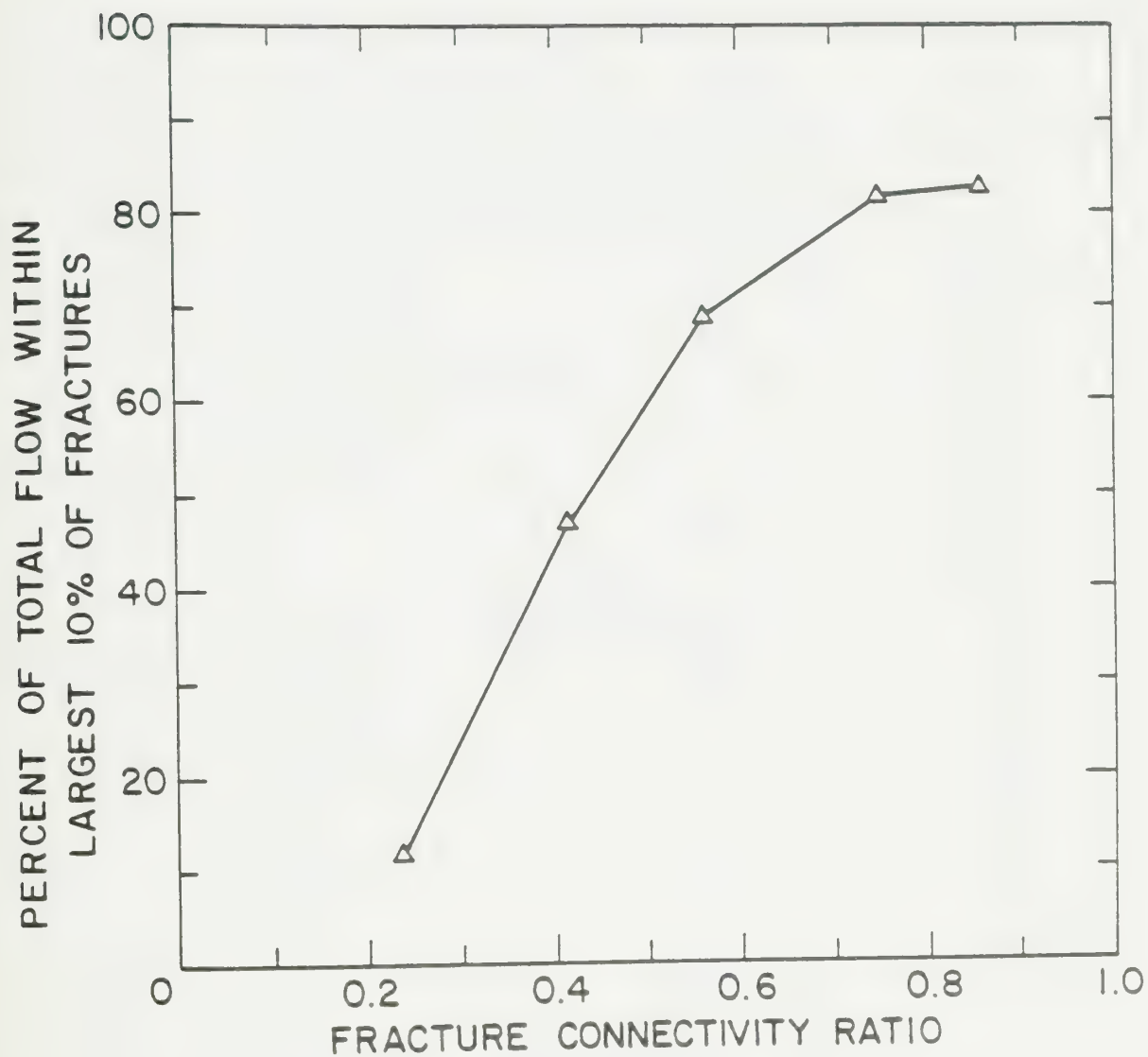


Figure 24: Impact of connectivity on domination of flow by largest fractures

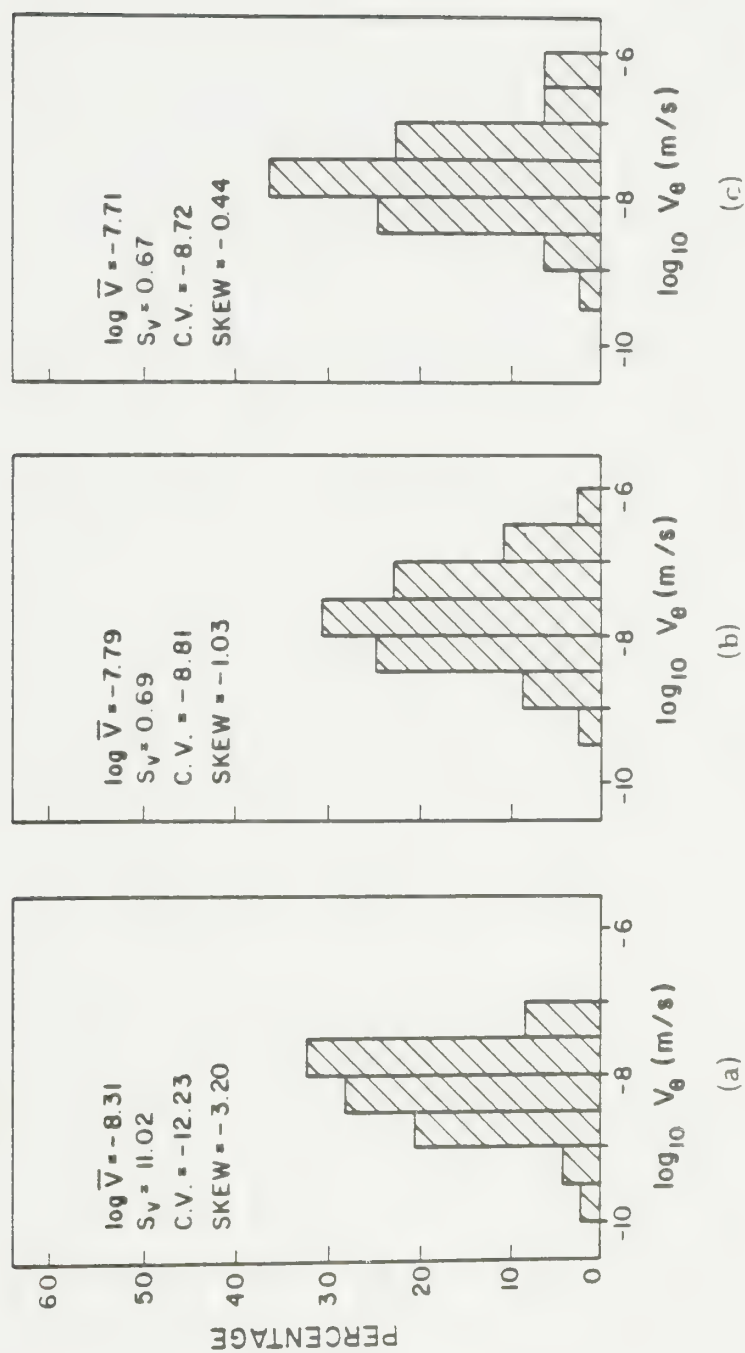


Figure 25: Histograms showing velocity distribution with changing connectivity. (a) Fracture connectivity ratio = 0.24 ; (b) Fracture connectivity ratio = 0.56 ; (c) Fracture connectivity ratio = 0.86.

4.2.2 Transport Properties

Concentration contours for three different fracture connectivity ratios are shown on Figure 26 (a), (b), and (c). Most apparent is that at any given time, the tracer has advanced much more rapidly through the better-interconnected networks than the poorly-interconnected ones. This could have been anticipated from the effect of increasing interconnection on flow velocities within the network.

The velocity vectors in Figures 21 (a), (b), and (c) demonstrate a shift in the location of high-velocity regions with changing fracture connectivity. Comparison of the concentration contours in Figures 25 (a), (b), and (c) with Figures 21 (a), (b), and (c) demonstrate that the distribution of the tracer in the fracture network follows this shift. In Figure 26 (a), the tracer is advancing at a somewhat more rapid rate in the upper part of the network, whereas in Figure 26 (c), transport is strongly influenced by the high-velocity regions in the lower part of the diagram. If changes in fracture connectivity create high-velocity pathways, the spatial distribution of contaminants can be profoundly influenced. Again, these preferred pathways would be difficult to predict using either a continuum or a dual-porosity approach.

Macroscopic breakthrough curves for three different values of connectivity are presented in Figure 27. In Section 4.1, it was noted that although changes in the variability of fracture apertures had a significant effect on the spatial distribution of contaminants in a fracture network, they had a minor influence on the macroscopic transport properties of the system. Figure 27 indicates that this is not true of the present simulations. Changes in fracture connectivity have a marked impact on the rate of travel of a tracer within fracture networks. As in the previous simulations, the macroscopic breakthrough curves are asymmetrical, asymptotically approaching a relative concentration of 1 even for the highly

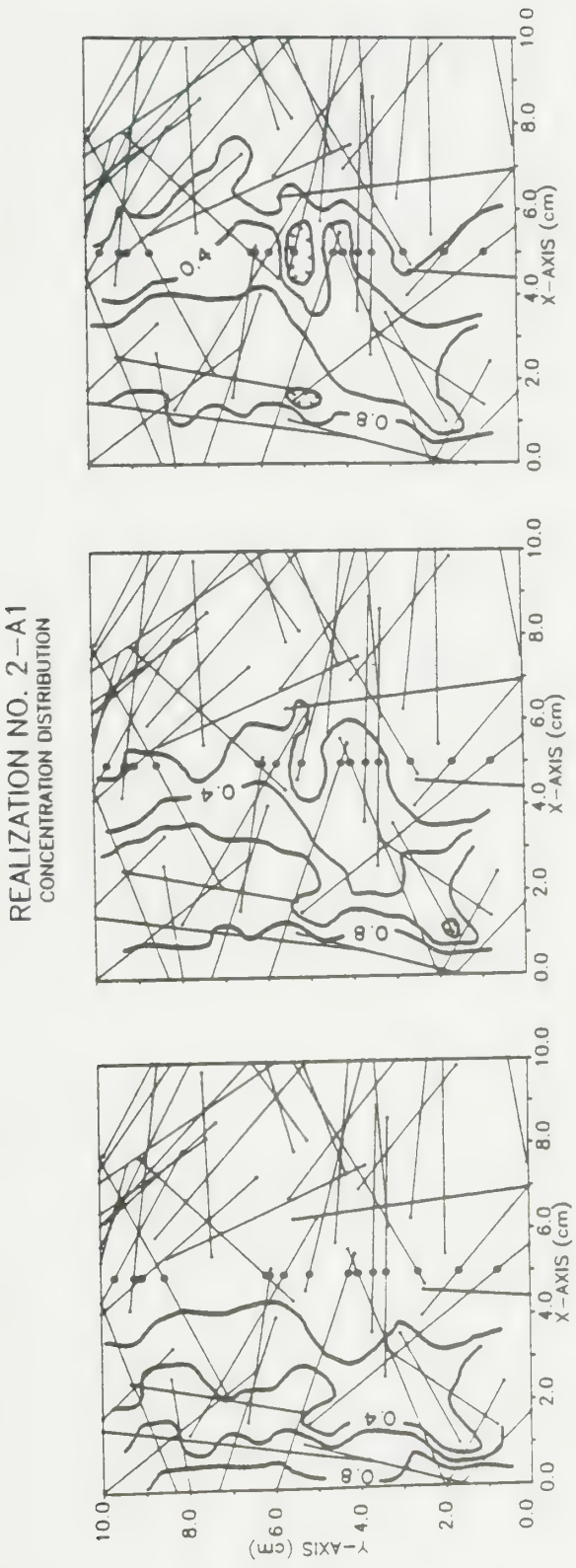


Figure 26: Concentration distributions for three different connectivities.

(a) Fracture connectivity ratio = 0.24. Results are shown at 5, 10, and 15 days

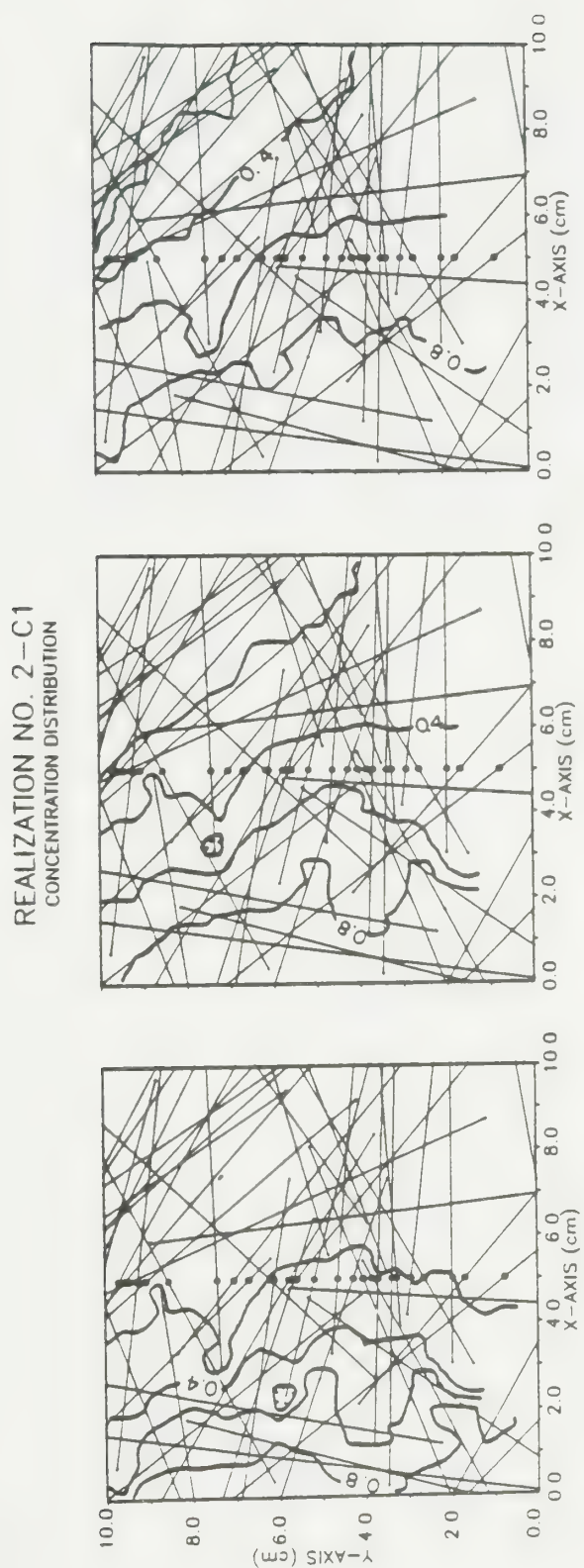


Figure 26: Concentration distributions for three different connectivities.

(b) Fracture connectivity ratio = 0.56. Results are shown at 5, 10, and 15 days

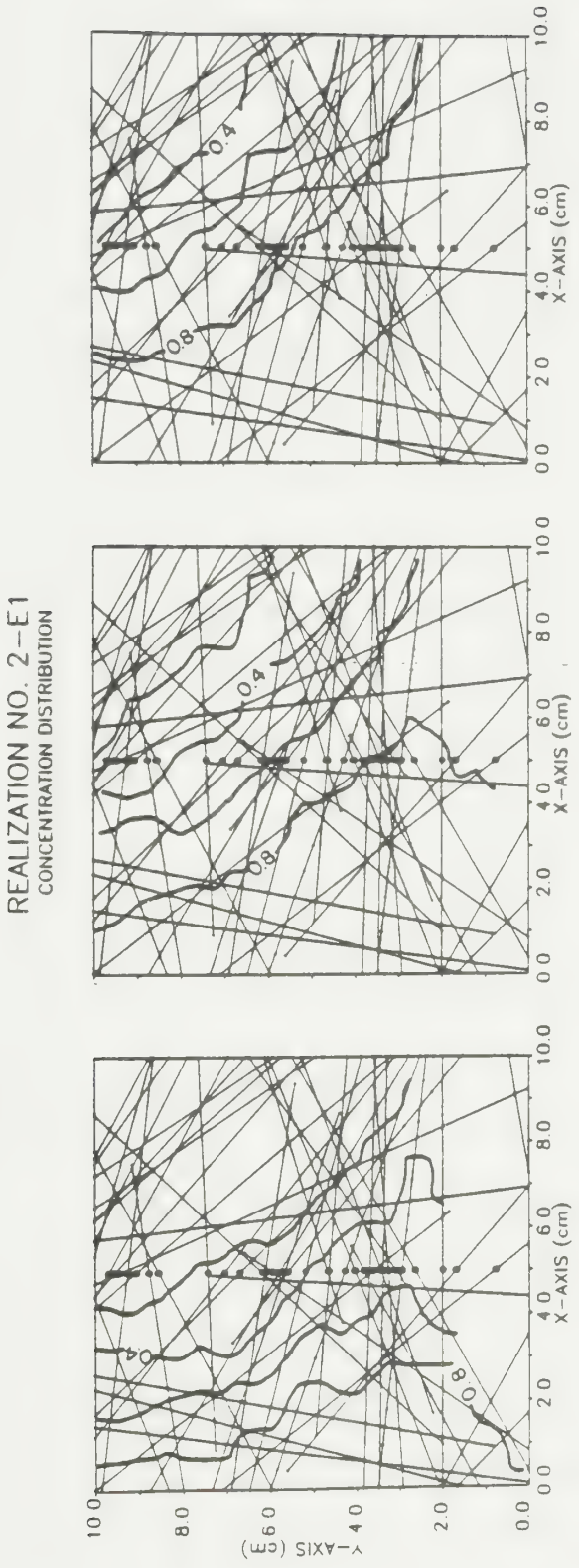


Figure 26: Concentration distributions for three different connectivity ratios.

(c) Fracture connectivity ratio = 0.86. Results are shown at 5, 10, and 15 days

interconnected networks. Because the proportion of deadend fracture regions decreases with increasing connectivity, the asymptotic behavior of the highly interconnected networks cannot solely be the result of diffusion to these regions.

Table 3 summarizes the macroscopic transport parameters for the different degrees of fracture interconnection. Although the bulk hydraulic conductivity increased by a factor of 40 with increasing connectivity, the tracer velocity only increased by half an order of magnitude. Similar to the result of the previous simulations, macroscopic transport appears to be less sensitive to fracture geometry than the bulk flow parameters are. The macroscopic dispersion coefficient appears even less sensitive to changes in fracture connectivity than to changes in fracture aperture variability. The difference in the shape of the breakthrough curves shown on Figure 27 is related primarily to the difference in tracer velocity rather than the macroscopic dispersion coefficient. The relative insensitivity of macroscopic dispersion to those geometrical parameters tested bodes favorably for the applicability of the continuum concept for transport in fractured media, provided a reliable means of determining input parameters can be developed.

Figure 28 demonstrates how the macroscopic dispersion coefficient and transport velocity change with changing connectivity. As in the previous simulations (Figure 18), no consistent trend can be observed in the macroscopic dispersion coefficient, nor is there any apparent relationship to the travel velocity. The standard deviation of the velocity distribution definitely does not seem to govern the macroscopic dispersion coefficient; if it did, the macroscopic dispersion coefficient and possibly also the skewness of the breakthrough curve should have diminished with increasing connectivity. Interestingly, although the standard deviation of the velocity distribution decreases with increasing connectivity, the ratio of the tracer residence time to fluid residence time t_p/t_f generally increases.

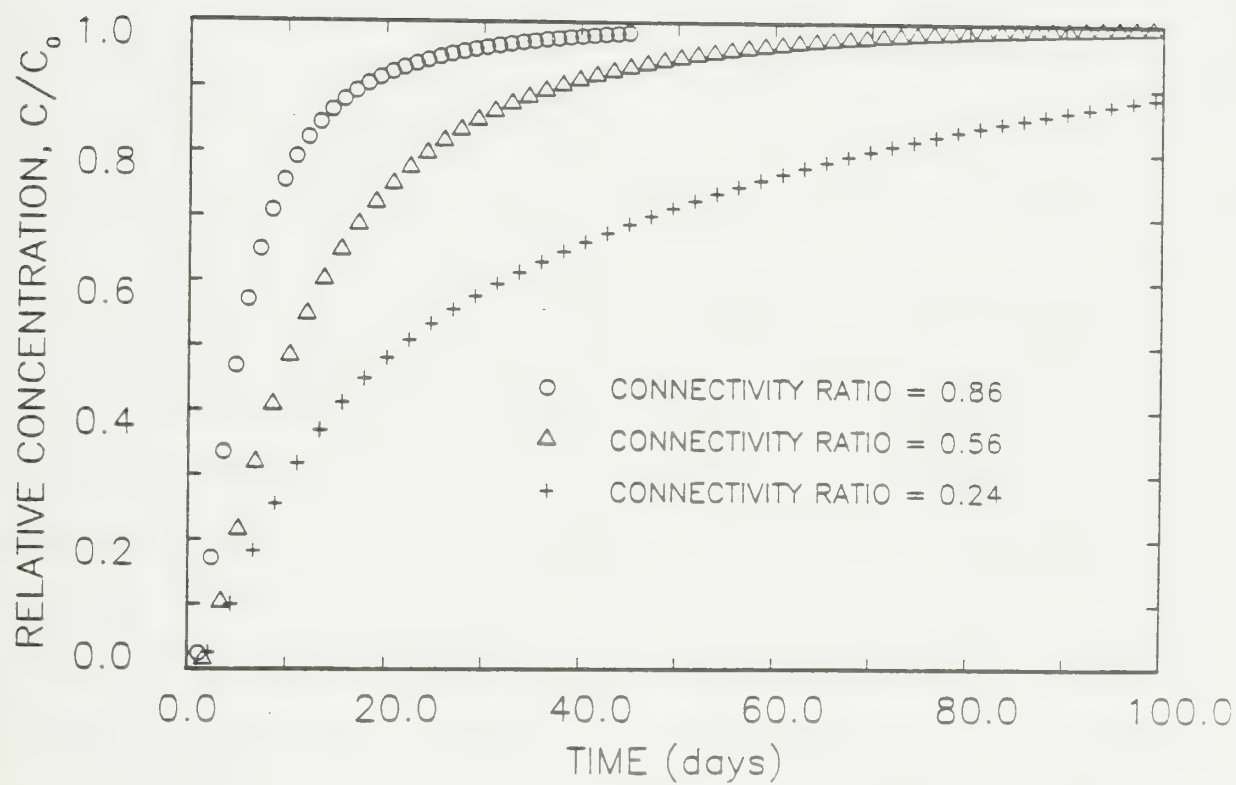


Figure 27: Macroscopic breakthrough curves for three different fracture connectivities

Table 3

Effect of increasing fracture connectivity on macroscopic transport parameters

| Computed value of parameter | Fracture connectivity ratio | | | | |
|-----------------------------------|-----------------------------|-----------------------|-----------------------|-----------------------|-----------------------|
| | 0.24 | 0.42 | 0.56 | 0.75 | 0.86 |
| $(v_x)_{tr}$ (m/day) | 1.48×10^{-3} | 2.84×10^{-3} | 3.66×10^{-3} | 5.98×10^{-3} | 7.53×10^{-3} |
| t_r/t_f | 0.9727 | 1.8071 | 2.2997 | 2.0376 | 2.0059 |
| D_L (m ² /day) | 1.46×10^{-4} | 1.21×10^{-4} | 1.16×10^{-4} | 1.56×10^{-4} | 1.58×10^{-4} |
| S_k | 1.3202 | 1.2677 | 1.3265 | 1.4929 | 1.5174 |

The ratio of the tracer residence time to the fluid residence time shown on Table 3 more than doubles with increasing connectivity. This suggests that even though the spread of the flow velocities diminishes, fracture regions that may have an insignificant role in flow through the network may still be important for transport. This could have a damping influence on the changes in the bulk hydraulic behavior, possibly explaining why macroscopic transport is less sensitive to changes in geometrical parameters. The results may mean that as transport is dominated by a few preferred pathways within a network, transport within the remaining pathways, which is influenced by diffusive mixing at intersections, becomes more important.

Finally, Figure 29 presents a comparison of velocities obtained from several different approaches with the velocity of the tracer in the network. As expected, the theoretical velocity based on Snow's model (equation 14) and the effective velocity calculated on the basis of bulk hydraulic conductivity converge with

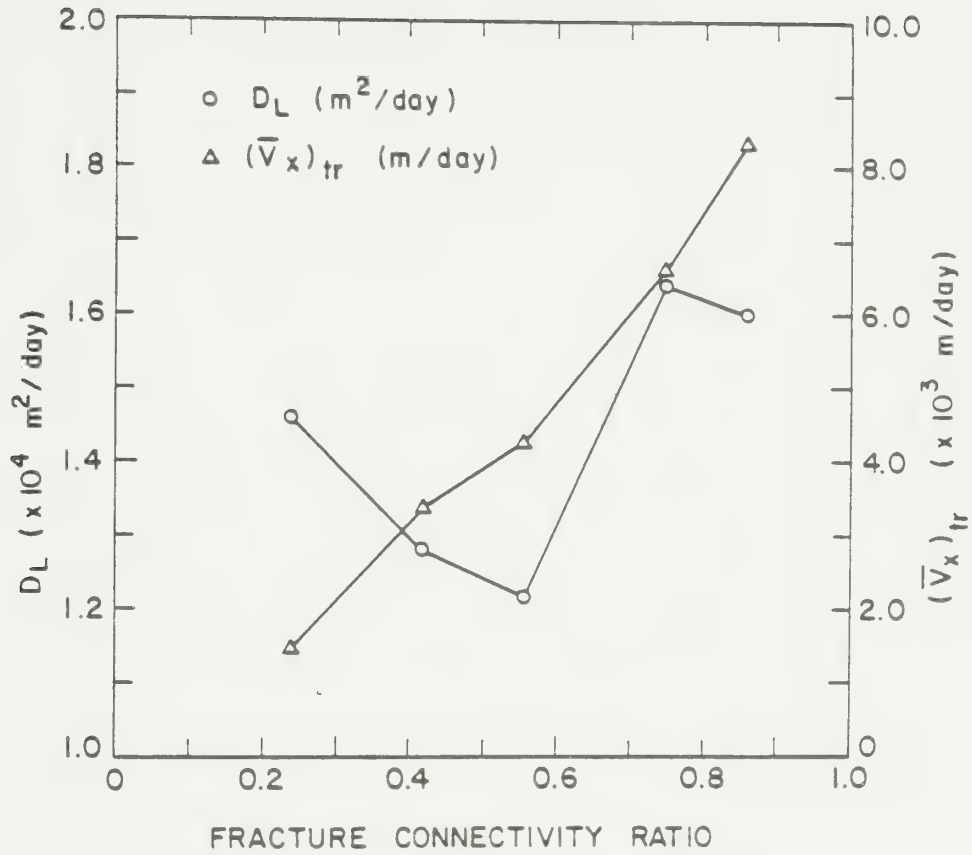


Figure 28: Effect of increasing connectivity on macroscopic dispersion and transport velocity.

increasing connectivity. Both approaches may significantly overestimate the tracer's rate of travel through the network. The effective velocity approach is much less successful at predicting the tracer's velocity than in the case of changing aperture standard deviation. Again, the arithmetic mean velocity underestimates the rate at which the tracer travels.

The most successful technique at predicting the tracer's velocity is the weighted average approach. The close correspondence of the values further supports the hypothesis that although flow and transport on a local scale may be dominated by a few preferred pathways, the entire volume of the fractures may be accessed during macroscopic transport.

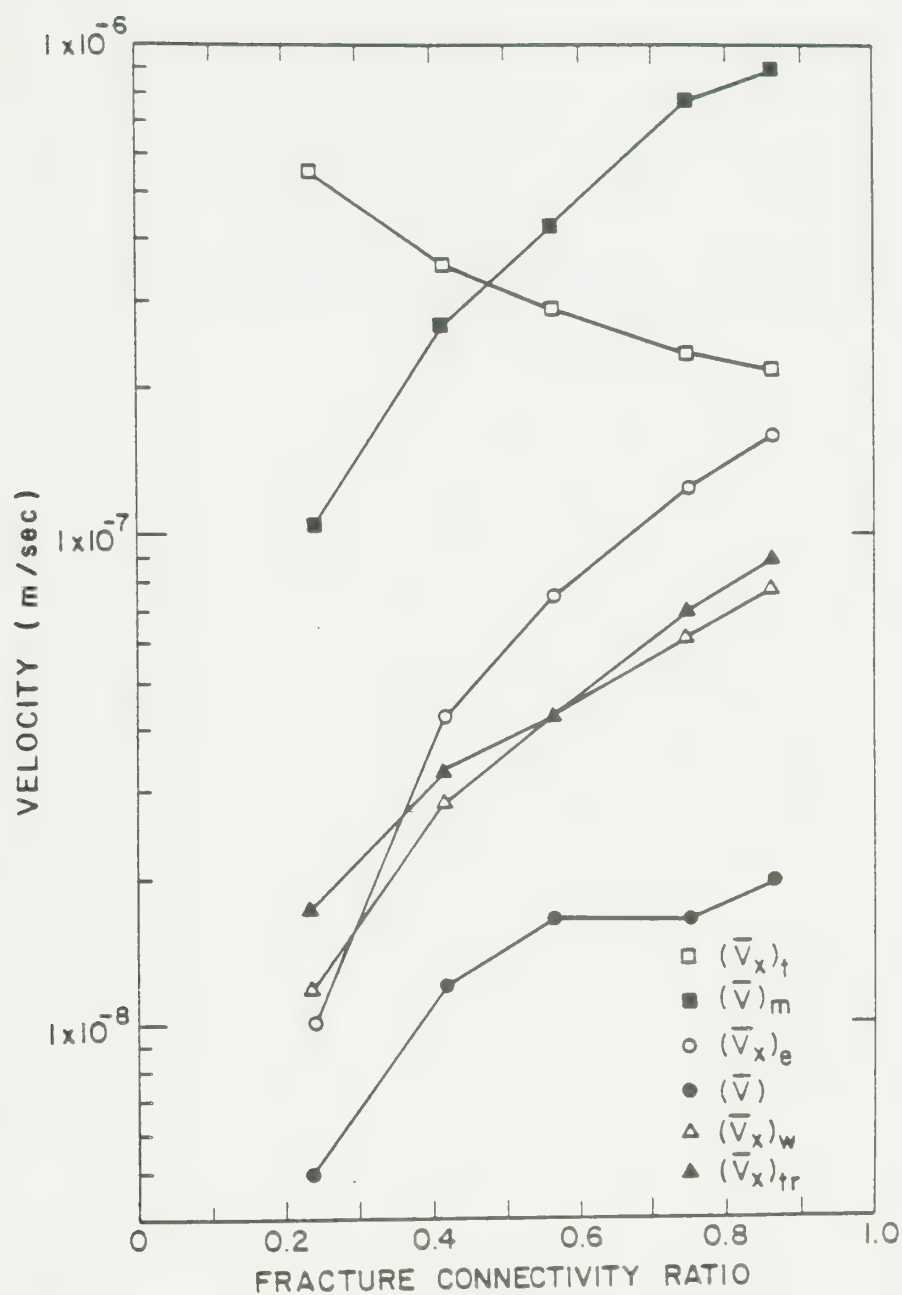


Figure 29:

Comparison of velocities obtained using different approaches for several connectivities. $(v_x)_{tr}$ calculated from equation (14); $(v)_m$ is maximum velocity in network; $(v_x)_e$ is calculated from $(K_x)_e$ and n_e ; (v) is arithmetic mean; $(v_x)_w$ is weighted average; $(v_x)_{tr}$ is travel velocity of center of mass.

Chapter V

IMPACT OF ATTENUATION MECHANISMS ON SOLUTE TRANSPORT

5.1 Effect of Sorption/Ion Exchange

The behavior of most contaminants of environmental concern in groundwater is affected by geochemical reactions that cause a transfer of the contaminant from the liquid to the solid phase or a conversion of the contaminant from one species to another with different physicochemical characteristics; conservative solutes are rarely of practical concern. One important class of reactions for contaminants present in groundwater at trace concentrations consists of sorption and ion-exchange reactions. When the occurrence of these geochemical processes is taken into account, the transport equation can be written in one dimension as:

$$\partial c / \partial t = D_L \partial^2 c / \partial x^2 - v \partial c / \partial x - Q \quad (28)$$

where Q is a general source-sink term describing the net rate of production or loss of the contaminant under consideration.

The model most commonly used to describe this source-sink term in the case of adsorption or ion-exchange reactions in homogeneous, saturated porous media was first developed in the study of chromatography (Lapidus and Amundson, 1952):

$$\partial c / \partial t = D_L \partial^2 c / \partial x^2 - v \partial c / \partial x - \rho_b / \theta \partial s / \partial t \quad (29)$$

where ρ_b is the bulk density of the porous medium and Θ is the porosity. Whether this model is really suitable for the description of transport with ion exchange or sorption in porous media is in doubt; assumptions, limitations, and alternative conceptual models are reviewed by Rao et al. (1979) and Gillham and Cherry (1982), among others.

Despite its potential limitations, this model can be modified for extension to transport in fractured media. As discussed by Burkholder (1976) according to Freeze and Cherry (1979), ρ_b/Θ is a macroscopic concept introduced purely for convenience. On the premise that adsorption and ion exchange reactions are much more closely related to the surface area in contact with the fluid than to the mass of the medium, a more rigorous but less convenient approach might be to use the unit surface area of the medium as a reference quantity, thus giving Q as:

$$Q = A \partial s / \partial t \quad (30)$$

where A is the surface area to void-space ratio of the fracture. Thus, for a fracture of length L and width W ,

$$A = \frac{\text{surface area of fracture}}{\text{volume of fracture}} = \frac{2LW}{LW(2b)} = \frac{1}{b} \quad (31)$$

If $s = f(c)$, i.e. if the reaction is reversible, non-hysteretic, attains equilibrium instantaneously, and can be described by a reaction isotherm, then

$$\partial s / \partial t = ds/dc \partial c / \partial t \quad (32)$$

and if the reaction isotherm is linear,

$$ds/dc = \text{constant} = K_a \quad (33)$$

where K_a is the fracture distribution coefficient defined on a per-unit-surface-area basis. Substituting (30), (31), (32), and (33) into equation (28):

$$\partial c / \partial t = D_L \partial^2 c / \partial x^2 - v \partial c / \partial x - K_a / b \partial c / \partial t \quad (34)$$

In a continuum, retardation of solutes via sorption or ion exchange is commonly described with a constant retardation factor R :

$$R = 1 + \rho_b / \Theta K_d \quad (35)$$

from which

$$\partial c / \partial t = D_L / R \partial^2 c / \partial x^2 - v / R \partial c / \partial x \quad (36)$$

The apparent velocity is uniformly retarded through the medium by this factor R , just as the effective dispersion coefficient is reduced.

Similarly, within an individual fracture of uniform aperture, the retardation factor can be defined as:

$$R = 1 + K_a / b \quad (37)$$

Because of the dependence of retardation in fractured media on the fracture aperture, however, retardation will not be uniform in a system consisting of a variety of apertures. Compared to the retardation experienced in the fracture of mean aperture $\mu_{ln} 2b$, retardation will be greater in the smaller fractures and less in the larger fractures. Because there is no one-to-one correspondence between fracture aperture and flow velocity in a system of finite fractures, the effective velocity v/R distribution of the retarded solute may have a different form than the actual flow velocity distribution. This introduces the possibility of retardation as a dispersive mechanism quite different from the conventional interpretation of apparent dispersion in porous media. This effect has been noted by Neretnieks et al. (1982) for a single fracture of varying aperture.

To test the significance of this process, transport with retardation (eq. (34)) was simulated for the fracture network shown in Figure 1 (a) and for the various aperture distributions examined in Section 4.1. The hydraulic properties of the fracture networks are the same as those described in Section 4.1 and illustrated in Figures 8 through 12; the results of the retarded case can be compared with those for the unretarded case shown on Figures 14 through 15. For convenience in interpreting the results, the value of K_a was selected so that for the mean fracture aperture ($\ln 2b = -7.824$ cm), the retardation factor R is exactly equal to 10; thus, $K_a = 1.8 \times 10^{-5}$ m. Only in the uniform aperture case will the macroscopic retardation factor equal 10.

Histograms comparing the distributions of the effective velocity v/R for the nonretarded case ($K_a = 0$) and the retarded case ($K_a = 1.8 \times 10^{-5}$) for three values of $\sigma_{\ln 2b}$ are shown on Figure 30. For $\sigma_{\ln 2b} = 0.0$, the mean effective velocity in the retarded case is one order of magnitude smaller than in the nonretarded case, as expected, and the standard deviation S_v is the same. As $\sigma_{\ln 2b}$ increases, the frequency of fractures smaller than the mean increases relative to that of fractures larger than the mean; thus, the mean value of v/R decreases by slightly more than one order of magnitude as $\sigma_{\ln 2b}$ increases. It might be inferred from this that retardation in a fractured medium is greater than that predicted on the basis of the mean aperture. As shown below, such an assumption would be fallacious. Illustrating the lack of a unique correspondence between the fracture aperture and the flow velocity, the sample standard deviation S_v is greater in the retarded case than in the nonretarded case for $\sigma_{\ln 2b} > 0$. If skewness in arrival time distribution is directly related to the standard deviation of the effective velocity distribution, then a Fickian model of dispersion should be even less appropriate for the retarded solutes than for the nonretarded solutes.

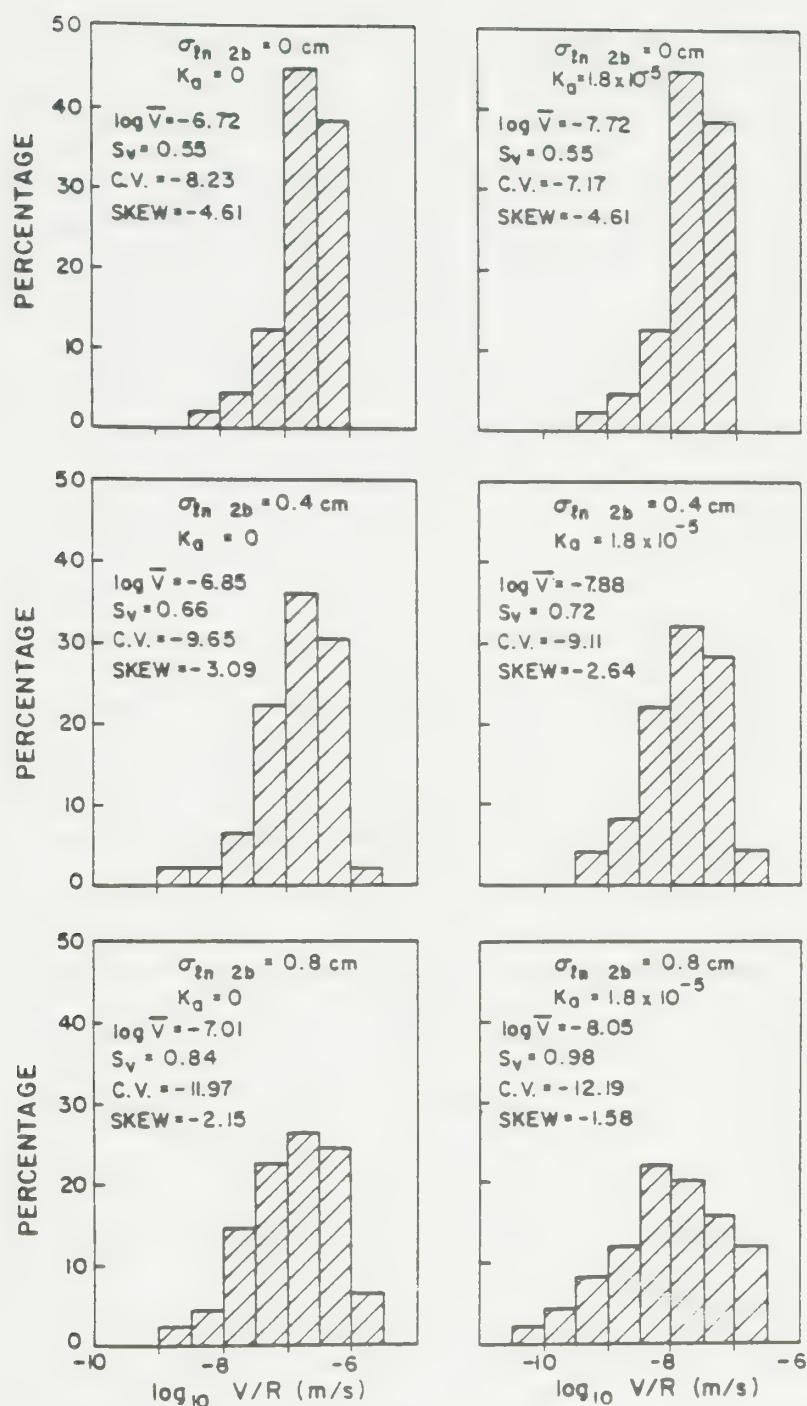


Figure 30:

Histograms comparing effective velocity v/R distributions for a nonretarded and a retarded case. The retardation factor R is equal to 10 for the fracture of mean aperture

Figure 31 (a), (b), and (c) illustrates the concentration distributions in the fracture network at three different times. Because the times selected are greater by a factor of 10 than those used in preparing Figure 14(a), (b), and (c), the contours should lie in exactly the same positions in Figure 31 and in Figure 14 if retardation were uniform. As expected, this is in fact the case with Figure 31 (a), the uniform aperture example. From the effective velocity distributions for the variable aperture cases, it might be expected that the reactive solute would be retarded by a factor greater than 10. That this is not true is apparent from comparing Figure 31 (b) with Figure 14 (b) and Figure 31 (c) with Figure 14 (c). Although it was shown in earlier sections that transport may not be dominated by the largest fractures, it is clearly not dominated by the smallest fractures either, in which the retardation factor would be greater than 10. The solute in the retarded case has penetrated a greater distance through the network, suggesting that the spatial distribution of contaminants is controlled by fractures larger than the mean, i.e. in those fractures for which the retardation factor is less than 10.

Figure 32 shows the macroscopic breakthrough curve for the retarded solute. The time scale in this figure has been reduced by a factor of 10 to facilitate a comparison with the macroscopic breakthrough curve for the nonretarded case (Figure 15). As expected, the results for the uniform aperture case are identical for the retarded and nonretarded solute. The reactive solute breakthrough curves, however, are significantly different in appearance for both the variable aperture cases. Although variations in fracture aperture proved relatively unimportant as a factor in macroscopic transport for a conservative tracer, they can be more significant when coupled with ion exchange or sorption reactions.

Table 4 shows the macroscopic transport parameters calculated from the breakthrough curves for the different aperture distributions tested. If the effec-

REALIZATION NO. 4-A1
CONCENTRATION DISTRIBUTION

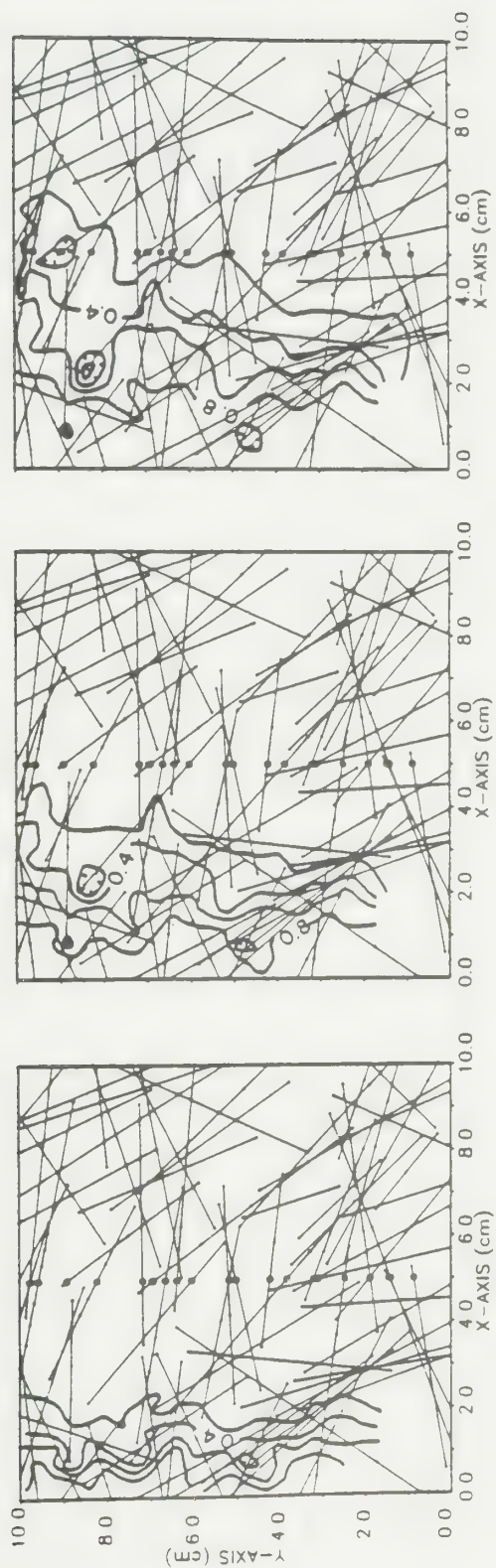


Figure 31: Concentration distributions for retarded solute ($K_a = 1.8 \times 10^{-5}$ m).

(a) $\sigma_{\ln 2b} = 0.0$ case. Results are shown at 5, 10, and 15 days

REALIZATION NO. 4-C1
CONCENTRATION DISTRIBUTION

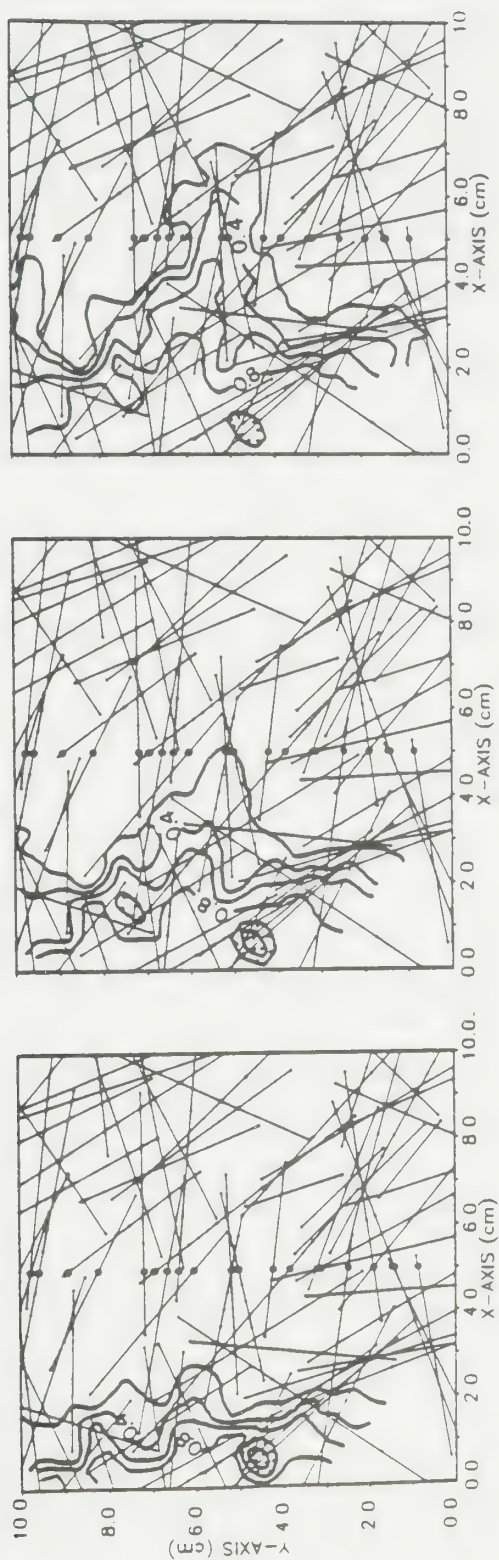


Figure 31: Concentration distributions for retarded solute ($K_a = 1.8 \times 10^{-5} \text{ m}$).

(b) $\sigma_{\ln 2b} = 0.4$ case. Results are shown at 5, 10, and 15 days

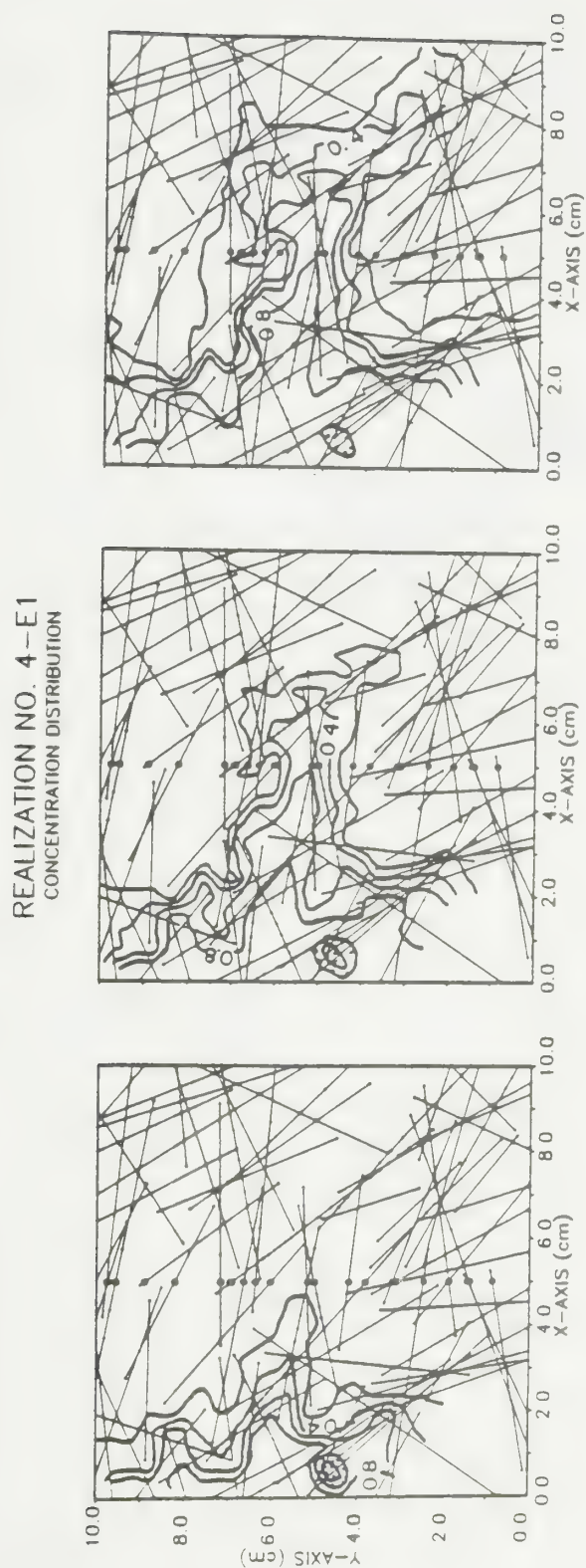


Figure 31: Concentration distributions for retarded solute ($K_a = 1.3 \times 10^{-3}$ m).

(c) $\sigma_{\ln 2b} = 0.8$ case. Results are shown at 5, 10, and 15 days

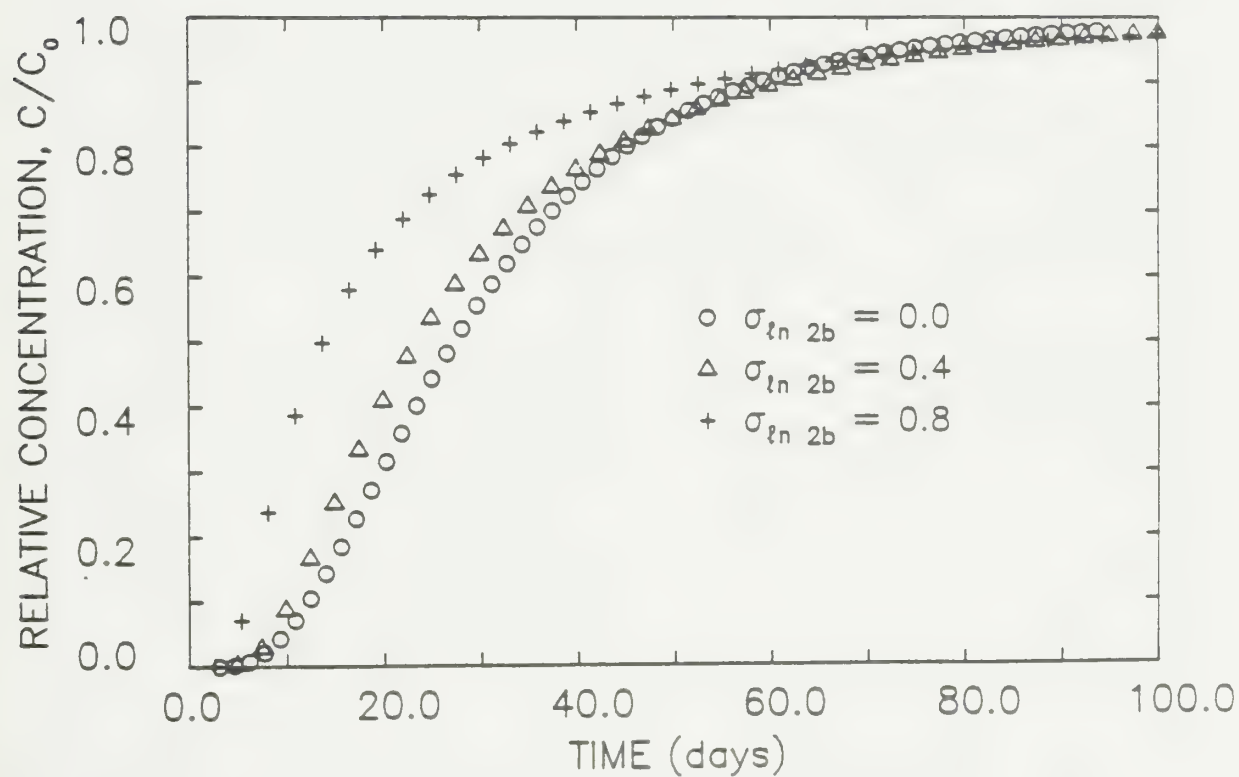


Figure 32: Macroscopic breakthrough curves for retarded solute.

tive retardation factor R is defined on the basis of its impact on the mean tracer residence time t_r for the nonreactive case, it can be seen that the effective retardation factor shows a progressive decrease with increasing aperture variability. Thus, predicting retardation factors in a continuum on the basis of the mean fracture aperture and equation (34), or simulating transport of retarded solutes in geometrically simplified fracture systems in which all the fractures have the mean aperture value may substantially underestimate the effective velocity of a contaminant. Erickson (1983) has proposed a method for determining an appropriate retardation factor for an equivalent porous medium approximation; this approach is based on the fracture porosity n_e without reference to whether this porosity comprises a few large fractures or many small ones. Such an approach could either underestimate or overestimate the residence time of a reactive solute.

Table 4 also shows the retardation factor that would have been expected for the largest 10% of the fractures. The observed value of R is intermediate between that that would be expected for the largest fractures and that for the mean fracture aperture. From the observed retardation factor, the 'effective' fracture aperture can be calculated; this value is also shown in Table 4. The effective aperture for transport is greater than the mean aperture by a relatively small amount (33% for $\sigma_{\ln 2b} = 0.8$) in comparison to the difference between the largest and the mean fracture aperture (87% for $\sigma_{\ln 2b} = 0.8$). These results lend weight to the previous observation that transport is not dominated by the largest fractures, although it clearly is controlled by fractures with apertures greater than the mean value.

With R defined on the basis of the mean arrival time, the longitudinal macroscopic dispersion coefficient D_L for the reactive solute can be determined from

Table 4

Effect of increasing variability in fracture aperture on macroscopic transport for a reactive solute

| Computed value of parameter | Ln standard deviation of fracture aperture distribution | | | | |
|--------------------------------|---|-----------------------|-----------------------|-----------------------|-----------------------|
| | 0.0 | 0.2 | 0.4 | 0.6 | 0.8 |
| $(v_x)_{tr}/R$ (m/d) | 1.72×10^{-3} | 1.81×10^{-3} | 1.87×10^{-3} | 3.16×10^{-3} | 2.67×10^{-3} |
| R | 9.9997 | 9.7293 | 8.8995 | 7.0216 | 6.4527 |
| R for largest 10% of fractures | 10.0000 | 6.7-8.1 | 4.8-6.5 | 2.9-5.2 | 2.1-3.8 |
| effective aperture (cm) | 4.00×10^{-4} | 4.12×10^{-4} | 4.60×10^{-4} | 5.98×10^{-4} | 6.60×10^{-4} |
| D_L/R (m^2/day) | 1.92×10^{-5} | 1.77×10^{-5} | 2.09×10^{-5} | 3.70×10^{-5} | 3.25×10^{-5} |
| D_L (m^2/day) | 1.92×10^{-4} | 1.72×10^{-4} | 1.86×10^{-4} | 2.60×10^{-4} | 2.10×10^{-4} |
| S_k | 0.7582 | 0.9060 | 1.0926 | 1.2291 | 1.4466 |

the computed value of D_L/R . Just as in the case of the nonretarded solute, D_L does not show a consistent trend with increasing $\sigma_{ln} 2b$. Except for the uniform aperture case and the $\sigma_{ln} 2b = 0.8$ case, the dispersion coefficient for the retarded solute is greater than that for the nonretarded solute, suggesting that under the circumstances simulated, retardation may affect macroscopic dispersion.

For two of the cases ($\sigma_{ln} 2b = 0.2$ and $\sigma_{ln} 2b = 0.4$), the coefficient of skewness of the arrival time distribution is greater for the retarded solute than for the nonretarded solute; for the other cases, this parameter was smaller or the same. Thus, although the standard deviation of the effective velocity distribution was greater for the retarded case, this does not appear to have a major impact on the

extent to which macroscopic dispersion can be described as a diffusive process. Incorporating retardation in the transport equation thus seems to affect the rate at which contaminants are carried through a system more than the dispersive characteristics of the medium, at least for the conditions simulated in the present study.

5.2 Effect of Diffusion to Deadend Fracture Segments

Diffusion of a tracer to deadend fracture segments probably represents an insignificant attenuation mechanism for most rock types in comparison to diffusion to intact matrix material (including diffusion to microfractures), and may well also be secondary in comparison to diffusion to slow-flowing regions of fluid. Other studies of transport in stochastic-discrete fracture systems (Schwartz et al., 1982, 1983; Smith and Schwartz, 1984) have accordingly trimmed deadend fracture regions from the network. The transport simulation technique used in these other studies also neglects diffusive transfer of solutes into fractures with very small fluid fluxes; retention of mass in the network may therefore be underestimated.

It was not possible to test the importance of diffusion to fractures containing little flow by removing them from the network; to do so would have altered the hydraulic properties of the system. The grid generator was however designed so that deadend fracture segments could either be retained or trimmed. To examine the importance of diffusion to deadend fractures as an attenuation mechanism, the transport simulations shown in Figure 14 (a), (b), and (c) (Section 4.1) were repeated without the deadend fracture segments. The fracture network is shown again on Figure 33(a); Figure 33(b) shows the trimmed grid system. For this network, the deadend fracture regions represent approximately 20% of the total

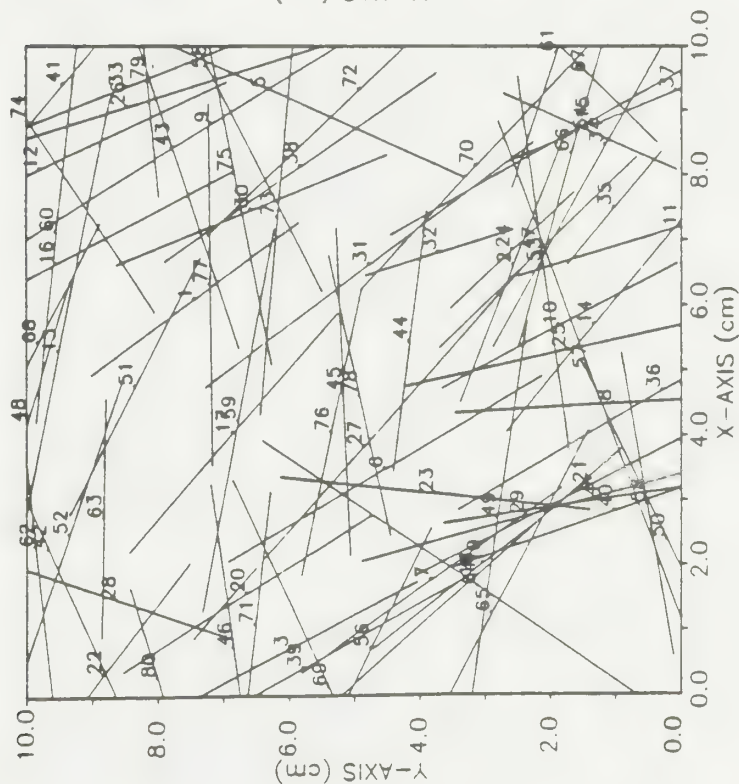
fracture volume. If the fracture system were in fact three-dimensional, some of these 'deadend' segments would have actually intersected other fractures out of the plane of the diagram.

Figure 34(a), (b), and (c) shows the concentration distributions in the fracture network at three different times. In comparing these contours with the hydraulically equivalent systems shown in Figure 14(a), (b), and (c), note that omitting the deadend fractures removes the irregularity imparted by the presence of diffusion to deadend fracture segments. This locally advances the position of each contour. Even so, it appears that the tracer is travelling through the trimmed network at a slightly more rapid rate than in the untrimmed network.

Figure 35 compares macroscopic breakthrough curves for two aperture realizations of the trimmed and untrimmed system. The difference in the apparent velocity produced by diffusion to deadend regions is more apparent than in the concentration contours. It is obvious that, at least at the flow velocities considered here, diffusion to deadend fracture segments can represent a significant attenuative mechanism.

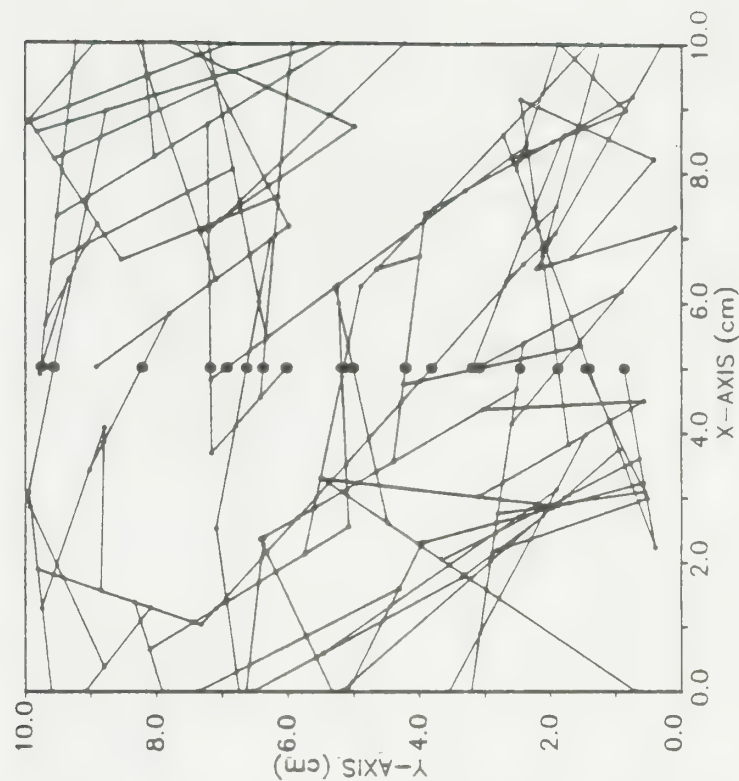
Table 5 shows the macroscopic transport parameters for the trimmed case. In comparison with the parameters shown in Table 2, the tracer velocities are approximately 20% greater. For the geometry shown in Figure 33, the presence of the deadend fracture regions decreases the macroscopic dispersion coefficient. This is contrary to what was expected on the basis of an analogy between transport in fracture networks with deadend regions and transport in tubes with stagnant pockets (Aris, 1959). Further studies should be performed to indicate whether this is a general result. The effect on the macroscopic dispersion coefficient diminishes with increasing $\sigma_{ln} 2b$.

REALIZATION NO. 5-A1
FRACTURE SYSTEM



(a)

REALIZATION NO. 5-A1
GRID SYSTEM



(b)

Figure 33: Fracture network with deadend fractures 'trimmed'. (a) Original fracture network; (b) Grid system with deadend fracture segments removed

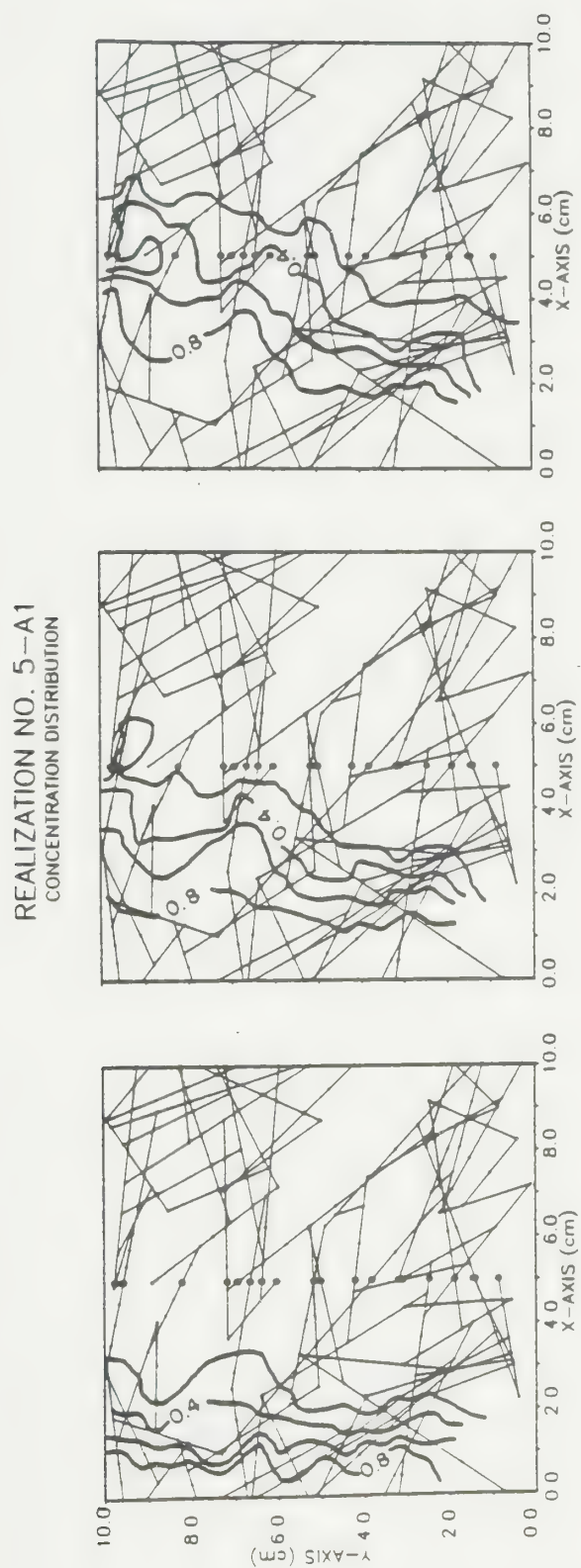


Figure 34: Concentration contours for 'trimmed' grid systems.

(a) $\sigma_{n2b} = 0.0$ case. Results are shown at 0.5, 1.0, and 1.5 days.

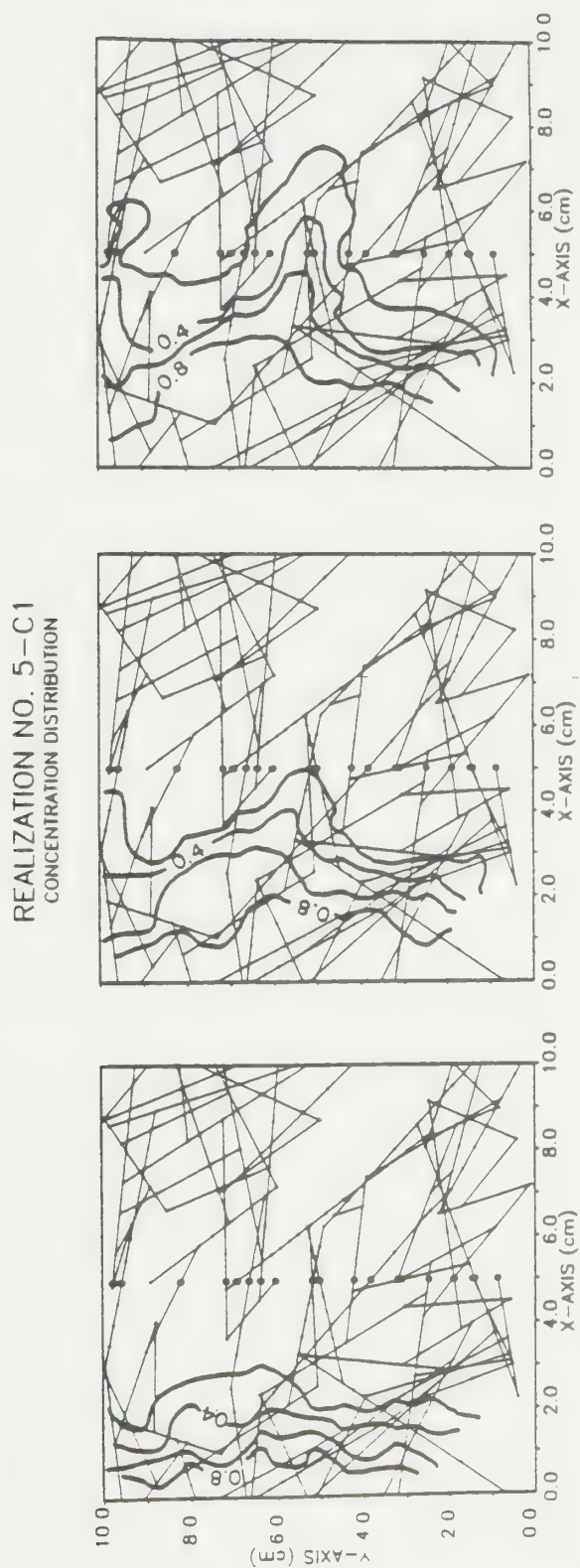


Figure 34:

Concentration contours for 'trimmed' grid systems.

(b) $\sigma_{\ln 2b} = 0.4$ case. Results are shown at 0.5, 1.0, and 1.5 days.

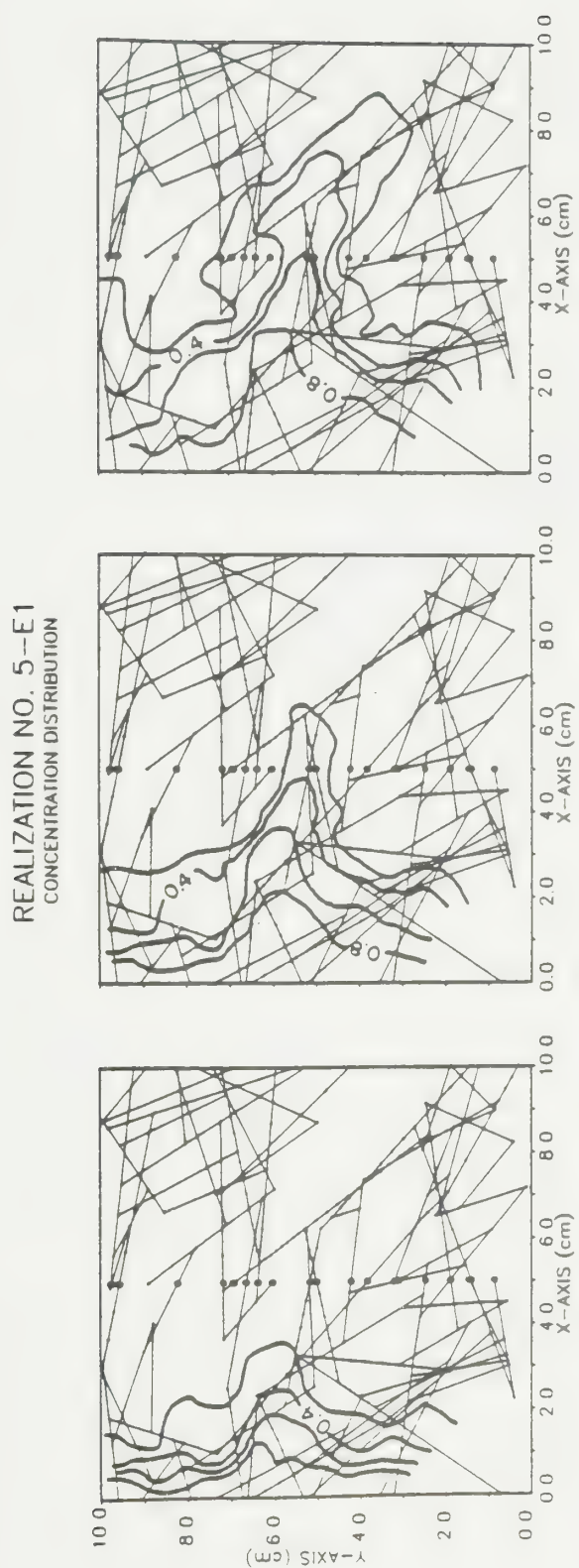


Figure 34: Concentration contours for 'trimmed' grid systems.

(c) $\sigma_{\ln 2b} = 0.8$ case. Results are shown at 0.5, 1.0, and 1.5 days.

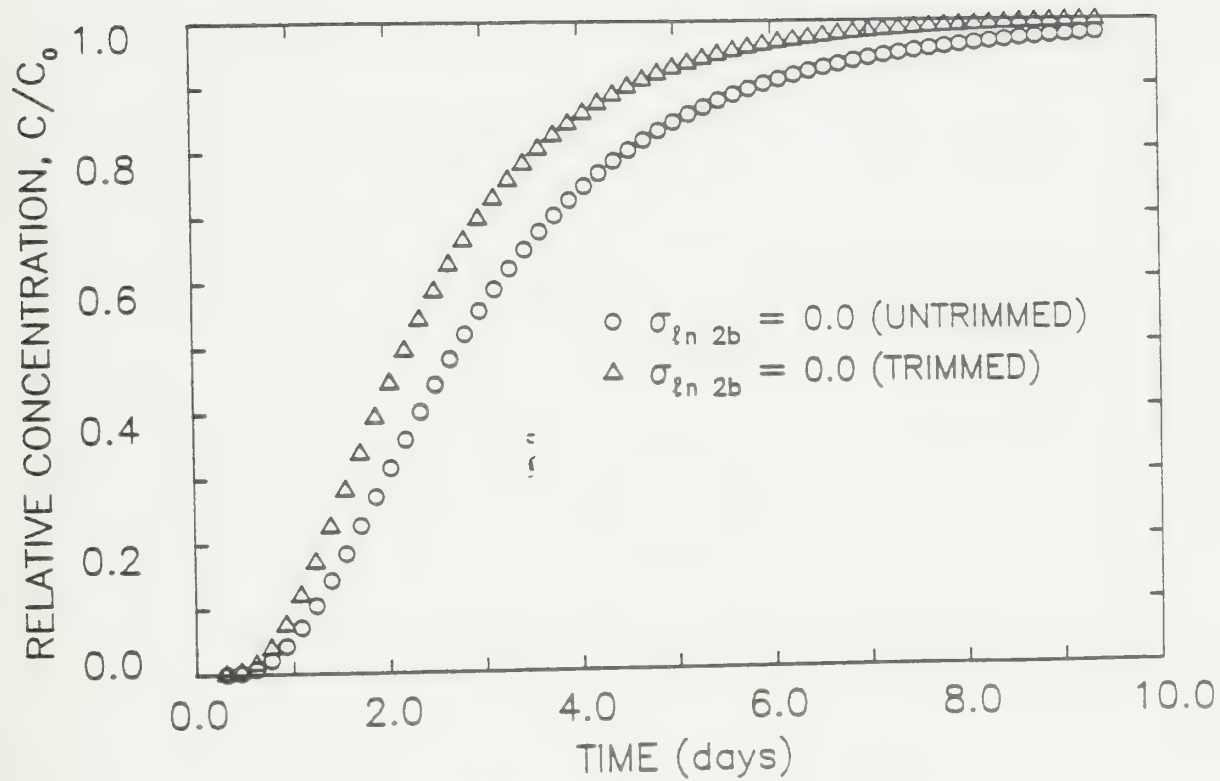


Figure 35: Macroscopic breakthrough curves for cases in which dead-end fractures have been 'trimmed'.

(a) $\sigma_{ln} 2b = 0.0$ case

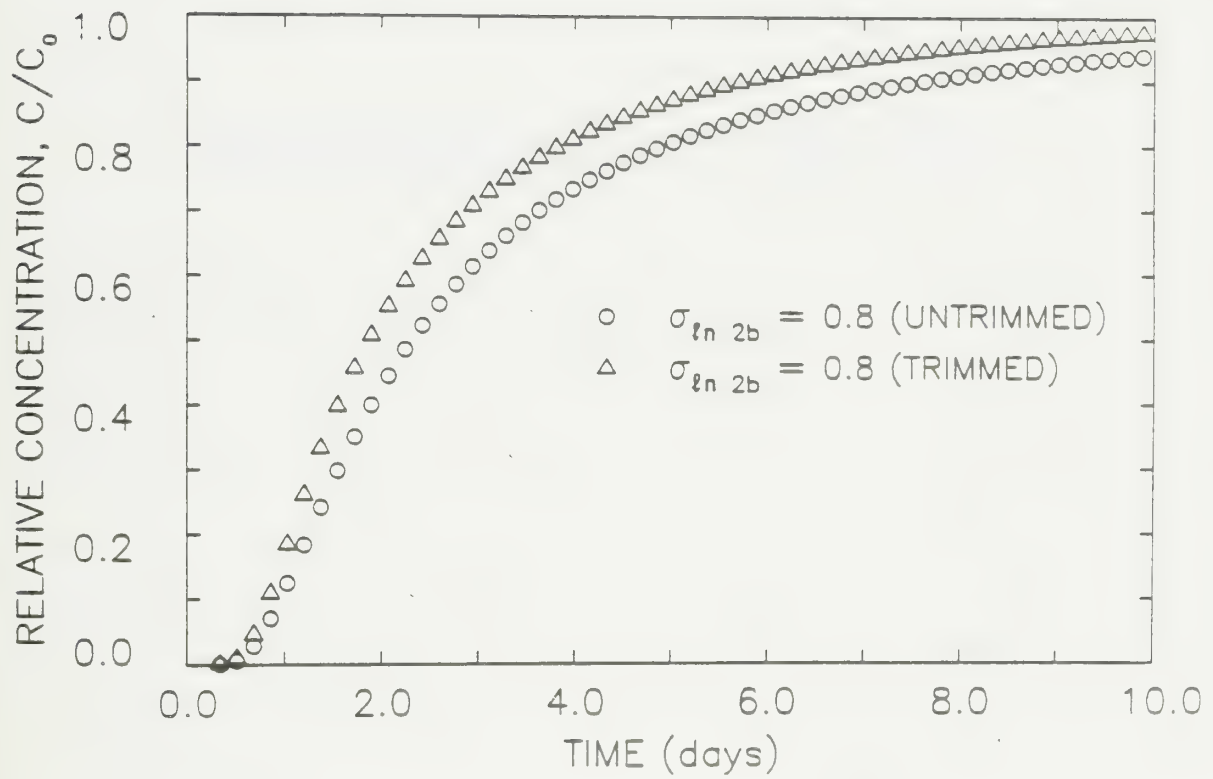


Figure 35: Macroscopic breakthrough curves for cases in which dead-end fractures have been 'trimmed'.

(b) $\sigma_{ln 2b} = 0.8$ case

In all of the cases tested, the skewness of the breakthrough curve is less in the trimmed case than in the untrimmed case. Although the curves still asymptotically approach a relative concentration of 1, this result would tend to support the hypothesis that diffusion to stagnant or essentially stagnant regions of flow is a significant factor in the non-Fickian tendencies of the macroscopic dispersion. As shown below for the example with the different connectivities, this may not always be the case.

Table 5

Comparison of macroscopic transport parameters for different values of $\sigma_{\ln 2b}$ without deadend fracture segments

| Computed value of parameter | Ln standard deviation of fracture aperture distribution | | | | |
|-----------------------------------|---|-----------------------|-----------------------|-----------------------|-----------------------|
| | 0.0 | 0.2 | 0.4 | 0.6 | 0.8 |
| $(v_x)_{tr}$ (m/day) | 2.16×10^{-2} | 2.22×10^{-2} | 2.10×10^{-2} | 2.82×10^{-2} | 2.13×10^{-2} |
| t_r/t_f | 0.9764 | 0.9649 | 0.9918 | 1.0451 | 0.9902 |
| D_L (m^2/day) | 2.16×10^{-4} | 1.86×10^{-4} | 1.89×10^{-4} | 2.53×10^{-4} | 2.29×10^{-4} |
| S_k | 0.6698 | 0.8004 | 0.9704 | 1.1354 | 1.3465 |

The closeness of the ratio of the tracer residence time to the fluid residence time t_r/t_f to the uniform-flow value of 0.95 for $\sigma_{\ln 2b} = 0.0$ and 0.2 suggests that in these cases, transport is relatively uniformly distributed through the fracture network. Diffusion to near-stagnant regions tentatively appears to be a more important attenuation mechanism in fracture networks characterized by a greater variability in aperture, as shown by the larger values of this ratio. The greater

tendency for flow to be dominated in a few fractures (shown by the unevenness of the velocity profile in Figure 10) causes the tracer to preferentially follow a few pathways within the network, thereby increasing the concentration gradient between adjacent regions and increasing the diffusive flux from the high-velocity pathways to the near-stagnant regions. This is analagous to the advection-diffusion concept for stratified porous media (Gillham et al., 1984).

The importance of the deadend fractures should be closely related to the fraction of the total fracture volume they comprise. To test this, the transport simulations for the changes in fracture connectivity were repeated without the deadend fractures. The network with the smallest connectivity ratio contains approximately 27% deadend fractures by volume, whereas the network with the greatest connectivity only contains 6% deadend fracture volume. The results of this simulation are shown on Table 6, and can be compared to the untrimmed results presented on Table 3. The presence of deadend fractures causes the tracer to be retarded by 26% in relation to the results in Table 6 for a connectivity ratio of 0.24; this retardation diminishes to 8% for a connectivity ratio of 0.86. Figure 36 compares macroscopic breakthrough curves for trimmed and untrimmed cases for two different degrees of interconnection. The greater importance of diffusion to deadend fracture segments in the poorly-interconnected case is apparent.

The macroscopic dispersion coefficients were again greater in the absence of deadend fractures. In the present case, however, the breakthrough curves for the simulations without the deadend fracture segments show a greater degree of skewness, contrary to the trend observed for the simulations with different values of $\sigma_{ln} 2b$.

Table 6

Comparison of macroscopic transport parameters for different connectivities without deadend fractures

| Calculated value of parameter | Fracture connectivity ratio | | | | |
|-------------------------------------|-----------------------------|-----------------------|-----------------------|-----------------------|-----------------------|
| | 0.24 | 0.42 | 0.56 | 0.75 | 0.86 |
| $(v_x)_{tr}$ (m/day) | 2.00×10^{-3} | 3.38×10^{-3} | 4.23×10^{-3} | 6.57×10^{-3} | 8.30×10^{-3} |
| t_r/t_f | 0.7196 | 1.5174 | 1.9905 | 1.8543 | 1.8439 |
| D_L (m ² /day) | 1.69×10^{-4} | 1.28×10^{-4} | 1.22×10^{-4} | 1.64×10^{-4} | 1.50×10^{-4} |
| S_k | 1.3739 | 1.3197 | 1.4019 | 1.5844 | 1.6186 |

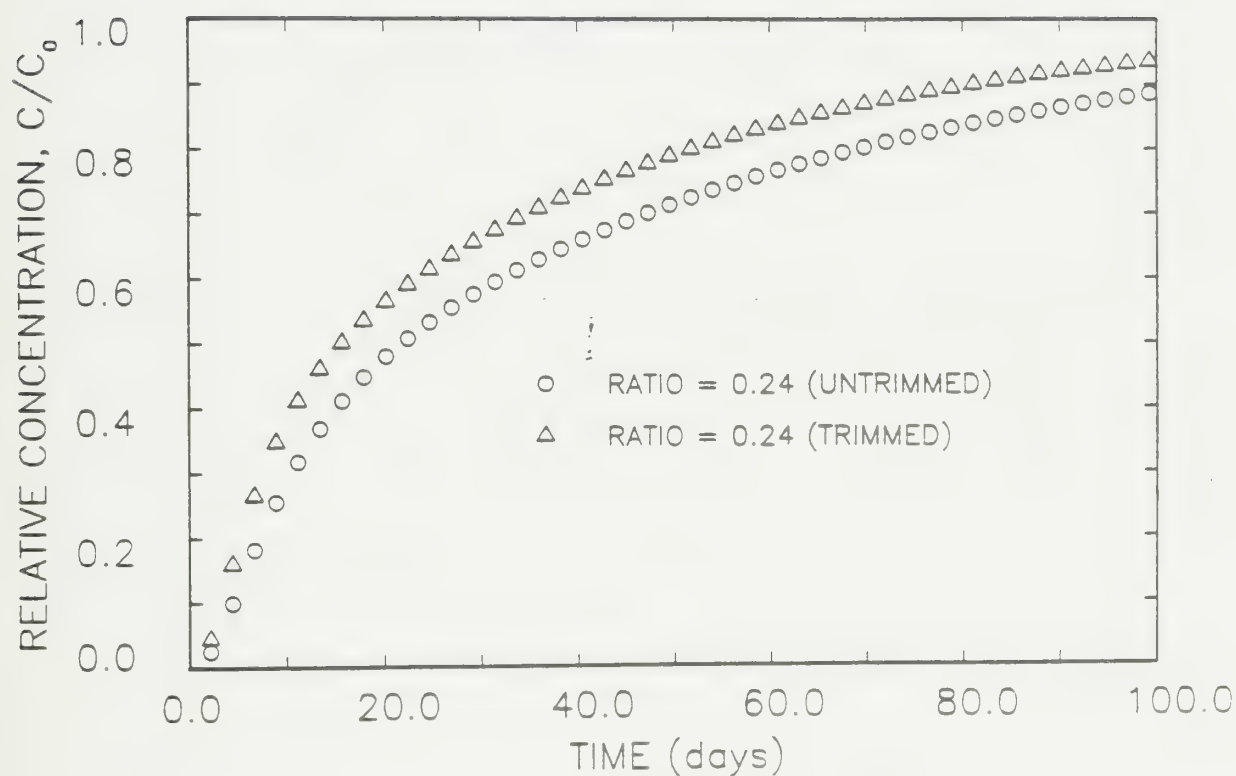


Figure 36: Breakthrough curves for two connectivity values showing relative importance of diffusion to deadend fractures.

(a) fracture connectivity ratio = 0.24

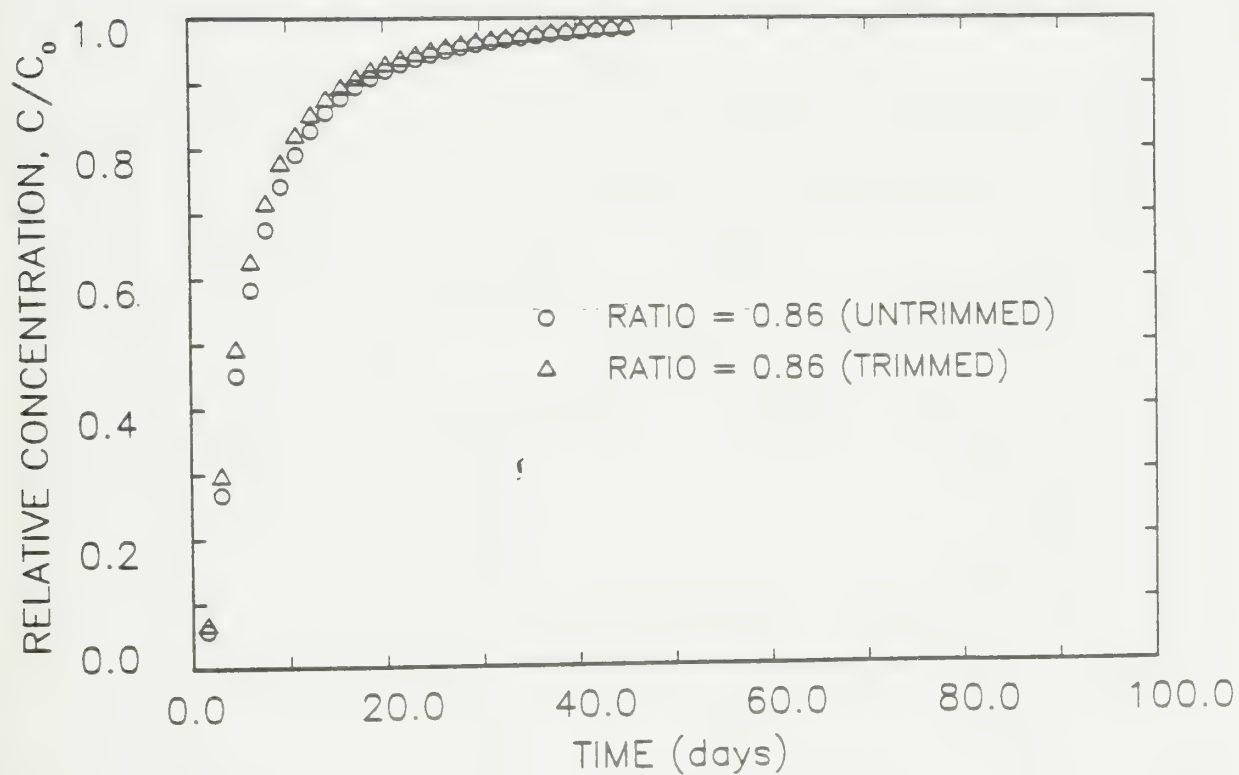


Figure 36: Breakthrough curves for two connectivity values showing relative importance of diffusion to deadend fractures.

(b) fracture connectivity ratio = 0.86

5.3 Scale-Dependence of Dispersion in Fracture Networks

Recent observations of dispersion in porous media have shown that field-observed dispersion coefficients increase with the scale of the problem under consideration; there is a growing body of literature documenting or explaining this scale-dependence of dispersion (Schwartz, 1977; Anderson, 1979; Sudicky and Cherry, 1979; Pickens and Grisak, 1981; Gelhar and Axness, 1983; Sudicky, 1983). This scale effect is produced as a tracer encounters heterogeneities that produce mixing at a scale greater than that of the porous medium REV. By analogy, it might also be expected that macroscopic dispersion in a fractured medium will exhibit a similar scale-dependence if an expanding zone of contamination encounters pathways with substantially different velocities, creating mixing at a scale greater than that occurring within an individual fracture or a few fractures with similar flow velocities.

Schwartz et al. (1983) examined whether the dispersive character of a fracture system could be described via a constant dispersivity or a simple dispersivity function using a numerical model. From equation (6), it can be seen that if a medium has a constant dispersion coefficient, then the time rate of change in the variance of the mass distribution in the longitudinal direction $d\sigma_x^2/dt$ should be constant with travel time. Schwartz et al. found that this parameter was not a constant, indicating that the classical concept of dispersion as a Fickian process may not adequately describe dispersion in fractured media. Nor did $d\sigma_x^2/dt$ follow a consistent relationship with time, limiting the validity of using dispersivity functions as proposed by Pickens and Grisak (1981) for the characterization of dispersion in fractured media.

The scale-dependence of dispersion was examined in the present study by testing the results of one realization with the 'observation' nodes positioned at

five different distances in the longitudinal direction. The fracture network used is the same one shown on Figure 1 (a) with a value of 0.4 for $\sigma_{ln} 2b$. Because the results are obtained in the form of the temporal variance σ_t^2 rather than the spatial variance σ_x^2 , a different approach from that employed by Schwartz et al. (1983) is required to analyze the scale-dependence of dispersion.

From equation (8), it can be seen that the temporal variance of the tracer distribution can be equated to

$$\sigma_t^2 = 2D_L t_r^2 / (v_x)_{tr} x \quad (38)$$

Since $t_r = x / (v_x)_{tr}$, this can be rearranged as

$$\sigma_t^2 = 2D_L x / (v_x)_{tr}^3 \quad (39)$$

If both D_L and $(v_x)_{tr}$ are constant, the temporal variance σ_t^2 is proportional to x , the distance traveled. If, however, $(v_x)_{tr}$ is not a constant, but the dispersion coefficient can be equated to the product of a constant longitudinal dispersivity and $(v_x)_{tr}$ (equation 5), then

$$\sigma_t^2 = 2 (v_x)_{tr} x / (v_x)_{tr}^3 \quad (40)$$

and σ_t^2 should be proportional to $x / (v_x)_{tr}^2$.

Macroscopic breakthrough curves for four different distances are shown on Figure 37. These curves clearly show that the macroscopic tracer velocity is not a stationary function within this fracture network. The moment analyses of the breakthrough curves are presented in Table 7. The observed tracer velocity varies by at least as much as 20% from one location to another. The macroscopic dispersion coefficient does not show any consistent trend with distance, although it does increase or decrease with the tracer velocity. If dispersion in fractured

media can be characterized with the concept of a constant dispersivity, then changes in the dispersion coefficient with changing velocity are to be expected. The ratio of the dispersion coefficient to the tracer velocity, however, does not show a consistent trend, nor is it a constant, as might have been expected if macroscopic dispersion in fractured media can be described by a constant or a scale-dependent dispersivity α_L .

Whether a scale effect exists within the size of the simulation domain was further tested by plotting σ_t^2 versus the ratio $x/(v_x)_{tr}^2$, as shown on Figure 38. If no scale effect is present, this plot should be linear. At one point, the curve shows a negative slope. This does not mean that the tracer distribution actually contracts; as shown on Table 7, the temporal variance progressively increases with distance. Although the results are not entirely conclusive, the curve on Figure 38 appears to be slightly concave upward, suggesting that the effective dispersion might increase with distance. It is possible that the size of the transport domain is too small in relation to the scale of the fractures to permit the development of a marked scale effect. Further work is required, both to determine whether macroscopic dispersion at any one distance is linearly proportional to the tracer velocity, and also to provide a basis for predicting the magnitude of any scale effect that might exist.

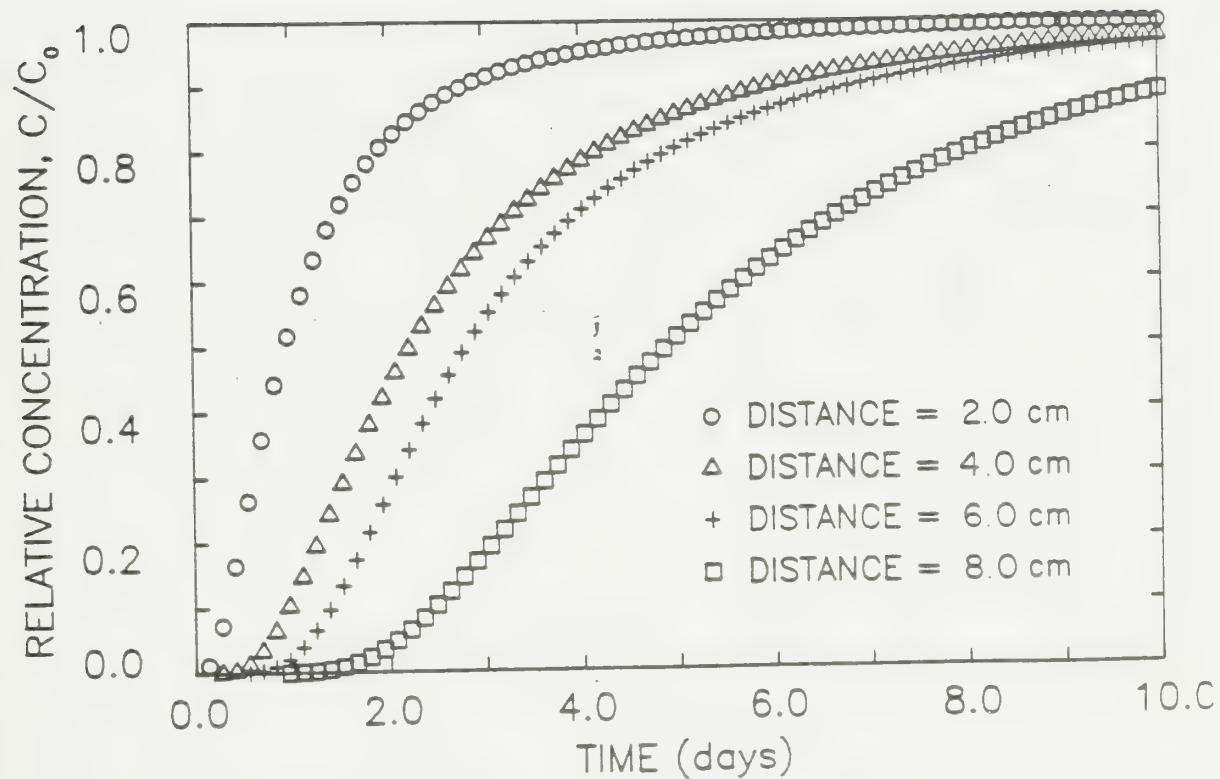


Figure 37: Macroscopic breakthrough curves for four different locations within a single fracture network

Table 7

Change in macroscopic transport parameters with distance from
the source within a single fracture network

| Computed value of parameter | Distance from inflow boundary (m) | | | | |
|-----------------------------------|-----------------------------------|-----------------------|-----------------------|-----------------------|-----------------------|
| | 0.02 | 0.04 | 0.05 | 0.06 | 0.08 |
| $(v_x)_{tr}$ (m/day) | 1.81×10^{-2} | 1.56×10^{-2} | 1.66×10^{-2} | 1.89×10^{-2} | 1.51×10^{-2} |
| σ_t^2 (days ²) | 4.97×10^{-2} | 3.43×10^{-1} | 4.80×10^{-1} | 5.60×10^{-1} | 1.72×10^0 |
| D_L (m ² /day) | 1.95×10^{-4} | 1.60×10^{-4} | 1.80×10^{-4} | 1.86×10^{-4} | 1.77×10^{-4} |
| S_k | 1.2104 | 1.1552 | 1.0711 | 1.1221 | 0.7920 |

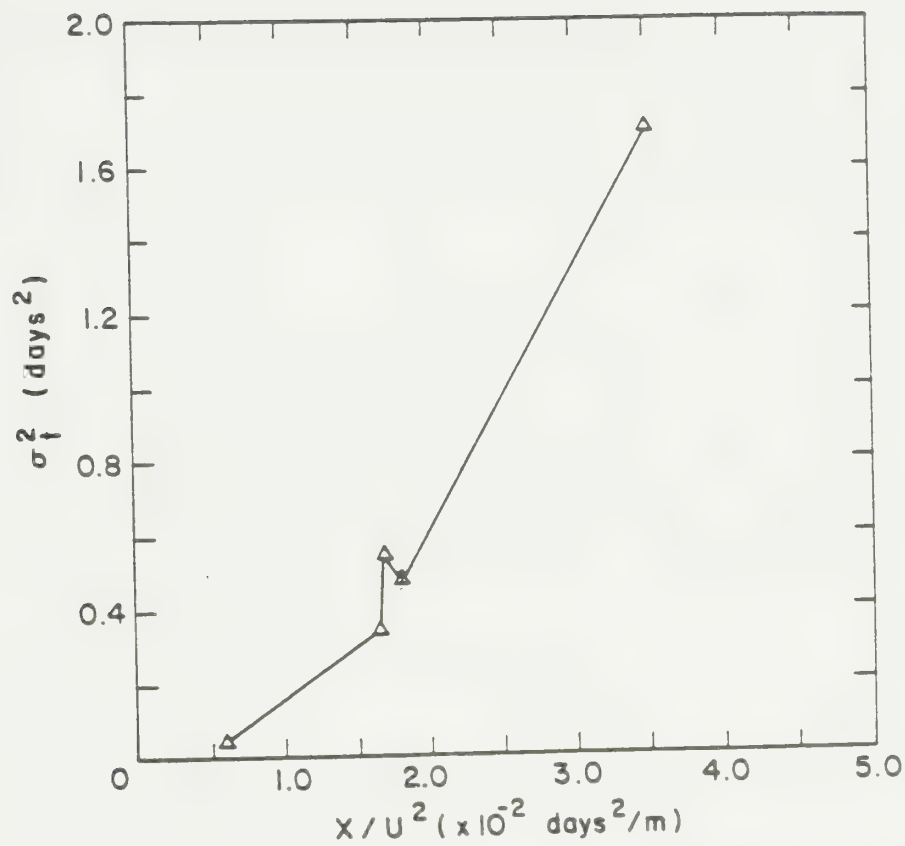


Figure 38: Results of investigation of scale-dependence of dispersion

5.4 Matrix Diffusion in Fracture Networks

Diffusion to the matrix has been shown to have a potentially important effect on the attenuation of contaminants traveling through a single fracture or in a system of parallel fractures (Tang et al., 1981; Sudicky and Frind, 1982). It was not possible to test the significance of this process in a network of finite fractures in the present study owing to the difficulty involved in discretizing the matrix regions, although the results of this study may have several implications.

Within a single fracture, the equation governing transport with diffusion to the matrix is identical to equation (34) except for the nature of the source/sink term.

$$\partial c / \partial t = D_L \partial^2 c / \partial x^2 - v \partial c / \partial x - q/b \quad (41)$$

Other terms can be added to account for sorption onto the fracture walls or radioactive decay (Tang et al., 1981). The source/sink term q represents the diffusive flux into the matrix, and can be expressed using Fick's first law as

$$q = -\Theta \tau D_0 \partial c' / \partial z \quad (42)$$

where τ is the matrix tortuosity and $\partial c' / \partial z$ is the concentration gradient in the matrix at the interface with the fracture.

Using a finite element model, Grisak and Pickens (1980) assessed the sensitivity of matrix diffusion to changes in the fracture aperture size and flow velocity. Their results demonstrate that, other factors remaining constant, much more matrix diffusion would occur in small fractures than in large ones, as is obvious from the form of equation (41). Similarly, matrix diffusion is a much more significant attenuation mechanism at low flow velocities than at high velocities, as was demonstrated on a more rigorous basis by Tang et al. (1981). Section 5.1

showed that on a local scale, transport in the absence of matrix diffusion is dominated by high-velocity pathways in larger-than-average fractures. The similarity of equations (34) and (41) suggests this may also be true of transport in the presence of matrix diffusion.

Another important factor in the amount of attenuation introduced by matrix diffusion may be the tendency of a contaminant to follow preferred pathways within a fracture network. It is apparent that the greater surface area a contaminant is exposed to, the greater the diffusive loss from the fractures. Factors that increase the tendency of a network to develop preferred high-velocity pathways along relatively large fractures, such as a large degree of variability in the apertures, may reduce the effectiveness of matrix diffusion by exposing the solute to a smaller surface area than if the same volume of contaminant were distributed among a large number of smaller fractures. When combined with the smaller diffusive flux from a single large fracture than from a single small fracture, the effectiveness of matrix diffusion may be further limited.

The results of the present study, however, also suggest that at least within the realm of flow velocities considered, this tendency may be counteracted to some extent by the transfer of contaminants via molecular diffusion to the remaining regions of the fracture network. The close correspondence of a conservative tracer's velocity through the network to the weighted flow velocity, the large ratios of tracer residence time to fluid residence time, and the relatively large retardation introduced by diffusion to deadend fracture segments all suggest that in the present simulations, the tracer was accessing most of the fractures. This will cause a contaminant to be exposed to considerably more surface area than if transport were restricted to the largest fractures in the network. If the importance of diffusive transfer to relatively stagnant fracture fluid regions is

true for most conditions of concern in fractured porous media, then significantly more attenuation via matrix diffusion may occur than in the absence of diffusion within fractures. A critical area for future research will be to test the relative importance of these effects by incorporating matrix diffusion in a stochastic-discrete fracture network model.

Chapter VI

IMPLICATIONS OF RESULTS

6.1 Sensitivity of Stochastic-Discrete Fracture Model to Changes in Geometric Parameters

The results of the present study are of necessity based on a very small number of realizations. For this reason, no definitive statements can be made concerning the sensitivity of transport to uncertainty in the statistical parameters describing the geometry of a fracture network. The results do however provide insight into the mechanisms governing transport in fracture networks, which allows some general conclusions to be drawn.

On a local scale, flow and transport in fractured media are both very sensitive to uncertainties in the statistical parameters describing the geometry of a fracture network. The spatial distribution of flow velocities and fluid discharges changes markedly as the variability in the sizes of fracture apertures increases. Both flow and contaminant transport begin to follow preferred pathways, produced wherever there is a fortuitously interconnected series of larger, more permeable features. These pathways need not be restricted to the largest features in a network, but can comprise medium-sized features if the accessibility of the largest features is limited by their being linked only to small fractures. The largest features need neither dominate flow nor transport in a finite network. The sensitivity of flow and transport on a local scale to changes in geometrical

parameters can be expected to greatly complicate attempts to predict transport over short distances or efforts to monitor groundwater contamination in fractured media.

Transport within a fracture network is, however, likely to be strongly influenced by fractures with apertures larger than the mean value, as proven by the simulations incorporating retardation. Attempts to predict contaminant retardation based on a mean fracture aperture may significantly underestimate the rate of transport in a fractured medium. Because both estimating fracture apertures from hydraulic testing and estimating mean fracture apertures from bulk hydraulic conductivity assuming perfect interconnection will generally underestimate the true values, overpredicting solute retardation in fractured media via sorption reactions or matrix diffusion is a potentially serious problem.

One of the most important factors governing flow and transport in fractured media appears to be the connectivity of fractures, a somewhat nebulous concept to attempt to apply to real systems. The hydraulic properties of finite fracture networks are very different from those of networks of infinite fractures. The bulk hydraulic conductivity of a finite fracture network may be orders of magnitude less, depending on the connectivity. This could introduce errors of an order of magnitude or more in the effective aperture estimate even if the bulk hydraulic conductivity were accurately known and reliable estimates were available of fracture density, which is rarely the case. If the effective porosity is computed from this estimated mean aperture, the effective velocity may be overestimated. The extent to which this could be countered by the greater predicted sorption and matrix diffusion introduced by a too-small aperture representation primarily depends on the specific solute and on the rock porosity.

Although neither the bulk hydraulic conductivity nor the weighted flow velocity changed much with changing aperture standard deviation, their sensitivity to connectivity suggests that the vagaries of interconnection may dominate the bulk hydraulic response of a fracture network. Repetitive realizations with the same aperture distribution may be expected to exhibit a very different response, depending on the specifics of interactions between individual fractures. If this is the case, then an inverse approach to estimating the parameters describing the fracture aperture distribution may not provide very reliable results. Complete Monte Carlo simulations may be required to assess the uncertainty in the hydraulic response associated with a known aperture distribution.

Macroscopic transport in fractured media appeared to be remarkably insensitive to changes in aperture standard deviation for the single network geometry tested, as long as the tracer was conservative. The extent of fracture interconnection was a much more important parameter, at least as far as the mean residence time of a conservative tracer was concerned. This mean residence time was much less sensitive to changes in connectivity than the fluid residence time was, however. Diffusion to deadend fracture segments and slow regions of flow may have a damping influence on the rate of transport expected from the spatial distribution of velocities within preferred pathways or expected from the bulk hydraulic conductivity and effective porosity. The tracer residence time for all of the simulations was slightly to significantly greater than the fluid residence time. Part of this was shown to be due to diffusion to deadend fracture segments; the remainder may be primarily due to transport of a tracer within near-stagnant regions of flow, where it is retained for long periods of time. Transfer of solutes to such zones is enhanced by the presence of molecular diffusion within fractures. Because of this transfer to the entire volume of fractures, the rate at

which a tracer was observed to travel through the simulated networks was much more closely related to the path length-weighted average flow velocity than to the velocities along the preferred pathways. More simulations need to be performed to substantiate this result; these should be performed at different hydraulic gradients to determine the point at which this time-dependent diffusive transfer becomes subsidiary to advection in the high-velocity regions.

The present simulations did not uncover any clear relationship between macroscopic dispersion and any other parameter. Macroscopic dispersion was remarkably insensitive to changes in fracture geometry for the limited number of realizations tested, much more so than the average residence time of a conservative tracer was. Whether macroscopic dispersion within a single network increases as some function of the average velocity should be tested with simulations at different hydraulic gradients; such results may show that macroscopic dispersion was largely controlled by diffusion in the present study.

6.2 Applicability of Dual-Porosity Models

The applicability of current dual-porosity models to the study of transport in fractured porous media will depend primarily on the purpose of the simulation and on the manner in which the parameters are estimated. Clearly such models will be much more useful for systems of evenly-spaced, highly-interconnected, near-uniform fractures such as are found in some sedimentary units than in the highly erratic fracture systems more common in crystalline rocks. If the fracture densities and apertures are known, a dual-porosity model may greatly overestimate fracture flow velocities because of the assumption of perfect interconnection. Perfect interconnection provides greater access to diffusion sites, however, and the overall effect on contaminant attenuation is difficult to predict.

If fracture apertures are estimated based on measured bulk hydraulic conductivity and known fracture density, both flow velocities and fracture apertures could be underestimated. Solute retardation and matrix diffusion would then be overestimated.

A potentially serious limitation of current dual-porosity models is their assumption of simple (sub-orthogonal) fracture geometries and simple aperture distributions (rarely more than bimodal). Flow and transport are thus evenly distributed through the network, causing contaminants to contact a greater surface area of rock for matrix diffusion. This is very different from the situation that may well occur within real fracture networks owing to differences in fracture aperture or interconnection. The extent to which the limited spatial distribution of contaminants may be counteracted by molecular diffusion to regions not participating as actively in flow merits further investigation.

Because dual-porosity models may either overestimate or underestimate contaminant arrival times, no blanket statement concerning the reliability of their predictions to field-scale problems is possible. Although they represent invaluable conceptual tools for illustrating how certain parameters can control solute transport in fractured porous media, as with any other model, they should only be applied with a clear understanding of their limitations.

6.3 Applicability of Continuum Models

The question of the applicability of continuum models for the simulation of solute transport in fractured media is partly related to the validity of a Fickian model of dispersion. In the present study, the observed macroscopic dispersion was not strictly Fickian. Macroscopic breakthrough curves were strongly 'tailed', asymptotically approaching a relative concentration of 1. The extent to which

this is caused by a capacitance effect introduced by diffusion to essentially stagnant regions of fluid and the extent to which the averaging technique contributes cannot be determined. The similarity of results for individual nodes to the macroscopic results suggests that the averaging technique is not entirely responsible. Diffusion to deadend fracture segments was observed to decrease macroscopic dispersion for the limited number of realizations tested; this process also affected the skewness of the breakthrough curves, though not in a consistent manner. It should be noted that at least over relatively short distances, diffusion to the matrix will greatly increase the non-Fickian tendencies of macroscopic dispersion.

Even though the macroscopic dispersion was not strictly Fickian, transport in the present study could still be closely represented at any one distance by a dispersion model. The applicability of this model to larger systems, or to a variety of points within the same system, needs further testing. Although a tracer travelled at a rate close to the weighted flow velocity in those networks studied, this result may not hold for all downgradient locations. The lack of stationarity of the macroscopically-observed velocity field complicated attempts to assess the scale-dependence of dispersion. This may be a common problem at a field scale.

The macroscopic dispersion coefficient appeared relatively insensitive to changes in fracture geometry. This result should be tested using a large number of realizations to see if it is possible to correlate macroscopic dispersion with any geometric parameter. It may be that the insensitivity of the dispersion coefficient can be explained by control via molecular diffusion, or possibly the dispersion coefficient is simply not sensitive to those parameters tested over the scale of the simulations. If this insensitivity is true in general of conditions representative of real fractured media, the applicability of a continuum concept is

avored. Problems remain in parameter estimation and in the technique's potential inability to predict contaminant transport on a local scale. Because of averaging, contaminants may travel at a much more rapid rate on a local scale than on a macroscopic scale.

Smith and Schwartz (1984) recently proposed an alternative to the traditional continuum approach. Their method involves applying a particle-tracking technique to a stochastically-generated discrete-fracture network, developing probability distribution functions describing particle displacement from the results; these then form the basis for the continuum model. Neglecting molecular diffusion in the fracture networks may represent an important limitation, depending on the flow regime. As with the present simulations, this technique may be highly sensitive to boundary effects; the velocity distribution of a large region is unlikely to bear much relationship to that of a small region owing to the difference in distance from arbitrarily-imposed boundary conditions and possibly different degrees of interconnection within the flow domain. The question of the size of an appropriate REV for simulating transport with any approach based on stochastically-generated fracture networks must be closely examined before its use can be widely adopted.

6.4 Areas for Future Research

The present study barely touched upon many issues of potential importance to the description of transport in fractured media. Areas for future research abound; a few are described here.

Many more statistical geometrical parameters could be subjected to a sensitivity analysis, and many more realizations need to be performed to substantiate some of the findings of this study. The present study, in accordance with Smith

and Schwartz (1984), showed bulk flow and transport in a fracture network to be relatively insensitive to changes in the fracture aperture standard deviation. Whether this is also true of the mean aperture is worth investigating. The sensitivity of flow or transport on a local scale to changes in fracture orientation distribution should also be investigated. Long et al. (1982) found an equivalent porous medium approach to be more appropriate for the representation of flow in fracture networks as the variability in fracture orientations increased; the impact this might have on transport is not readily apparent. The sensitivity of the present results to changes in fracture connectivity suggests that efforts to characterize this parameter in real systems would be useful. An additional potentially important factor may be the sensitivity of stochastically-generated discrete-fracture transport results to the boundary conditions imposed and to the size of the domain with respect to the length of the fractures. The present results are only based on a few realizations; many more would be required before the uncertainty introduced by errors in statistical geometrical input parameters can be fully assessed.

The two-dimensional stochastic-discrete fracture model developed in the present study certainly contains areas for improvement. Consideration should be given to incorporating the effects of fracture roughness, to variability in aperture along an individual fracture, to extending the network to a three-dimensional array of fractures, and to incorporating the effects of matrix diffusion. The first parameter is relatively straightforward except for uncertainties in the relationship between fracture roughness and hydrodynamic dispersion within individual fractures. The last two areas may entail a major effort. For media in which the matrix is comprised of microfractures, diffusion to the matrix could be incorporated by generating such features in the same manner as the rest of the frac-

tures. This would avoid the necessity of discretizing the matrix blocks, but might require considerable computational effort. The present model assumes no correlation between fracture aperture and length. For some fractured media, such an assumption may be unrealistic. If there is a relationship between fracture aperture and length, then the tendency of the largest fractures to dominate flow may be much greater than was observed in the present study. This could be tested by incorporating a correlation function between fracture length and aperture.

Finally, the applicability of a Fickian model of macroscopic dispersion in fractured media needs further study. The macroscopic dispersion coefficients observed were curiously insensitive to changes in fracture geometry at the scale of the present study; whether this is true of real systems, whether it would be true of other realizations, whether it represents a limitation of the small size of the networks, or whether the macroscopic dispersion was diffusion-controlled may be important questions. Testing the system at different hydraulic gradients, and examining the scale-dependence of dispersion in a large fracture network may provide a better appreciation of the limitations of a Fickian model to the description of macroscopic dispersion in fractured media.

REFERENCES

- Anderson, M. P., Using models to simulate the movement of contaminants through groundwater flow systems, *CRC Crit. Rev. Environ. Control*, 9, 97-156, 1979.
- Anderssen, A. S., and E. T. White, Parameter estimation by the weighted moments method, *Chem. Eng. Sci.* 26, 1203-1221, 1971
- Aris, R., On the dispersion of solute in a fluid flowing through a tube. *Proc. Roy. Soc. A*, 235, 67-77, 1956.
- Bear, J., *Dynamics of Fluids in Porous Media*, American Elsevier, N.Y., 764 pp., 1972.
- Bibby, R., Mass transport in dual porosity media, *Water Resour. Res.*, 17, 1075-1081, 1981.
- Burkholder, H. C., Methods and data for predicting nuclide migration in geologic media, *Intern. Symp. Management of Wastes from the LWR Fuel Cycle*, Denver, Colo., 1976.
- Castillo, E., Krizek, R. J., and G. M. Karadi, Comparison of dispersion characteristics in rock, in *Proceedings, Second Int. Symp. on Fundamentals of Transport Phenomena in Porous Media*, Guelph, Ontario, University of Guelph, Office of Continuing Education, 2, 778-797, 1972a.
- Castillo, E., Karadi, G. M., and R. J. Krizek, Unconfined flow through jointed rock, *Water Resour. Bull.*, 8, 266-281, 1972b.
- Coats, K. H., and B. D. Smith, Dead-end pore volume and dispersion in porous media, *Soc. Pet. Eng. Jour.*, 4, 73-84, 1964.
- Collins, R. J., Bandwidth reduction by automatic renumbering, *Int. Jour. for Numerical Methods in Engineering*, 6, 345-356, 1973.
- Cruden, D. M., Describing the size of discontinuities, *Int. J. Rock Mech. Min. Sci. Geomech Abstr.*, 14, 133-137, 1977.
- Daus, A. D., Frind, E. O., and E. A. Sudicky, Comparative error analysis in finite element formulations of the advection-dispersion equation, submitted to *Advances in Water Resour.*, 1983.
- Erickson, K. L., Approximations for adapting porous media radionuclide transport models to analysis of transport in jointed, porous rock, in *Scientific Basis for Nuclear Waste Management*, VI, Materials Research Society Ann. Mtg. Proceedings, Boston, MA, D. A. Brookins,

ed., 15, 473-480, 1983.

Freeze, R. A., and J. A. Cherry, Groundwater, Prentice-Hall, Inc., Englewood Cliffs, New Jersey, 604 pp., 1979.

Gale, J. E., Assessing the permeability characteristics of fractured rock, in Recent Trends in Hydrogeology, T. N. Narasimhan, ed., Geol. Soc. Amer. Spec. Paper 189, 163-181, 1982.

Gale, J. E., Witherspoon, P. A., Wilson, C. R., and A. Rouleau, Hydrogeological characterization of the Stripa site. OECD/NEA Stripa Project Workshop, October 25-27, 1982.

Gelhar, L. W., and C. L. Axness, Three-dimensional stochastic analysis of macrodispersion in aquifers. Water Resour. Res., 19, 161-180, 1983.

Gillham, R. W., and J. A. Cherry, Contaminant migration in saturated unconsolidated geological deposits, in Recent Trends in Hydrogeology, T. N. Narasimhan, ed., Geol. Soc. Amer. Spec. Paper 189, p. 31-62, 1982.

Gillham, R. W., Sudicky, E. A., Cherry, J. A., and E. O. Frind, An advection-diffusion concept for solute transport in heterogeneous unconsolidated geological deposits, Water Resour. Res., 20, 369-378, 1984.

Grisak, G. E., and J. A. Cherry, Hydrogeologic characteristics and response of fractured till and clay confining a shallow aquifer, Canadian Geotech. Jour., 12(1), 23-43, 1975.

Grisak, G. E., Cherry, J. A., Vanhof, J. A., and J. P. Blumle, Hydrogeologic and hydrogeochemical properties of fractured till in the Interior Plains Region, in Proc. Conf. Glacial Till, Spec. Publ. No. 12, Royal Soc. Canada, R. F. Legget (ed), 304-335, 1976.

Grisak, G. E., and J. F. Pickens, Solute transport through fractured media 1, The effect of matrix diffusion, Water Resour. Res., 16, 719, 1980.

Huyakorn, P. S., Lester, B. H., and J. W. Mercer, An efficient finite element technique for modeling transport in fractured porous media, 1. Single species transport, Water Resour. Res., 19, 841-854, 1983a.

Huyakorn, P. S., Lester, B. H., and J. W. Mercer, An efficient finite element technique for modeling transport in fractured porous media, 2. Nuclide decay chain transport, Water Resour. Res., 19, 1286-1296, 1983b.

Iwai, K., Fundamental studies of fluid flow through a single fracture. PhD thesis, University of California, Berkeley, 208 p., 1976.

Kreft, A., and A. Zuber, On the physical meaning of the dispersion equation and its solutions for different initial and boundary conditions, Chem. Eng. Sci., 33, 1471-1480, 1978.

Krizek, R. J., Karadi, G. M., and Socias, E., Dispersion of a contaminant in fissured rock, in Proc. Symp. Percolation through Fissured Rock. Intern.

Soc. Rock Mech., Stuttgart, 1972.

Lapidus, L., and N. R. Amundson, Mathematics of adsorption in beds, VI, The effect of longitudinal diffusion in ion exchange and chromatographic columns, J. Phys. Chem., 56, 984-995, 1952.

Levenspiel, O., Chemical Reaction Engineering, John Wiley and Sons, N. Y., 501 pp., 1962.

Long, J. C. S., Remer, J. S., Wilson, C. R., and Witherspoon, P. A., Porous media equivalents for networks of discontinuous fractures, Water Resour. Res., 18(3), 645-658, 1982.

Mercado, A., The spreading pattern of injected water in a permeability stratified aquifer, in Proc. of Intern. Assoc. Sci. Hydrol., Symp., Haifa, Publ. No., 72, 23-26, 1967.

Mixon, F. O., Whitaker, D. R., and J. C. Orcutt, Axial dispersion and heat transfer in liquid-liquid spray towers, A. I. Ch. E. J., 13, 21-28, 1967.

Neretnieks, I., Diffusion in the rock matrix: an important factor in radionuclide retardation? Jour. Geophys. Res., 85, 4379-4397, 1980.

Neretnieks, I., A note on fracture flow dispersion mechanisms in the ground, Water Resour. Res., 19, 364-370, 1983.

Neretnieks, I., Eriksen, T., and P. Tahtinen, Tracer movement in a single fissure in granitic rock: some experimental results and their interpretation, Water Resour. Res., 18(4), 849-858, 1982.

Neuzil, C. E., and J. V. Tracy, Flow through fractures, Water Resour. Res., 17(1), 191-199, 1981.

Noorishad, J., and M. Mehran, An upstream finite element method for solution of transient transport equation in fractured porous media, Water Resour. Res., 18, 588-596, 1982.

Nunge, R. J., and Gill, W. N., Mechanisms affecting dispersion and miscible displacement, in Flow through Porous Media, Amer. Chem. Soc., Washington, Washington, D. C., 179-195, 1970.

Ogata, A., and R. B. Banks, A solution of the differential equation of longitudinal dispersion in porous media, U. S. Geol. Surv., Prof. Paper 411-A, A1-A7, 1961.

Parsons, R. W., Permeability of idealized fractured rock, Soc. Pet. Eng. J., 6, 126-136, 1966.

Perkins, T. K., and O. C. Johnston, A review of diffusion and dispersion in porous media, Soc. Pet. Eng. Jour., 3, 70-84, 1963.

Philip, J. R., The theory of dispersal during laminar flow in tubes, I, Australian J. Phys., 16, 287-299, 1963.

- Pickens, J. F., and G. E. Grisak, Scale-dependent dispersion in a stratified granular aquifer, *Water Resour. Res.*, 17(4), 1191-1211, 1981.
- Pinder, G. F., and W. G. Gray, *Finite Element Simulation in Surface and Subsurface Hydrology*, Academic Press, N. Y., 295 pp., 1977.
- Priest, S. D., and J. A. Hudson, Discontinuity spacings in rock, *Int. J. Rock Mech. Min. Sci. Abstr.*, 13, 135-148, 1976.
- Rao, P. S. C., Davidson, J. M., Jessup, R. E., and H. M. Selim, Evaluation of conceptual models for describing nonequilibrium adsorption-desorption of pesticides during steady-flow in soils, *Soil Sci. Soc. Am. J.*, 43, 22-28, 1979.
- Rasmuson, A., and I. Neretnieks, Migration of radionuclides in fissured rock: the influence of micropore diffusion and longitudinal dispersion, *J. Geophys. Res.*, 86, 3749, 1981.
- Rouleau, A., and Gale, G., Statistical characterization and numerical simulation of a fracture system for hydrogeological purposes, in *Proceedings, Intern. Groundwater Symposium on Groundwater Resources Utilization and Contaminant Hydrogeology*, Montreal, Canada, v. 1, 188-196, 1984.
- Saffman, P. G., Dispersion due to molecular diffusion and macroscopic mixing in flow through a network of capillaries, *J. Fluid Mech.*, 7, 194-208, 1960.
- Sampson, R. J., *Surface II Graphics System (Revision One)*, Kansas Geological Survey, 239 p., 1978.
- Schwartz, F. W., Macroscopic dispersion in porous media: The controlling factors, *Water Resour. Res.*, 13(4), 743-752, 1977.
- Schwartz, F. W., Smith, L., and A. S. Crowe, Stochastic analysis of groundwater flow and contaminant transport in a fractured rock system, in *Scientific Basis for Nuclear Waste Management, Materials Research Society Annual Mtg., Proceedings*, Boston, Mass, v. VI, S. V. Topp, ed., 457-463, 1982.
- Schwartz, F. W., Smith, L., and A. S. Crowe, A stochastic analysis of macroscopic dispersion in fractured media, *Water Resour. Res.*, 19, 1253-1265, 1983.
- Simon, R., and F. J. Kelsey, The use of capillary tube networks in reservoir performance studies: I. Equal-viscosity miscible displacements, *Soc. Pet. Eng. Jour.*, 11, 99-112, 1971.
- Smith, L., and F. W. Schwartz, Macroscopic dispersion in a fractured rock mass, in *Proceedings, International Groundwater Symposium on Groundwater Resources Utilization and Contaminant Hydrogeology*, Montreal, Canada, v. II, 539-548, 1984.
- Snow, D. T., A parallel plate model of fractured permeable media, PhD thesis, Univ. of Calif., Berkeley, 331 p., 1965.
- Snow, D. T., Rock fracture spacings, openings, and porosities, *J. Soil Mech.*

- Found. Div., Proc. Amer. Soc. Civil Engrs., 94, 73-91, 1968.
- Snow, D. T., Anisotropic permeability of fractured media, Water Resour. Res., 5, 1273-1289, 1969.
- Snow, D. T., The frequency and apertures of fractures in rock, Int. J. Rock Mech. Min. Sci., 7, 23, 1970.
- Sudicky, E. A., An advection-diffusion theory of contaminant transport for porous media, PhD thesis, Univ. of Waterloo, 203 pp., 1983.
- Sudicky, E. A., and J. A. Cherry, Field observations of tracer dispersion under natural flow conditions in an unconfined sandy aquifer, Water Pollut. Res. Can., 14, 1-17, 1979.
- Sudicky, E. A., and E. O. Frind, Contaminant transport in fractured porous media: analytical solutions for a system of parallel fractures. Water Resour. Res., 18, 1634-1642, 1982.
- Tang, D. H., Frind, E. O., and Sudicky, E. A., Contaminant transport in fractured porous media: analytical solution for a single fracture, Water Resour. Res., 17, 555-564, 1981.
- Taylor, G. I., Dispersion of soluble matter in solvent flowing slowly through a tube, Proc. Royal Soc. A., 1137, 186-203, 1953.
- Taylor, G. I., Diffusion and mass transport in tubes, Proc. Phys. Soc. London, 67, 857-859, 1954.
- Turner, G. A., The frequency response of some illustrative models of porous media, Chem. Eng. Sci., 10, 14-21, 1959.
- Wilson, C. R., and P. A. Witherspoon, An investigation of laminar flow in fractured rocks, Geotechnical Report No. 70-6, University of California, Berkeley, 1970.

APPENDIX A: FRACTURE GENERATION, FLOW, AND TRANSPORT MODELS

Four computer models were used in simulating advective-dispersive transport in fracture networks. Program FRACGEN generates a fracture network and a grid system; program FRACFLOW simulates steady-state flow through the fracture system and calculates the average flow velocity within each fracture segment; program FRACDISC calculates the dispersion coefficient and retardation factor for each fracture segment and rediscrretizes the grid system to minimize numerical dispersion; and program FRACTRAN simulates advective-dispersive transport within the fracture network. The programs are included at the end of this Appendix. They are all fully documented and self-explanatory. Extra information concerning input and output files is provided below. The first three programs all call plotting functions designed for a Nicolet Zeta 3653sx drum plotter (or equivalent device).

Fracture Generation Program

Program FRACGEN is set up to read and write from six external devices. FI 18 is the primary input file, which must be provided by the user. Any parameters generated by the program are written to FI 19. If simulations are being run with one or more parameters held constant, the appropriate portions of this output file can be embedded back into FI 18 for subsequent runs. FI 20 is the primary output file summarizing the geometry of the fracture network and parameters such as

the theoretical hydraulic conductivity and effective porosity. FI 21 is generated as the primary input file for program FRACFLOW. If only fracture apertures are being generated and the grid system stays the same so that no plotting is required (KPLOT = 0), this file will not be generated. The input file from the base case can however be used as an input file for FRACFLOW, substituting the new apertures contained in FI 19. FI 22 contains values of the (base 10) logarithms of fractures; this file is used to generate histograms. Finally, the fracture network and grid system are contained in the plotfile.

Fracture Flow Program

Program FRACFLOW also uses six external devices. FI 25 is the primary input file; most of this is generated by program FRACGEN as described in the input documentation. FI 26 is the primary output file summarizing the hydraulic head values at the nodes, the elemental flow velocities, discharges, and Reynolds numbers, the maximum, average, and weighted average velocities, and the bulk flow parameters. FI 27 contains head values generated by this program which are used as input for SURFACE II contouring programs. FI 28 contains (base 10) logarithms of elemental velocities; these are used to generate histograms. FI 29 contains elemental velocities in a format suitable for input to program FRACDISC. The grid system (for superposition of hydraulic head contours) and the velocity vectors are plotted on the plotfile.

Fracture Rediscretization Program

Program FRACDISC uses five devices. FI 25 is the primary input file. The same file used as input for program FRACFLOW can be used with minor changes, such as embedding FI 29 generated by FRACFLOW. FI 26 is the primary output

file; it contains the Peclet and Courant numbers for the new elements. FI 27 is generated as an input file for program FRACTRAN. FI 28 contains the (base 10) logarithms of the effective (V/R) velocities for preparing histograms. The plot-file contains the new grid system for superposition of the concentration contours.

Fracture Transport Program

Program FRACTRAN uses eight files. FI 25 is the input file generated by program FRACDISC. FI 26 contains the number of time steps and the macroscopic concentrations for breakthrough curve generation. FI 28 contains concentrations at selected times for contouring with SURFACE II. FI 29 contains values of dimensionless time, and FI 30 contains values of actual time. Finally, FI 31 contains concentrations for a designated individual node.

HAMILTON PUBLIC LIBRARY



3 2022 21333730 2